Synthesis of Diverse Compounds using Mannofuranose as a Chiral Scaffold

By

Penny L. Miner

Submitted in Partial Fulfillment of the Requirements

for the Degree of

Master of Science

in the Chemistry Program

YOUNGSTOWN STATE UNIVERSITY

August, 2004

Synthesis of Diverse Compounds using Mannofuranose as a Chiral Scaffold

Penny L. Miner

I hereby release this to the public. I understand that this thesis will be made available from the OhioLINK ETD Center and the Maag Library Circulation Desk for public access. I also authorize the University or other individuals to make copies of this thesis as needed for scholarly research.

Signature: Penny L. Miner 7/27/04

Penny L. Miner — Date

Approvals:

7/27/04

Dr. Peter Norris — Date
Thesis Advisor

7/27/04

Dr. John Jackson — Date
Committee Member

7/27/04

Dr. Timothy Wagner — Date
Committee Member

7/28/04

Dr. Peter J. Kasvinsky — Date
Dean of Graduate Studies

Thesis Abstract

This project involves the convenient methods for the synthesis of mannofuranose derivatives. The parallel synthesis method provided an advantage to multiple compound synthesis of *N*-glycosides such as mannosyl triazoles. The synthesis of *N*-glycoside analogs from available precursors is studied using Huisgen 1,3-dipolar cycloadditions and the modified catalyst version. Manipulation of the isopropylidene protecting groups on mannose is also explored. The methods and results of each compound obtained are described in detail.

Acknowledgements

I would like to first express my thanks to the YSU Department of Chemistry and the School of Graduate Studies for allowing me to pursue my degree. A special thank you goes to Dr. John Jackson and Dr. Timothy Wagner for not only being members of my thesis committee, but also giving me their time when I needed it. Also, thank you to Ray Hoff and Dr. Daryl Mincey for giving me the resources to start off my career.

A special thanks to my Mom and Dad for the foundation you gave me, which has allowed me to achieve my goals and dreams. Most of all I want to thank my husband, Rob, for all his love, support, and understanding though the years. To my kids, Dominique, Amber, and Austin, I want to say thank you for all your love even when I couldn't be there.

I must also thank all the people in the Norris Research Group particularly Travis, Dave, Rakesh, Dan, Brian and Yuri for making life in the lab more enjoyable. I would like to especially thank Yuri Root for giving me all the help at the beginning of my M.S. degree.

Finally, I must thank Dr. Peter Norris for seeing my potential and giving me a chance to develop as a chemist. I can't express my gratitude enough for all the knowledge you have given me but also your caring support when I needed it.

Table of Contents

Title Page.....i

Signature Page.....ii

Abstract.....iii

Acknowledgements.....iv

Table of Contents.....v

List of Tables.....vi

List of Schemes.....vi

List of Equations.....vi

List of Figures.....ix

Introduction.....1

Statement of Problem.....15

Results and Discussion.....16

1. Precursors to mannofuranosyl azide
2. Selective deprotection and manipulation of glycosyl azide **4**
3. 1,3-Dipolar cycloadditions of mannosyl azide **4**
4. Additional deprotection and manipulation of triazole **9**
5. Precursors to triazole oligosaccharide synthesis
6. Disaccharide and trisaccharide heterocycle formation

Future Investigation.....43

Experimental.....44

General Procedures

References.....74

Appendix A NMR Spectra, Mass Spectra.....79

Appendix B X-ray.....149

List of Tables

Table 1: Mannosyl azide (**4**) cycloadditions (uncatalyzed).....24

Table 2: Mannosyl azide **4** cycloadditions with copper catalyst 28

Table 3: Alkyne reagents 52

Table 4: Alkyne reagents 56

Table 5: Sugar-alkyne precursors.....64

Table 6: Yields of sugar alkynes 65

List of Schemes

Scheme 1: Copper-catalyzed 1,2,3-triazole formation.....7

Scheme 2: Synthesis of Fuc-T inhibitor.....7

Scheme 3: Preparation of a carbohydrate scaffold.....14

Scheme 4: Synthesis of azidodeoxy sugar **4**.....17

Scheme 5: 1) Huisgen 1,3-dipolar cycloaddition mechanism; 2) Copper(I)-catalyzed Huisgen 1,3-dipolar cycloaddition.....23

List of Equations

Equation 1: Formation of 2,3:5,6-di-*O*-isopropylidene-α-D-mannofuranose.....17

Equation 2: Selective deprotection of mannofuranosyl azide **4**.....19

Equation 3: Selective tosylation of 1-azido-1-deoxy-2,3-*O*-isopropylidene-β-D-mannofuranose.....20

Equation 4: Formation of 1,6-diazido-1,6-di-deoxy-2,3-*O*-isopropylidene-β-D-mannofuranose (**7**).....21

Equation 5: Protection of free hydroxyl in **7**.....22

Equation 6: 1-(2,3:5,6-Di-*O*-isopropylidene-β-D-mannofuranosyl)-1*H*-[1,2,3] triazol-4,5-dicarboxylic acid diethyl ester (**9**).....24

Equation 7: 1-(2,3:5,6-Di-*O*-isopropylidene-β-D-mannofuranosyl)-1*H*-[1,2,3] triazol-4-(and 5-)-carboxylic acid ethyl esters (**10a/10b**).....25

Equation 8: 1-(2,3:5,6-Di-*O*-isopropylidene-β-D-mannofuranosyl)-1*H*-[1,2,3] triazol-4-(and 5-)-carboxylic acids (**11a/11b**).....26

Equation 9: 1-(2,3:5,6-Di-*O*-isopropylidene-β-D-mannofuranosyl)-1*H*-[1,2,3] triazol-4-(and 5-)-carboxylic acid trimethylsilyl esters (**12a/12b**).....26

Equation 10: 1-(2,3:5,6-Di-*O*-isopropylidene-β-D-mannofuranosyl)-4-(and 5-) -phenyl-1*H*-[1,2,3]triazole (**13a/13b**).....27

Equation 11: Bis(triazole) **14**.....27

Equation 12: 1-(2,3:5,6-Di-*O*-isopropylidene-β-D-mannofuranosyl)-1*H*-[1,2,3] triazol- 4-carboxylic acid ethyl ester (**10a**).....29

Equation 13:1-(2,3:5,6-Di-*O*-isopropylidene-β-D-mannofuranosyl)-1*H*-[1,2,3] triazol-4-carboxylic acid (**11a**).....29

Equation 14:1-(2,3:5,6-Di-*O*-isopropylidene-β-D-mannofuranosyl)-1*H*-[1,2,3] triazol-4-carboxylic acid trimethylsilyl ester (**12a**).....30

Equation 15: 1-(2,3:5,6-Di-*O*-isopropylidene-β-D-mannofuranosyl)-4-phenyl-1*H*-[1,2,3]triazole (**13a**).....30

Equation 16: 1-(2,3:5,6-Di-*O*-isopropylidene-β-D-mannofuranosyl)-1*H*-[1,2,3]-triazol-4-yl methanol (**15**).....31

Equation 17: 1-(2,3-*O*-Isopropylidene-β-D-mannofuranosyl)-1*H*-[1,2,3]triazol-4,5-dicarboxylic acid diethyl ester (**16**).....32

Equation 18: 1-(2,3-*O*-Isopropylidene-5,6-di-*O*-acetyl-β-D-mannofuranosyl)-1*H*-[1,2,3]triazol-4,5-dicarboxylic acid diethyl ester (**17**).....33

Equation 19: Attempted formation of 1-β-D-mannofuranosyl-1*H*-[1,2,3]triazol-4,5-dicarboxylic acid diethyl ester (**18**).....34

Equation 20: 1-(2,3:5,6- Di-*O*-isopropylidene-β-D-mannofuranosyl)-1*H*-[1,2,3]-triazol-4,5-dicarboxylic acid diamide (**19**).....34

Equation 21: Benzoylation of **16**.....35

Equation 22: 1,2:3,4-Di-*O*-isopropylidene-6-((prop-2-ynyloxy)methyl)-D-galactopyranose (**22**).....36

Equation 23: Synthesis of compound **23**.....37

Equation 24: Synthesis of alkyne **25**.....37

Equation 25: 1,2-*O*-isopropylidene-3,5-di-*O*-(prop-2-ynyloxy)-D-xylofuranose (**27**).....38

Equation 26: Synthesis of compound **28**.....39

Equation 27: Synthesis of compound **29**.....40

Equation 28: Synthesis of compound **30**.....41

Equation 29: Synthesis of compound **31**.....41

List of Figures

Figure 1: The different forms of D-mannose 2

Figure 2: The D- and L-mannose configurations 3

Figure 3: Example of *O*-glycoside 4

Figure 4: Comparison of *O*-glycoside and *C*-glycoside 5

Figure 5: AZT and Spicamycin 6

Figure 6: Parallel Synthesis 9

Figure 7: Mixture Synthesis 10

Figure 8: Somatostatin mimic and RGD sequence mimic.....13

Figure 9: 2,3:5,6-Di-*O*-isopropylidene-α-D-mannofuranose (**1**).....16

Figure 10: X-ray structure for 1-(2,3:5,6-di-*O*-isopropylidene-β-D-manno-furanosyl)-1*H*-[1,2,3]triazol-4,5-dicarboxylic acid diethyl ester (**9**).....25

Figure 11: Compound **31** X-ray structure 36

Figure 12: 400 MHz ^{1}H NMR spectrum of diacetone D-mannofuranose (**1**).....80

Figure 13: 400 MHz ^{1}H NMR spectrum of mannosyl chloride **3**.....81

Figure 14: 400 MHz ^{1}H NMR spectrum of mannosyl azide **4**.....82

Figure 15: 100 MHz ^{13}C NMR spectrum of mannosyl azide **4**.....83

Figure 16: 400 MHz ^{1}H NMR spectrum of 1-azido-1-deoxy-2,3-*O*-isopropylidene-β-D-mannofuranose **5**.....84

Figure 17: 100 MHz ^{13}C NMR spectrum of 1-azido-1-deoxy-2,3-*O*-isopropylidene-β-D-mannofuranose **5**.....85

Figure 18: Mass spectrum of 1-azido-1-deoxy-2,3-*O*-isopropylidene-β-D-manno-furanose **5**.....86

Figure 19: 400 MHz ^{1}H NMR spectrum of 1-azido-1-deoxy-2,3-*O*-isopropylidene-6-*p*-toluenesulfonyl-β-D-mannofuranose (**6**).....87

Figure 20: 100 MHz ^{13}C NMR spectrum of 1-azido-1-deoxy-2,3-*O*-isopropylidene-6-*p*-toluenesulfonyl-β-D-mannofuranose (**6**).....88

Figure 21: Mass spectrum of 1-azido-1-deoxy-2,3-*O*-isopropylidene-6-*p*-toluenesulfonyl-β-D-mannofuranose (**6**).....89

Figure 22: 400 MHz ^{1}H NMR spectrum of 1,6-diazido-1,6-dideoxy-2,3-*O*-isopropylidene-β-D-mannofuranose (**7**).....90

Figure 23: 100 MHz ^{1}C NMR spectrum of 1,6-diazido-1,6-dideoxy-2,3-*O*-isopropylidene-β-D-mannofuranose (**7**).....91

Figure 24: Mass spectrum of 1,6-diazido-1,6-dideoxy-2,3-*O*-isopropylidene-β-D-mannofuranose (**7**).....92

Figure 25: 400 MHz ^{1}H NMR spectrum of 5-acetyl-1,6-diazido-1,6-dideoxy-2,3-*O*-isopropylidene-β-D-mannofuranose (**8**).....93

Figure 26: 400 MHz ^{1}H NMR spectrum of mannofuranosyl-1*H*-[1,2,3]triazol-4,5-dicarboxylic acid diethyl ester (**9**).....94

Figure 27: 100 MHz ^{13}C NMR spectrum of mannofuranosyl-1*H*-[1,2,3]triazol-4,5-dicarboxylic acid diethyl ester (**9**).....95

Figure 28: Mass spectrum of mannofuranosyl-1*H*-[1,2,3]triazol-4,5-dicarboxylic acid diethyl ester (**9**).....96

Figure 29: 400 MHz ^{1}H NMR spectrum of mannofuranosyl-1*H*-[1,2,3]triazol-4-(and 5-)-carboxylic acid ethyl esters (**10a/10b**).....97

Figure 30: 400 MHz ^{1}H NMR spectrum of mannofuranosyl-1*H*-[1,2,3]triazol-4-(and 5-)-carboxylic acids (**11a/11b**).....98

Figure 31: 400 MHz ^{1}H NMR spectrum of mannofuranosyl-1*H*-[1,2,3]triazol-4-(and 5-)-carboxylic acid trimethylsilyl esters (**12a/12b**).....99

Figure 32: 400 MHz ^{1}H NMR spectrum of mannofuranosyl-1*H*-[1,2,3]triazol-4-carboxylic acid ethyl ester (**10a**).....100

Figure 33: 100 MHz ^{13}C NMR spectrum of mannofuranosyl-1*H*-[1,2,3]-triazol-4-carboxylic acid ethyl ester (**10a**).....101

Figure 34: Mass spectrum of mannofuranosyl-1*H*-[1,2,3]triazol-4-carboxylic acid ethyl ester (**10a**).....102

Figure 35: 400 MHz ^{1}H NMR spectrum of mannofuranosyl-1*H*-[1,2,3]triazol-4-carboxylic acid (**11a**).....103

Figure 36: 100 MHz ^{13}C NMR spectrum of mannofuranosyl-1*H*-[1,2,3]triazol-4-carboxylic acid (**11a**).....104

Figure 37: Mass spectrum of mannofuranosyl-1*H*-[1,2,3]triazol-4-carboxylic acid (**11a**).....105

Figure 38: 400 MHz ^{1}H NMR spectrum of mannofuranosyl-1*H*-[1,2,3]triazol-4-carboxylic acid trimethylsilyl ester (**12a**).....106

Figure 39: 400 MHz ^{1}H NMR spectrum of mannofuranosyl-4-phenyl-1*H*-[1,2,3]-triazole (**13a**) 107

Figure 40: 100 MHz ^{13}C NMR spectrum of mannofuranosyl-4-phenyl-1*H*-[1,2,3]triazole (**13a**).....108

Figure 41: Mass spectrum of mannofuranosyl-4-phenyl-1*H*-[1,2,3]triazole (**13a**).....109

Figure 42: 400 MHz ^{1}H NMR spectrum of mannofuranosyl-1,6-*H*-[1,2,3]triazol-4,5-dicarboxylic acid diethyl esters (**14**).....110

Figure 43: 100 MHz ^{13}C NMR spectrum of mannofuranosyl-1,6-*H*-[1,2,3]triazol-4,5-dicarboxylic acid diethyl esters (**14**).....111

Figure 44: Mass spectrum of mannofuranosyl-1,6-1*H*-[1,2,3]triazol-4,5-dicarboxylic acid diethyl esters (**14**).....112

Figure 45: 400 MHz ^{1}H NMR spectrum of mannofuranosyl-1*H*-[1,2,3]triazol-4-yl methanol (**15**).....113

Figure 46: 100 MHz ^{13}C NMR spectrum of mannofuranosyl-1*H*-[1,2,3]-triazol-4-yl methanol (**15**).....114

Figure 47: Mass spectrum of mannofuranosyl-1*H*-[1,2,3]triazol-4-yl methanol (**15**).....115

Figure 48: 400 MHz ^{1}H NMR spectrum of 1-(2,3-*O*-isopropylidene-β-D-mannofuranosyl)-1*H*-[1,2,3]triazol-4,5-dicarboxylic acid diethyl ester (**16**).....116

Figure 49: Mass spectrum of 1-(2,3-*O*-isopropylidene-β-D-mannofuranosyl)-1*H*-[1,2,3]triazol-4,5-dicarboxylic acid diethyl ester (**16**).....117

Figure 50: 400 MHz ^{1}H NMR spectrum of 1-(5,6-di-*O*-acetyl-2,3-*O*-isopropylidene-β-D-mannofuranosyl)-1*H*-[1,2,3]triazol-4,5-dicarboxylic acid diethyl ester (**17**).....118

Figure 51: 400 MHz ^{1}H NMR spectrum of mannofuranosyl-1*H*-[1,2,3]-triazol-4,5-dicarboxylic acid diamide (**19**).....119

Figure 52: 100 MHz ^{13}C NMR spectrum of mannofuranosyl-1*H*-[1,2,3]-triazol-4,5-dicarboxylic acid diamide (**19**).....120

Figure 53: Mass spectrum of mannofuranosyl-1*H*-[1,2,3]-triazol-4,5-dicarboxylic acid diamide (**19**).....121

Figure 54: 400 MHz ^{1}H NMR spectrum of Bis(ester) **20**.....122

Figure 55: 100 MHz ^{13}C NMR spectrum of Bis(ester)**20**.....123

Figure 56: Mass NMR spectrum of Bis(ester) **20**.....124

Figure 57: 400 MHz ^{1}H NMR spectrum of 1,2:3,4-di-*O*-isopropylidene-6-(prop-2-ynyloxy)-D-galactopyranose (**22**).....125

Figure 58: 100 MHz ^{13}C NMR spectrum of 1,2:3,4-di-*O*-isopropylidene-6-(prop-2-ynyloxy)-D-galactopyranose (**22**).....126

Figure 59: Mass spectrum of 1,2:3,4-di-*O*-isopropylidene-6-(prop-2-ynyl-oxy)-D-galactopyranose (**22**).....127

Figure 60: 400 MHz ^{1}H NMR spectrum of diacetone-D-mannose alkyne **23**.....128

Figure 61: 100 MHz ^{13}C NMR spectrum of diacetone-D-mannose alkyne **23**.....129

Figure 62: Mass spectrum of diacetone-D-mannose alkyne **23**.....130

Figure 63: 400 MHz ^{1}H NMR spectrum of diacetone-D-glucofuranose alkyne **25**...131

Figure 64: 100 MHz ^{13}C NMR spectrum of diacetone-D-glucofuranose alkyne **25**.132

Figure 65: Mass spectrum of diacetone-D-glucofuranose alkyne **25**.....133

Figure 66: 400 MHz ^{1}H NMR spectrum of 1,2-*O*-isopropylidene-3,5-di-*O*-(prop-2-ynyloxy)-D-xylofuranose (**27**).....134

Figure 67: 100 MHz ^{13}C NMR spectrum of 1,2-*O*-isopropylidene-3,5-di-*O*-(prop-2-ynyloxy)-D-xylofuranose (**27**).....135

Figure 68: Mass spectrum of 1,2-*O*-isopropylidene-3,5-di-*O*-(prop-2-ynyloxy)-D-xylofuranose (**27**).....136

Figure 69: 400 MHz ^{1}H NMR spectrum of bistriazole **28**.....137

Figure 70: 100 MHz ^{13}C NMR spectrum of bistriazole **28**.....138

Figure 71: Mass spectrum of bistriazole **28**.....139

Figure 72: 400 MHz ^{1}H NMR spectrum of triazole **29**, a disaccharide analog 140

Figure 73: 100 MHz ^{13}C NMR spectrum of triazole **29**, a disaccharide analog 141

Figure 74: Mass spectrum of triazole **29**, a disaccharide analog 142

Figure 75: 400 MHz ^{1}H NMR spectrum of triazole **30**, a disaccharide analog 143

Figure 76: 100 MHz ^{13}C NMR spectrum of triazole **30**, a disaccharide analog 144

Figure 77: Mass spectrum of triazole **30**, a disaccharide analog 145

Figure 78: 400 MHz ^{1}H NMR spectrum of triazole **31**, a disaccharide analog.....146

Figure 79: 100 MHz ^{13}C NMR spectrum of triazole **31**, a disaccharide analog.....147

Figure 80: Mass spectrum of triazole **31**, a disaccharide analog 148

Figure 81: X-ray structure for 1-(2,3:5,6-di-*O*-isopropylidene-β-D-manno-furanosyl)-1*H*-[1,2,3]triazol-4,5-dicarboxylic acid diethyl ester (**9**).....150

Figure 82: X-ray structure compound **31**, a disaccharide analog.....164

Introduction:

Over the past thirty-five years carbohydrate chemistry has seen a surge of interest from both chemical and biological perspectives. These molecules have been understood to play vital roles in food, pharmaceutical, and agrochemical industries. The history of carbohydrate chemistry can be traced back to Emil Fischer in the late 1800's where his research on the parent sugars laid the foundation of modern carbohydrate chemistry. Until the advances of spectroscopy in the 1960's this subdivision of organic chemistry was considered repetitive and limited. By the 1970's these molecules were recognized as chiral starting materials in the synthesis of non-carbohydrates and biological materials, and this discovery laid the foundation for the study of carbohydrates in biological processes, a science recently labeled "glycobiology."[1]

The science of glycobiology is the study of the structure and biosynthesis of molecules such as glycoproteins or glycolipids. The scope of this science ranges from the properties of complex biomolecules to the synthetic chemistry of carbohydrates.[2] Carbohydrates (sugars) form important elements of glycolipids and glycoproteins and can be found as a single linear unit or as branched molecules. Simple carbohydrates have the general molecular formula $C_n(H_2O)_n$ and are considered hydrates of carbon. Monosaccharides are the chemical unit from which all members of the carbohydrate family are built, and cannot be hydrolyzed into a simpler unit. The grouping of monosaccharides is dependent on the number of carbons attached, the orientation of the hydroxyl groups, as well as whether they are polyhydroxylated aldehydes (aldoses) or polyhydroxylated ketones (ketoses). Carbohydrates are classified under four general terms: monosaccharides, disaccharides, oligosaccharides, or polysaccharides.[3] Glucose,

mannose, and galactose are examples of monosaccharides. Glucose is the most naturally abundant, and it alone plays a central role in biochemistry. Monosaccharides can exist in three main distinct forms: acyclic form; the furanose ring (five-membered): and the pyranose ring (six-membered) while in solution (Figure 1).

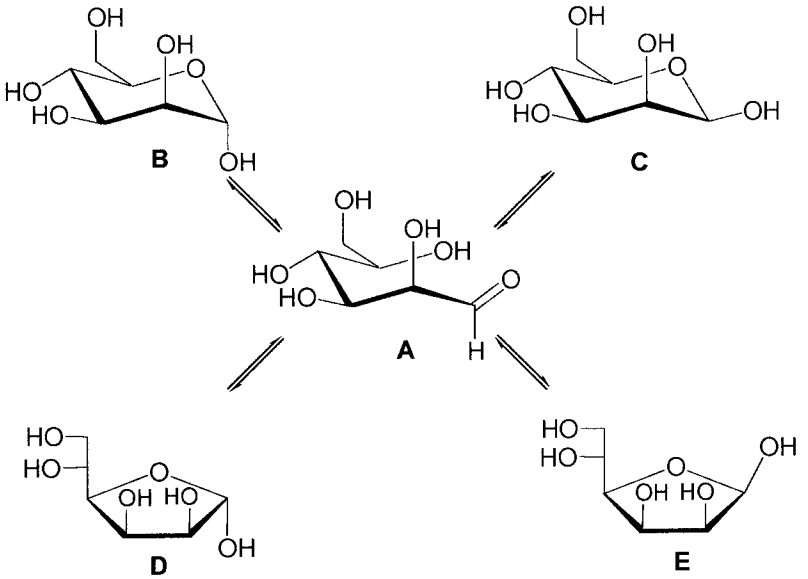

Figure 1: The different forms of D-mannose

The formation of the rings occurs when the hydroxyl group attached at carbon four or carbon five attacks the carbonyl carbon of the aldehyde. This is demonstrated for D-mannose (Figure 1). When the *aldehydo* form (Figure 1, **A**) cyclizes from nucleophilic attack by the –OH group at carbon five, the six-membered ring (Figure 1, **B** and **C**) results to give the pyranose form. The sugar will cyclize to give the five-membered ring, the furanose form (Figure 1, **D** and **E**), if the *aldehydo* form undergoes nucleophilic attack from the –OH group at carbon four. In the *aldehydo* form C-1 is sp^2 hybridized and therefore can undergo attack from the top or bottom position to provide the mixture of

alpha (α) (Figure **1, B** and **D**) and beta (β) (Figure **1, C** and **E**) anomers. The alpha (α) configurations are given to sugars where the hydroxyl group at carbon one (anomeric) are pointing in the axial position (below the plane of the molecule). The beta (β) arrangement is specified when the hydroxyl group at the anomeric carbon is pointing equatorial (above the plane of the molecule).[4] The interconversion between the alpha and beta anomers, known as mutarotation, occurs quickly in the presence of an acid or base.[5]

All monosaccharides are given the notations D or L in reference to the orientation of the hydroxyl group at the first stereocenter from the bottom of the Fischer projection. In the example of D-mannose, the hydroxyl group is positioned on the right side of the chain, and with L-mannose the hydroxyl group is oriented to the left (Figure 2). D and L sugars are mirror images of each other, however most naturally occurring sugars are D isomers.

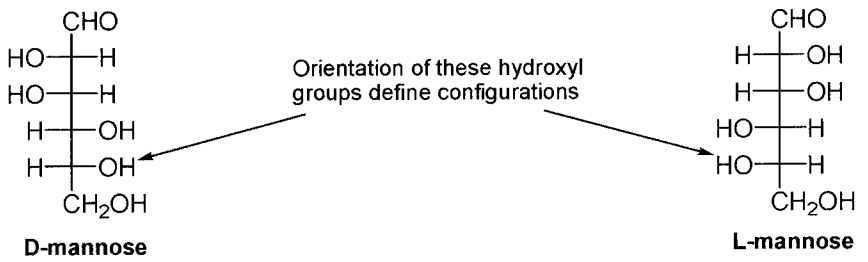

Figure 2: The D- and L-mannose configurations

The entire group of carbohydrates can be divided into many subdivisions, two of the most important being glycosides and amino sugars. Glycosides have become an important subdivision due to their importance in biological processes and medicinal development. Glycosides are characterized by the replacement of the anomeric hydroxyl group with any other functionality, for example *-OR, -CR,* or *-NR.* The result is

glycosidic linkages, which are classified as *O*-glycoside, *C*-glycoside, and *N*-glycoside respectively.

O-Glycosides can be found everywhere in Nature from animals, plants, and microbiological sources. Microbial glycosides have been shown to have particular significance in regards to antibiotic activity. Daunomycin, an *O*-glycoside (Figure 3), is useful in fighting leukemias and soft-tissue sarcomas. A need for these compounds has been the major stimulus to the development of new synthetic methods, however naturally occurring enzymes, such as glycohydrolases mediate the breakdown of *O*-glycosides. Due to this reason, researchers now look to synthesize inhibitors and sugars that mimic these natural compounds, but are not easily hydrolyzed. Such compounds are generally called "glycomimetics" (carbohydrate mimics).

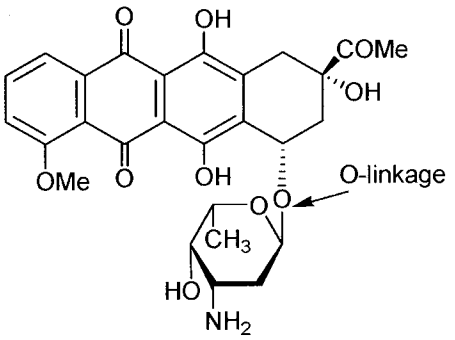

Daunomycin

Figure 3: Example of *O*-glycoside

Since *O*-glycosides are easily susceptible to biodegradation, synthetic chemists have had to develop more stable analogs with similar medicinal characteristics. A major focus has been in the formation of *C*-glycosides due to their ability to withstand

degradation from hydrolytic and enzymatic processes within biological systems.[6] The work done by Kishi and co-workers on the conformational characteristics of *C*- and *O*-glycosides has shown that the small energy differences among conformers allows for their interchange without any major problems.[7] Linhardt and coworkers have investigated the biological activity of sialyl-Tn, an *O*-glycoside (Figure 4) versus the *C*-glycoside analog. Sialyl-Tn has been found to be part of the HIV envelope glycoprotein, gp120, and also part of the glycoproteins present on the surface of cancer cells.[8]

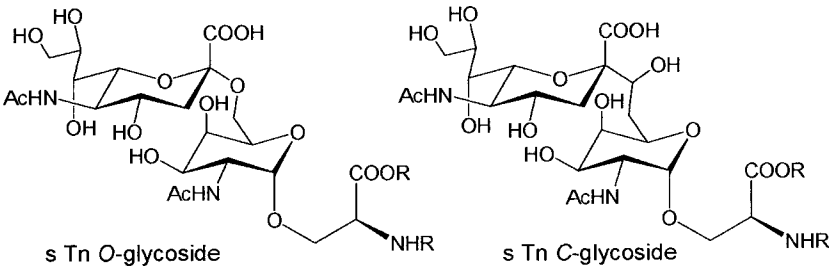

Figure 4: Comparison of *O*-glycoside and *C*-glycoside

Another type of glycomimetic studied extensively are *N*-glycosides, which include naturally occurring microbiological metabolites, nucleosides, nucleotides and nucleic acids. Synthesis of naturally occurring *N*-glycoside analogs has become extremely important within medicinal chemistry. Nucleosides, such as 2',3'-dideoxynucleosides, have been used as anticancer and antiviral drugs. There was an explosion of interest in these compounds when it was discovered that several had activity against the human immunodeficiency virus. Structural analogs, such as AZT (Figure 5), mimic their counterparts during DNA synthesis, however when the 2',3'-dideoxynucleosides are accepted by the DNA polymerase and are incorporated within the

growing chain, the absence of a 3'-hydroxyl group prohibits the elongation of the DNA. Nucleoside analogs work primarily by inhibiting chain elongation or by competitive inhibition.[9]

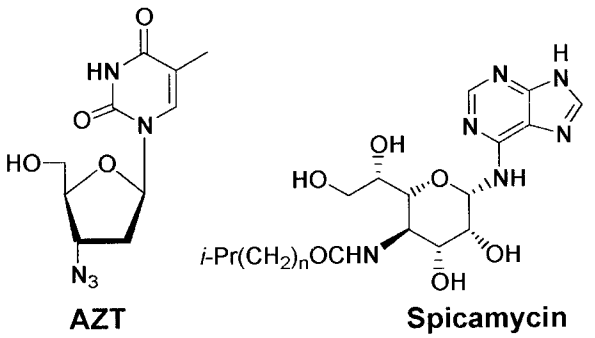

Figure 5: AZT and Spicamycin

Chida and co-workers have synthesized an analog of the naturally occurring antitumor antibiotic, spicamycin (Figure 5).[10] Spicamycin is a member of a family of compounds, which differ in Nature only by the length of the fatty acid chain portion of the molecule (shown above as n). The point of interest in this compound is where the adenine is linked to the nucleoside through the N^6 amino group, instead of the 9-position.[11]

In recent years, interest surrounding 1,2,3-triazole synthesis has increased. This is due in part to the fact that unlike amides, triazoles are not subject to hydrolytic cleavage and are almost impossible to oxidize or reduce.[12] The major stumbling block was to control 1,4- versus 1,5-regioselectivity in the formation of the heterocycle. Meldal and co-workers reported regiospecifc 1,3-dipolar cycloaddition of terminal alkynes to azides utilizing copper(I)-catalysis (Scheme 1) to produce peptidotriazoles on solid support.[13]

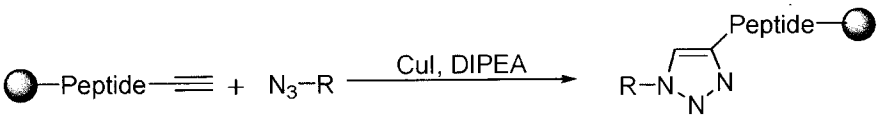

Scheme 1: Copper-catalyzed 1,2,3-triazole formation

Sharpless and Wong employed the same methodology as Meldel but used the knowledge that azides are extremely stable towards H_2O, O_2, and a variety of aqueous solutions and mild reducing environments common to biological systems.[14] They chose to examine fucosyltranferases, which are responsible for the final glycosylation step in biosynthesis and expression of various saccharides. The synthesis of glycomimetics of this system has been problematic until now when Sharpless and Wong were able to synthesize an inhibitor of α-1,3-fucosyltranferase (Fuc-T) in the presence of water and alcohols as the solvent system using Cu(I) as a catalyst in the reaction (Scheme 2). They showed that advances in triazole synthesis have made it possible to be able to work with unprotected groups and therefore allow for the screening of the crude aqueous reaction solutions.[15]

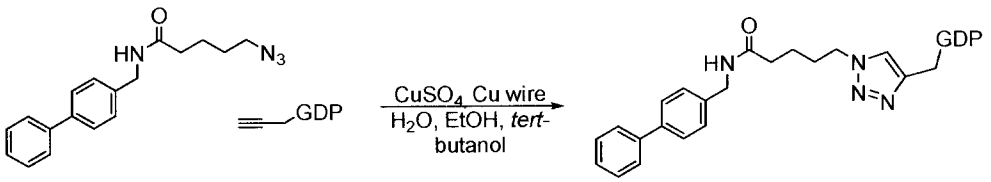

Scheme 2: Synthesis of Fuc-T inhibitor

In the last twenty years, insight into the biological processes underlying disease states have increased dramatically, due in part to the emergence of molecular biology, especially the genomic sciences. With this escalation, the number of suitable attack points

has increased the number of treatment routes,[16] therefore the "one by one" synthesis theory began to radically change in order to meet the growing demands for the development of new compounds for discovering new drugs. This new way of thinking introduced a rapidly growing new scientific field, *Combinatorial Chemistry*. The principle behind this new field is that all substances synthesized can be deduced from a selected set of monomers used in the synthesis. Combinatorial chemistry has the ability to generate large numbers of structurally diverse molecules, which in turn may reduce the drug discovery timeline. The early methods owe their roots to solid-phase peptide synthesis, which revolutionized pharmaceutical research.[17]

Modern combinatorial chemistry involves both the synthesis and screening of large sets of libraries. The synthetic methods are classified into two categories, parallel synthesis leading to individual compounds and combinatorial synthesis leading to mixtures. Combinatorial synthetic methods are where the number of synthesized compounds increases exponentially with the number of executed steps. These methods can produce either mixtures or series of individual compounds.[18]

When the number of synthesized compounds remains constant with increasing executed steps, this is termed parallel synthesis. The underlying principle is the geometrical expansion of both the number and the diversity of compounds in a product set that is achieved by matrix construction of a row of functionally identical but diverse building blocks with a column of diverse building blocks that have complementary functionality (Figure 6).[19] This method is used in preparing series of individual compounds.

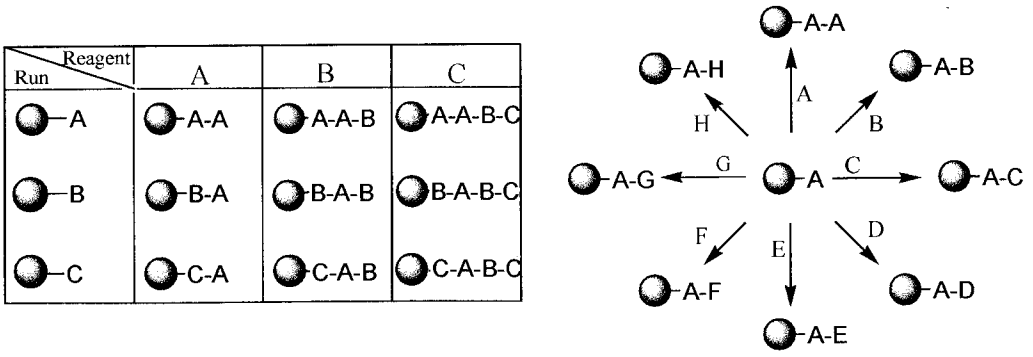

Figure 6: Parallel Synthesis[20]

In 1984 Geysen and colleagues introduced the multipin method, which originally was used for the parallel synthesis of arrays of peptides, however the method was later applied to preparing other organic libraries. The multipin device is considered the prototype of the modern automated synthesizers.[21]

Furka and colleagues in 1988 invented the "portioning-mixing" (split) method. This method is used to make libraries based on real combinatorial principles. Merrifield's solid phase procedure exemplified this by creating a tetrapeptide library using only three amino acids. The synthesis is executed by three simple steps, which are repeated. The first is dividing the solid support into equal portions, and then coupling each individually with a different amino acid. Lastly, the portions are mixed, and the procedure then repeats (Figure 7).[22]

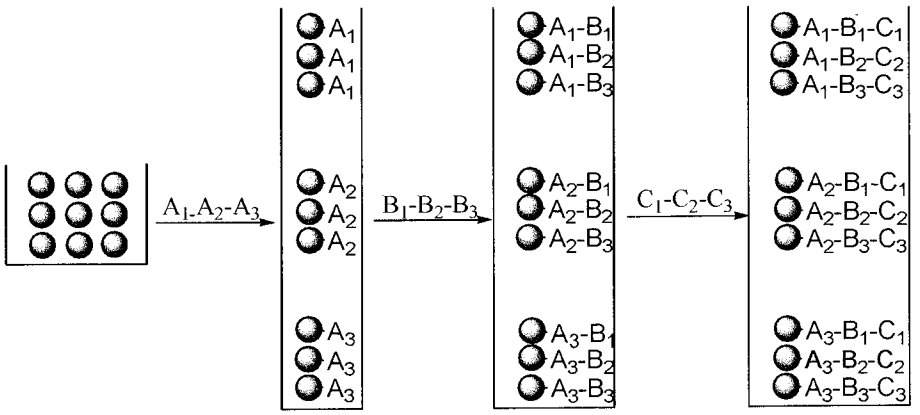

Figure 7: Mixture Synthesis[20]

In 1988, Parmley and Smith introduced a biological method of preparation of peptide libraries. As with Furka's method, this too was based on combinatorial principles. Billions of peptide sequences were prepared and then attached to the outer end of the coat proteins of a phage. The drawback was that increasing the peptide to protein size allowed for the disruption of the function of the outer coat proteins.[23]

Today, the preferred drug candidates are small organic molecules with emphasis on libraries of diverse individual compounds. Conditions that were once developed for solution reactions are being adapted and optimized for solid phase methods, which offer many advantages and are best suited for parallel synthesis. To achieve high yields, reagents are used in excess. Washings easily remove this excess and the product can be cleaved from the resin in a relatively pure form, therefore eliminating the need for extensive chromatography. Another advantage is that supported reagents make safe previously toxic, odorous, or explosive reagents. The supported reagents can be mixed with each other without interactions between them. The main obstacles that need to be overcome include reaction rates that are often slower than their homogeneous analogues,

the support needs to be compatible with the reaction conditions, and the reagents can be expensive to prepare as well as the loading can be low, therefore limiting the scale of the experiment.[24]

Although peptide libraries continue to play an active role in finding new drug targets, there is a trend towards smaller libraries produced on a milligram scale that target compounds with molecular weights not exceeding 500 daltons.[25] Since proteins tend to exert their biological activity through only small regions of their folded surface, their functions could in principle be reproduced in much smaller designer molecules that maintain the crucial surfaces. Many options for modifications, such as introduction of constraints, cyclization, or replacement (partial or full) of the peptidic backbone can be provided by sugar amino acids (SAA).

In particular sugar amino acids are ideal peptidomimetic scaffolds; they may function as structural pharmacophores depending on their substituents, in addition to the amino and carboxyl functions. Sugar amino acids can adopt secondary turns or helical structures, they can substitute a single amino acid, and SAAs can be functionalized with hydrophobic side chains to replace hydrophobic residues.[26] Smith *et al.* have reported the use of a pyranoid SAA scaffold to inhibit mammalian ribonucleotide reductase based on the bound conformation of heptapeptide *N*-AcFTLDADF.[27]

The growing demands for development of new molecule entities for discovering new drugs and materials has organic chemists looking for new concepts. A closer look into biological recognition turned chemists to a class of naturally occuring compounds, the carbohydrates. When compared to amino acids, carbohydrates are attractive scaffolds due to the fact that there are numerous eligible stereogenic centers to manipulate.

Carbohydrates are present in pyranosidic or furanosidic form and this cyclic form is an added advantage due to the conformational rigidity for biological interactions.[28] They provide a defined three-dimensional spatial arrangement of substituents that are highly functionalized, thereby providing the "essential combinatorial density."[29]

In order for carbohydrates to be used as a scaffold, a strategy based on orthogonally stable protecting groups must be employed; there must be selective deprotection at each hydroxyl group. Moreover, the remaining protecting groups must remain stable and unaffected during the substitution reactions. Finally, the anchoring to solid phase reagents must remain stable during all protecting, deprotecting, and side chain manipulations, but be able to detach from the target compound undestroyed.[30]

Hirschmann and colleagues first recognized the unique characteristics of monosaccharides when they described the synthesis of bioactive somatostatin mimics from the natural sugar D-glucose. By knowing that the biological activity is due to the interaction of the β-turn type I fragment *Phe-Trp-Lys-Thr* with the receptor, Hirschmann *et al.* attached appropriate side chains to glycidic scaffolds in the proper spatial arrangement, which in turn inhibits the release of several hormones (Figure 8).[31] Nicolau *et al.* have also reported the use of carbohydrates to mimic non-carbohydrate bioactive compounds. The mimics synthesized were of the *Arg-Gly-Asp* (RGD) sequence. This sequence is responsible for the adhesion of extracellular matrix glycoproteins.[32]

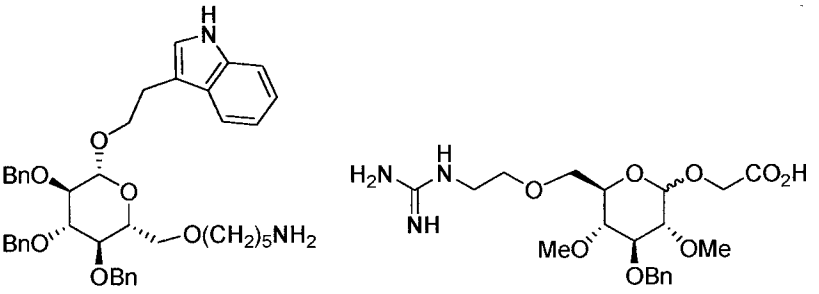

Somatostatin mimic RGD sequence

Figure 8: Somatostatin mimic and RGD sequence mimic

In the preceding examples, the potential glycidic scaffold was only partially exploited since only a couple of the hydroxyl groups were manipulated. Kunz and colleagues developed a synthetic route that modified all five positions of galactopyranose. Starting with an acetylated galactopyranose, they attached a thioglycoside anchor to the anomeric carbon and then removed the remaining *O*-acetyl groups. The remaining free hydroxyl groups were treated with *tert*-butyl diphenylsilyl chloride/imidazole and then 2,2-dimethoxypropane to afford selective protection on O6 with TBDPS and an isopropylidene group at O3 and O4. Upon removal of the isopropylidene group there would be three secondary hydroxyl groups, so in order to distinguish them the hydroxyl group at C2 was acetylated. Selective acidolysis removed the isopropylidene group thus allowing Kunz to be able to manipulate these two groups. Regioselective allylation at the 3-OH and then acid-catalyzed addition of ethyl vinyl ether at the 4-OH provided a workable scaffold with varying protecting groups (Scheme 3). Although no biological activities were given, this approach promises access to new lead

structures.[33] However, the problem of orthogonal protection of numerous hydroxyl groups is still a difficult one to solve.

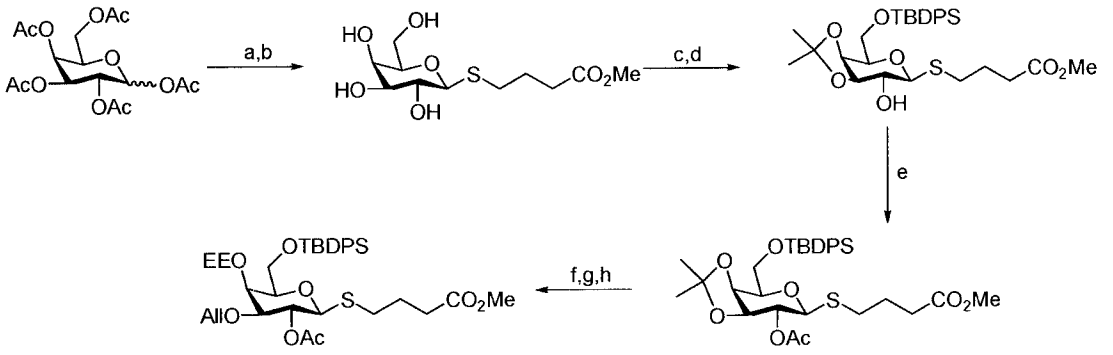

Scheme 3: Preparation of a carbohydrate scaffold: a) HS-$(CH_2)_3CO_2Me/BF_3{\cdot}Et_2O$; b) NaOMe, MeOH; c) *t*-$BuPh_2SiCl$/imidazole; d) 2,2-dimethoxypropane; e) Ac_2O/pyridine; f) ethane-1,2-dithiol; g) Bu_2SnO, AllBr, Bu_4NI; h) ethyl vinyl ether

The primary objective of combinatorial chemistry in modern drug discovery is to obtain large numbers of compounds; the complexity of carbohydrates can be exploited to achieve this. The mimics being synthesized are small in size, maintain solubility under physiological conditions, and are amenable to detailed studies. With further modifications in and on the rings, new syntheses of compounds can be expected and exploited.

Statement of problem:

The primary objective of combinatorial chemistry in modern drug discovery is to obtain large numbers of compounds; the complexity of carbohydrates can be exploited to achieve this. The mimics being synthesized should be small in size, maintain solubility under physiological conditions, and be amenable to detailed studies. With further modifications in and on the carbohydrate rings, new synthesis of compounds can be developed. Using this concept, a new set of mannofuranose derivatives will be developed, that may potentially be tested for biological activity.

Results and Discussion:

1) Precursors to mannofuranosyl azide

As was previously stated in the introduction, working with carbohydrates is often problematic due to the numerous free hydroxyl groups. Therefore, measures must be taken to protect hydroxyl groups from undesired reactions. In this research, the protecting groups of choice are isopropylidene groups because the desired mannose sugar is trapped in the furanose form upon acid-catalyzed acetalation. This type of protection allows for the hydroxyl group at C-1 to remain untouched and the alcohols at C-2 and C-3 as well as C-5 and C-6 to be protected with isopropylidene groups.

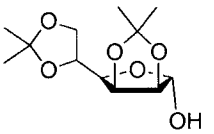

1

Figure 9: 2,3:5,6-Di-*O*-isopropylidene-α-D-mannofuranose (**1**)

2,3:5,6-Di-*O*-isopropylidene-α-D-mannofuranose (**1**) was synthesized by reacting D-mannose (**2**) with acetone and a catalytic amount of sulfuric acid while stirring (Equation 1).[34] TLC was used to monitor the progress of the reaction (1:1 hexane:ethyl acetate). The appearance of a spot less polar then the starting material, which stays at the baseline, indicated reaction within several hours. The reaction was neutralized with sodium carbonate and refluxed for an hour. Upon completion of refluxing and evaporating, a white/yellow solid was produced, which was then purified by recrystallization from methanol.

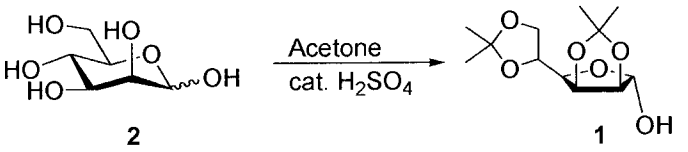

Equation 1: Formation of 2,3:5,6-di-*O*-isopropylidene-α-D-mannofuranose

Proton nuclear magnetic resonance spectra (^{1}H NMR) were taken of the protected sugar to prove it was produced. The appearance of four signals at 1.32, 1.37, 1.45, and 1.46 ppm are indicative of the methyl protons of the isopropylidene groups; moving downfield a doublet at 2.56 ppm is the proton from the hydroxyl group at C-1. Next on the spectrum at 4.06 ppm is a multiplet for the two hydrogens found at C-6. At 4.18 ppm, a doublet of doublets signifies the proton at C-4 while at 4.40 ppm a doublet of doublets of doublets exists for H-5. This pattern is exhibited because of coupling with the geminal protons at C-6 and the C-4 proton. A doublet at 4.61 ppm for H-2 is present while a doublet of doublets at 4.81 ppm belongs to the proton at C-3. The furthest signal downfield at 5.38 ppm is a doublet, which is the proton at C-1. This shift is due to the proton being attached to the anomeric carbon, which is attached to two electronegative oxygen atoms.

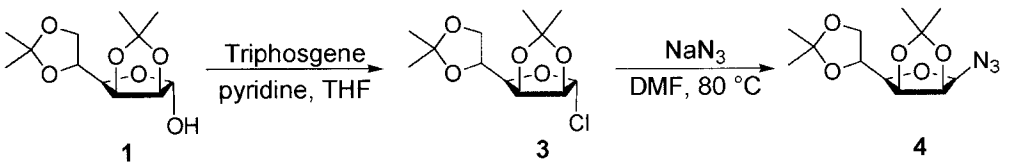

Scheme 4: Synthesis of azidodeoxy sugar **4**

The synthesis of 2,3:5,6-di-*O*-isopropylidene-α-D-mannofuranosyl chloride (**3**, Scheme 4)[35] began by dissolving the starting sugar **1** in anhydrous tetrahydrofuran

(THF), and then adding triphosgene to the solution. Next, pyridine was added dropwise to the reaction flask while being stirred. A whitish yellow precipitate immediately formed upon the addition of the pyridine. The reaction was monitored by TLC (3:1 hexane: ethyl acetate), which showed the consumption of the starting material and formation of a new spot. Upon filtration of the salt that formed the solution was evaporated to give a yellow syrup. A ^{1}H NMR spectrum was obtained of the chlorinated sugar **3** that showed a shift of the peak for H-1 from 5.38 ppm to 6.05 ppm due to the electronegativity of the chlorine. The singlet that appears at 6.05 ppm shows that the product is the α-anomer and H-1 and H-2 have a dihedral angle of 90°.

Due to the chloride being a good leaving group, reaction with sodium azide gave the azide **4** *via* S_N2 (Scheme 4). 2,3:5,6-Di-*O*-isopropylidene-α-D-mannofuranosyl chloride was dissolved in *N*,*N*-dimethylformamide (DMF), sodium azide was added, and the reaction was heated to 80 °C. The reaction was monitored by TLC (3:1 hexane:ethyl acetate), which showed the consumption of the starting material **3**. Proton and carbon NMR were obtained for the product.

The ^{13}C spectrum shows four signals at 25.5, 26.3, 26.4, and 28.1 ppm for the methyl groups on the isopropylidene protecting groups, and peaks at 67.8, 73.9, 79.6, 80.5, 82.1, and 90.1 ppm correlate to the carbons C-1 through C-6 on the sugar and at 90.1 ppm for the anomeric carbon. The remaining two peaks, 110.3 and 114.6 ppm, correspond to the quaternary carbons of the protecting groups. ^{1}H NMR indicates a shift for the anomeric proton from 6.05 ppm to a doublet at 4.45 ppm with a coupling constant of 3.66 Hz due to coupling with H-2.

2) Selective deprotection and manipulation of glycosyl azide 4

When working with a carbohydrate scaffold, employing a protection scheme that can be selectively manipulated is of the utmost importance. Fleet and co-workers had to use selective deprotection when assembling spirodiketopiperazines on mannofuranose. Their chemistry caused no anomeric equilibration nor any isomerisation to mannopyranose isomers. Under acidic conditions, anomers with the nitrogen function *cis* to the 2,3-diol are more stable than those that are *trans*.[36] Using their conditions, 1-azido-1-deoxy-2,3:5,6-di-*O*-isopropylidene-β-D-mannofuranose was selectively deprotected at C-5 and C-6 using aqueous acetic acid.

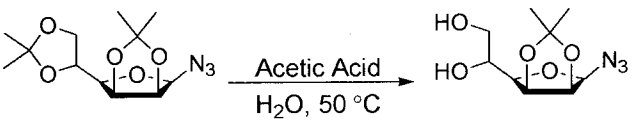

4 **5**

Equation 2: Selective deprotection of mannofuranosyl azide **4**

The synthesis of 1-azido-1-deoxy-2,3-*O*-isopropylidene-β-D-mannofuranose (**5**) from compound **4** was a relatively simple task (Equation 2). The azido sugar was dissolved in a 1:1 mixture of glacial acetic acid and water and the reaction was heated to 50 °C and monitored by TLC (ethyl acetate). TLC of the reaction showed a spot with a much lower R_f than the starting material. The solvents were evaporated, and the residue was evaporated with toluene twice, which lead to a yellow syrup.

The ^{1}H NMR spectrum of **5** showed only two peaks at 1.37 and 1.56 ppm, which indicates the removal of the isopropylidene group from C-5 and C-6. Moving further downfield at 3.75 and 3.90 ppm are a set of doublet of doublets corresponding to the two protons at C-6, which is a shift from a 4.11 ppm multiplet in the starting compound **4**.

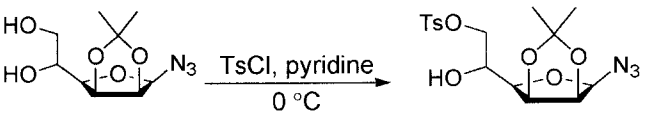

5 **6**

Equation 3: Selective tosylation of 1-azido-1-deoxy-2,3-*O*-isopropylidene-β-D-mannofuranose

At this point, 1-azido-1-deoxy-2,3-*O*-isopropylidene-β-D-mannofuranose has two free hydroxyl groups for manipulation. The reactivities of the primary and secondary alcohols are different, therefore this fact was used to selectively add a leaving group to the primary alcohol. Selective tosylation of the primary hydroxyl group began by first dissolving the deprotected azido sugar in pyridine and lowering the temperature to 0 °C. Next, *p*-toluenesulfonyl chloride was added to the mixture, which was then allowed to stir until TLC showed consumption of the starting material (Equation 3). Once no more change was occurring, water was added and stirred for ten minutes. The sugar was extracted with methylene chloride, evaporated, and purified by flash column chromatography. The product **6** was isolated in a low yield of around 30%. Multiple attempts with varying reagents and reaction conditions were carried out in hopes of increasing the yield, however the above procedure seemed to work best.

After purification, proton NMR showed a singlet peak at 2.44 ppm for the methyl group on the tosylate. Moving downfield a doublet at 2.64 ppm correlates to the free hydroxyl group at C-5. The only major shift within the sugar region was the pair of protons at C-6, which moved from 3.75 and 3.90 ppm to 4.2 ppm (a multiplet) due to the electronegativity of the sulfonyl group. Continuing downfield are two sets of doublets, at 7.36 and 7.82 ppm, which signify the *para*-substituted aromatic ring of the tosylate. The

^{13}C spectrum had four signals at 129.1, 131.0, 133.4, and 146.1 ppm, which belong to the phenyl group. Further examination showed two peaks at 25.7 and 26.4 ppm for the methyl carbons of the protecting group; also at 23.0 ppm is a signal for the benzylic methyl group.

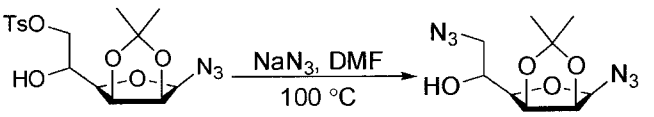

6 7

Equation 4: Formation of 1,6-diazido-1,6-di-deoxy-2,3-*O*-isopropylidene-β-D-mannofuranose (**7**)

Because the tosylate is a good leaving group, reaction with sodium azide in DMF gave the diazide sugar **7** *via* S_N2 reaction (Equation 4). TLC showed a spot that burned at a higher R_f value compared to the starting material. The product was extracted to afford **7** in 89% yield. The ^1H NMR spectrum showed the change of the C-6 signals compared to the starting material at 4.2 ppm, which now shows a multiplet at 3.64 ppm. This is due to the removal of the leaving group and replacement with N_3, which shields the C-6 protons and moves the signal upfield. The remaining spectrum peaks are similar to the starting material spectrum. Due to the shielding effects, the ^{13}C NMR spectrum provided evidence of the attachment of the azide at C-6 with a signal at 55.2 ppm for C-6, a change from 72.7 ppm in the starting material.

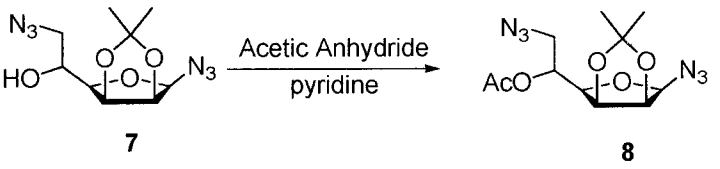

7 8

Equation 5: Protection of free hydroxyl in **7**

To ensure no side reactions occurred, compound **7** was acetylated with acetic anhydride in pyridine (Equation 5). The reaction was left stirring and monitored by TLC. Upon completion a ^{1}H NMR was taken, in which at 2.11 ppm appeared a signal corresponding to the methyl group of the acetyl group. Moving further downfield, the two protons at C-6 are now marked by two sets of doublets of doublets at 3.78 and 3.87 ppm. The proton at C-5 is deshielded, due to the addition of the acetate protecting group, therefore moving the multiplet from 4.19 ppm in the starting material to 5.29 ppm in the spectrum of **8**.

3) 1,3-Dipolar cycloadditions of mannosyl azide 4.

Azides and alkynes are extremely energetic, but the azide is also the one of the least reactive functional groups in organic chemistry. This stability allows for them to be inert towards biological molecules as well as reactions within biological systems, such as dimerization or hydrolysis. The Huisgen 1,3-dipolar cycloaddition mechanism allows for the glycosyl N atom to attack the alkyne carbon and this prompts the π electrons to attack the terminal N atom to afford an aromatic 1,2,3-triazole compound, in a concerted process (Scheme 5).[37] The downfall of this process is the possibility of regioisomers (1,4 and 1,5) being formed when unsymmetrical alkynes are employed.

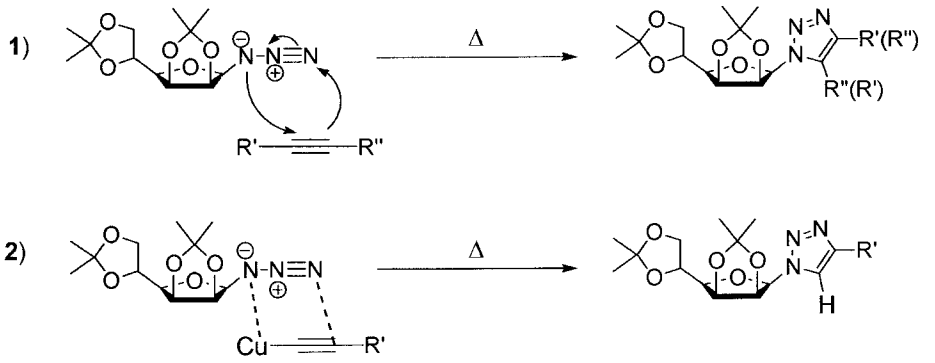

Scheme 5: 1) Huisgen 1,3-dipolar cycloaddition mechanism; 2) Copper-(I)-catalyzed Huisgen 1,3-dipolar cycloaddition

Almost simultaneously, several groups reported successful regiospecific 1,4-substituted [1,2,3]-triazole synthesis from terminal alkynes using a copper(I) catalyst (Scheme 5).[13,37,38] The copper(I)-catalyzed triazole formation has proven to be a very powerful reaction due to the production of one isomer and the bio-compatibility of the reagents. Hence, synthesis of mannosyl triazole heterocycles was investigated by using the Huisgen 1,3-dipolar cycloaddition as well its modified copper(I)-catalyzed version.

1-Azido-1-deoxy-2,3:5,6-di-*O*-isopropylidene-β-D-mannofuranose (**4**) reacted with six different alkynes (Table 1) to afford a variety of compounds using the unmodified Huisgen 1,3-dipolar cycloaddition. By using the parallel synthetic method, these compounds were prepared in series and purified on silica columns. The reaction with diethylacetylene dicarboxylate provided the highest yield, however no reaction was observed with diphenyl acetylene. This particular reaction is believed to have been blocked by the large substituents on the alkyne. Reaction times were varied with this alkyne but no change from the starting material on the TLC plate was observed.

Starting material	Alkyne	Product	% Yield	Ratio of Isomers**
4	Diethylacetylene dicarboxylate	**9**	90	N/A
	Ethyl propiolate	**10a/b**	70	9:1
	Propiolic acid	**11a/b**	70	5:1
	Trimethylsilyl propiolate	**12a/b**	Crude	-
	Phenyl Acetylene	**13a/b**	Crude	-
	Diphenyl Acetylene	N/R	-	-
7	Diethylacetylene dicarboxylate	**14**	89	N/A

*In general: isomer **a** = 1,4-product: isomer **b** = 1,5-product **ratio determined by proton NMR

Table 1: Mannosyl azide (**4**) cycloadditions (uncatalyzed)

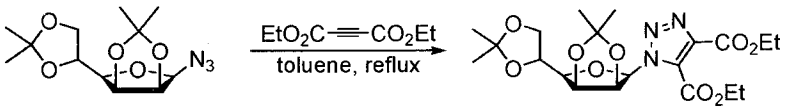

4 **9**

Equation 6: 1-(2,3:5,6-Di-*O*-isopropylidene-β-D-mannofuranosyl)-1*H*-[1,2,3]triazol-4,5-dicarboxylic acid diethyl ester (**9**)

Reaction of glycosyl azide **4** with diethylacetylene dicarboxylate afforded a single isomer **9** as expected (Equation 6). TLC results showed a UV-active spot that burned at a lower R_f than the starting material. After column purification, the white residue was recrystallized with ethyl acetate to afford a clear crystal. Investigation of the ^1H NMR spectrum showed the disappearance of the anomeric proton doublet at 4.45 ppm and the appearance of a new signal at 6.29 ppm, an indication that the triazole had been formed. New signals were observed at 1.39 ppm and 4.41 ppm corresponding to methyl and methylene protons, respectively of the two ethyl esters. The ^{13}C NMR spectrum also showed the signals at 15.1 and 15.4 ppm belonging to the methyl carbons on the ethyl esters and at 131.9 ppm and 140.1 ppm that correspond to the triazole carbons. The crystal was of sufficient quality for diffraction, and this proved the configuration of the product to be β (Figure 10). Also, this proves that compound **3** (mannosyl chloride) was indeed α since the glycosyl azide **4** is achieved *via* S_N2.

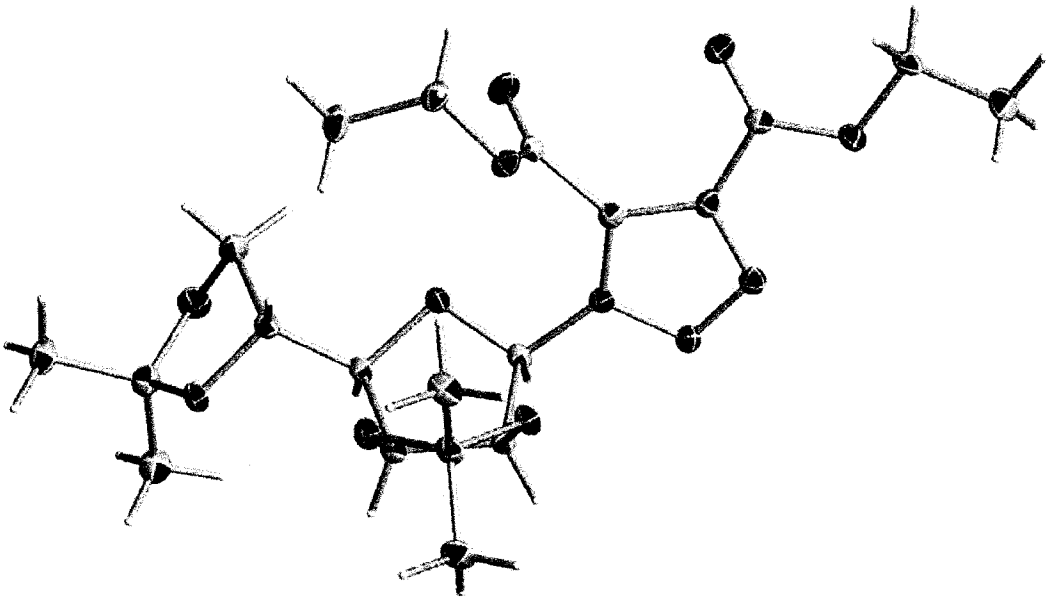

Figure 10: X-ray structure for 1-(2,3:5,6-di-*O*-isopropylidene-β-D-mannofuranosyl)-1*H*-[1,2,3]triazol-4,5-dicarboxylic acid diethyl ester (**9**)

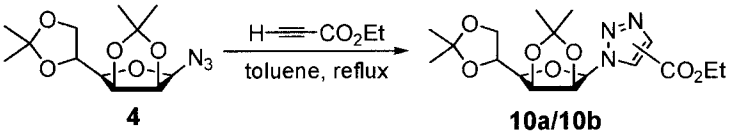

4 **10a/10b**

Equation 7: 1-(2,3:5,6-Di-*O*-isopropylidene-β-D-mannofuranosyl)-1*H*-[1,2,3]triazol-4-(and 5-)-carboxylic acid ethyl esters (**10a/10b**)

Following the protocol previously mentioned mannosyl azide **4** was reacted with ethyl propiolate (Equation 7) to afford triazole isomers (**10a/10b**). Examination of the TLC plate showed a UV active spot that burned lower than the starting material. The ^{1}H NMR spectrum showed the presence of the methyl and methylene protons of the $CO_2CH_2CH_3$ groups at 1.36 ppm and 4.48 ppm respectively. Moving downfield the protons on the triazole ring of the isomers are observed at 8.12 ppm and 8.32 ppm. The remaining protons are at similar positions to the starting material.

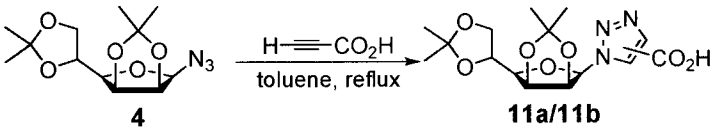

Equation 8: 1-(2,3:5,6-Di-*O*-isopropylidene-β-D-mannofuranosyl)-1*H*-[1,2,3]triazol-4-(and 5-)-carboxylic acids (**11a/11b**)

The formation of compounds **11a/11b** involves the concerted reaction of glycosyl azide **4** with propiolic acid (Equation 8). Again the reaction was monitored by TLC, which indicated the formation of the triazole with a UV-active spot that burned at a lower R_f value. Investigation of the proton NMR spectrum showed the appearance of two singlets at 7.77 ppm and 8.25 ppm that correspond to the heterocycle ring. The carboxylic acid proton was not present on the spectrum. The anomeric proton appeared as a doublet at 6.05 ppm, a change from 4.45 ppm in the starting material.

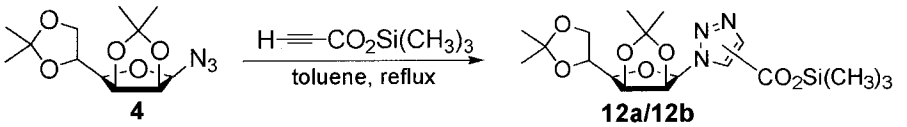

Equation 9: 1-(2,3:5,6-Di-*O*-isopropylidene-β-D-mannofuranosyl)-1*H*-[1,2,3]triazol-4-(and 5-)-carboxylic acid trimethylsilyl esters (**12a/12b**)

Similar reaction of **4** with trimethylsilyl propiolate (Equation 9) gave a mixture of isomers (**12a/12b**). TLC revealed a UV-active spot that also burned at a lower R_f than the starting material. Purification of this product was hampered by the fact that it decomposed on the silica column before separation could take place. The crude ^{1}H NMR had the appearance of two singlets at 8.32 ppm and 7.90 ppm indicating the formation of isomeric triazoles. Also, appearing in the spectrum are two signals at 7.74 and 8.40 ppm which are believed to correspond to isomeric triazoles from which the silyl group has been lost.

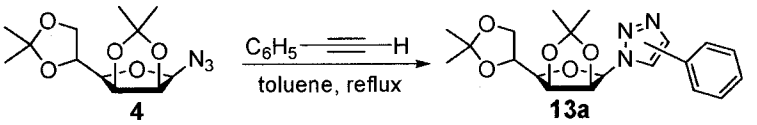

Equation 10: 1-(2,3:5,6-Di-*O*-isopropylidene-β-D-mannofuranosyl)-4-(and 5-)-phenyl-1*H*-[1,2,3]triazole (**13a/13b**)

Following the same procedure as described previously, phenyl acetylene was reacted with compound **4** (Equation 10). Monitoring by TLC, the reaction proceeded very slowly, with the appearance of a new spot at lower R_f, however the starting material was not consumed entirely after twenty-four hours. Formation of the triazole ring was apparent by proton NMR with peaks at 7.65 ppm and 8.06 ppm, which indicates that isomers are present.

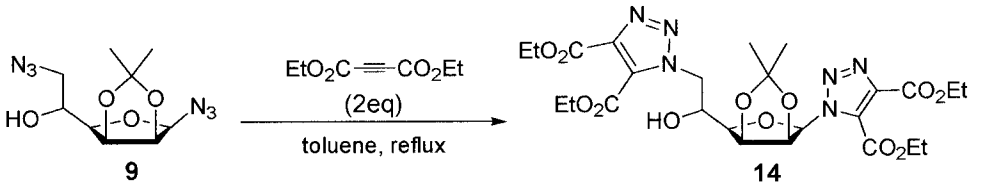

Equation 11: Bis(triazole) **14**

At this point compound **9** was revisited as a starting azide donor in heterocycle synthesis (Equation 11). The procedure previously described was used except for the use of 2 equivalents of DEAD. Inspection of the TLC plate showed a new spot with a lower R_f than the starting material. Examination of the ^{1}H NMR showed that most of the sugar protons moved downfield; the biggest shift was the anomeric proton from 4.48 ppm in the starting compound to 6.42 ppm. Also shown in the spectrum is a multiplet for the methylene protons at 4.41 ppm that overlaps the geminal protons at C-6, and at 1.38 ppm is a set of overlapping triplets for the methyl protons of the esters. Analysis of the ^{13}C NMR spectrum showed the carbonyl carbons at 159.5 ppm, 159.8 ppm, and a double

intensity peak at 160.9 ppm, as well as the triazole carbons at 131.8 ppm, 133.5 ppm, and 140.3 ppm and 140.3 ppm. Proceeding upfield peaks are found at 62.9 ppm, 63.0 ppm, 64.1 ppm, and 64.2 ppm, as well as 15.1 ppm and 15.4 ppm, which correspond to the methylene and methyl carbons, respectively. Mass spectral data shows an M+ at 611.3 that corresponds to the calculated molecular weight of 610.6 with the addition of a proton.

All the results of cycloadditions reported previously gave a mixture of isomers for an unsymmetrical alkyne, however as stated the aid of a copper(I) catalyst with terminal alkynes affords only one isomer.[13,38] 1-Azido-1-deoxy-2,3:5,6-di-*O*-isopropylidene-β-D-mannofuranose (**4**) was reacted with five different terminal alkynes (Table 2) to afford a variety of compounds using the modified Huisgen 1,3-dipolar cycloaddition. The parallel synthesis approach was again used to prepare these compounds and purification was carried out on a silica column. The yield for phenyl acetylene was increased from a low yield of ~30% to 67% yield. However, reaction with trimethylsilyl propiolate afforded a mixture of two compounds, which could not be purified due to decomposition on the silica column. Conditions were varied and reaction times monitored in order to achieve optimal yields.

Starting Material	Alkyne	Product	% Yield
4	Ethyl propiolate	**10a**	81
	Propiolic acid	**11a**	50
	Trimethylsilyl propiolate	**12a**	-
	Phenyl Acetylene	**13a**	67
	Propargyl Alcohol	**15**	57

Table 2: Mannosyl azide **4** cycloadditions with copper catalyst

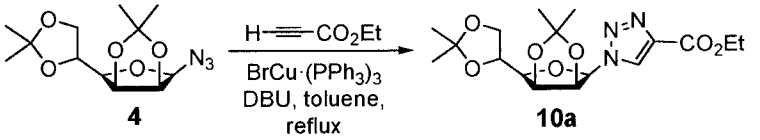

Equation 12: 1-(2,3:5,6-Di-*O*-isopropylidene-β-D-mannofuranosyl)-1*H*-[1,2,3]triazol-4-carboxylic acid ethyl ester (**10a**)

Mannosyl azide **4**, ethyl propiolate, and 1,8-diazabicyclo[5.4.0]undec-7-ene (DBU) were dissolved in toluene. The mixture was allowed to dissolve entirely before the copper catalyst[38b] was added (Equation 12). Once all reactants were added, the reaction was allowed to reflux gently until TLC showed the disappearance of the starting material. Examination of the TLC plate once again showed a UV-active spot that burned with a lower R_f than the starting material. Investigation of ^{1}H NMR spectrum revealed only one isomer had formed with a peak at 8.35 ppm indicating the triazole was present. The anomeric proton appears at 6.15 ppm as a doublet, a change from 4.45 ppm in the starting material. Looking further upfield at 4.45 ppm an overlapping quartet is found corresponding to the ethyl group of the ester. A triplet for the $OCH_2\underline{CH_3}$ overlaps a methyl isopropylidene singlet at 1.45 ppm. The ^{13}C NMR spectrum showed the appearance of a signal at 161.5 ppm, which corresponds to the carbonyl carbon of the carboxylic acid ester. The two triazole carbons were found at 129.3 and 140.8 ppm.

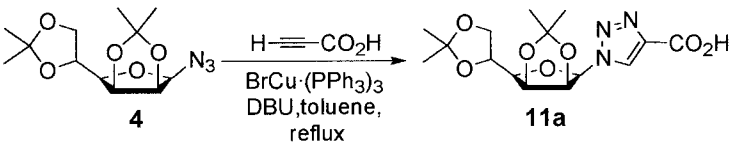

Equation 13: 1-(2,3:5,6-Di-*O*-isopropylidene-β-D-mannofuranosyl)-1*H*-[1,2,3]triazol-4-carboxylic acid (**11a**)

Similar reaction of **4** with propiolic acid again gave one isomer (Equation 13). TLC showed total consumption of the starting material and a UV-active spot that burned. The triazole proton could be seen at 8.35 ppm on the ^{1}H NMR spectrum, however the carboxylic acid proton was not present on the spectrum.

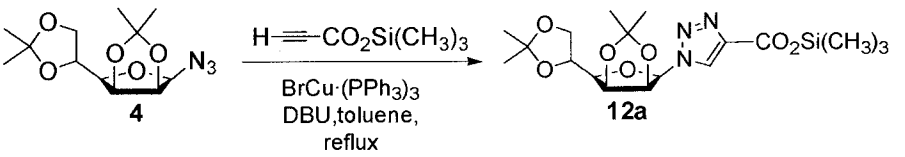

Equation 14: 1-(2,3:5,6-Di-*O*-isopropylidene-β-D-mannofuranosyl)-1*H*-[1,2,3]triazol-4-carboxylic acid trimethylsilyl ester (**12a**)

The cycloaddition to give compound **12a** involves the concerted reaction of glycosyl azide **4** with trimethylsilyl propiolate (Equation 14). The reaction was monitored by TLC, which showed the formation of a new UV-active spot that burned. The ^{1}H NMR of the product was inconclusive although a signal at 8.35 ppm suggest that the triazole had formed.

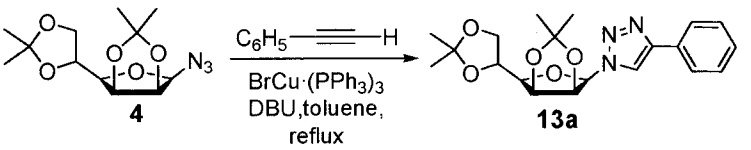

Equation 15: 1-(2,3:5,6-Di-*O*-isopropylidene-β-D-mannofuranosyl)-4-phenyl-1*H*-[1,2,3]triazole (**13a**)

The uncatalyzed reaction with phenyl acetylene and compound **4** was an extremely slow reaction with a poor yield, however when phenyl acetylene was reacted in the presence of the catalyst, the yield and reaction time improved tremendously. Compound **13a** was isolated as a single isomer in 67% yield. Proton NMR clearly shows

the triazole proton at 8.07 ppm. Moving slightly upfield are three peaks corresponding to the phenyl group at 7.35 ppm, 7.44 ppm, and 7.84 ppm. The protecting groups on the mannofuranose ring are found at 1.36 ppm, 1.40 ppm, 1.47 ppm, and 1.60 ppm. The carbon NMR spectrum showed the appearance of two signals, at 129.2 and 148.2 ppm provided further evidence the triazole had formed the four different phenyl carbons are found from 121.4 to 131.5 ppm.

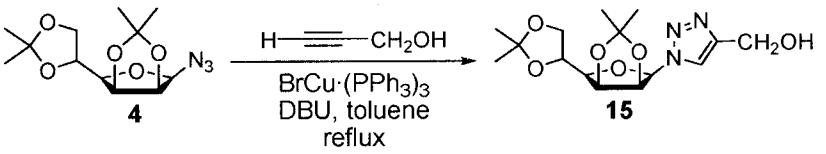

4 15

Equation 16: 1-(2,3:5,6-Di-*O*-isopropylidene-β-D-mannofuranosyl)-1*H*-[1,2,3]triazol-4-yl methanol (**15**)

Using the same protocol as above, propargyl alcohol was reacted with compound **4** (Equation 16). As expected TLC showed a new lower spot that was UV-active and burned. Analysis of ^{1}H NMR revealed the formation of only one isomer. At 2.45 ppm a broad peak appears to represent the alcohol proton. Moving downfield at 4.85 ppm a doublet signifies the $C\underline{H}_2OH$ group and a singlet at 7.89 ppm corresponds to the triazole proton. Investigation of the ^{13}C NMR spectrum confirmed the formation of the triazole with two signals at 123.7 and 148.5 ppm for the triazole carbons. Also, there was a peak at 57.2 ppm for the carbon of the primary alcohol ($\underline{C}H_2OH$).

4) Additional deprotection and manipulation of triazole 9

As previously stated, working with a carbohydrate scaffold requires a protection scheme that can be manipulated selectively throughout the scaffold construction. Using

this philosophy, 1-(2,3:5,6-di-*O*-isopropylidene-β-D-mannofuranosyl)-1*H*-[1,2,3]triazol-4,5-dicarboxylic acid diethyl ester (**9**) was deprotected, manipulated, as well as reprotected when necessary.

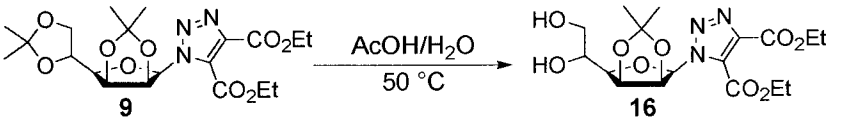

9 **16**

Equation 17: 1-(2,3-*O*-Isopropylidene-β-D-mannofuranosyl)-1*H*-[1,2,3]triazol-4,5-dicarboxylic acid diethyl ester (**16**)

The synthesis of 1-(2,3-*O*-isopropylidene-β-D-mannofuranosyl)-1*H*-[1,2,3]triazol-4,5-dicarboxylic acid diethyl ester (**16**) from compound **9** was achieved by reaction with glacial acetic acid and water in a 1:1 ratio and heating it to 50 °C (Equation 17). The TLC plate revealed a spot that burned with a lower R_f. Examination of the ^1H NMR spectrum shows the disappearance of two peaks at 1.39 ppm and 1.47 ppm, which signifies the removal of the isopropylidene group at C-5 and C-6. Integration of the two signals present at 1.20 ppm and 1.26 ppm are for 6H's each, corresponding to the two methyl groups of the isopropylidene group and the methyl group on the esters, respectively. Moving downfield an alcohol peak is found at 3.35 ppm. The anomeric proton remains at approximately the same chemical shift as in the starting material.

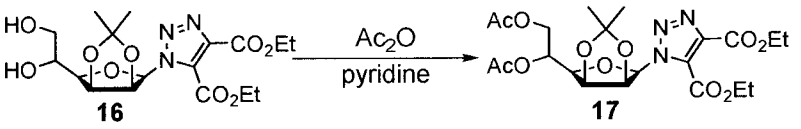

Equation 18: 1-(2,3-*O*-Isopropylidene-5,6-di-*O*-acetyl-β-D-mannofuranosyl)-1*H*-[1,2,3]triazol-4,5-dicarboxylic acid diethyl ester (**17**)

To further ensure that compound **16** was produced, it was reacted with acetic anhydride and pyridine to produce diacetate **17** (Equation 18). Consumption of the starting material was seen by examination of the TLC plate; a new spot had formed with a higher R_f. Analysis of the proton NMR spectrum showed the appearance of two new singlets at 2.06 ppm and 2.07 ppm, which relate to the methyl on each acetyl protecting group. Moving further downfield the geminal protons for C-6 appear at 4.28 overlapping each other. At 4.41 ppm a multiplet for five hydrogens appears corresponding to the overlapping of the C-5 proton and the methylene groups of the esters. The C-4 proton appears as a doublet of doublets at 4.69 ppm, a shift from 3.85 ppm in the starting material.

Now that it was known that selective deprotection could take place, full deprotection was investigated. The main issue was to ensure that the heterocycle remained intact during this process. It was determined that using a strong acid, even diluted 50% H_2SO_4, would sever the triazole ring immediately. After various condition changes, it was found that even the slow addition of 5% HCl would only partially remove the isopropylidene groups (Equation 19).

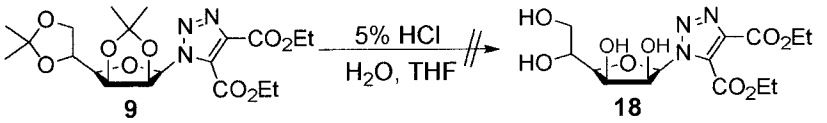

Equation 19: Attempted formation of 1-β-D-mannofuranosyl-1*H*-[1,2,3]triazol-4,5-dicarboxylic acid diethyl ester (**18**)

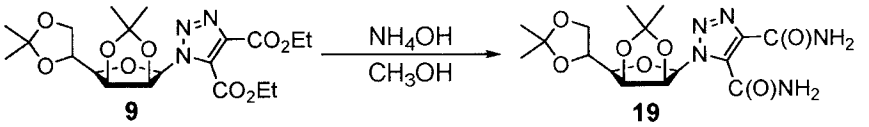

Equation 20: 1-(2,3:5,6- Di-*O*-isopropylidene-β-D-mannofuranosyl)-1*H*-[1,2,3]triazol-4,5-dicarboxylic acid diamide (**19**)

The manipulation of the carboxylic ethyl esters seemed a logical step in hopes of being able to eventually complex a metal with the sugar. In order for this to happen the glycosyl triazole **9** must have the esters replaced with amides. The synthesis of compound **19** from glycosyl triazole **9** was achieved by bubbling ammonia gas through the reaction (Equation 20). Inspection of the ^{1}H NMR spectrum showed the disappearance of the methyl groups at 1.39 ppm as well as the ethyl signals at 4.41 ppm. Moving downfield at 6.87 ppm the anomeric proton is found to have shifted from 6.25 ppm in the starting material **9**. The ^{13}C spectrum showed the appearance of two signals at 159.9 ppm and 164.9 ppm, which are the carbonyl carbons. Moving upfield at 132.0 ppm and 139.4 ppm, two peaks for the carbons of the triazole are found. The mass of compound **19** was calculated as 397.16 and found to be 398.2 (+H).

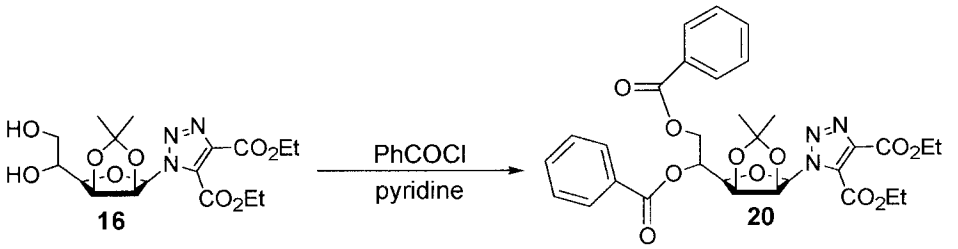

Equation 21: Benzoylation of **16**

With the procedure for selectively removing the protecting group at C-5 and C-6 worked out, the next scheme was to manipulate the alcohols into esters. Triazole **16** was dissolved in pyridine, and two equivalents benzoyl chloride were added (Equation 21), which lead to a mixture of two products. Isolated by flash column chromotagraphy (1:1 hexane: ethyl acetate), clean proton NMR spectra were obtained. Furthest downfield three signals appeared at 7.38 ppm, 7.51 ppm, and 8.01 ppm, which correspond to the benzoyl groups. Moving upfield the proton at C-4 shifted from 3.85 ppm to 4.19 ppm due to the addition of the esters at C-5 and C-6. The remaining peaks were similar to the starting material. In the ^{13}C spectrum, signals appear at 159.7 ppm, 160.9 ppm, 161.0 ppm and 167.9 ppm, which belong to carbonyl carbons. The benzene ring carbons appear from 129.4 ppm to 140.0 ppm. This product was identified as bis(ester) **20**.

5) Precursors to triazole oligosaccharide synthesis

In the aforementioned heterocyclic compounds, the terminal alkynes used were purchased from Aldrich and Acros. In order to expand the triazole synthesis into disaccharides and trisaccharides, unsymmetrical sugar alkyne precursors needed to be made. In order for this to occur, each sugar chosen had to employ a protecting scheme

that is complimentary to the reaction conditions. The following explores the synthesis of four different sugar alkynes.

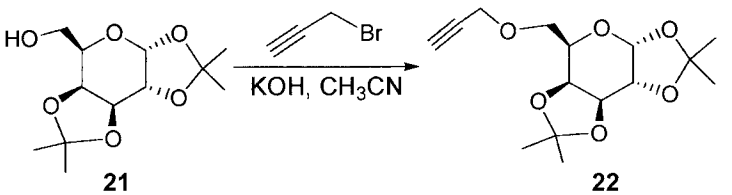

21 22

Equation 22: 1,2:3,4-Di-*O*-isopropylidene-6-((prop-2-ynyloxy)methyl)-D-galactopyranose (**22**)

Diacetone D-galactopyranose was dissolved in acetonitrile and potassium hydroxide was added. Once dissolved, propargyl bromide was added to the reaction flask (Equation 22). TLC was used to monitor the reaction, until total consumption of the starting material was observed. The mixture was then evaporated and redissolved in water and methylene chloride (1:1). The organic phase was extracted with methylene chloride, and the organic layers combined and dried over magnesium sulfate and evaporated. The final product was purified on a silica gel column to afford 1.17 g (3.9 mmol) of a brown solid. Inspection of the ^{1}H NMR spectrum showed the appearance of a signal at 2.45 ppm, which signifies the alkyne proton. Moving downfield the geminal protons at C-6 are now two sets of doublets of doublets at 3.69 ppm and 3.79 ppm. Analysis of the ^{13}C spectrum showed two signals at 69.8 ppm and 71.6 ppm, which relate to the alkyne carbons. The carbons for the sugar appear from 71.8 ppm to 97.4 ppm. The protecting group methyls appear at 25.7 ppm, 26.2 ppm, 27.2 ppm and 27.3 ppm.

5.90 ppm as a doublet. Analysis of the ^{13}C spectrum shows two signals at 82.6 and 83.9 ppm for the alkyne carbons, at 68.3 ppm is a peak for the CH_2 group linking the alkyne to the sugar, and the anomeric carbon is found at 106.2 ppm.

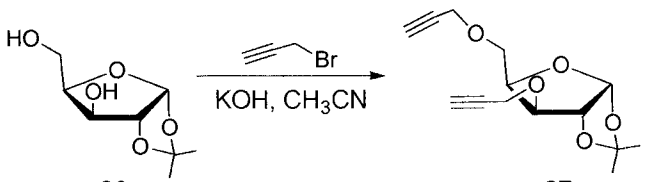

26 **27**

Equation 25: 1,2-*O*-isopropylidene-3,5-di-*O*-(prop-2-ynyloxy)-D-xylofuranose (**27**)

Once again the same procedure was followed by reacting compound **26** with propargyl bromide to afford bis(alkyne) **27** (Equation 25). Inspection of the TLC showed the appearance of a new spot with a higher R_f than the starting material. Compound **27** was produced as a brown solid in 73% yield. Proton NMR was taken to prove that the two alkynes had been attached. Analysis of the spectrum showed the appearance of two signals at 2.47 and 2.50 ppm signifying the two different alkyne protons. At 4.22 ppm a multiplet appears for the two propargyl ethers and the anomeric proton appears at 5.92 ppm. Examination of the ^{13}C spectrum shows four signals from 80.0 to 82.6 ppm for the carbons of the two alkyne groups. Also shown are two peaks for the CH_2 groups next to the alkynes at 58.9 and 59.8 ppm; the two methyl groups from the isopropylidene group are at 27.6 and 28.0 ppm.

6) Disaccharide and trisaccharide heterocycle formation

In the introduction, *N*-glycosides were mentioned with regards to their importance in Nature. It was also stated that interest surrounding 1,2,3-triazole synthesis has exploded due to their high degree of stability in biological systems. Previously, heterocycles produced from unsymmetrical alkynes and mannosyl azide **4** were investigated, now the four sugar alkynes and mannosyl azide are explored in hopes of producing various disaccharide and trisaccharide analogs.

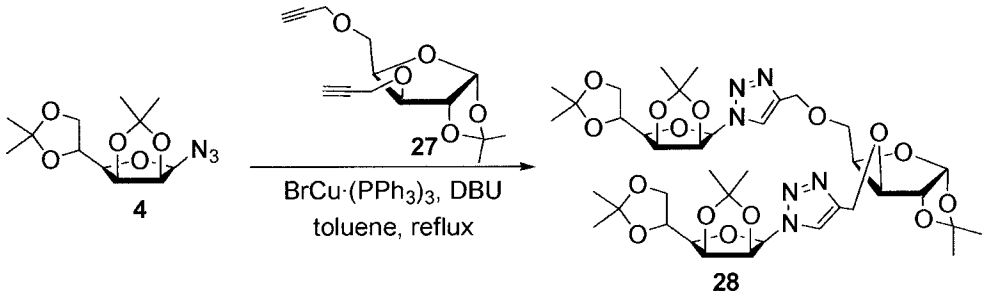

Equation 26: Synthesis of compound **28**

Mannosyl azide **4** was reacted with xylose bis(alkyne) **27** to afford a trisaccharide analog (**28**, Equation 26). The azide and alkyne were dissolved in toluene and DBU was added. Then the catalyst $BrCu\cdot(PPh_3)_3$ was introduced into the reaction mixture, which was then allowed to reflux. TLC was used to monitor the progress of the reaction. Upon complete consumption of the starting material, the solution was evaporated and the product purified by flash chromotagraphy. Examination of the ^1H NMR spectrum showed two signals at 7.87 and 7.89 ppm which relate to the two triazole rings. Moving upfield at 5.89 and 6.08 ppm are a doublet and a double set of doublets for the anomeric proton on xylose and the two mannose sugars, respectively. From 1.30 to 1.63 ppm there are eight peaks, two that integrate to three protons for the methyls of the isopropylidene groups.

Analysis of the carbon NMR spectrum showed four signals at 129.4, 129.5, 133.0, and 133.1 ppm, which correspond to the four triazole carbons. There are also six peaks, four of which have double intensity, from 25.3 to 28.2 ppm belonging to the carbons of the protecting groups. The mass spectrum was obtained and found to be 837.5 (M+1).

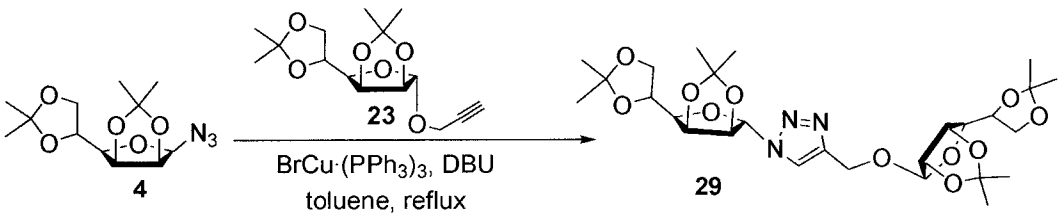

Equation 27: Synthesis of compound **29**

Compound **29** was formed by using the previously described procedure with mannosyl azide **4** and compound **23** (Equation 27). The reaction was monitored by TLC (1:1 hexane: ethyl acetate), which showed a spot with a lower R_f than the starting material. Analysis of the ^1H NMR spectrum showed that the triazole had indeed formed with the appearance of the signal at 7.82 ppm. Continuing upfield at 5.08 and 6.08 ppm a singlet and a doublet can be found relating to the mannosyl *O*-glycoside anomeric proton and mannosyl *N*-glycoside anomeric proton, respectively. At 1.29 to 1.56 ppm, eight signals appear which relate to the isopropylidene protecting groups. Inspection of the ^{13}C spectrum showed two signals at 124.4 and 144.6 ppm, which belong to the triazole carbons. The anomeric carbons for the mannosyl and glycosyl portions are found at 89.8 and 106.6 ppm, respectively. Mass spectrometry found a protonated molecular ion of 584.5 a.m.u.

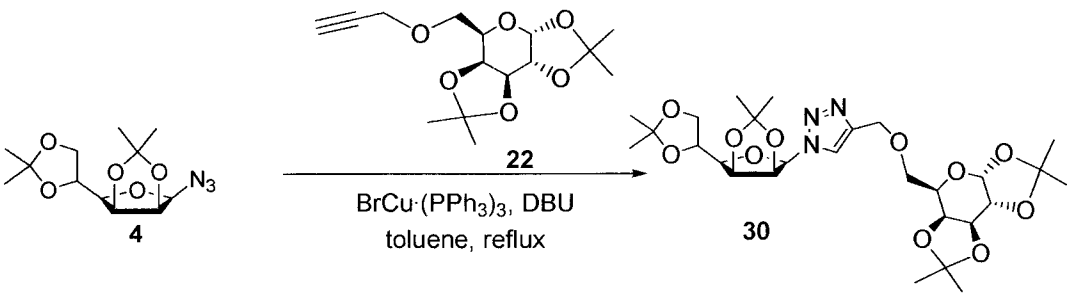

Equation 28: Synthesis of compound **30**

Mixing glycosyl azide **4** and the galactose alkyne **22** as previously described afforded compound **30** a white solid in 73% yield (Equation 28). Analysis of the ^{1}H NMR spectrum showed the appearance of a singlet at 7.87 ppm corresponding to the triazole proton. Two doublets are found at 5.52 and 6.07 ppm for the two anomeric protons of galactose and mannose, respectively, and from 1.31 to 1.55 ppm are seven peaks (integration of one is 6H's), which correspond to the eight methyl groups of the isopropylidene protecting groups. Inspection of the ^{13}C spectrum showed two peaks at 145.6 and 124.5 ppm for the two triazole carbons and the anomeric carbons are found at 97.4 and 109.6 ppm for mannose and galactose, respectively. Mass spectrometry found the mass to be 584.4 a.m.u. (M +1).

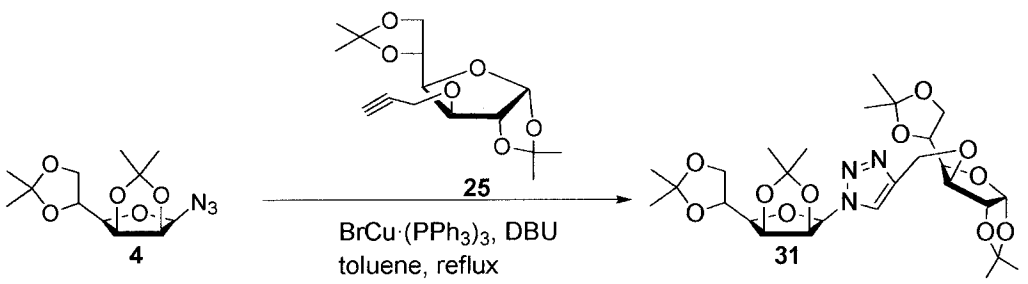

Equation 29: Synthesis of compound **31**

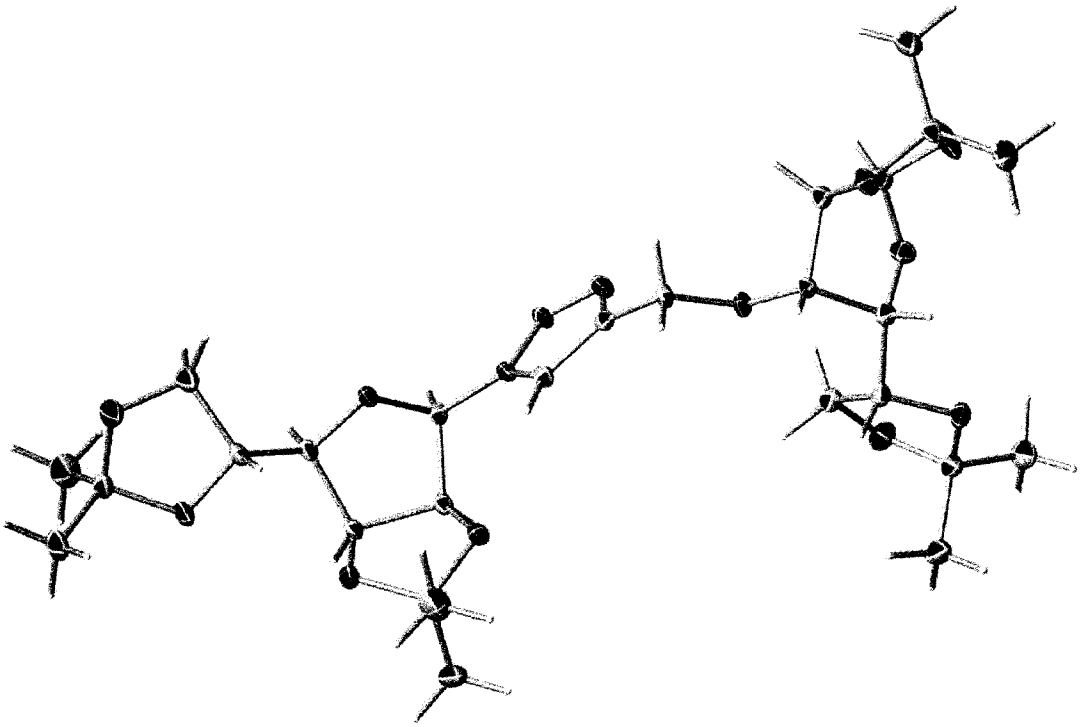

Figure 11: Compound **31** X-ray structure

Compound **31** was produced using the same procedures as described above. Mannosyl azide **4** and glucosyl alkyne **25** were combined with $BrCu{\cdot}(PPh_3)_3$ to attain compound **31**, a clear crystal in 71% yield (Equation 29). Proton NMR revealed a signal at 7.86 ppm for the triazole proton, and two peaks appear at 5.86 and 6.09 ppm, which represent the glucose and mannose anomeric protons, respectively. Eight signals from 1.29 to 1.56 ppm signify the methyl groups of the protecting groups. Examination of the ^{13}C NMR spectrum revealed two peaks at 124.5 and 145.2 ppm for the triazole carbons; the anomeric carbons are found at 89.9 and 106.3 ppm. The mass of **31** was calculated at 583.3 a.m.u. and was found to be 584.4 (M +1). Recrystallization of the product yielded crystals of X-ray quality (Figure 11).

Future Investigations

The formation of mannosyl *N*-glycoside analogs needs to be investigated further. Approaches toward the synthesis of mannosyl triazoles need to be explored in order to increase yields as well as to avoid decomposition of unpurified product. Deprotection of all the isopropylidene groups will prove useful in manipulating mannose as a carbohydrate scaffold as well as end products being potentially tested for biological activity. Once these obstacles are overcome, a wider variety of mannofuranose derivatives may be synthesized.

Experimental:

General Procedures

Reaction progress was monitored by thin layer chromatography (TLC) with UV light detection since most of the reaction materials are UV-active. The TLC plate was treated with a 5% sulfuric acid/ethanol solution to burn the reaction material to provide indication of the carbohydrate product. Isolation of products was achieved by recrystallization and flash chromatography, which was performed with 32-63 μm, 60-Å silica gel. A Bruker Esquire-HP 1100 mass spectrometer was used for low-resolution MS and a Micromass LCT was used for high resolution. A Varian Gemini 2000 NMR system was used for ^{1}H and ^{13}C NMR spectroscopy at 400 MHz and 100 MHz respectively, using $CDCl_3$ or D_6-DMSO as solvents. Proton and carbon chemical shifts (δ) are recorded in parts per million (ppm). Splitting patterns of multiplets are labeled as follows: s (singlet), d (doublet), dd (doublet of doublets), ddd (doublet of doublet of doublets), t (triplet), q (quartet), and m (multiplet) with coupling constants (J) measured in Hz. X-ray diffraction was also used to determine the solid-state crystal structure of two of the compounds produced herein. For both samples, data was collected using a Bruker SMART APEX 4K CCD Single Crystal Diffractometer at 100 K; Mo (K_α) radiation.

Preparation of 2,3:5,6-di-*O*-isopropylidene-α-D-mannofuranose (1) from D-mannose (2).

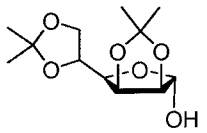

In a flame-dried 2000 mL Erlenmeyer flask equipped with a drying tube and magnetic stir bar, D-mannose (20.0 g, 107.4 mmol) was dissolved in acetone (750 mL) at room temperature. Concentrated H_2SO_4 (14 mL) was added in 2 mL portions every five minutes and the reaction was allowed to stir until TLC (1:1, hexane : ethyl acetate) showed consumption of starting material. The reaction was neutralized with Na_2CO_3 (excess) and filtered. Charcoal and Na_2CO_3 were added to the filtrate and the mixture was refluxed for an hour. The reaction was cooled, filtered, and evaporated. The solid was recrystallized from methanol to afford 18.8 g of **2** (67%, m.p. = 119-121 °C).

^{1}H NMR ($CDCl_3$): δ 1.32 (s, 3H, -CH_3), 1.37 (s, 3H, -CH_3), 1.45 (s, 3H, -CH_3), 1.46 (s, 3H, -CH_3), 2.77 (d, 1H, -OH, J = 2.6 Hz), 4.06 (m, 2H, H-6, H-6'), 4.18 (dd, 1H, H-4, J = 3.7, 7.3 Hz), 4.40 (m, 1H, H-5), 4.61 (d, 1H, H-2, J = 5.9 Hz), 4.81 (dd, 1H, H-3, J = 3.7, 5.9 Hz), 5.38 (d, 1H, H-1, J = 2.2 Hz).

Preparation of 2,3:5,6-di-*O*-isopropylidene-α-D-mannofuranosyl chloride (3) from 2,3:5,6-di-*O*-isopropylidene-α-D-mannofuranose (1).

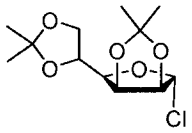

In a 500 mL flame-dried round bottom flask fitted with a septum and magnetic stir bar, 2,3:5,6-di-*O*-isopropylidene-α-D-mannofuranose (**1**) (24.0 g, 92.2 mmol) was dissolved in THF (250 mL). To the reaction triphosgene (10.9 g, 36.9 mmol) was added and the flask placed in an ice bath. Pyridine (4.8 mL) was added dropwise, and the mixture was allowed to stir for 4 hours until the TLC (3:1 hexane: ethyl acetate, product $R_f = 0.58$) showed consumption of the starting material. The mixture was filtered and the precipitate washed with THF. The filtrate was reduced to produce 22.85 g (82.2 mmol) of **3** as a yellow syrup (87%).

^{1}H NMR ($CDCl_3$): δ 1.35 (s, 3H, -CH_3), 1.41 (s, 3H,-CH_3), 1.48 (s, 6H, 2 x -CH_3), 4.00 (dd, 1H, H-6, J = 4.4, 8.8 Hz), 4.08 (dd, 1H, H-6', J = 6.2, 8.8 Hz), 4.19 (dd, 1H, H-4, J = 3.7, 7.9 Hz), 4.42 (ddd, 1H, H-5, J = 4.4, 6.2, 10.6 Hz), 4.87 (dd, 1H, H-3, J = 3.7, 5.9 Hz), 4.93 (d, 1H, H-2, J = 5.9 Hz), 6.08 (s, 1H, H-1).

Preparation of 2,3:5,6-di-*O*-isopropylidene-β-D-mannofuranosyl azide (4) from 2,3:5,6-di-*O*-isopropylidene-α-D-mannofuranosyl chloride (3).

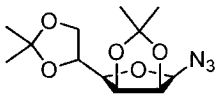

In a 500 mL round bottom two neck flask equipped with a thermometer adapter and magnetic stir bar, 2,3:5,6-di-*O*-isopropylidene-α-D-mannofuranosyl chloride (**3**) (22.85 g, 82.2 mmol) was dissolved in DMF (250 mL). NaN_3 (26.7 g, 410.8 mmol) was added and the mixture was heated to 80 °C until TLC (3:1 hexane : ethyl acetate, product R_f = 0.32) showed total consumption of the starting material. Upon completion, the reaction was diluted with water (100 mL) and then extracted with methylene chloride (3 x 20 mL). The organic phase was washed with water (20 mL). The organic layer was collected and dried over magnesium sulfate. Evaporation of the solvent gave a brown waxy solid identified as **4** (22.5 g, 78.9 mmol) in 96% yield.

^{1}H NMR ($CDCl_3$): δ 1.36 (s, 3H, -CH_3), 1.38 (s, 3H, -CH_3), 1.44 (s, 3H, -CH_3), 1.55 (s, 3H, -CH_3), 3.59 (dd, 1H, H-4, J = 3.7, 7.7 Hz), 4.11 (m, 2H, H-6, H-6'), 4.40 (d, 1H, H-1, J = 3.7 Hz), 4.45 (m, 1H, H-5), 4.67 (dd, 1H, H-2, J = 3.7, 5.9 Hz), 4.77 (dd, 1H, H-3, J = 3.3, 5.9 Hz).

^{13}C NMR ($CDCl_3$): δ 25.6, 26.3, 26.4, 28.2, 67.9, 74.0, 79.6, 80.6, 82.2, 90.1, 110.3, 114.6.

Preparation of 1-azido-1-deoxy-2,3-*O*-isopropylidene-β-D-mannofuranose (5) from 2,3:5,6-di-*O*-isopropylidene-β-D-mannofuranosyl azide (4).

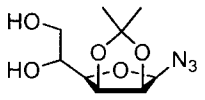

In a 500 mL two neck round bottom flask equipped with a thermometer adapter and magnetic stir bar, 2,3:5,6-di-*O*-isopropylidene-β-D-mannofuranosyl azide (**4**) (6.0 g, 21.0 mmol) was dissolved in 1:1 glacial acetic acid and water (150 mL : 150 mL). The reaction was heated to 50 °C for 3 hours or until TLC (ethyl acetate, product $R_f = 0.34$) showed disappearance of compound **4**. The residue after evaporation *in vacuo* was evaporated with toluene (2 x 100 mL) to afford **5** as a clear syrup in 84% yield.

^{1}H NMR (D_6-DMSO): δ 1.37 (s, 3H, -CH_3), 1.56 (s, 3H, -CH_3), 3.67 (dd, 1H, H-4, J = 4.0, 8.4 Hz), 3.75 (dd, 1H, H-6, J = 5.5, 11.4 Hz), 3.90 (dd, 1H, H-6', J = 3.3, 11.7 Hz), 4.10 (m, 1H, H-5), 4.46 (d, 1H, H-1, J = 3.7 Hz), 4.69 (dd, 1H, H-2, J = 3.7, 6.2 Hz), 4.84 (dd, 1H, H-3, J = 4.0, 6.2 Hz).

Preparation of 1-azido-1-deoxy-2,3-*O*-isopropylidene-6-*p*-toluenesulfonyl-β-D-mannofuranose (6) from 1-azido-1-deoxy-2,3-*O*-isopropylidene-β-D-mannofuranose (5).

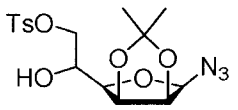

In a 100 mL round bottom flask equipped with a magnetic stir bar and septum 1-azido-1-deoxy-2,3-*O*-isopropylidene-β-D-mannofuranose (**5**) (3.25 g, 13.4 mmol) was dissolved in pyridine (60 mL). *p*-Toluenesulfonyl chloride (3.06 g, 16.0 mmol) was added and the temperature lowered to 0 °C. The mixture was stirred until TLC (ethyl acetate) showed the disappearance of the starting material. Water (12 mL) was mixed with the reaction for ten minutes. The mixture was poured over ice and then extracted with methylene chloride (3 x 10 mL). The combined organic layers were washed with water (10 mL). The organic layer was dried over magnesium sulfate, evaporated, and purified by elution from a column of silica gel (1:1 hexane: ethyl acetate) to afford a white solid in 29% yield.

^{1}H NMR ($CDCl_3$): δ 1.34 (s, 3H, -CH_3), 1.50 (s, 3H, -CH_3), 2.45 (s, 3H, -PhC$\underline{H_3}$), 2.64 (d, 1H, -OH, J = 5.5 Hz), 3.58 (dd, 1H, H-4, J = 4.0, 8.1 Hz), 4.17 (m, 2H, H-6, H-6'), 4.34 (m, 2H, H-1, H-5), 4.66 (dd, 1H, H-2, J = 3.7, 5.9 Hz), 4.81 (dd, 1H, H-3, J = 4.0, 6.2 Hz), 7.35 (d, 2H, Ar-H), 7.81 (d, 2H, Ar-H).

^{13}C NMR ($CDCl_3$): δ 22.9, 25.7, 26.4, 68.7, 72.7, 77.9, 80.6, 82.0, 90.2, 114.8, 129.1(double intensity), 131.0 (double intensity), 133.4, 146.1.

m/z calculated: 399.41 *m/z* found (APCI): 391.3 (M –N_2 + H_2O)

Preparation of 1,6-diazido-1,6-dideoxy-2,3-*O*-isopropylidene-β-D-mannofuranose (7) from 1-azido-1-deoxy-2,3-*O*-isopropylidene-6-*p*-toluenesulfonyl-β-D-mannofuranose (6).

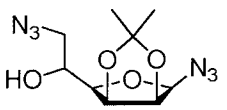

In a 50 mL two neck round bottom flask equipped with a magnetic stir bar and thermometer adapter, 1-azido-1-deoxy-2,3-*O*-isopropylidene-6-*p*-toluenesulfonyl-β-D-mannofuranose (**6**) (0.50 g, 1.3 mmol) was dissolved in DMF (15 mL). NaN_3 (0.41 g, 6.3 mmol) was added and the mixture heated to 100 °C until TLC (2:1 hexane: ethyl acetate) showed no starting material. The reaction was cooled and poured over water (25 mL). The organic product was extracted into methylene chloride (3 x 15 mL) and back extracted with water (10 mL). The organic extract was dried over magnesium sulfate and reduced to afford **7** as a yellow syrup in 89% yield.

^{1}H NMR ($CDCl_3$): δ 1.36 (s, 3H, -CH_3), 1.56 (s, 3H, -CH_3), 2.52 (d, 1H, -OH, J = 5.1 Hz), 3.48 (dd, 1H, H-6, J = 5.9, 12.8 Hz), 3.64 (m, 2H, H-4, H-6'), 4.18 (m, 1H, H-5), 4.48 (d, 1H, H-1, J = 3.7 Hz), 4.70 (dd, 1H, H-2, J = 3.7, 6.2 Hz), 4.84 (dd, 1H, H-3, J = 4.0, 6.2 Hz).

^{13}C NMR ($CDCl_3$): δ 25.8, 26.5, 55.2, 70.1, 79.1, 80.8, 82.1, 90.2, 114.9.

m/z calculated: 270.11 *m/z* found (APCI): 243.1 (M - N_2, + H)

Preparation of 5-*O*-acetyl-1,6-diazido-1,6-dideoxy-2,3-*O*-isopropylidene-β-D-manno-furanose (8) from 1,6-diazido-1,6-dideoxy-2,3-*O*-isopropylidene-β-D-manno-furanose (7).

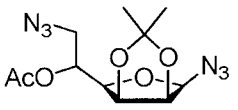

A 25 mL round bottom flask containing 1,6-diazido-1,6-dideoxy-2,3-*O*-isopropylidene-β-D-mannofuranose (**7**) (0.271 g, 1.0 mmol) dissolved in pyridine (2 mL) and acetic anhydride (1 mL) was equipped with a septum and magnetic stir bar. The reaction mixture was allowed to stir until TLC (1:1 hexane: ethyl acetate) showed consumption of starting material. Ice water (5 mL) was added to the reaction. The mixture was extracted with methylene chloride (3 x 10 mL) and back extracted with dilute H_2SO_4 (10 mL). The organic layer was dried over magnesium sulfate and reduced to yield **8** as a yellow syrup (95%).

^{1}H NMR ($CDCl_3$): δ 1.32 (s, 3H, -CH_3), 1.52 (s, 3H, -CH_3), 2.12 (s, 3H, -C(O)C$\underline{H}_3$), 3.56 (dd, 1H, H-6, J = 4.8, 13.5 Hz), 3.78 (dd, 1H, H-6', J = 2.6, 13.5 Hz), 3.88 (dd, 1H, H-4, J = 3.7, 7.7 Hz), 4.45 (d, 1H, H-1, J = 3.3 Hz), 4.67 (dd, 1H, H-2, J = 3.7, 5.9 Hz), 4.73 (dd, 1H, H-3, J = 3.7, 5.9 Hz), 5.29 (ddd, 1H, H-5, J = 2.6, 4.8, 10.6 Hz).

Synthesis of carbohydrate-derived triazoles *via* uncatalyzed cycloadditions on mannosyl azide 4.

In six 15 x 150 mm test tubes, mannosyl azide **4** (210 mg, 0.74 mmol) was dissolved in toluene (5.0 mL) and placed on the parallel synthesizer rack. A different alkyne (1 equivalent) was added to each test tube. The reactions were refluxed at 110 °C for up to twenty-four hours or until the TLC (3:1 hexane: ethyl acetate) showed consumption of starting material. The mixtures were evaporated *in vacuo* and purified on a column of silca gel.

Alkynes	Alkynes
Diethylacetylene dicarboxylate	Trimethylsilyl propiolate
Ethyl propiolate	Phenyl acetylene
Propiolic acid	Diphenyl acetylene

Table 3: Alkyne reagents

1-(2,3:5,6-Di-*O*-isopropylidene-β-D-mannofuranosyl)-1*H*-[1,2,3]triazol-4,5-dicarboxylic acid diethyl ester (9).

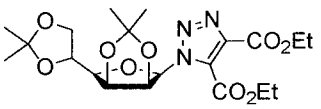

^{1}H NMR ($CDCl_3$): δ 1.27 (s, 3H, -CH_3), 1.29 (s, 3H, -CH_3), 1.39 (m, 9H, -CH_3, 2 x -OCH_2CH_3), 1.47 (s, 3H, -CH_3), 4.00 (dd, 1H, H-4, J = 4.0, 8.1 Hz), 4.17 (m, 2H, H-6, H-6'), 4.41 (m, 4H, -OCH_2CH_3), 4.65 (m, 1H, H-5), 4.94 (dd, 1H, H-3, J = 4.0, 5.9 Hz), 5.08 (dd, 1H, H-2, J = 4.4, 6.2 Hz), 6.29 (d, 1H, H-1, J = 4.7 Hz).

^{13}C NMR ($CDCl_3$): δ 15.1, 15.4, 25.7, 26.1, 26.3, 28.2, 62.9, 64.0, 67.7, 73.7, 77.9, 80.5, 81.8, 91.7, 110.5, 115.8, 131.9, 140.1, 159.7, 160.9.

m/z calculated: 455.19 *m/z* found (APCI): 456.1 (M + H)

m.p. = 122-124 °C

1-(2,3:5,6-Di-*O*-isopropylidene-β-D-mannofuranosyl)-1*H*-[1,2,3]triazol-4-(and 5-)-carboxylic acid ethyl esters (10a/10b).

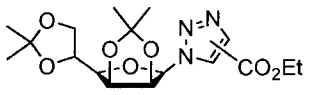

^{1}H NMR ($CDCl_3$): δ 1.35 (s, 3H, -CH_3), 1.42 (m, 6H, -CH_3, -$CH_2\underline{CH_3}$), 1.46 (s, 3H, -CH_3), 1.57 (s, 3H, -CH_3), 3.83 (dd, 1H, H-4, J = 3.7, 7.7 Hz), 4.07 (dd, 1H, H-6, J = 4.0, 8.8 Hz), 4.13 (dd, 1H, H-6', J = 6.2, 9.1 Hz), 4.45 (m, 3H, H-5, -$C\underline{H_2}CH_3$), 4.92 (dd, 1H, H-2, J = 3.7, 5.9 Hz), 4.98 (dd, 1H, H-3, J = 3.7, 5.9 Hz), 6.18 (d, 1H, H-1, J = 6.18 Hz), 8.16 (s, 1H, triazole-H), 8.35 (s, 1H, triazole-H).

1-(2,3:5,6-Di-*O*-isopropylidene-β-D-mannofuranosyl)-1*H*-[1,2,3]triazol-4-(and 5-)-carboxylic acids (11a/11b).

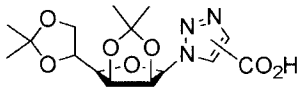

^{1}H NMR ($CDCl_3$): δ 1.34 (s, 3H, -CH_3), 1.39 (s, 3H, -CH_3), 1.46 (s, 3H, -CH_3), 1.56 (s, 3H, CH_3), 3.86 (dd, 1H, H-4, J = 3.3, 7.7 Hz), 4.10 (m, 2H, H-6, H-6'), 4.52 (m, 1H, H-5), 4.93 (dd, 1H, H-2, J = 3.7, 6.2 Hz), 4.99 (dd, 1H, H-3, J = 4.4, 6.2 Hz), 6.22 (d, 1H, H-1, J = 3.67 Hz), 7.72, 7.93, 8.41 (s, each 1H, 2 x triazole-H, -CO_2H).

1-(2,3:5,6-Di-*O*-isopropylidene-β-D-mannofuranosyl)-1*H*-[1,2,3]triazol-4-(and 5-)-carboxylic acid trimethylsilyl esters (12a/12b).

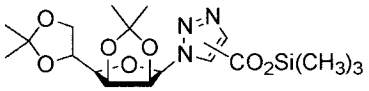

^{1}H NMR ($CDCl_3$): δ 0.415 (s, 3H, -CH_3), 1.35 (s, 3H, -CH_3), 1.40 (s, 3H, -CH_3), 1.47 (s, 3H, -CH_3), 1.57 (s, 3H, -CH_3), 3.80 (m, 1H, H-4), 4.10 (m, 2H, H-6, H-6'), 4.50 (m, 1H, H-5), 4.91 (m, 1H, H-2), 4.97 (m, 1H, H-3), 6.17 (m, 1H, H-1), 7.54, 7.91, 8.34, 8.42 (s, 1H each, triazole isomers).

1-(2,3-*O*-Isopropylidene-β-D-mannofuranosyl)-1,6-*H*-[1,2,3]triazol-4,5-dicarboxylic acid diethyl esters (14).

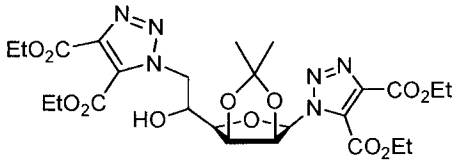

^{1}H NMR ($CDCl_3$): δ 1.15 (s, 3H, -CH_3), 1.24 (s, 3H, -CH_3), 1.38 (m, 12H, 4 x -$OCH_2\underline{CH_3}$), 3.11 (d, 1H, -OH, J = 5.5 Hz), 3.93 (dd, 1H, H-4, J = 4.8, 8.8 Hz), 4.42 (m, 10H, H-6, H-6', 4 x -$OC\underline{H_2}CH_3$), 4.70 (m, 1H, H-5), 4.95 (m, 1H, H-3), 5.10 (dd, 1H, H-2, J = 4.8, 5.9 Hz), 6.42 (d, 1H, H-1, J = 4.8 Hz).

^{13}C NMR ($CDCl_3$): δ 15.1 (double intensity), 15.4 (double intensity), 25.7, 26.0, 53.4, 62.9, 63.0, 64.1, 64.3, 69.1, 80.6, 81.3, 81.9, 91.9, 116.0, 131.8, 133.5, 140.30, 140.31, 159.6, 159.9, 160.9 (double intensity).

m/z calculated: 610.57 *m/z* found: 611.3 (M + H)

Synthesis of carbohydrate-derived triazoles *via* catalyzed cycloadditions on mannosyl azide 4.

In five 15 x 150 mm test tubes, mannosyl azide **4** (500 mg, 1.75 mmol) was dissolved in toluene (5.0 mL) and placed on the parallel synthesizer rack. A different alkyne (1 equivalent), DBU (3 equivalents) and $BrCu{\cdot}(PPh_3)_3$ (0.2 equivalent)[38b] was added to each test tube. The reactions were refluxed at 110 °C for up to sixteen hours or until the TLC (3:1 hexane: ethyl acetate) showed consumption of starting material. The mixtures were evaporated *in vacuo* and purified on a column of silica gel.

Alkynes	Alkynes
Ethyl propiolate	Phenyl acetylene
Propiolic acid	Propargyl alcohol
Trimethylsilyl propiolate	

Table 4: Alkyne reagents

1-(2,3:5,6-Di-*O*-isopropylidene-β-D-mannofuranosyl)-1*H*-[1,2,3]triazol-4-carboxylic acid ethyl ester (10a).

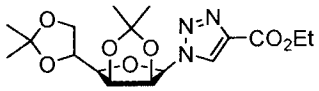

^{1}H NMR ($CDCl_3$): δ 1.38 (s, 3H, -CH_3), 1.45 (m, 6H, -CH_3, -$OCH_2C\underline{H}_3$), 1.50 (s, 3H, -CH_3), 1.60 (s, 3H, -CH_3), 3.80 (dd, 1H, H-4, J = 3.8, 7.8 Hz), 4.06 (dd, 1H, H-6, J = 4.2, 9.0 Hz), 4.14 (dd, 1H, H-6', J = 6.2, 9.2 Hz), 4.47 (m, 3H, H-5, -$OC\underline{H}_2CH_3$), 4.92 (dd, 1H, H-2, J = 3.6, 5.9 Hz), 4.98 (dd, 1H, H-3, J = 5.9, 3.7 Hz), 6.17 (d, 1H, H-1, J = 3.6 Hz), 8.35 (s, 1H, triazole-H).

^{13}C NMR ($CDCl_3$): δ 15.5, 25.2, 26.3, 26.6, 28.1, 62.4, 67.7, 73.7, 80.2, 80.4, 80.8, 89.8, 110.5, 114.8, 129.3, 140.7, 161.5.

m/z calculated: 383.39 *m/z* found: 384.2

1-(2,3:5,6-Di-*O*-isopropylidene-β-D-mannofuranosyl)-1*H*-[1,2,3]triazol-4-carboxylic acid (11a).

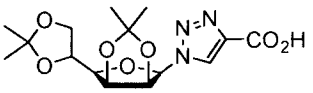

The proton NMR spectrum showed two products and suggests that the triazole has formed with a signal at 8.20 ppm, however both the proton and carbon spectra are inconclusive.

m/z calculated: 355.14 *m/z* found: 387.5 (M + CH_3OH)

1-(2,3:5,6-Di-*O*-isopropylidene-β-D-mannofuranosyl)-1*H*-[1,2,3]triazol-4-carboxylic acid trimethylsilyl ester (12a).

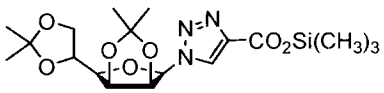

The ^1H NMR spectrum showed the appearance of two products. It suggests that the triazole had formed with a signal at 8.20 ppm, however the spectrum does not conclusively prove the structure of the product.

1-(2,3:5,6-Di-*O*-isopropylidene-β-D-mannofuranosyl)-4-phenyl-1*H*-[1,2,3]triazole (13a).

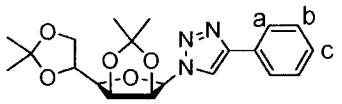

^{1}H NMR ($CDCl_3$): δ 1.36 (s, 3H, -CH_3), 1.41 (s, 3H, -CH_3), 1.48 (s, 3H, -CH_3), 1.61 (s, 3H, -CH_3), 3.80 (dd, 1H, H-4, J = 3.7, 7.7 Hz), 4.11 (dd, 1H, H-6, J = 4.4, 9.2 Hz), 4.15 (dd, 1H, H-6', J = 6.2, 9.2 Hz), 4.53 (ddd, 1H, H-5, J = 4.0, 6.2, 10.3 Hz), 4.92 (dd, 1H, H-2, J = 3.7, 5.9 Hz), 4.98 (dd, 1H, H-3, J = 3.7, 5.9 Hz), 6.14 (d, 1H, H-1, J = 3.7 Hz), 7.32 (d, 1H, Ar-H_c), 7.44 (t, 2H, Ar-H_b), 7.85 (d, 2H, Ar-H_a), 8.08 (s, 1H, triazole-H).

^{13}C NMR ($CDCl_3$): δ 25.2, 26.4, 26.7, 28.2, 67.9, 73.8, 80.2, 80.3, 80.8, 89.9, 110.5, 114.7, 121.4, 126.7 (double intensity), 129.2 (double intensity), 129.8, 131.5, 148.2.

m/z calculated: 387.43 *m/z* found: 388.3 (M + H).

1-(2,3:5,6-Di-*O*-isopropylidene-β-D-mannofuranosyl)-1*H*-[1,2,3]triazol-4-yl methanol (15).

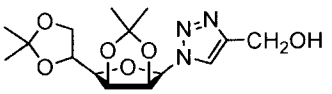

^{1}H NMR ($CDCl_3$): δ 1.35 (s, 3H, -CH_3), 1.40 (s, 3H, -CH_3), 1.47 (s, 3H, -CH_3), 1.58 (s, 3H, -CH_3), 2.46 (s, 1H, -OH), 3.77 (dd, 1H, H-4, J = 3.7, 7.7 Hz), 4.06 (dd, 1H, H-6, J = 4.0, 8.8 Hz), 4.12 (dd, 1H, H-6', J = 5.9, 8.8 Hz), 4.49 (ddd, 1H, H-5, J = 4.0, 5.9, 7.7 Hz), 4.82 (d, 2H, -C$\underline{H_2}$OH, J = 4.4 Hz), 4.88 (dd, 1H, H-2, J = 3.7, 6.2 Hz), 4.96 (dd, 1H, H-3, J = 4.0, 6.2 Hz), 6.10 (d, 1H, H-1, J = 3.7 Hz), 7.87 (s, 1H, triazole-H).

^{13}C NMR ($CDCl_3$): δ 25.2, 26.3, 26.7, 28.1, 57.2, 67.7, 73.7, 80.1, 80.2, 80.7, 89.7, 110.5, 114.7, 123.7, 148.5.

m/z calculated: 341.36 *m/z* found: 342.1 (M + 1)

Preparation of 1-(2,3-*O*-isopropylidene-β-D-mannofuranosyl)-1*H*-[1,2,3]triazol-4,5-dicarboxylic acid diethyl ester (16) from 1-(2,3:5,6-di-*O*-isopropylidene-β-D-mannofuranosyl)-1*H*-[1,2,3]triazol-4,5-dicarboxylic acid diethyl ester (9).

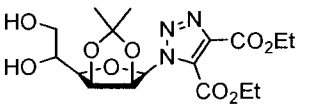

In a 50 mL two neck round bottom flask equipped with a thermometer adapter and magnetic stir bar, 1-(2,3:5,6-di-*O*-isopropylidene-β-D-mannofuranosyl)-1*H*-[1,2,3]-triazol-4,5-dicarboxylic acid diethyl ester (**9**, 0.455 g, 1 mmol) was dissolved in glacial acetic acid and water (1:1 acetic acid/water, 20 mL each) and heated to 50 °C. The reaction was monitored by TLC (100% ethyl acetate) until starting material was consumed. The mixture was reduced and the residue was reevaporated with toluene (2 x 10 mL) to afford **16** as a clear syrup (96%).

^{1}H NMR (D_6-DMSO): δ 1.20 (s, 6H, 2 x -CH_3), 1.27 (m, 6H, 2 x -$CH_2C\underline{H}_3$), 3.86 (dd, 1H, H-4, J = 3.3, 9.5 Hz), 4.30 (m, 6H, H-6, H-6', 2 x -$C\underline{H}_2CH_3$), 4.56 (m, 1H, H-5), 4.84 (dd, 1H, H-3, J = 3.3, 5.9 Hz), 5.01 (dd, 1H, H-2, J = 4.4, 5.9 Hz), 6.34 (d, 1H, H-1, J = 4.4 Hz).

m/z calculated: 415.40 *m/z* found: 416.0 (M + H)

Preparation of 1-(5,6-di-*O*-acetyl-2,3-*O*-isopropylidene-β-D-mannofuranosyl)-1*H*-[1,2,3]triazol-4,5-dicarboxylic acid diethyl ester (17) from 1-(2,3-*O*-isopropylidene-β-D-mannofuranosyl)-1*H*-[1,2,3]triazol-4,5-dicarboxylic acid diethyl ester (16).

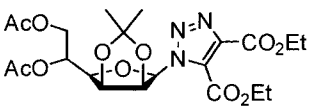

In a 50 mL round bottom flask equipped with a septum and magnetic stir bar 1-(2,3-*O*-isopropylidene-β-D-mannofuranosyl)-1*H*-[1,2,3]triazol-4,5-dicarboxylic acid diethyl ester (**16**) (0.399 g, 0.96 mmol) was dissolved in pyridine (5 mL) and acetic anhydride (2 mL). The mixture was left to stir until TLC (100% ethyl acetate) showed complete consumption of the starting material then the reaction was added to 50 mL of ice water. The mixture was extracted with methylene chloride (3 x 10 mL). The combined organic layers were dried over magnesium sulfate and evaporated to give **17** as a clear syrup (0.450 g, 94%).

^{1}H NMR ($CDCl_3$): δ 1.22 (s, 3H, -CH_3), 1.25 (s, 3H, -CH_3), 1.40 (m, 6H, 2 x -$CH_2\underline{CH_3}$), 4.30 (dd, 1H, H-4, J = 4.0, 8.1 Hz), 4.44 (m, 6H, H-6, H-6', 2 x -$\underline{CH_2}CH_3$), 4.90 (dd, 1H, H-3, J = 4.0, 5.9 Hz), 5.10 (dd, 1H, H-2, J = 4.4, 5.9 Hz), 5.52 (m, 1H, H-5), 6.36 (d, 1H, H-1, J = 4.4 Hz).

Preparation of 1-(2,3:5,6-di-*O*-isopropylidene-β-D-mannofuranosyl)-1*H*-[1,2,3]-triazol-4,5-dicarboxylic acid diamide (19) from 1-(2,3:5,6-di-*O*-isopropylidene-β-D-mannofuranosyl)-1*H*-[1,2,3]triazol-4,5-dicarboxylic acid diethyl ester (9).

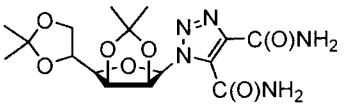

In a 250 mL three neck round bottom flask equipped with a gas inlet, septum, and magnetic stir bar, 1-(2,3:5,6-di-*O*-isopropylidene-β-D-mannofuranosyl)-1*H*-[1,2,3]-triazol-4,5-dicarboxylic acid diethyl ester (**9**) (2.0 g, 4.4 mmol) was dissolved in methanol (125 mL). Ammonia gas (produced by heating concentrated ammonium hydroxide, 250 mL) was bubbled into the reaction mixture until TLC (1:1 hexane : ethyl acetate) showed total consumption of starting material. Dilute HCl (5 mL) quenched the reaction, and the mixture was extracted with methylene chloride (3 x 20 mL). The combined organic layers were back-extracted with water (20 mL) and dried over magnesium sulfate. The remaining filtrate was evaporated *in vacuo* to yield a white solid (1.28 g, 3.3 mmol, 75%).

^{1}H NMR ($CDCl_3$): δ 1.18 (s, 3H, -CH_3), 1.28 (s, 3H, -CH_3), 1.40 (s, 3H, -CH_3), 1.48 (s, 3H, -CH_3), 4.04 (dd, 1H, H-4, J = 3.8, 7.8 Hz), 4.20 (dd, 1H, H-6, J = 5.9, 8.8 Hz), 4.24 (dd, 1H, H-6', J = 4.0, 8.8 Hz), 4.73 (ddd, 1H, H-5, J = 4.0, 5.9, 7.7 Hz), 4.94 (dd, 1H, H-3, J = 3.7, 5.9 Hz), 5.21 (dd, 1H, H-2, J = 4.4, 5.9 Hz), 6.41 (s, 2H, -NH_2), 6.88 (d, 1H, H-1, J = 4.7 Hz), 7.63 (s, 1H, -NH), 10.84 (s, 1H, -NH).

^{13}C NMR ($CDCl_3$): δ 26.0, 26.4, 26.5, 28.2, 68.1, 74.0, 80.8, 81.2, 81.6, 92.2, 110.5, 115.4, 132.1, 139.5, 159.9, 164.9.

m/z calculated: 397.16 *m/z* found: 398.2 (M + H).

Preparation of dibenzoate 20 from triazole 16.

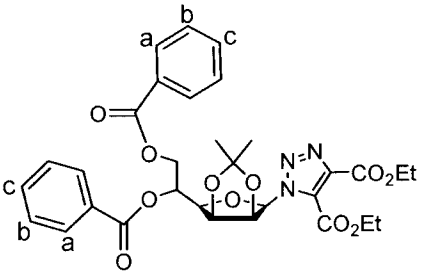

In a 25 mL round bottom flask equipped with a septum and magnetic stir bar 1-(2,3-*O*-isopropylidene-β-D-mannofuranosyl)-1*H*-[1,2,3]-triazol-4,5-dicarboxylic acid di-ethyl ester (**16**) (0.410 g, 1.0 mmol) was dissolved in dioxane (10 mL). To the reaction, pyridine (0.179 mL) and benzoyl chloride (0.253 mL) was added and the mixture stirred until TLC (100% ethyl acetate) showed no starting material remaining. The mixture was added to ice water (10 mL) and the organic layer was extracted with methylene chloride (3 x 10 mL). The combined organic layer was dried over magnesium sulfate, filtered, and the filtrate reduced. The product was purified on a column of silica gel (1:1 hexane: ethyl acetate) to afford a clear yellow syrup (0.225 g, 36%).

^{1}H NMR ($CDCl_3$): δ 1.25 (s, 3H, $-CH_3$), 1.30 (s, 3H, $-CH_3$), 1.40 (m, 6H, 2 x $-CH_2\underline{CH_3}$), 4.22 (dd, 1H, H-4, J = 4.0, 8.1 Hz), 4.44 (m, 6H, H-6, H-6', 2 x $-CH_2CH_3$), 4.68 (m, 1H, H-5), 5.09 (dd, 1H, H-3, J = 4.0, 5.9 Hz), 5.14 (dd, 1H, H-

2, J = 4.6, 5.9 Hz), 6.40 (d, 1H, H-1, J = 4.7 Hz), 7.45 (m, 4H, Ar-H_b), 7.59 (m, 2H, Ar-H_c), 8.08 (m, 4H, Ar-H_a).

^{13}C NMR ($CDCl_3$): δ 15.1 (double intensity), 15.3, 15.4, 25.7, 26.1, 63.0, 63.2, 64.2, 67.7, 69.1, 80.85, 80.90, 80.91, 81.8, 91.9, 115.9, 129.4 (triple intensity), 130.6 (triple intensity), 130.7, 132.1, 134.2 (double intensity), 140.1, 159.7, 160.9, 167.9.

m/z calculated: 623.61 *m/z* found: 624.2 (M + H).

Preparation of terminal sugar alkynes.

In four 25 mL round flasks equipped with a septum and magnetic stir bar, a different sugar precursor (1.15 g) (Table 5) was dissolved in acetronitrile (10 mL). To each flask, potassium hydroxide (3-6 equivalents) and propargyl bromide (3-6 equivalents) were added and the reactions were left stirring for up to 24 hours or until the TLC showed no starting material. The mixtures were evaporated *in vacuo* and partitioned between methylene chloride (25 mL) and water (25 mL). The organic phases were extracted with methylene chloride (3 x 20 mL). The combined organic layers were dried over magnesium sulfate, reduced, and purified by elution from a column of silica gel. The major fractions were collected and concentrated to obtain the product (yields Table 6).

Protected sugar	Protected sugar
Diacetone D-galactopyranose	Diacetone D-glucose
Diacetone D-mannofuranose	1,2-*O*-isopropylidene-D-xylofuranose

Table 5: Sugar alkyne precursors

Terminal Alkyne	Yield	R_f*
D-galactopyranose alkyne **21**	67%	0.65
D-mannofuranose alkyne **23**	69%	0.68
D-glucose alkyne **25**	62%	0.65
D-xylofuranose alkyne **27**	73%	0.65

* 1:1 hexane: ethyl acetate

Table 6: Yields of sugar alkynes

Preparation of 1,2:3,4-di-*O*-isopropylidene-6-(prop-2-ynyloxy)-D-galactopyranose (22) from diacetone D-galactopyranose (21).

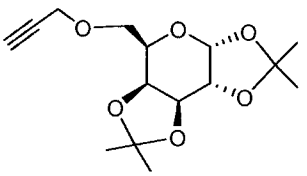

^{1}H NMR ($CDCl_3$): δ 1.33 (s, 3H, -CH_3), 1.35 (s, 3H, -CH_3), 1.46 (s, 3H, -CH_3), 1.55 (s, 3H, -CH_3), 2.44 (t, 1H, $\underline{H}CCCH_2$, J = 2.4 Hz), 3.67 (dd, 1H, H-6, J = 7.1, 10.1 Hz), 3.78 (dd, 1H, H-6', J = 5.2, 10.1 Hz), 4.00 (ddd, 1H, H-5, J = 1.9, 5.2, 7.1 Hz), 4.21 (d, 1H, -O$C\underline{H}_2$CCH, J = 2.4 Hz), 4.24 (d, 1H, -O$C\underline{H}_2$CCH, J = 2.4 Hz), 4.26 (dd, 1H, H-4, J = 1.8, 7.9 Hz), 4.32 (dd, 1H, H-2, J = 2.4, 5.1 Hz), 4.61 (dd, 1H, H-3, J = 2.4, 7.9 Hz), 5.55 (d, 1H, H-1, J = 5.1 Hz).

^{13}C NMR ($CDCl_3$): δ 25.7, 26.2, 27.2, 27.3, 59.7, 67.9, 69.8, 71.6, 71.8, 72.3, 75.8, 80.7, 97.4, 109.6, 110.3.

m/z calculated: 298.33 *m/z* found: 299.0 (M + H).

Preparation of alkyne 23 from diacetone-D-mannose (1).

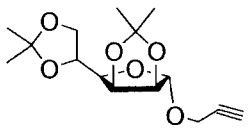

^{1}H NMR ($CDCl_3$): δ 1.33 (s, 3H, -CH_3), 1.38 (s, 3H, -CH_3), 1.46 (s, 3H, -CH_3), 1.48 (s, 3H, -CH_3), 2.44 (t, 1H, $\underline{H}CCCH_2$, J = 2.4 Hz), 3.96 (dd,1H, H-4, J = 3.6, 7.8 Hz), 4.06 (dd, 1H, H-6, J = 4.2, 8.7 Hz), 4.11 (dd, 1H, H-6', J = 6.2, 8.7 Hz), 4.19 (dd, 2H, -OC$\underline{H}_2$CCH, J = 2.3, 4.3 Hz), 4.41 (ddd, 1H, H-5, J = 4.3, 6.2, 7.8 Hz), 4.63 (d, 1H, H-2, J = 5.9 Hz), 4.79 (dd, 1H, H-3, J = 3.6, 5.9 Hz), 5.18 (s, 1H, H-1).

^{13}C NMR ($CDCl_3$): δ 25.7, 26.4, 27.1, 28.2, 55.3, 70.0, 74.1, 75.8, 78.8, 80.5, 81.7, 86.1, 105.9, 110.3, 113.7.

m/z calculated: 298.33 *m/z* found: 299.2 (M + H).

Preparation of alkyne 25 from diacetone-D-glucofuranose (24).

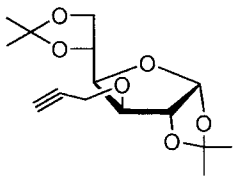

^{1}H NMR ($CDCl_3$): δ 1.30 (s, 3H, -CH_3), 1.34 (s, 3H, -CH_3), 1.41 (s, 3H, -CH_3), 1.49 (s, 3H, -CH_3), 2.52 (t, 1H, -$OCH_2CC\underline{H}$, J = 2.4 Hz), 3.98 (dd, 1H, H-4, J = 5.4, 8.6 Hz), 4.11 (m, 3H, H-5, H-6, H-6'), 4.26 (m, 3H, H-3, -$OC\underline{H_2}CCH$), 4.62 (d, 1H, H-2, J = 3.7 Hz), 5.87 (d, 1H, H-1, J = 3.7 Hz).

^{13}C NMR ($CDCl_3$): δ 26.6, 27.5, 28.0 (double intensity), 59.2, 68.3, 73.6, 76.1, 80.3, 82.1, 82.6, 83.9, 106.2, 110.0, 112.9.

m/z calculated: 298.33 *m/z* found: 299.3 (M + H).

Preparation of 1,2-*O*-isopropylidene-3,5-di-*O*-(prop-2-ynyloxy)-D-xylofuranose (27).

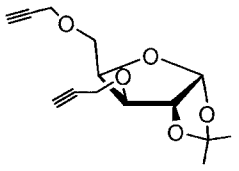

^{1}H NMR ($CDCl_3$): δ 1.32 (s, 3H, -CH_3), 1.50 (s, 3H, -CH_3), 2.47 (t, 1H, -$CH_2CC\underline{H}$, J = 2.6 Hz), 2.50 (t, 1H, -$CH_2CC\underline{H}$, J = 2.6 Hz), 3.72 (dd, 1H, H-5, J = 6.6, 10.0 Hz), 3.81 (dd, 1H, H-5', J = 5.6, 10.0 Hz), 4.11 (d, 1H, H-3, J = 3.1 Hz), 4.19-4.25 (m, 4H, 2 x -$OC\underline{H}_2CCH$), 4.40 (m, 1H, H-4), 4.62 (d, 1H, H-2, J = 3.8 Hz), 5.92 (d, 1H, H-1, J = 3.8 Hz).

^{13}C NMR ($CDCl_3$): δ 27.6, 28.0, 58.9, 59.8, 68.4, 75.8, 76.2, 80.0, 80.2, 80.6, 82.6, 83.4, 106.1, 112.9.

m/z calculated: 266.29 *m/z* found: 267.2 (M + H).

Preparation of bistriazole 28.

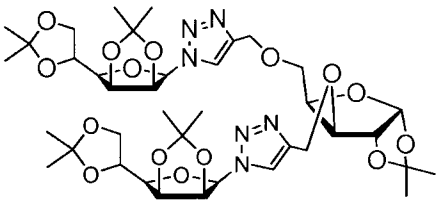

In a 50 mL round bottom flask equipped with a reflux condenser and magnetic stir bar mannosyl azide **4** (0.292 g, 1.0 mmol) and dialkyne **27** (0.150 g, 0.56 mmol) were dissolved in toluene (15 mL). To the reaction mixture, $BrCu{\cdot}(PPh_3)_3$ (0.157g, 0.17 mmol) and DBU (0.51 mL) were added and the solution was gently refluxed. Progression of the reaction was observed by TLC (1:1 hexane: ethyl acetate) until no further starting material remained. The reaction was evaporated *in vacuo* and purified by elution on a column of silica gel (2:1 hexane: ethyl acetate). The major fractions were concentrated to give 0.489g (57%, m.p. = 75-77 ˚C) of bistriazole **28** as a white solid.

^{1}H NMR ($CDCl_3$): δ 1.30, 1.34, 1.35 (3s, 9H total, 3 x -CH_3), 1.40, 1.47 (2s, 12H total, 4 x -CH_3), 1.56, 1.57, 1.64 (3s, 9H total, 3 x -CH_3), 3.73 to 4.96 (several m, 23H total, 2 x H-2 to H-6' mannofuranose, H-2 to H-5' xylofuranose, 3 x -O$\underline{CH_2}$), 5.90 (d, 1H, H-1 xylofuranose, J = 3.7 Hz), 6.07 (d, 1H, H-1 mannofuranose, J = 3.3 Hz), 6.09 (d, 1H, H-1 mannofuranose, J = 3.7 Hz), 7.87 (s, 1H, triazole-H), 7.89 (s, 1H, triazole-H).

^{13}C NMR ($CDCl_3$): δ 25.3 (double intensity), 26.3 (double intensity), 26.7 (double intensity), 27.5, 28.0, 28.2 (double intensity), 64.8, 65.8, 67.9 (double intensity), 70.0, 73.7 (double intensity), 80.2, 80.3 (double intensity), 80.4, 80.8, 83.2, 83.4,

89.8, 106.1, 110.5, 110.6, 112.7, 114.78, 114.79, 124.6 (double intensity), 129.4, 129.5, 132.9, 133.0, 133.1.

Exact mass *m/z* calculated: 859.3701 (M + Na) *m/z* found: 859.3705 (M + Na).

$[\alpha]_D$ (*c* 5.0, CH_2Cl_2) = +11°

Preparation of triazole 29, a disaccharide analog.

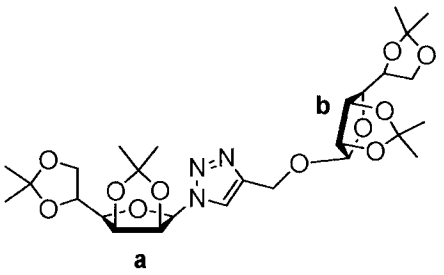

In a 50 mL round bottom flask equipped with a reflux condenser and magnetic stir bar mannosyl azide (0.774 g, 2.7 mmol) and alkyne **23** (0.890 g, 3.0 mmol) were dissolved in toluene (15 mL). To the mixture $BrCu{\cdot}(PPh_3)_3$ (0.554 g, 0.59 mmol) and DBU (1.33 mL) were added and the mixture was gently refluxed until TLC (1:1 hexane : ethyl acetate) showed total consumption of starting material. The reaction was reduced and purified on a column of silica gel. The major fractions were concentrated to give 1.11 g (1.9 mmol) of disaccharide **29** as a white solid (70%, m.p. = 64-66 °C).

^{1}H NMR ($CDCl_3$): δ 1.29, 1.33, 1.36, 1.37 (4s, 12H, 4 x -CH_3), 1.44 (overlapping 3s, 9H, 3 x -CH_3), 1.56 (s, 3H, -CH_3), 3.74 (dd, 1H, H-4_b, J = 3.7, 8.1 Hz), 3.96 (dd, 1H, H-4_a, J = 3.7, 8.1 Hz), 4.06 (m, 6H, (H-6, H-6')$_a$, (H-6, H-6')$_b$, -O$\underline{CH_2}$CNCH-), 4.39 (ddd, 1H, H-5_b, J = 4.4, 6.6, 8.1 Hz), 4.48 (m, 1H, H-5_a, J =

4.0, 5.9, 7.7 Hz), 4.61, 4.76 (2m, 2H, (H-2, H-3)$_b$, 4.86 (dd, 1H, H-2$_a$, J = 3.7, 5.9 Hz), 4.94 (dd, 1H, H-3$_a$, J = 3.7, 5.9 Hz), 5.08 (s, 1H, H-1$_b$), 6.08 (dd, 1H, H-1$_a$, J = 3.3 Hz), 7.82 (s, 1H, triazole-H).

^{13}C NMR ($CDCl_3$): δ 25.2, 25.7, 26.3, 26.4, 26.7, 27.1, 28.1, 28.2, 54.6, 61.4, 67.9, 68.1, 73.7, 74.2, 80.3, 80.6, 80.7, 81.6, 86.1, 89.8, 106.6, 110.3, 110.6, 113.6, 114.8, 124.4, 144.6.

Exact mass *m/z* calculated: 606.2639 (M + Na) *m/z* found: 606.2645 (M + Na).

$[\alpha]_D$ (*c* 5.0, CH_2Cl_2) = +3.5°

Preparation of triazole 30, a disaccharide analog.

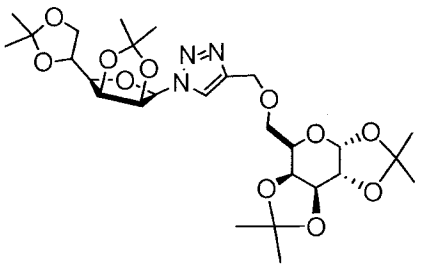

In a 50 mL round bottom flask equipped with a reflux condenser and magnetic stir bar mannosyl azide **4** (0.250 g, 0.88 mmol) and galactosyl alkyne **22** (0.288 g, 0.96 mmol) were dissolved in toluene (15 mL). $BrCu{\cdot}(PPh_3)_3$ (0.268 g, 0.29 mmol) and DBU (0.432 mL) were added to the reaction mixture. The reaction was allowed to gently reflux until TLC (1:1 hexane : ethyl acetate) showed no starting material remaining. The reaction was evaporated *in vacuo* and purified by elution on a column of silica gel. The major fractions were collected and concentrated to afford **30** as a white solid (0.37 g, 0.63

mmol, m.p. = 142-144 °C). The white solid was recrystallized in methanol, which gave a clear crystal.

^{1}H NMR ($CDCl_3$): δ 1.31 (s, 6H, 2 x -CH_3), 1.32, 1.38, 1.41, 1.44, 1.50, 1.55 (6s, 18H total, 6 x -CH_3), 3.63 to 4.94 (several m, 14H, H-2 to H-6' mannofuranose, H-2 to H-6' galactopyranose, -OC$\underline{H_2}$CNCH-), 5.52 (d, 1H, H-1 galactopyranose, J = 4.8 Hz), 6.07 (d, 1H, H-1 mannofuranose, J = 3.3 Hz), 7.87 (s, 1H, triazole-H).

^{13}C NMR ($CDCl_3$): δ 25.3, 25.7, 26.2, 26.3, 26.7, 27.2, 27.3, 28.2, 65.8, 67.9, 67.9, 70.3, 71.6, 71.8, 72.3, 73.7, 80.3, 80.7, 89.8, 97.4, 109.6 (double intensity), 110.2, 110.6, 114.8, 124.5, 145.6.

Exact mass *m/z* calculated: 606.2639 (M + Na) *m/z* found: 606.2627 (M + Na).

$[\alpha]_D$ (*c* 5.0, CH_2Cl_2) = -18.1°

Preparation of triazole 31, a disaccharide analog.

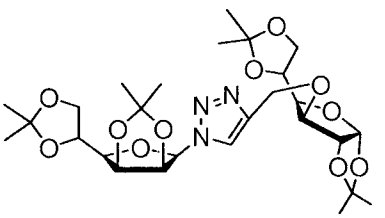

In a 50 mL round bottom flask equipped with a magnetic stir bar and reflux condenser mannosyl azide **4** (0.250 g, 0.88 mmol) and glucosyl alkyne (0.288 g, 0.96 mmol) were dissolved in toluene (15 mL). To the mixture $BrCu{\cdot}(PPh_3)_3$ (0.268 g, 0.29 mmol) and DBU (0.432 mL) were added. The reaction was allowed to gently reflux until TLC (1:1 hexane: ethyl acetate) showed total consumption of azide **4**. The reaction was

concentrated and purified by elution on a column of silica gel. The major fractions were concentrated to give 0.360 g (0.62 mmol, 73%, m.p. = 196-198 °C) of **30** as a white solid. The solid was recrystallized from methanol to give a crystal of sufficient quality for diffraction.

^{1}H NMR ($CDCl_3$): δ 1.29 (s, 3H, -CH_3), 1.33, 1.34 (2s, 6H total, 2 x -CH_3), 1.39 (s, 6H, 2 x -CH_3), 1.46, 1.48, 1.56 (3s, 9H total, 3 x -CH_3), 3.76 (dd, 1H, H-4 mannofuranose, J = 3.7, 8.1 Hz), 4.07 (m, 9H, H-6 and H-6' mannofuranose, H-3, H-4, H-5, H-6, and H-6' glucofuranose, -OC$\underline{H_2}$CNCH-), 4.50 (ddd, 1H, H-5 mannofuranose, J = 4.0, 5.9, 8.1 Hz), 4.61 (d, 1H, H-2 glucofuranose, J = 3.7 Hz), 4.87 (dd, 1H, H-2 mannofuranose, J = 3.6, 5.9 Hz), 4.96 (dd, 1H, H-3 mannofuranose, J = 3.7, 5.9 Hz), 5.88 (d, 1H, H-1 glucofuranose, J = 3.7 Hz), 6.10 (d, 1H, H-1 mannofuranose, J = 3.6 Hz), 7.87 (s, 1H, triazole-H).

^{13}C NMR ($CDCl_3$): δ 25.2, 26.3, 26.7 (double intensity), 27.4, 28.1 (double intensity), 28.3, 65.1, 68.0, 68.4, 73.7 (double intensity), 80.3, 80.35, 80.7, 82.2, 82.8, 83.6, 89.9, 106.3, 110.0, 100.7, 112.9, 114.8, 124.5, 145.2.

Exact mass *m/z* calculated: 606.2639 (M + Na) *m/z* found: 606.2645 (M + Na).

$[\alpha]_D$ (*c* 5.0, CH_2Cl_2) = +55.6°

References:

1. Collins, P., Ferrier, R. A., "Monosaccharides: Their Chemistry and Their Roles in Natural Products." Wiley: New York, New York, **1995**.
2. Arya, P., Barkley, A., "Combinatorial Chemistry toward Understanding the Function(s) of Carbohydrates and Carbohydrate Conjugates," *Chem. Eur. J.* **2001**, *7*, 555-563.
3. Carey, F.A., "Organic Chemistry," McGraw-Hill: Boston, Massachusetts, **2003**.
4. http://www.ncbi.nlm.nih.gov/books/bv.fcgi?call=bv.
5. http://www.ncbi.nlm.nih.gov/entrez/
6. Stick, R., "Carbohydrates: The Sweet Molecules of Life," Academic Press: San Diego, California, **2001**.
7. Kishi, Y., Wei, A., Boy, K. M., "Biological Evaluation of Rationally Modified Analogs of the H-Type II Blood Group Trisaccharide. A Correlation Between Solution Conformation and Binding Affinity," *J. Am. Chem. Soc.* **1995**, *117*, 9432-9436.
8. Linhardt, R., Kuberan, B., Sikkander, S., Tomiyama, H., "Synthesis of a *C*-Glycoside Analogue of sTn: An HIV- and Tumor-Associated Antigen," *Angew. Chem. Int. Ed.* **2003**, *42*, 2073-2075.
9. Liotta, D., Wilson, L., Hager, M., El-Kattan, Y. A., "Nitrogen Glycosylation Reactions Involving Pyrimidine and Purine Nucleoside Bases with Furanoside Sugars," *Synthesis*, **1995**, 1465-1479.
10. Chida, N., Suzuki, T., Suzuki, S., Yamada, I., Koashi, Y., Yamada, K., "Total Synthesis of Spicamycin," *J. Org. Chem.* **2002**, *67*, 2874-2880.

11. Fleet, G. W. J., Mons, S., "An Approach to the Generation of Simple Analogues of the Antitumour Agent Spicamycin," *Org. Biomol. Chem.* **2003**, *1*, 3685-3691.

12. Sharpless, K. B., Kolb, H. C., "The Growing Impact of Click Chemistry on Drug Discovery," *DDT*, **2003**, *24*, 1128-1137.

13. Meldal, M., Tornoe, C., Christensen, C., "Peptidotriazoles on Solid Phase: [1,2,3]-Triazoles by Regiospecific Copper(I)-Catalyzed 1,3-Dipolar Cycloadditions of Terminal Alkynes to Azides," *J. Org. Chem.* **2002**, *67*, 3057-3064.

14. Saxon, E., Bertozzi, C. R., "Cell Surface Engineering by a Modified Staudinger Reacton," *Science*, **2000**, *287*, 2007-2010.

15. Sharpless, K.B., Wong, C., Lee, L., Mitchell, M., Huang, S., Fokin, V., "A Potent and Highly Selective Inhibitor of Human α-1,3-Fucosyltransferase *via* Click Chemistry," *J. Am. Chem. Soc.* **2003**, *125*, 9588-9589.

16. Drews, J., "Drug Discovery: A Historical Perspective," *Science*, **2000**, *5460*, 1960-1964.

17. http://www.peptide.com

18. http://www.nyu.edu/classes/ytchang/book/e007.html

19. Gustafson, G. R., Baldino, C., O'Donnell, M., Sheldon, A., Tarsa, R., Verni, C., Coffen, D., "Incorporation of Carbohydrates and Peptides into Large Triazine-Based Screening Libraries Using Automated Parallel Synthesis," *Tetrahedron*, **1998**, *54*, 4051-4065.

20. Root, Y. Y., M.S. Thesis, Youngstown State University, **2003**.

21. Geysen, H. M., Meloen, R. H., Barteling, S. J., "Use of Peptide Synthesis to Probe Viral Antigens for Epitopes to a Resolution of a Single Amino Acid," *Proc. Natl. Acad. Sci. U.S.A.* **1984**, *81*, 3998-4002.

22. Furka, A., (editor), "Cornucopia of Peptides by Synthesis," *Proceedings of the 14th International Congress of Biochemistry*, **1988**, *5*, 47.

23. Wilson, S., Czarnik, A., "Combinatorial Chemistry: Synthesis and Application," Wiley: New York, New York, **1997**.

24. Bhalay, G., Dunstan, A., Glen, A., "Supported Reagents: Opportunities and Limitations," *Synlett*, **2000**, *12*, 1846-1859.

25. Maehr, H., "Combinatorial Chemistry in Drug Research from a New Vantage Point," *Bioorg. Med. Chem.* **1997**, *3*, 473-491.

26. Gruner, S., Locardi, E., Lohof, E., Kessler, H., "Carbohydrate-Based Mimetics in Drug Design: Sugar Amino Acids and Carbohydrate Scaffolds," *Chem. Rev.* **2002**, *102*, 491-514.

27. Smith, A. B., Sasho, S., Barwis, B. A., Sprengeler, P., Barbosa, J., Hirschmann, R., Cooperman, B. S., "Design and Synthesis of a Tetrahydropyran-Based Inhibitor of Mammalian Ribonucleotide Reductase," *Bioorg. Med. Chem. Lett.* **1998**, *8*, 3133.

28. Nicotra, F., Peri, F., Cipolla, L., Forni, E., "Carbohydrate-Based Scaffolds for the Generation of Sortiments of Bioactive Compounds," *Monatshefte fur Chemie*, **2002**, *133*, 369-382.

29. Sofia, M., Hunter, R., Chan, T, Vaughan, A., Dulina, R., Wang, H., Gange, D., "Carbohydrate-Based Small-Molecule Scaffolds for the Construction of Universal Pharmacophore Mapping Libraries," *J. Org. Chem.* **1998**, *63*, 2802-2803.

30. Kunz, H., Wunberg, T., Kallus, C., Opatz, T., Henke, S., Schmidt, W., "Carbohydrates as Multifunctional Chiral Scaffolds in Combinatorial Synthesis," *Angew. Chem. Int. Ed.* **1998**, *37*, 2503-2505.

31. Hirschmann, R., Nicolaou, K.C., Pietranico, S., Salvino, J., Laehy, E.M., Splengeler, P., Furst, G., Smith, A., Strader C., Cascieri, M., Candelore, M., Donaldson, C., Vale, W., Maechler, L., "Nonpeptidal Peptidomimetics with β-D-Glucose Scaffolding. A Partial Somatostatin Agonist Bearing a Close Structural Relationship to a Potent, Selective Substance P Antagonist," *J. Am. Chem. Soc.* **1992**, *114*, 9217-9218.

32. Nicolaou, K.C., Trujillo, J.L., Chibale, K., "Design, Synthesis and Biological Evaluation of Carbohydrate-Based Mimetics of cRGDFV," *Tetrahedron*, **1997**, *53*, 8751-8778.

33. Kunz, H., Kallus, C., Opatz, T., Wunberg, T., Schmidt, W., Henke, S., "Combinatorial Solid-Phase Synthesis Using D-Galactose as a Chiral Five-Dimension-Diversity Scaffold," *Tetrahedron Lett.* **1999**, *40*, 7783-7786.

34. Hanessian, S., "Preparative Carbohydrate Chemistry," Marcel Dekker, Inc., New York, New York, **1997**.

35. Norris, P., Cicchillo, R., "A Convenient Synthesis of Glycosyl Chlorides from Sugar Hemiacetals using Triphosgene as the Chlorine Source," *Carbohydr. Res.* **2000**, *328*, 431-434.

36. Fleet, G. W. J., Estevez, J., Burton, J., Estevez, R., Ardron, H., Wormald, M., Dwek, R., Brown, R., "Spirodiketopiperazines of Mannofuranose: Carbopeptoid α-

Amino Acid Esters at the Anomeric Position of Mannofuranose," *Tetrahedron Asymm.* **1998**, *9*, 2137-2154.

37. a) Kolb, H.C.; Finn, M.G.; Sharpless, K.B. "Click Chemistry: Diverse Chemical Function From a Few Good Reactions," *Angew. Chem. Int. Ed.*, **2001**, *40*, 2004-2021, and references cited therein.

    b) Sharpless, K. B., Lewis, W., Green, L., Grynszpan, F., Radic, Z., Carlier, P., Taylor, P., Finn, M.G., "Click Chemistry In Situ: Acetylcholinesterase as a Reaction Vessel for the Selective Assembly of a Femtomolar Inhibitor from an Array of Building Blocks," *Angew. Chem. Int. Ed.* **2002**, *41*, 1053-1057.

38. a) Sharpless, K. B., Rostovtsev, V., Green, L., Fokin, V., "A Stepwise Huisgen Cycloaddition Process: Copper(I)-Catalyzed Regioselective "Ligation of Azides and Terminal Alkynes," *Angew. Chem. Int. Ed.* **2002**, *41*, 2596-2599.

    b) Santoyo-Gonzalez, F., Perez-Balderas, F., Ortega-Munoz, M., Morales-Sanfrutos, J., Hernandez-Mateo, F., Calvo-Flores, F., Calvo-Asin, J., Isac-Garcia, J., " Multivalent Neoglycoconjugates by Regiospecific Cylcoaddition of Alkynes and Azides Using Organic-Soluble Copper Catalysts," *Org. Lett.* **2003,** *11*, 1951-1954.

Appendix A

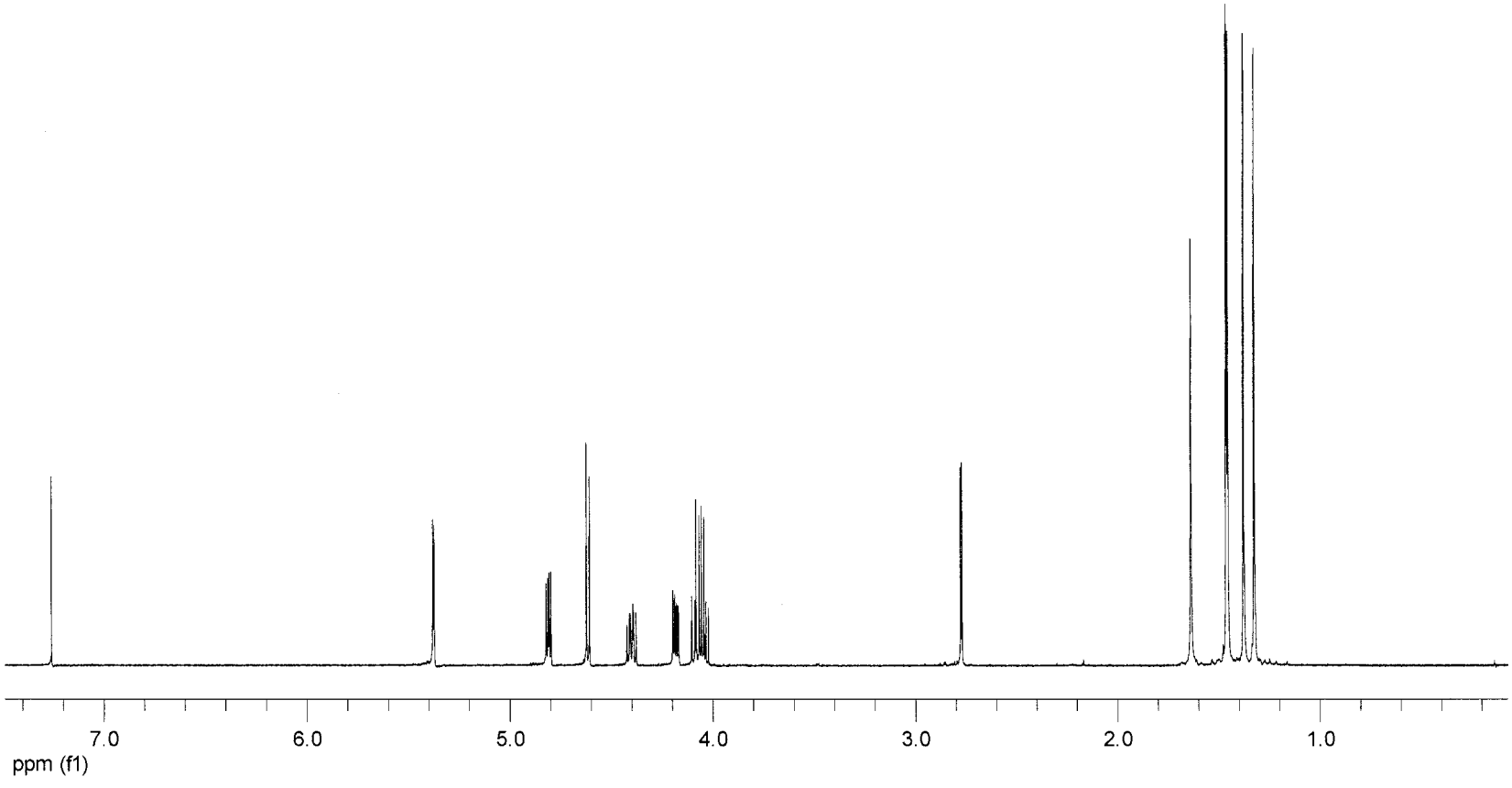

Figure 12: 400 MHz ^{1}H NMR spectrum of diacetone D-mannofuranose (**1**)

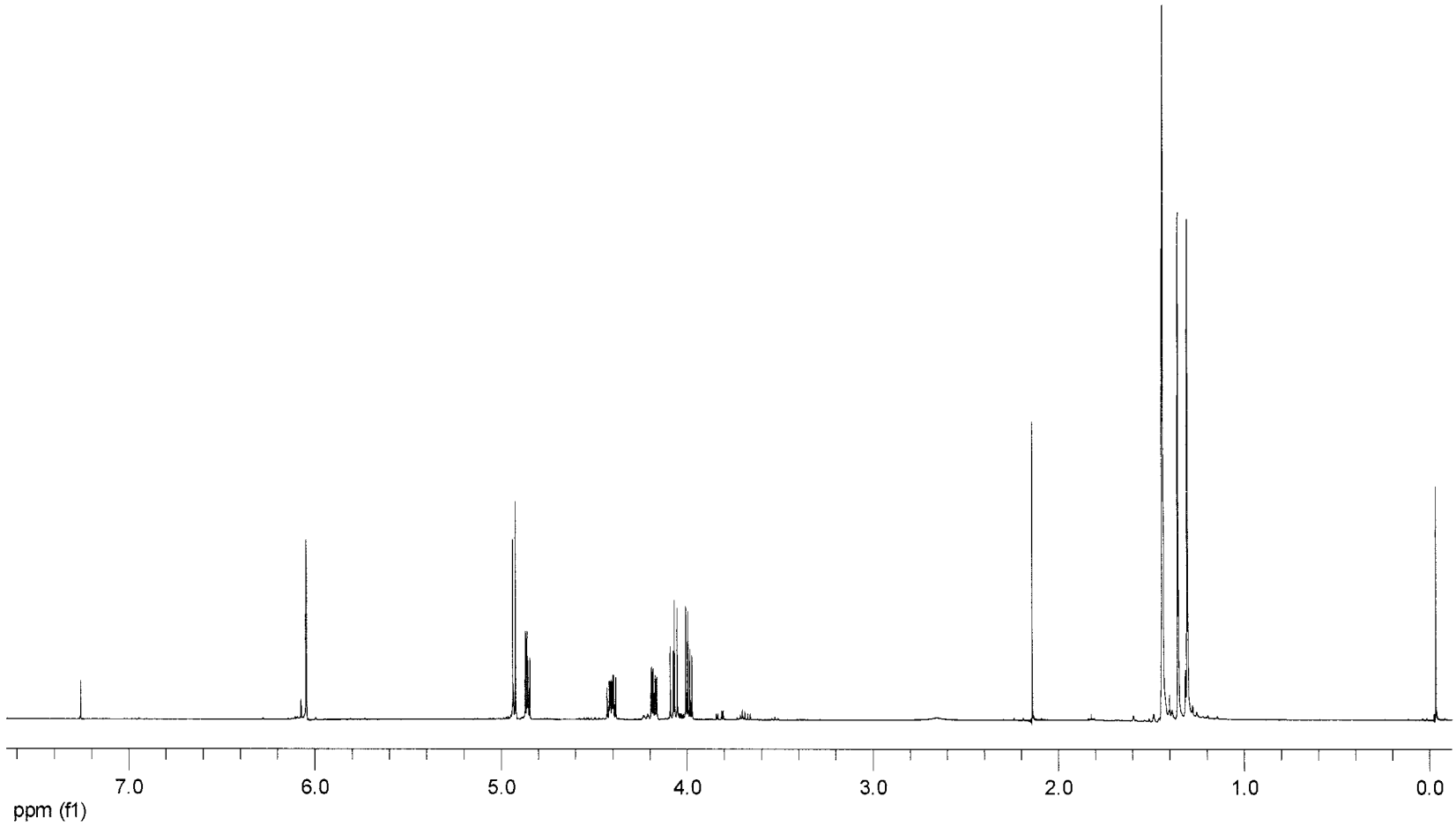

Figure 13: 400 MHz ^{1}H NMR spectrum of mannosyl chloride **3**

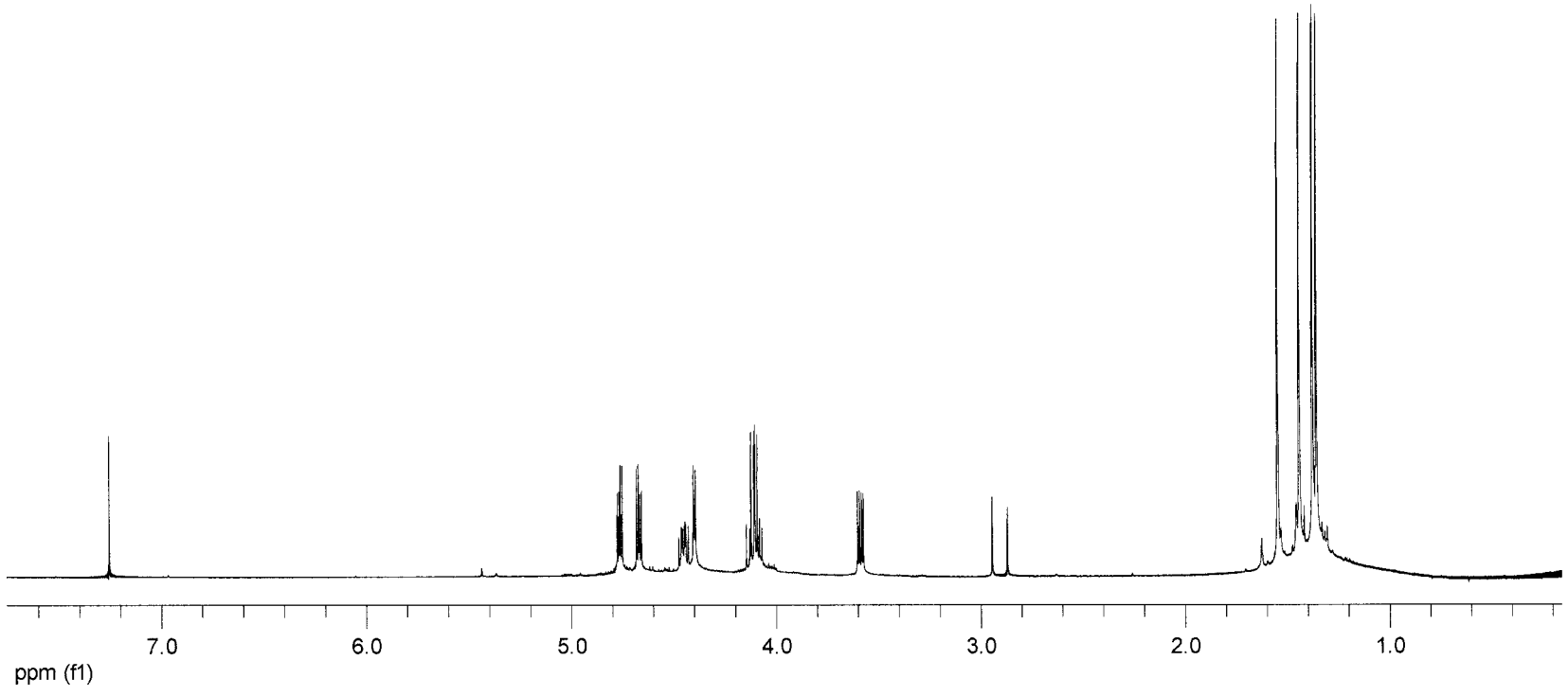

Figure 14: 400 MHz ^{1}H NMR spectrum of mannosyl azide **4**

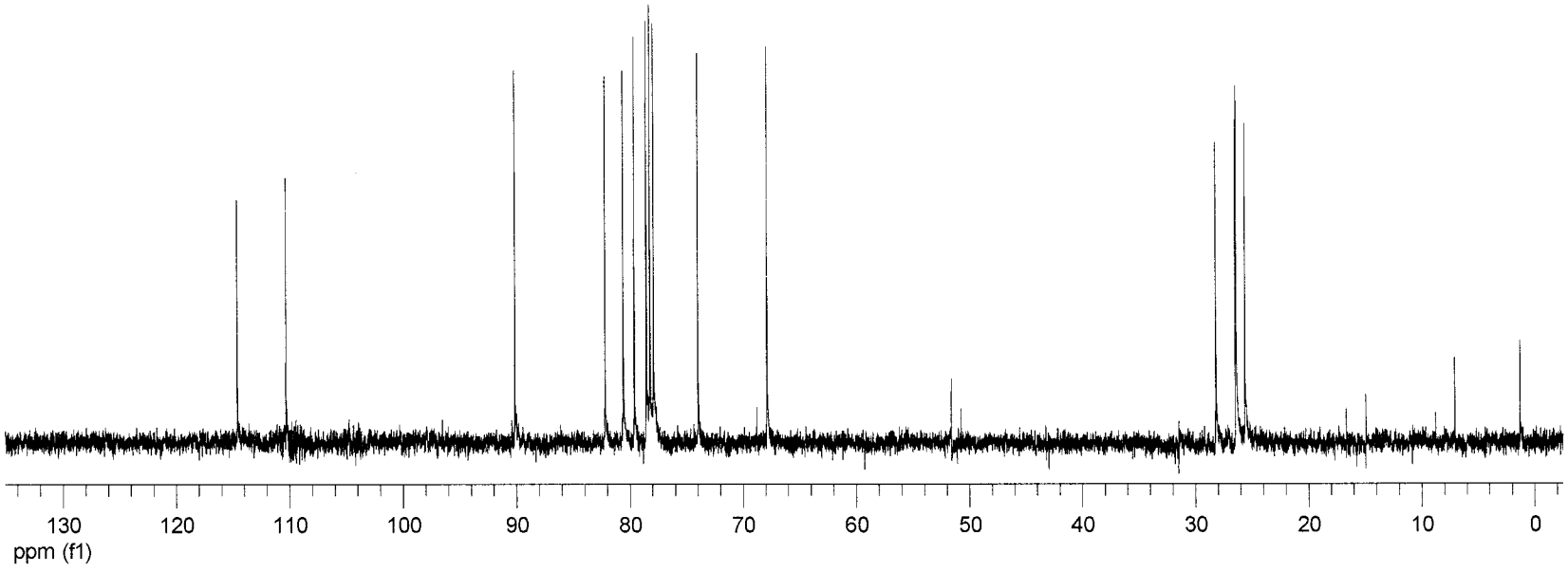

Figure 15: 100 MHz ^{13}C NMR spectrum of mannosyl azide **4**

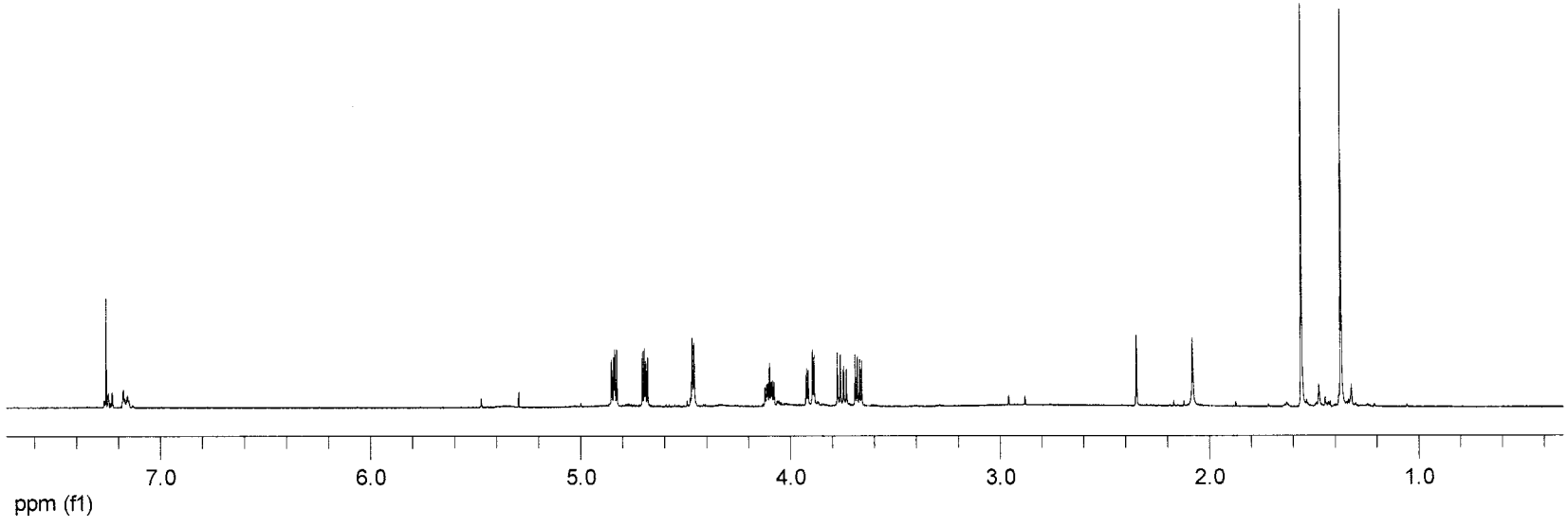

Figure 16: 400 MHz ^{1}H NMR spectrum of 1-azido-1-deoxy-2,3-*O*-isopropylidene-β-D-mannofuranose (**5**)

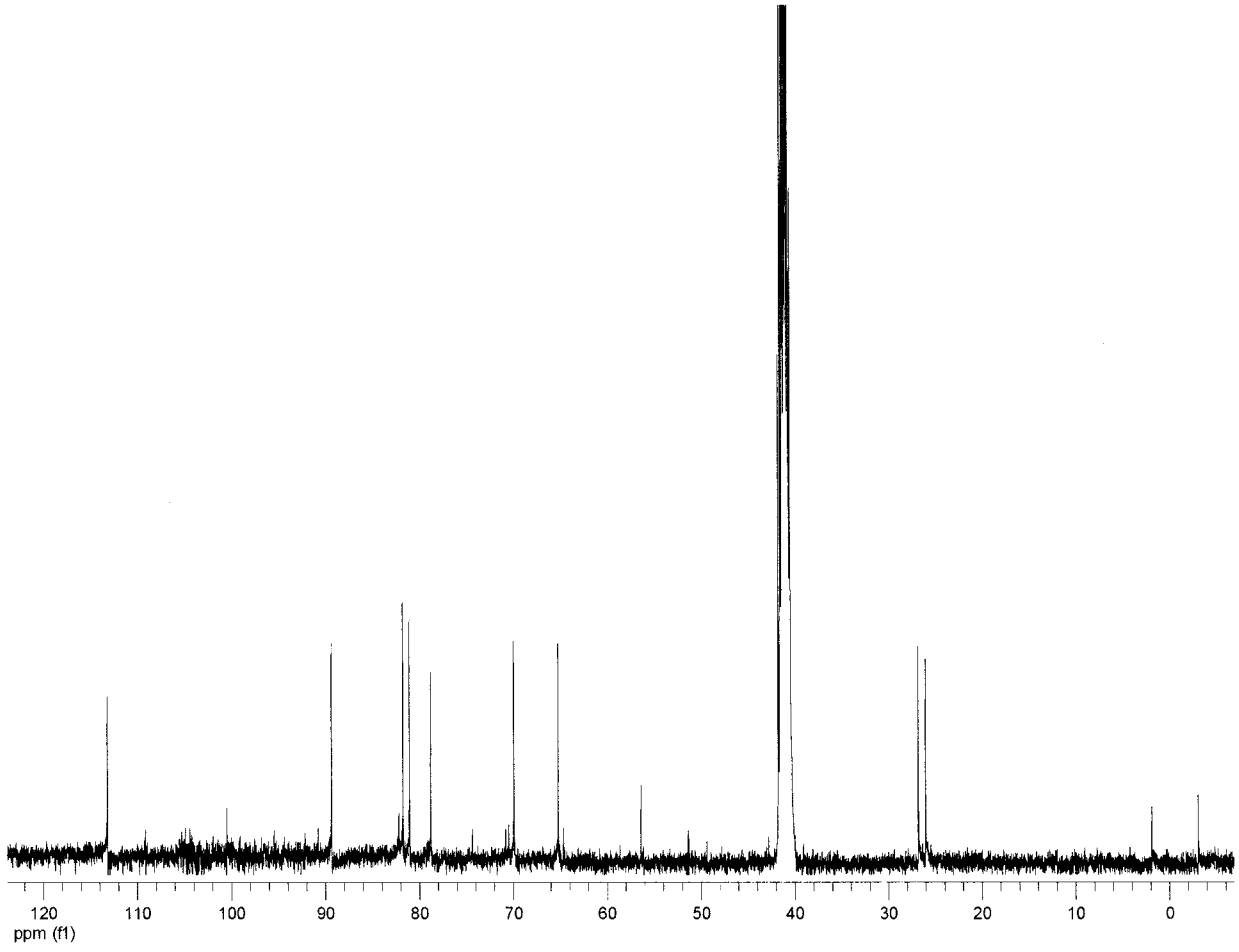

Figure 17: 100 MHz ^{13}C NMR spectrum of 1-azido-1-deoxy-2,3-*O*-isopropylidene-β-D-mannofuranose (**5**)

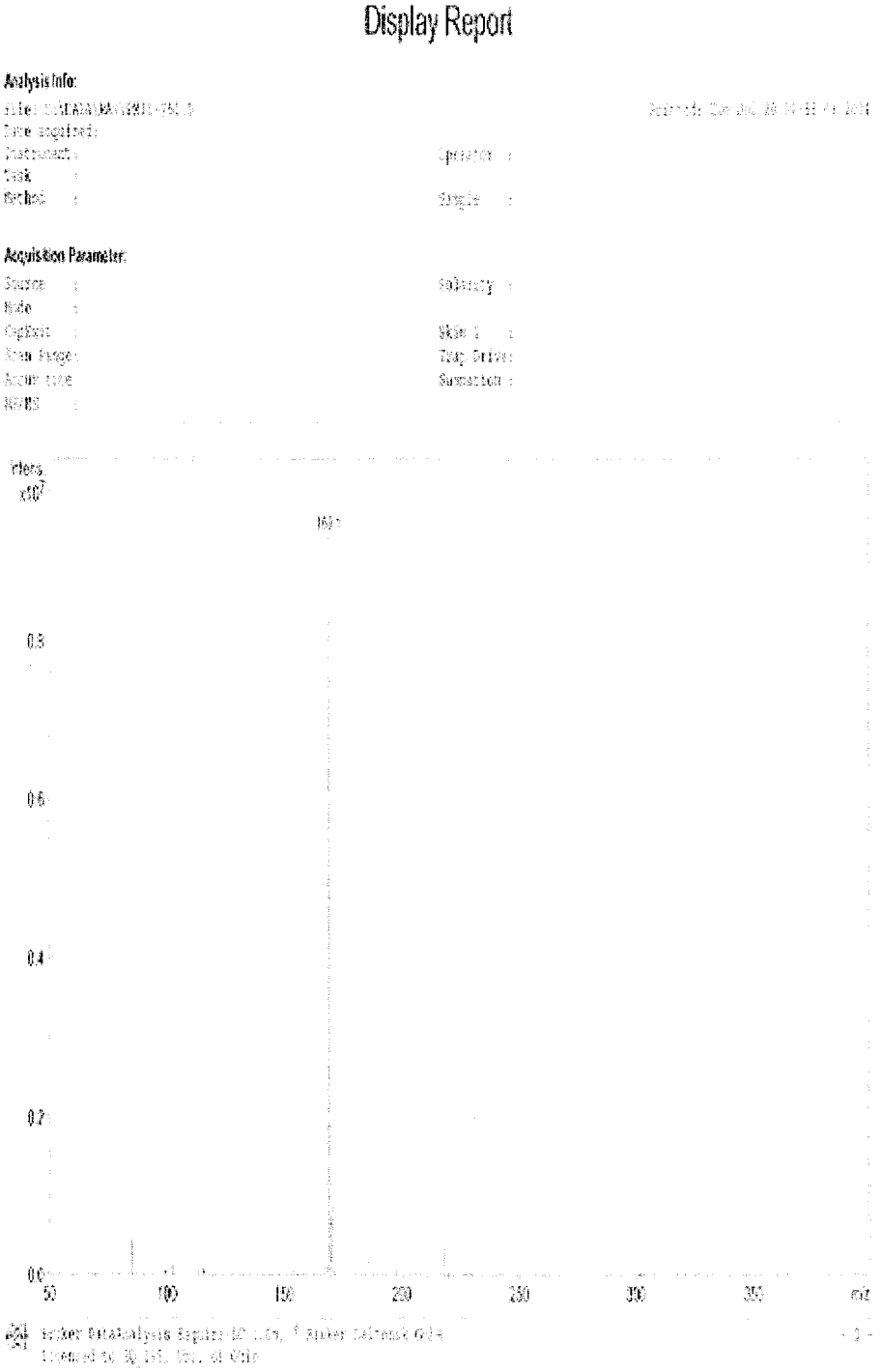

Figure 18: Mass spectrum of 1-azido-1-deoxy-2,3-*O*-isopropylidene-β-D-mannofuranose (**5**)

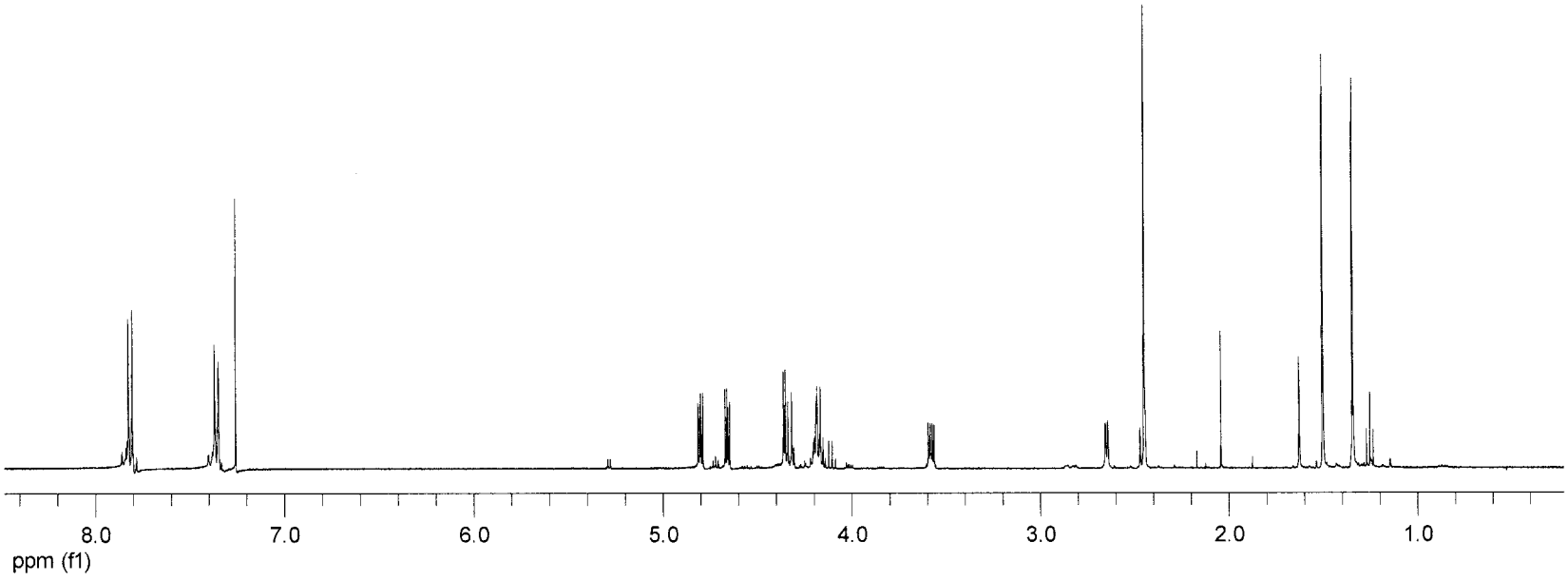

Figure 19: 400 MHz ^{1}H NMR spectrum of 1-azido-1-deoxy-2,3-*O*-isopropylidene-6-*p*-toluenesulfonyl-β-mannofuranose (**6**)

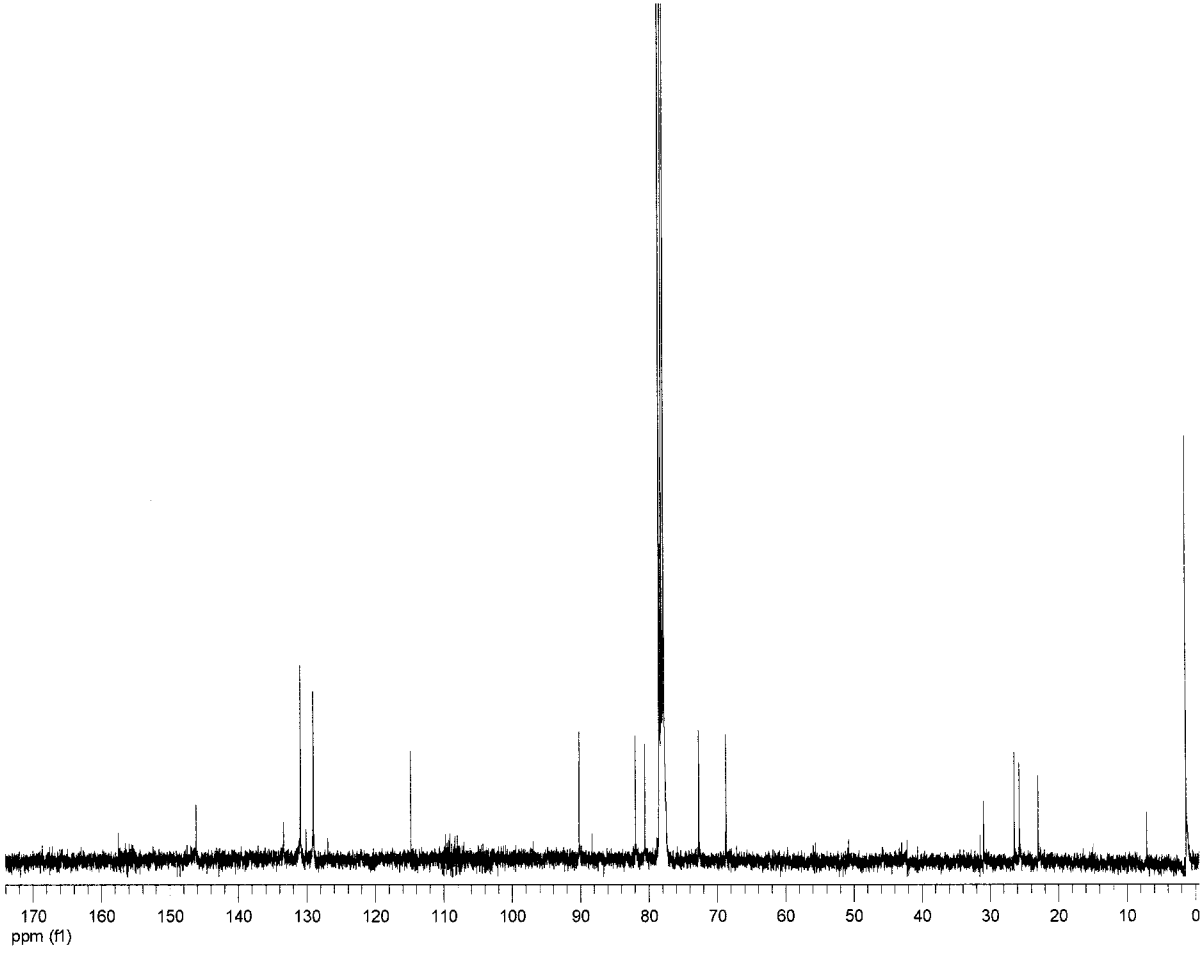

Figure 20: 100 MHz ^{13}C NMR spectrum of 1-azido-1-deoxy-2,3-*O*-isopropylidene-6-*p*-toluenesulfonyl-β-D-mannofuranose (**6**)

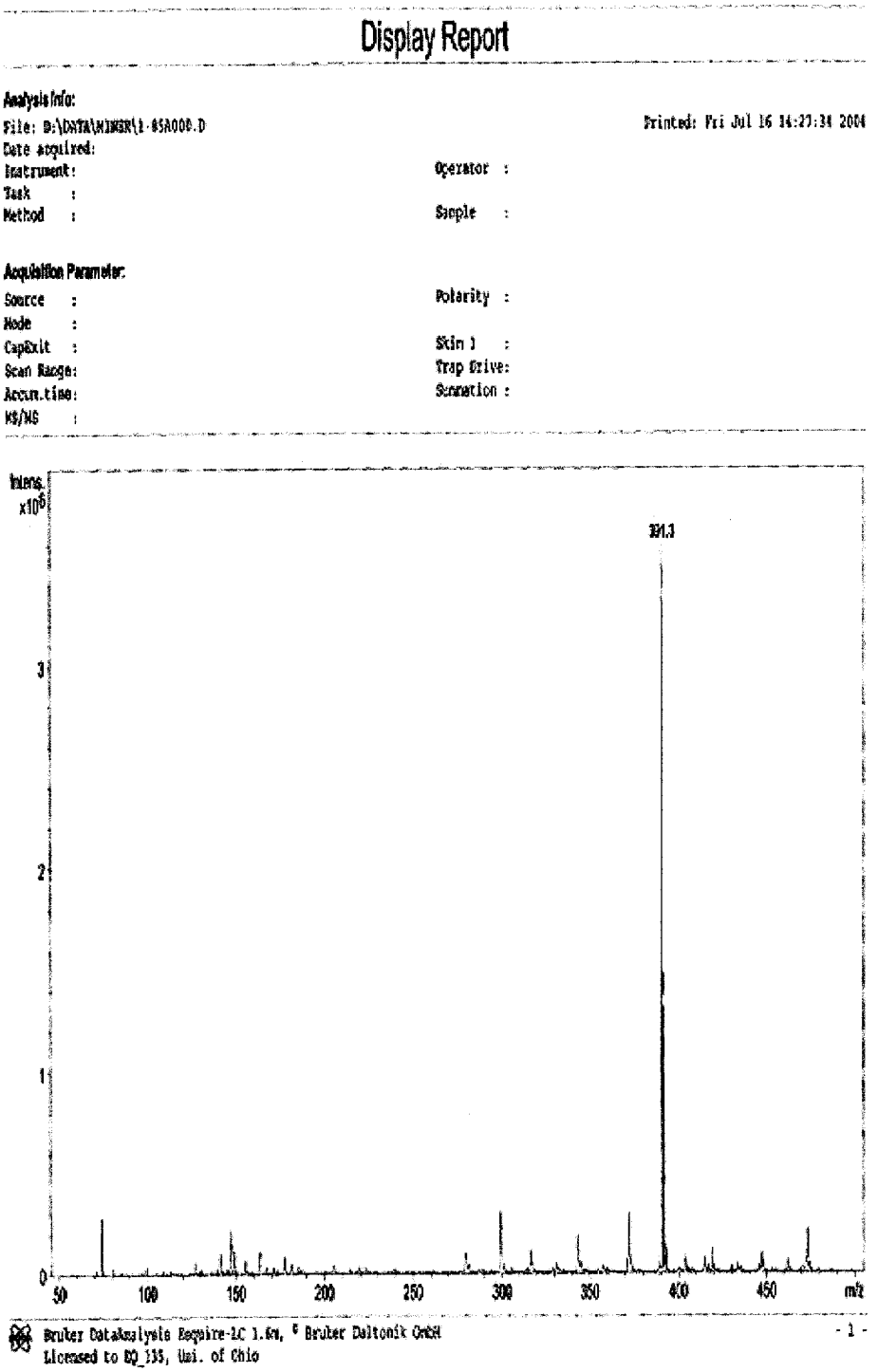

Figure 21: Mass spectrum of 1-azido-1-deoxy-2,3-*O*-isopropylidene-6-*p*-toluenesulfonyl-β-D-mannofuranose (**6**)

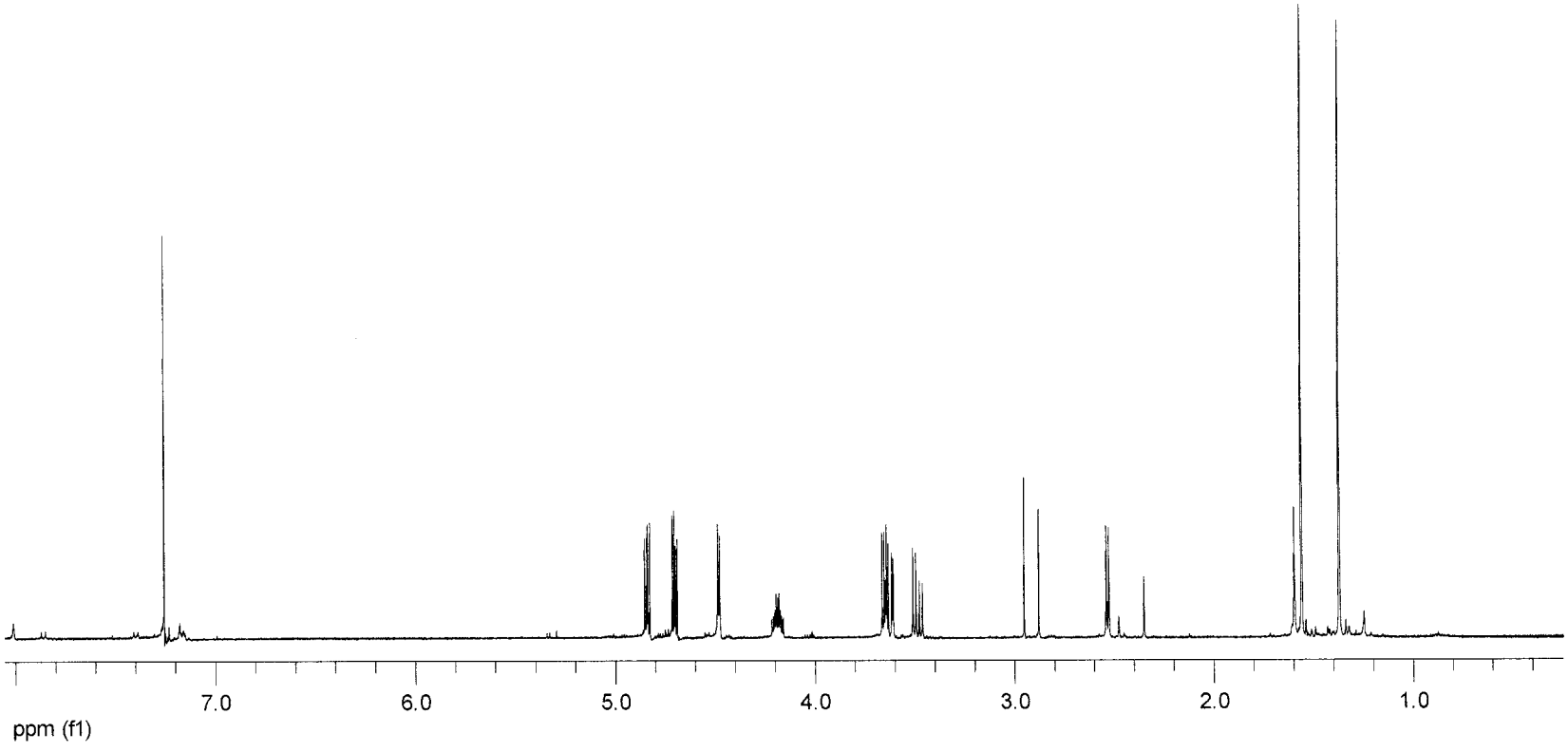

Figure 22: 400 MHz ^{1}H NMR spectrum of 1,6-diazido-1,6-dideoxy-2,3-*O*-isopropylidene-β-D-mannofuranose (**7**)

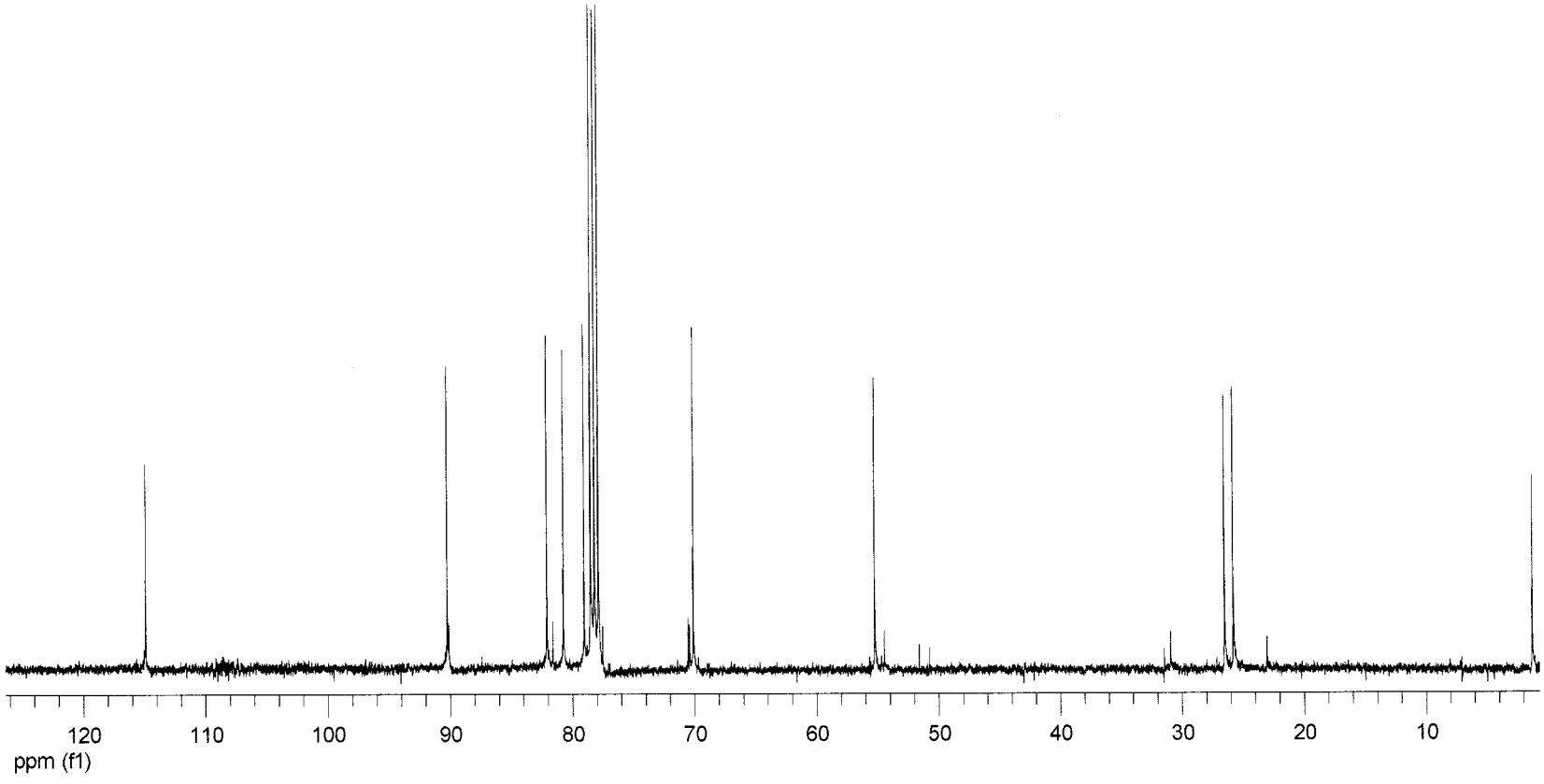

Figure 23: 100 MHz ^{1}C NMR spectrum of 1,6-diazido-1,6-dideoxy-2,3-*O*-isopropylidene-β-D-mannofuranose (**7**)

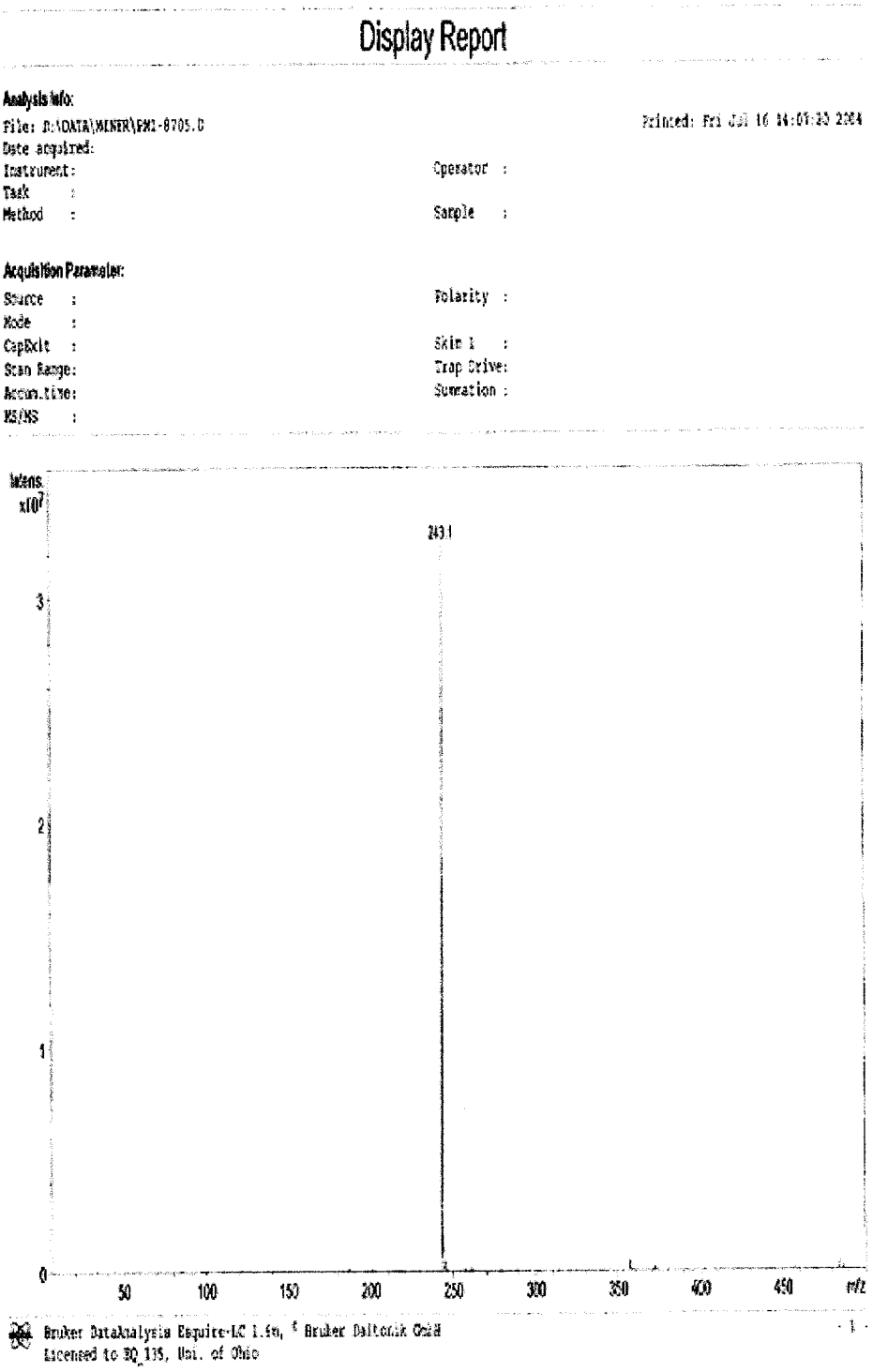

Figure 24: Mass spectrum of 1,6-diazido-1,6-dideoxy-2,3-*O*-isopropylidene-β-D-mannofuranose (**7**)

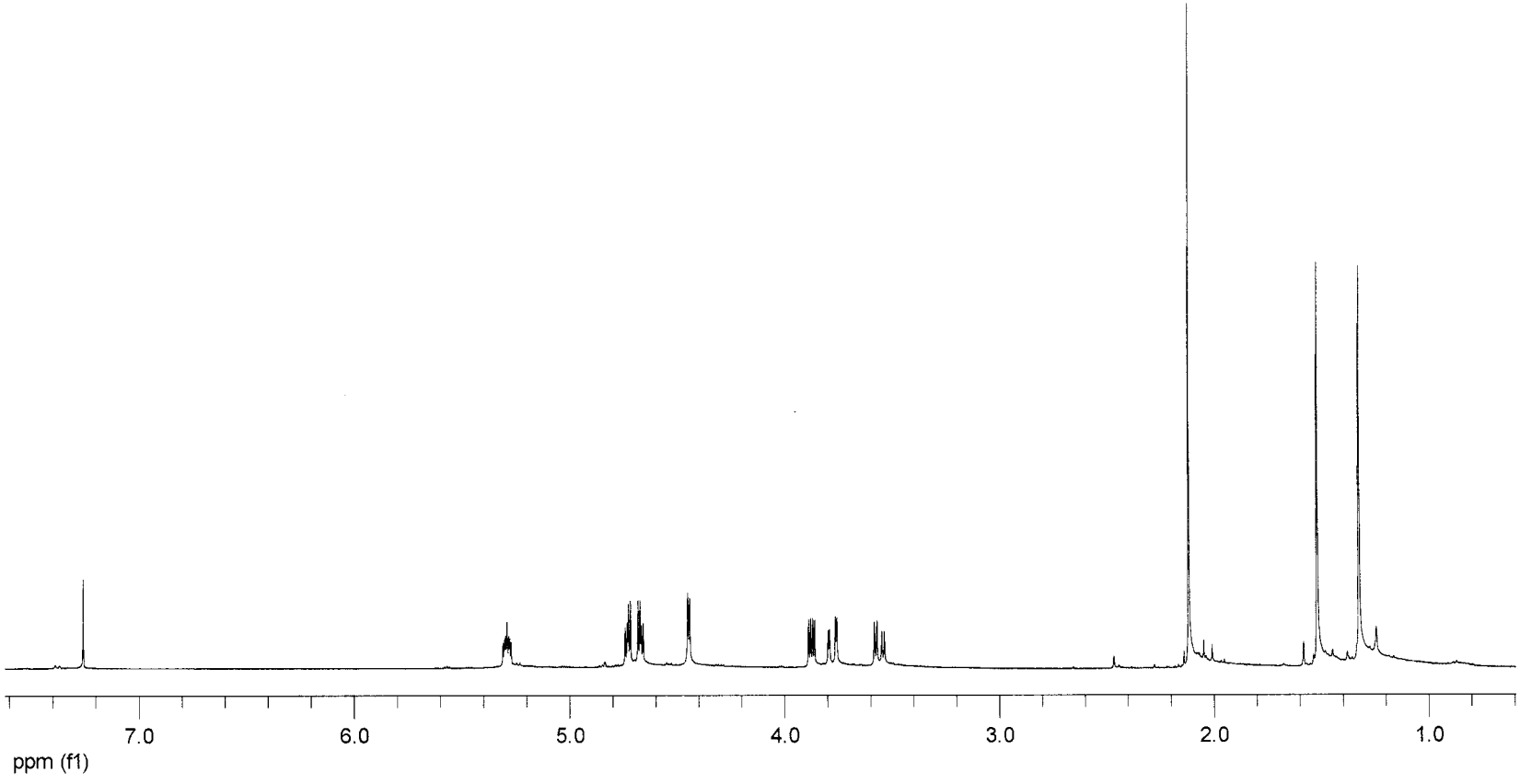

Figure 25: 400 MHz ^{1}H NMR spectrum of 5-acetyl-1,6-diazido-1,6-dideoxy-2,3-*O*-isopropylidene-β-D-manno-furanose (**8**)

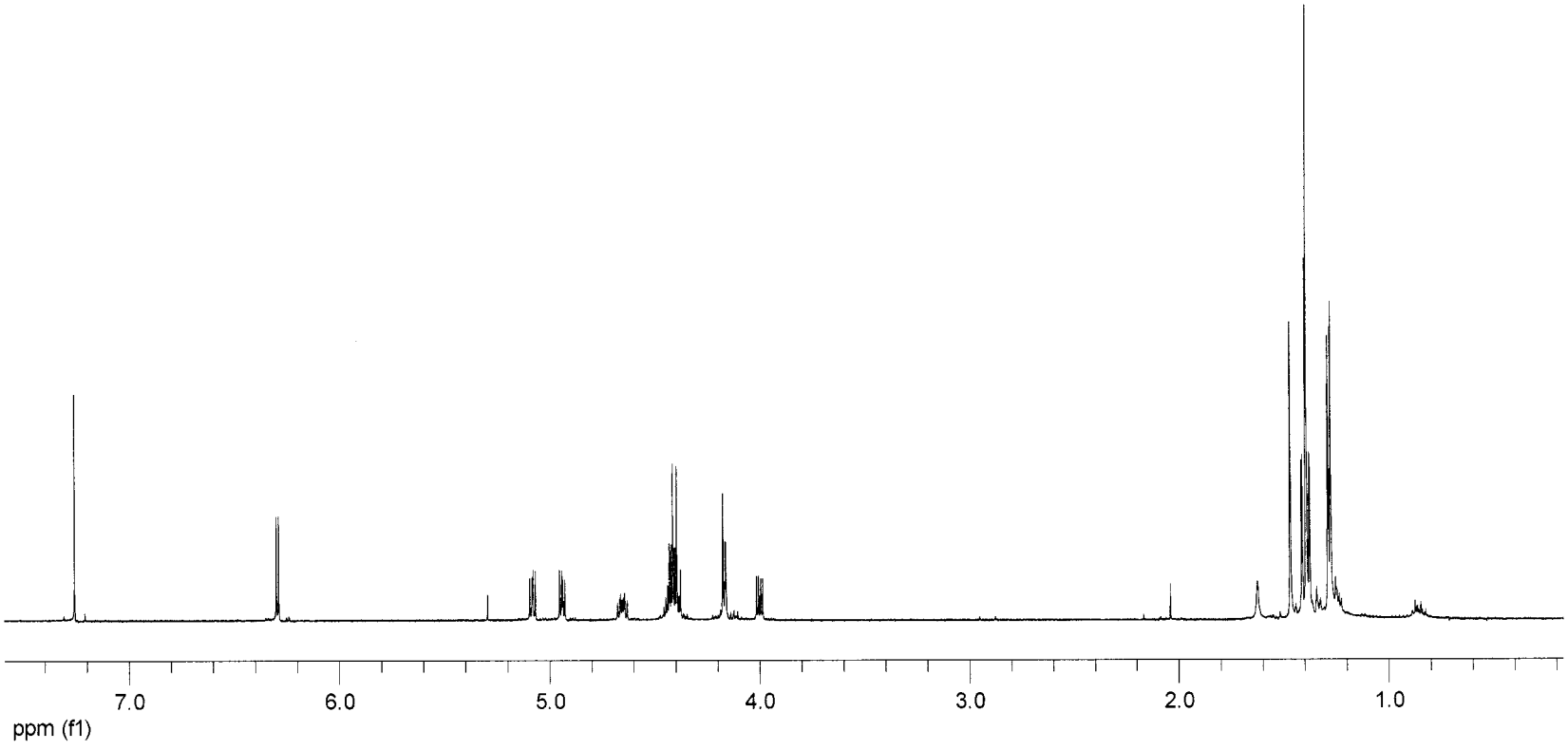

Figure 26: 400 MHz ^{1}H NMR spectrum of mannofuranosyl-1*H*-[1,2,3]triazol-4,5-dicarboxylic acid diethyl ester (**9**)

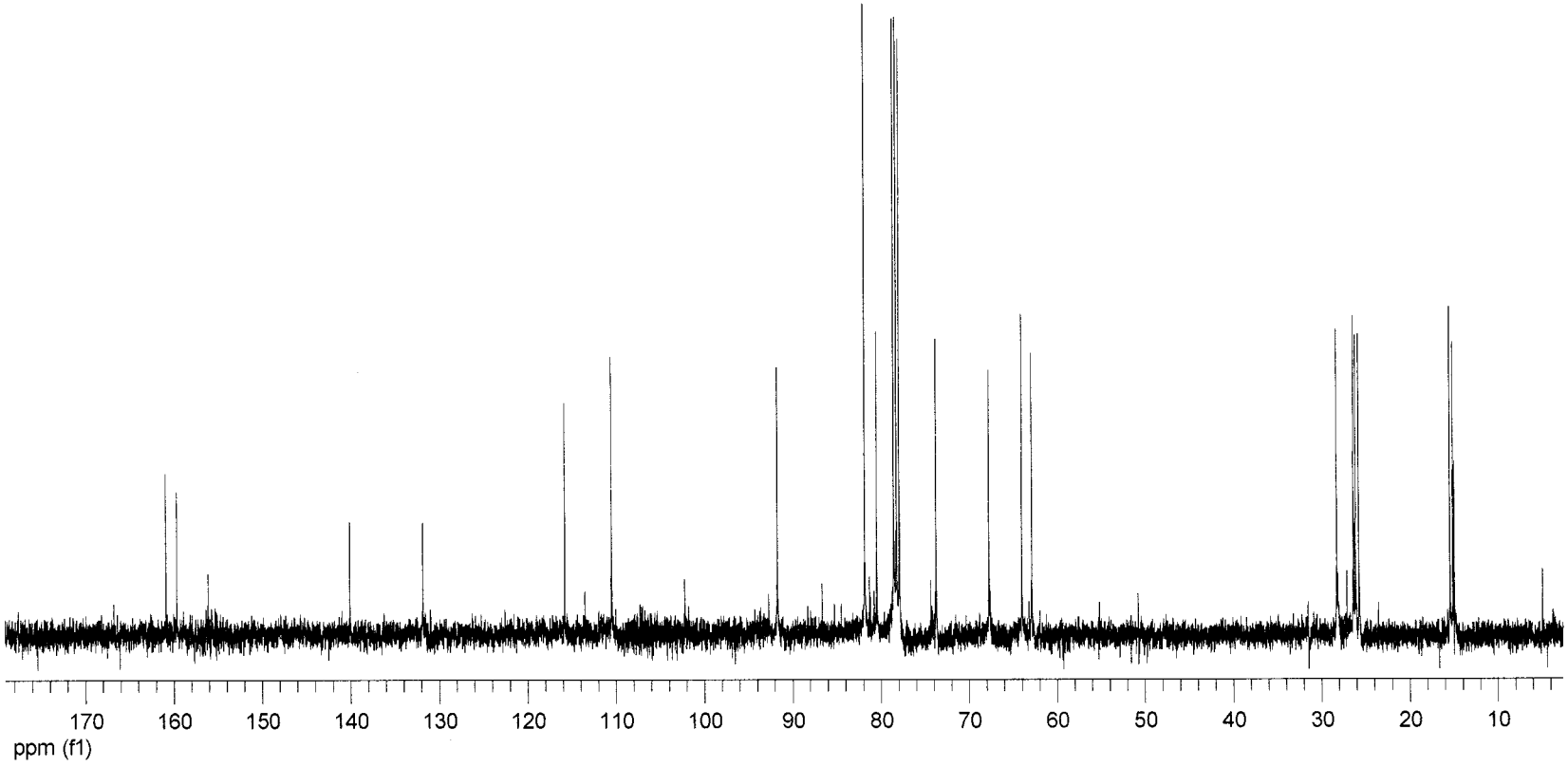

Figure 27: 100 MHz ^{13}C NMR spectrum of mannofuranosyl-1*H*-[1,2,3]triazol-4,5-dicarboxylic acid diethyl ester (**9**)

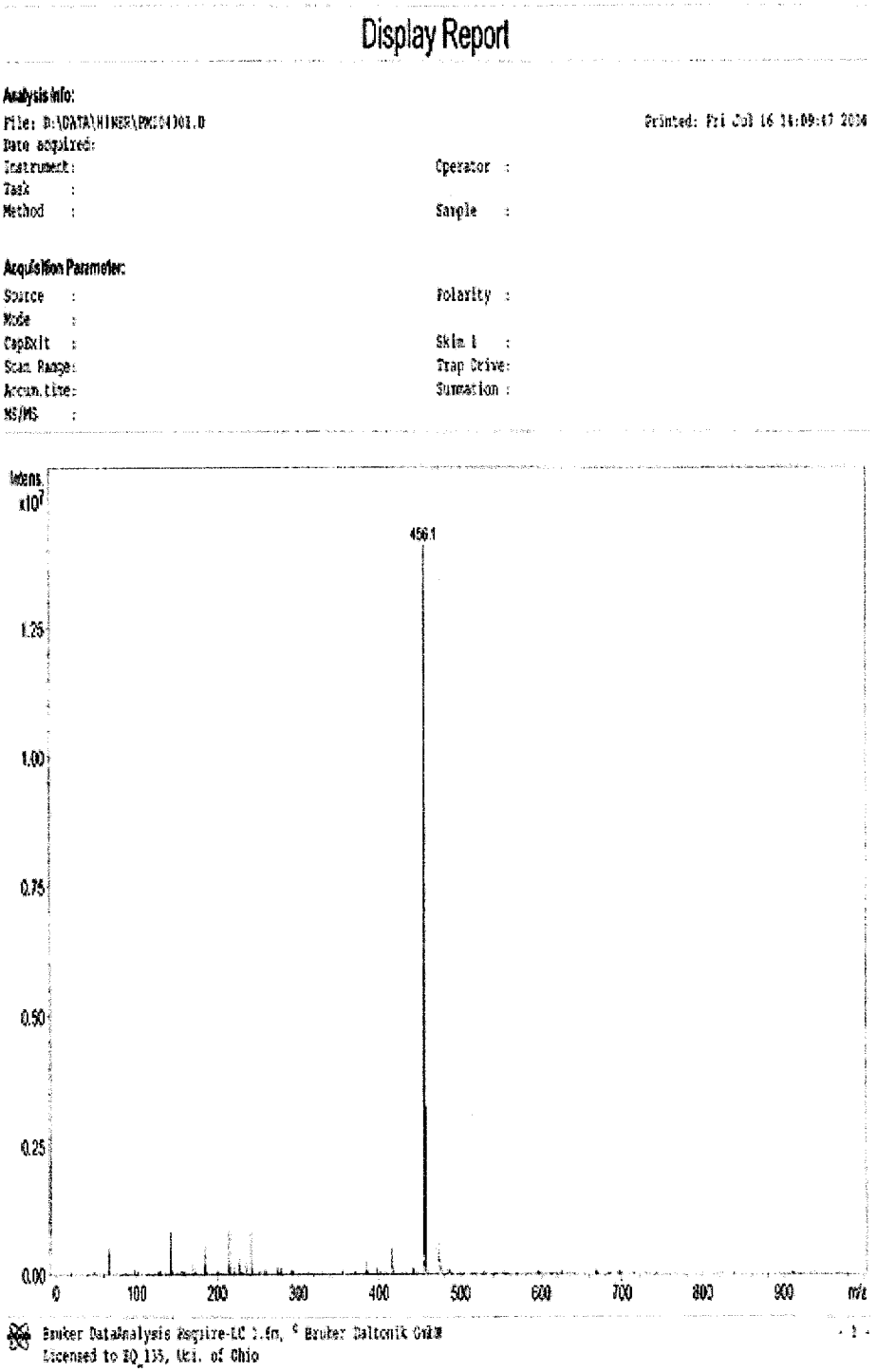

Figure 28: Mass spectrum of mannofuranosyl-1*H*-[1,2,3]triazol-4,5-dicarboxylic acid diethyl ester (**9**)

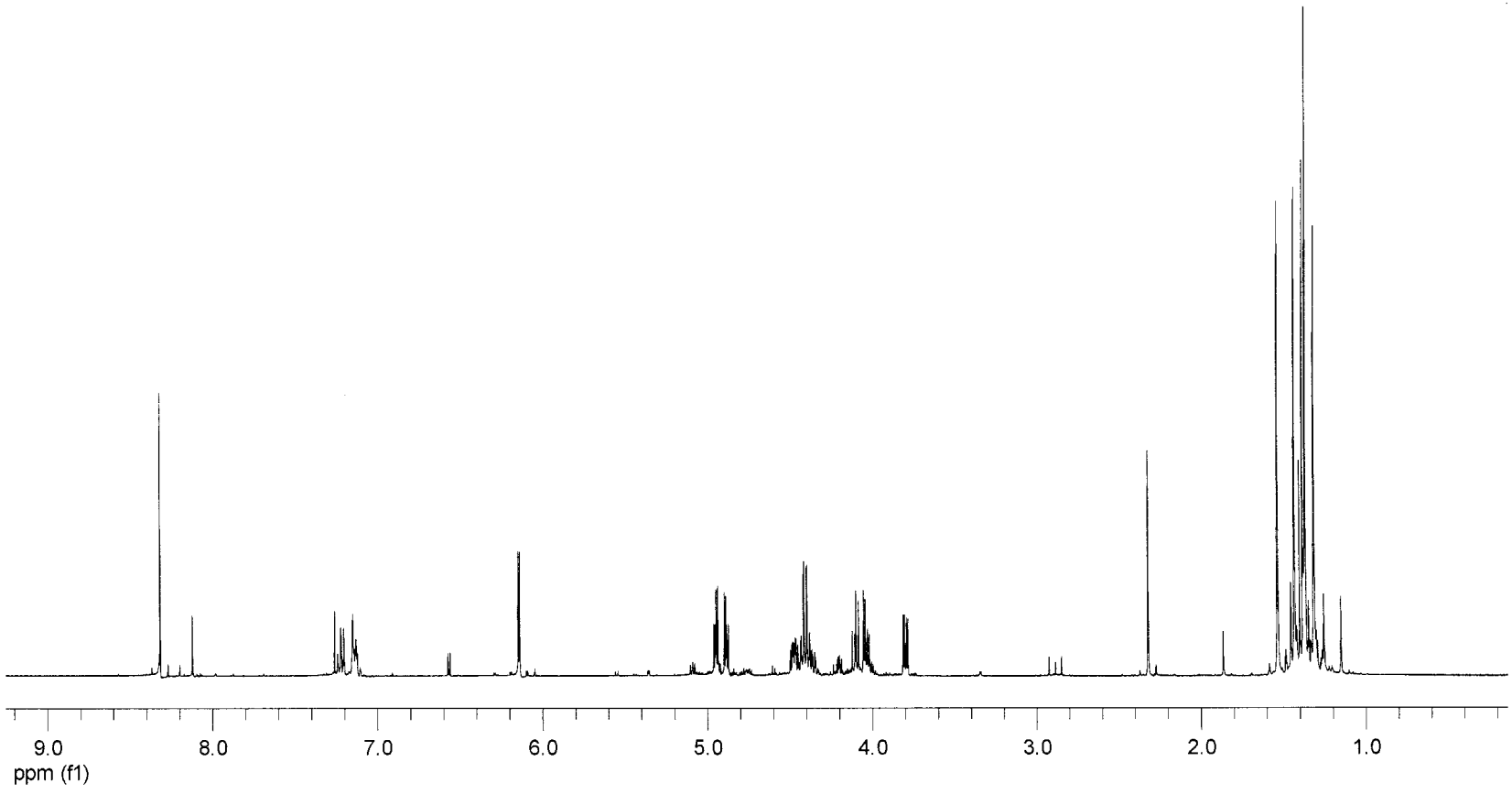

Figure 29: 400 MHz ^{1}H NMR spectrum of mannofuranosyl-1*H*-[1,2,3]triazol-4-(and 5-)-carboxylic acid ethyl esters (**10a/10b**)

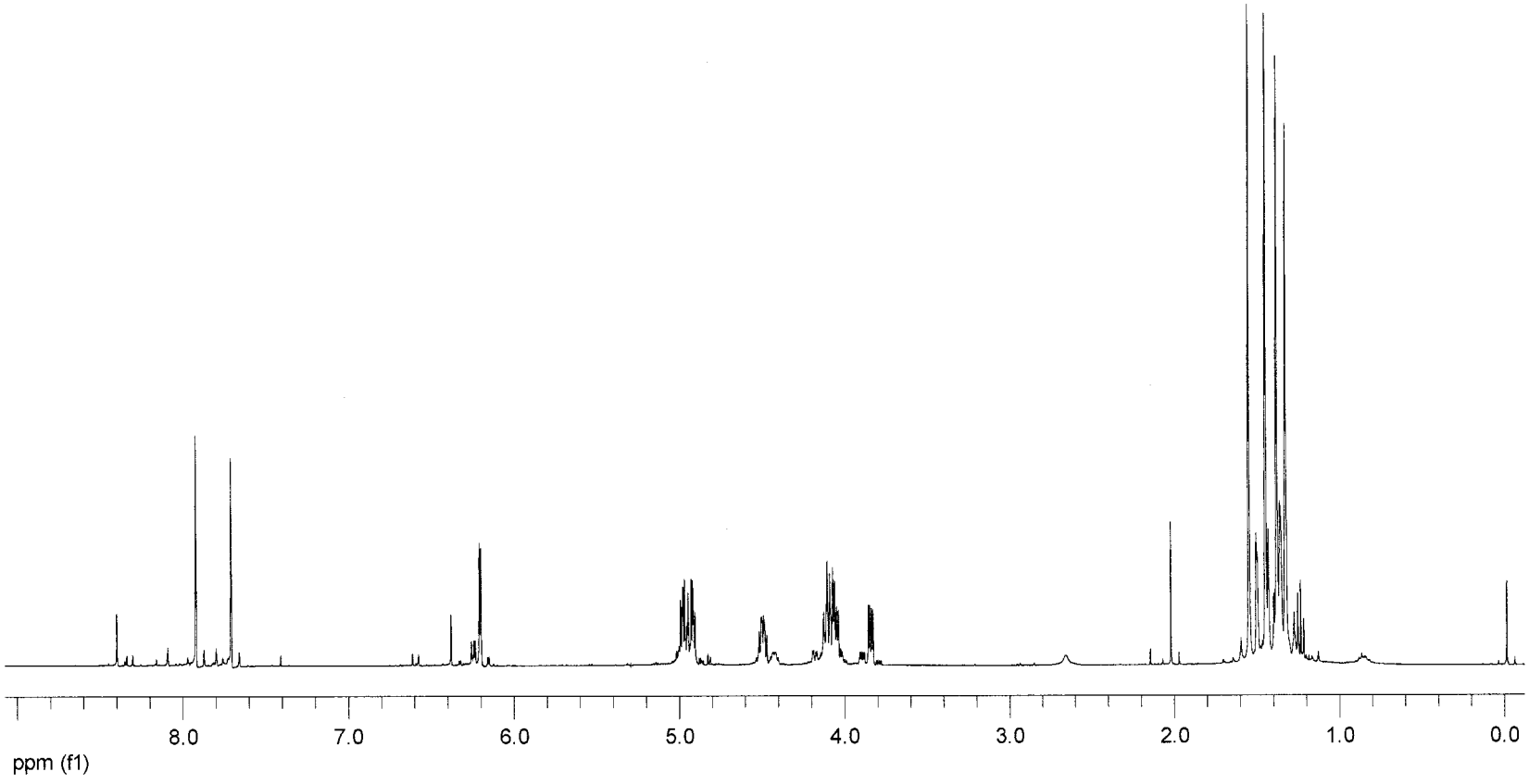

Figure 30: 400 MHz ^{1}H NMR spectrum of mannofuranosyl-1*H*-[1,2,3]triazol-4-(and 5-)-carboxylic acids (**11a/11b**)

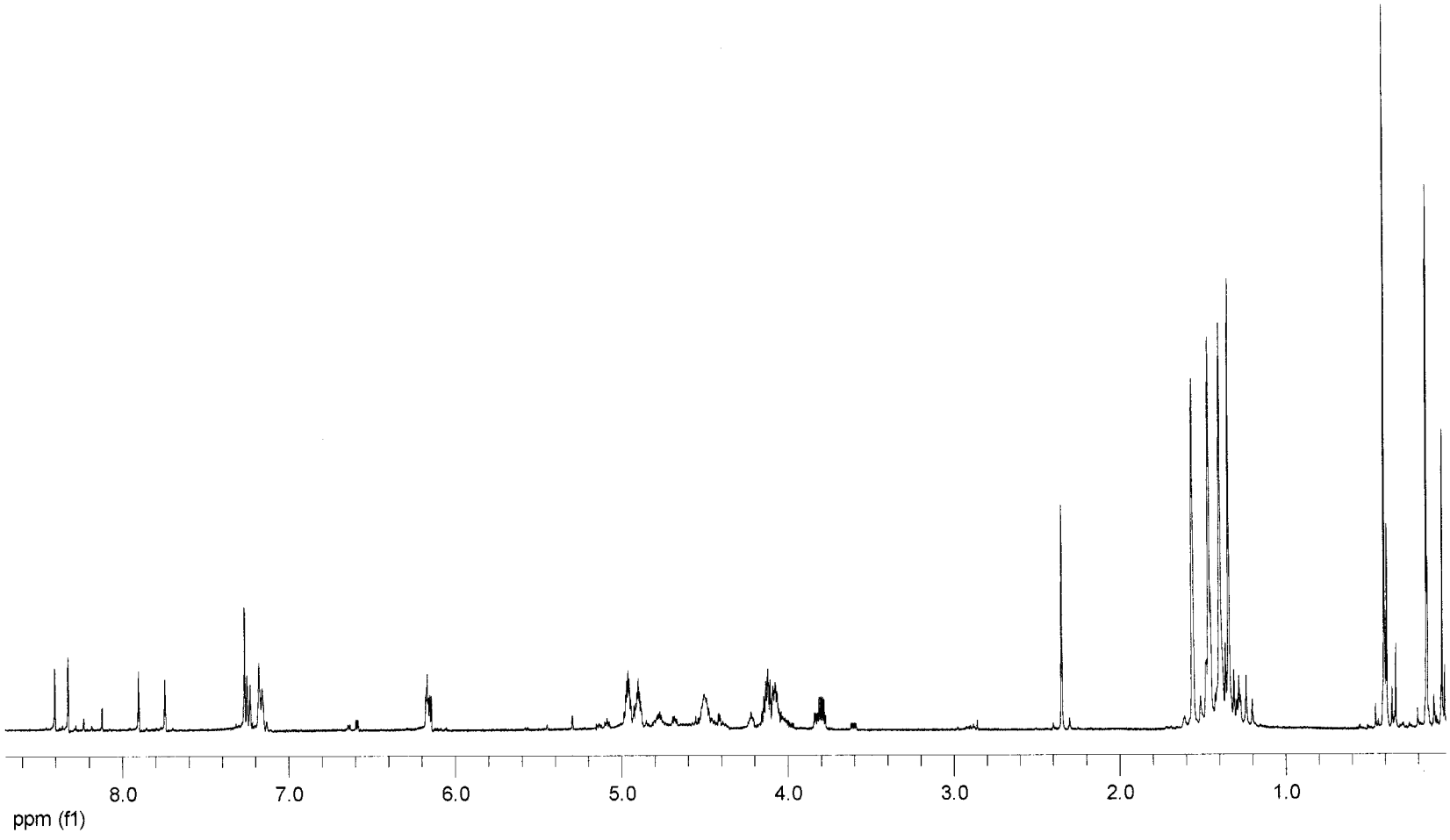

Figure 31: 400 MHz ^{1}H NMR spectrum of mannofuranosyl-1*H*-[1,2,3]triazol-4-(and 5-)-carboxylic acid trimethylsilyl esters (**12a/12b**)

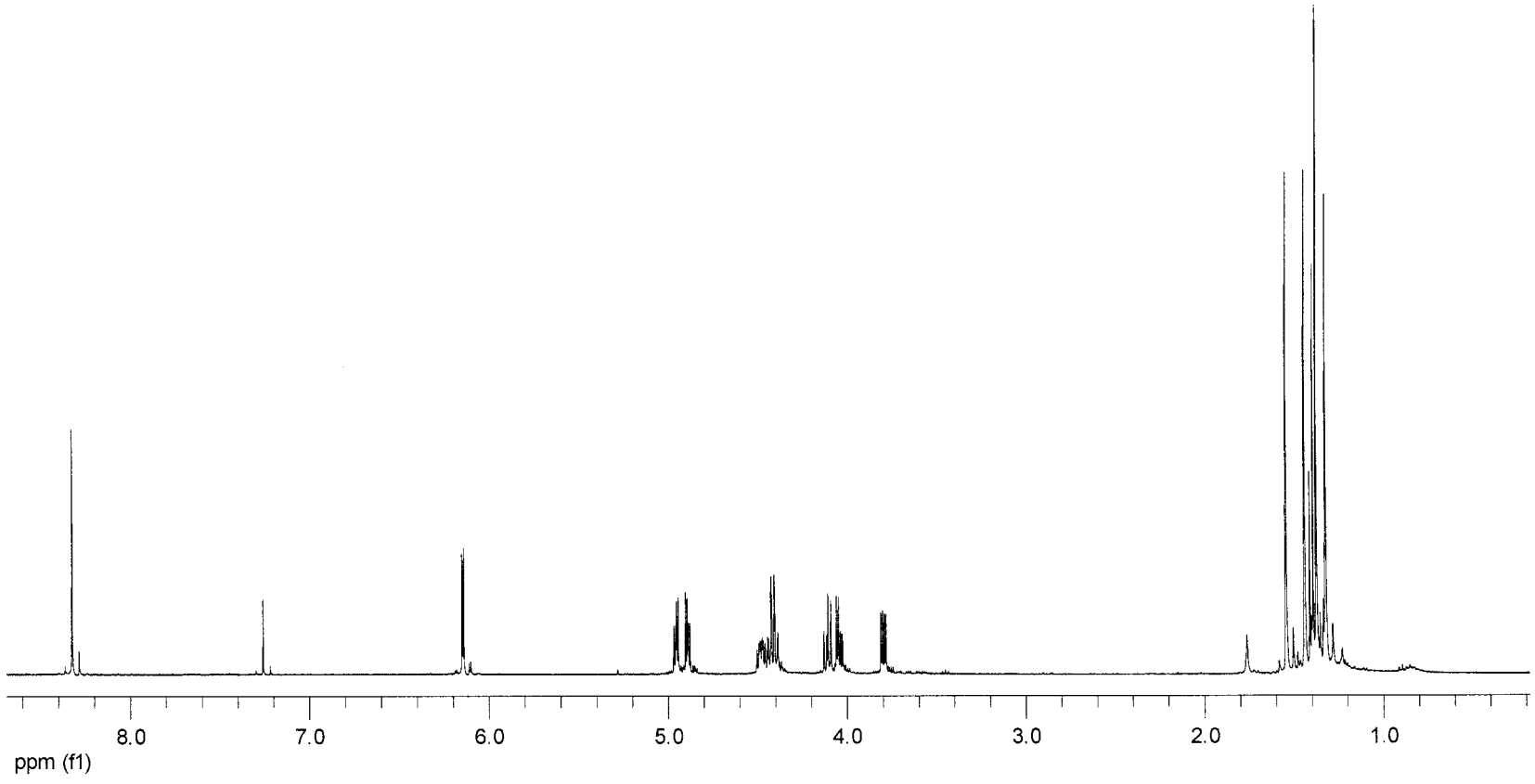

Figure 32: 400 MHz ^{1}H NMR spectrum of mannofuranosyl-1*H*-[1,2,3]triazol-4-carboxylic acid ethyl ester (**10a**)

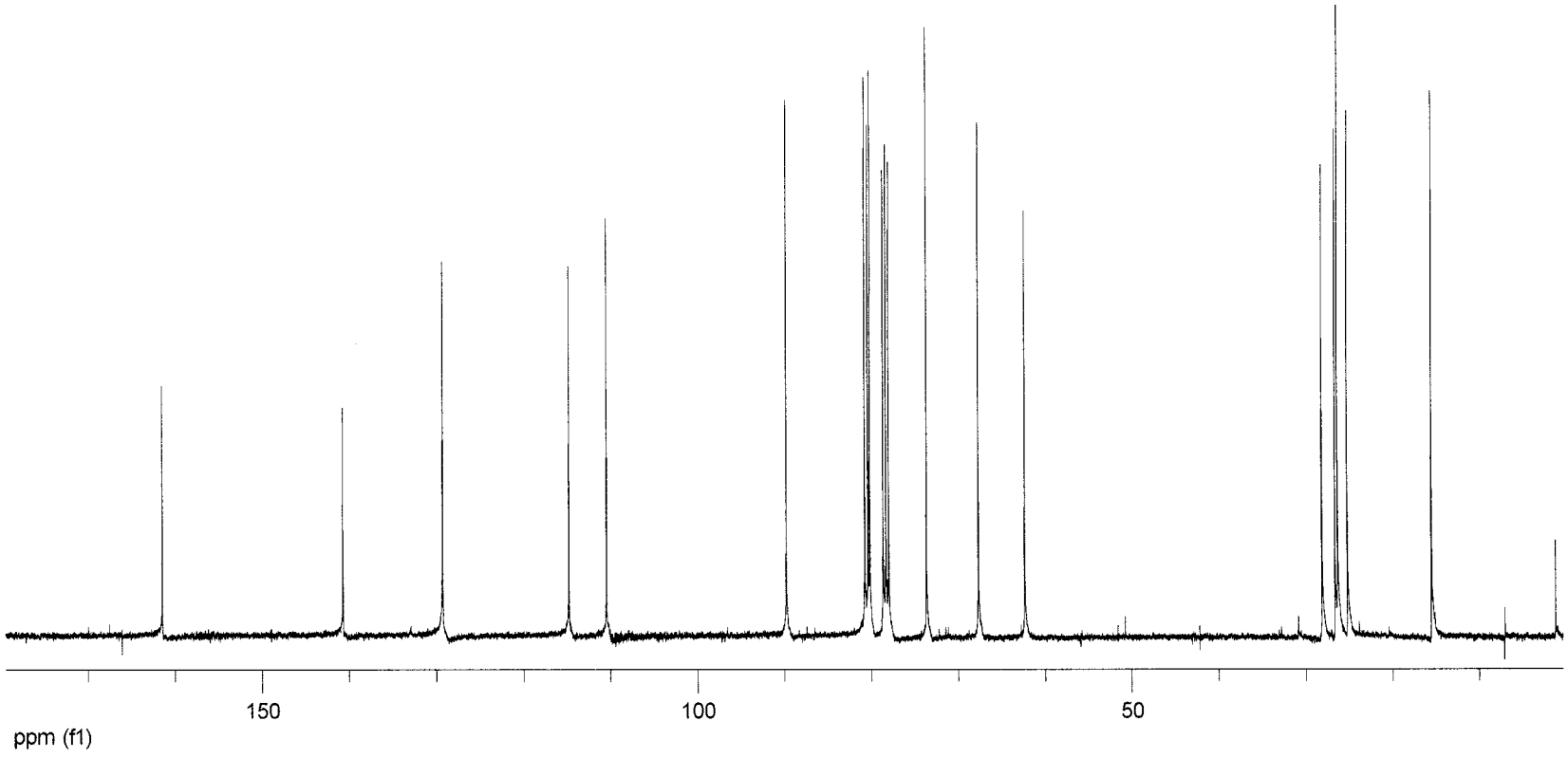

Figure 33: 100 MHz ^{13}C NMR spectrum of mannofuranosyl-1*H*-[1,2,3]triazol-4-carboxylic acid ethyl ester (**10a**)

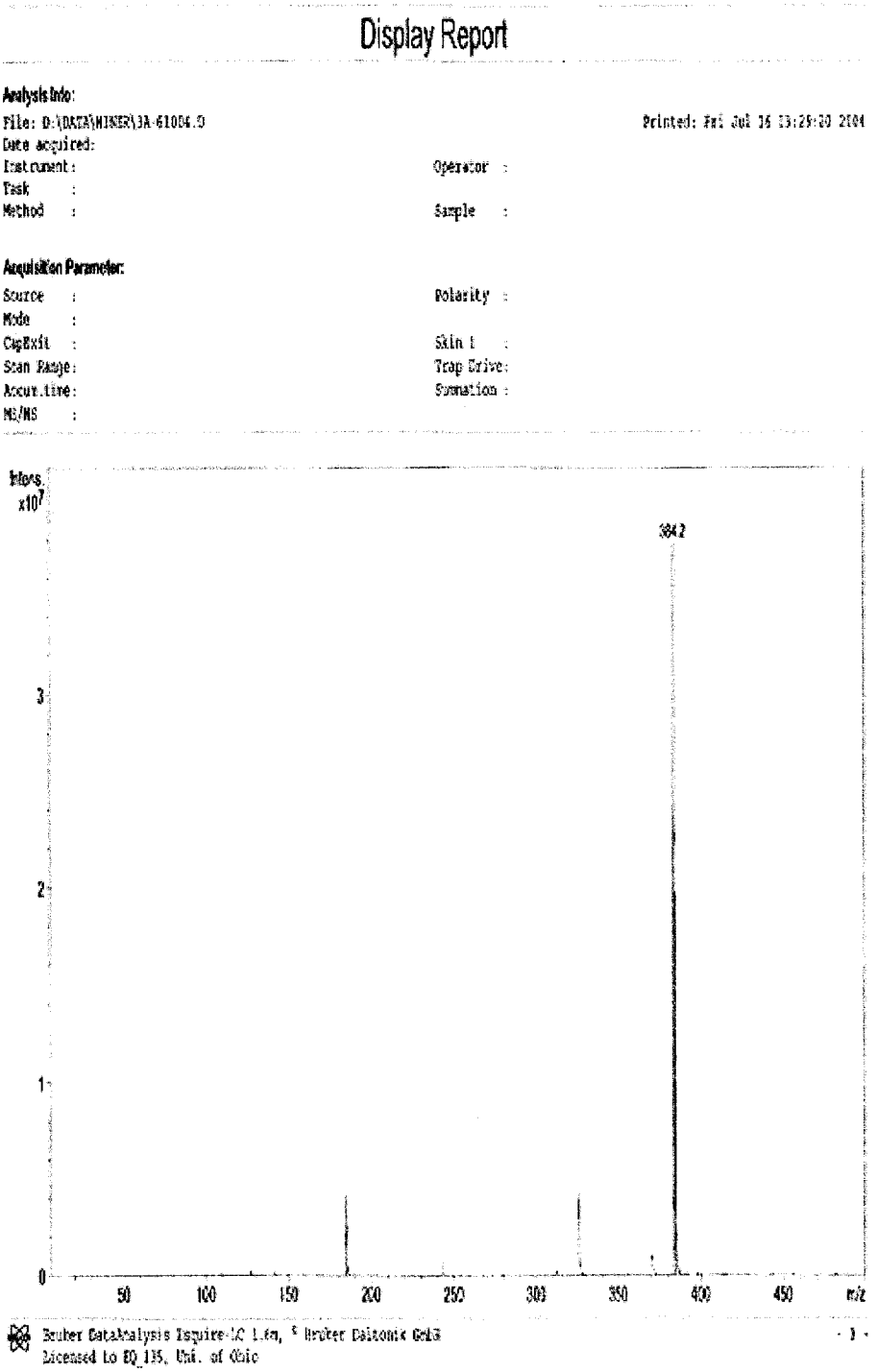

Figure 34: Mass spectrum of mannofuranosyl-1*H*-[1,2,3]triazol-4-carboxylic acid ethyl ester (**10a**)

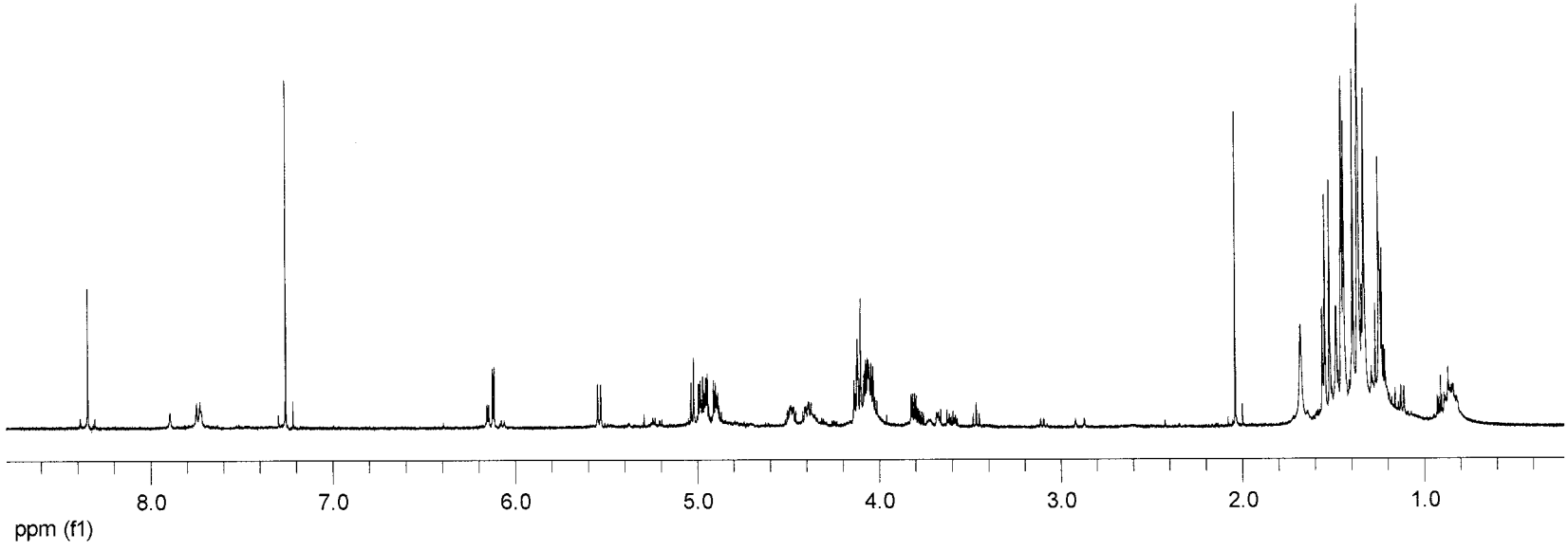

Figure 35: 400 MHz ^{1}H NMR spectrum of mannofuranosyl-1*H*-[1,2,3]triazol-4-carboxylic acid (**11a**)

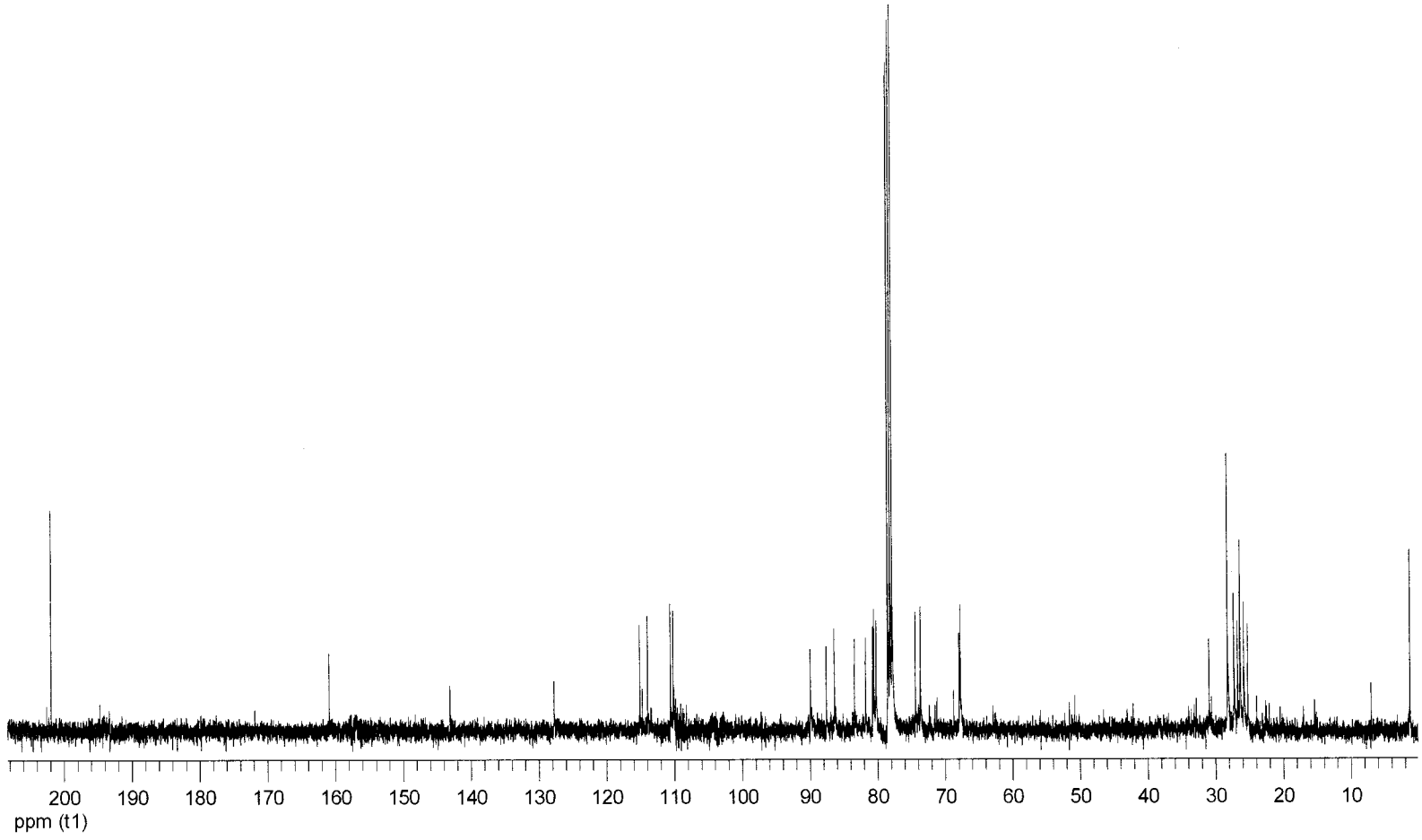

Figure 36: 100 MHz ^{13}C NMR spectrum of mannofuranosyl-1*H*-[1,2,3]triazol-4-carboxylic acid (**11a**)

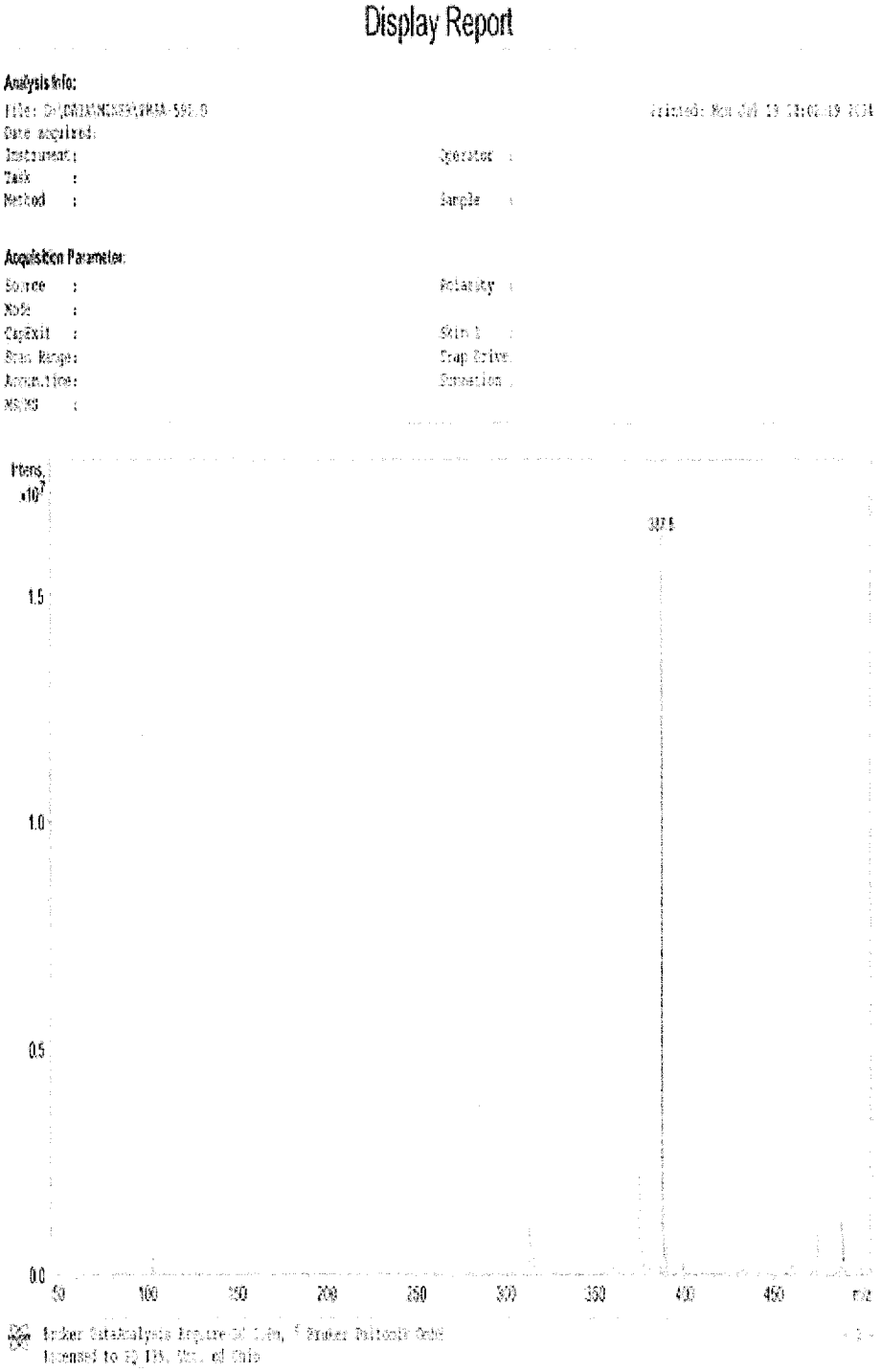

Figure 37: Mass spectrum of mannofuranosyl-1*H*-[1,2,3]triazol-4-carboxylic acid (**11a**)

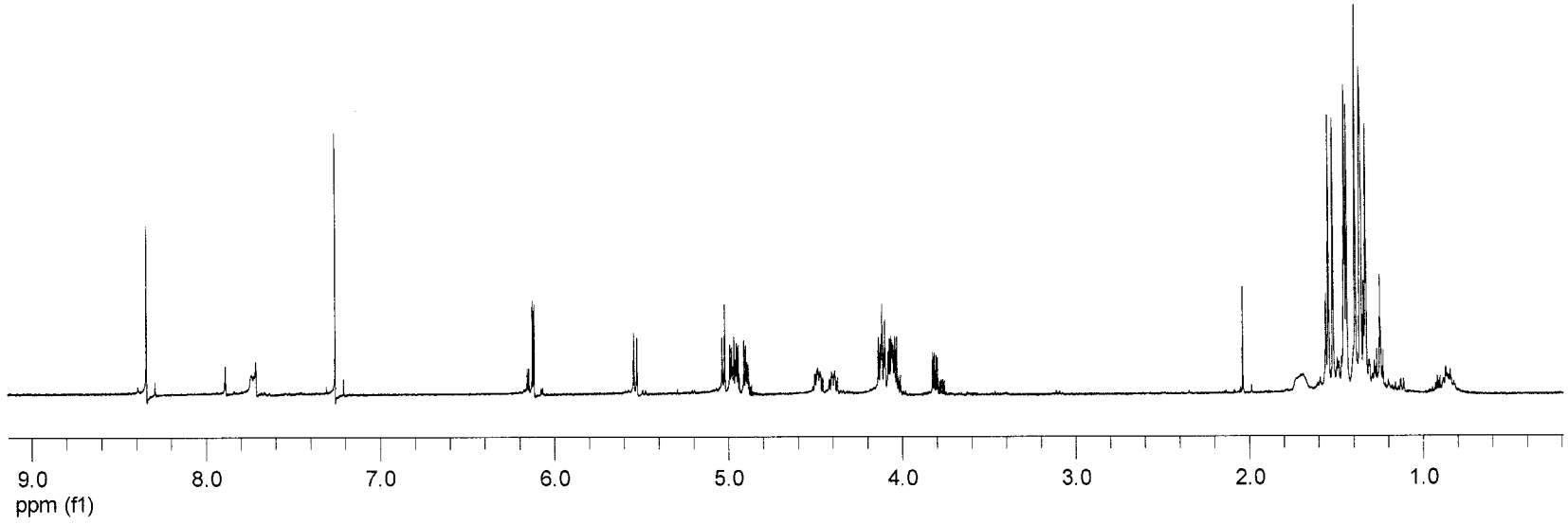

Figure 38: 400 MHz ^{1}H NMR spectrum of mannofuranosyl-1*H*-[1,2,3]triazol-4-carboxylic acid trimethylsilyl ester (**12a**)

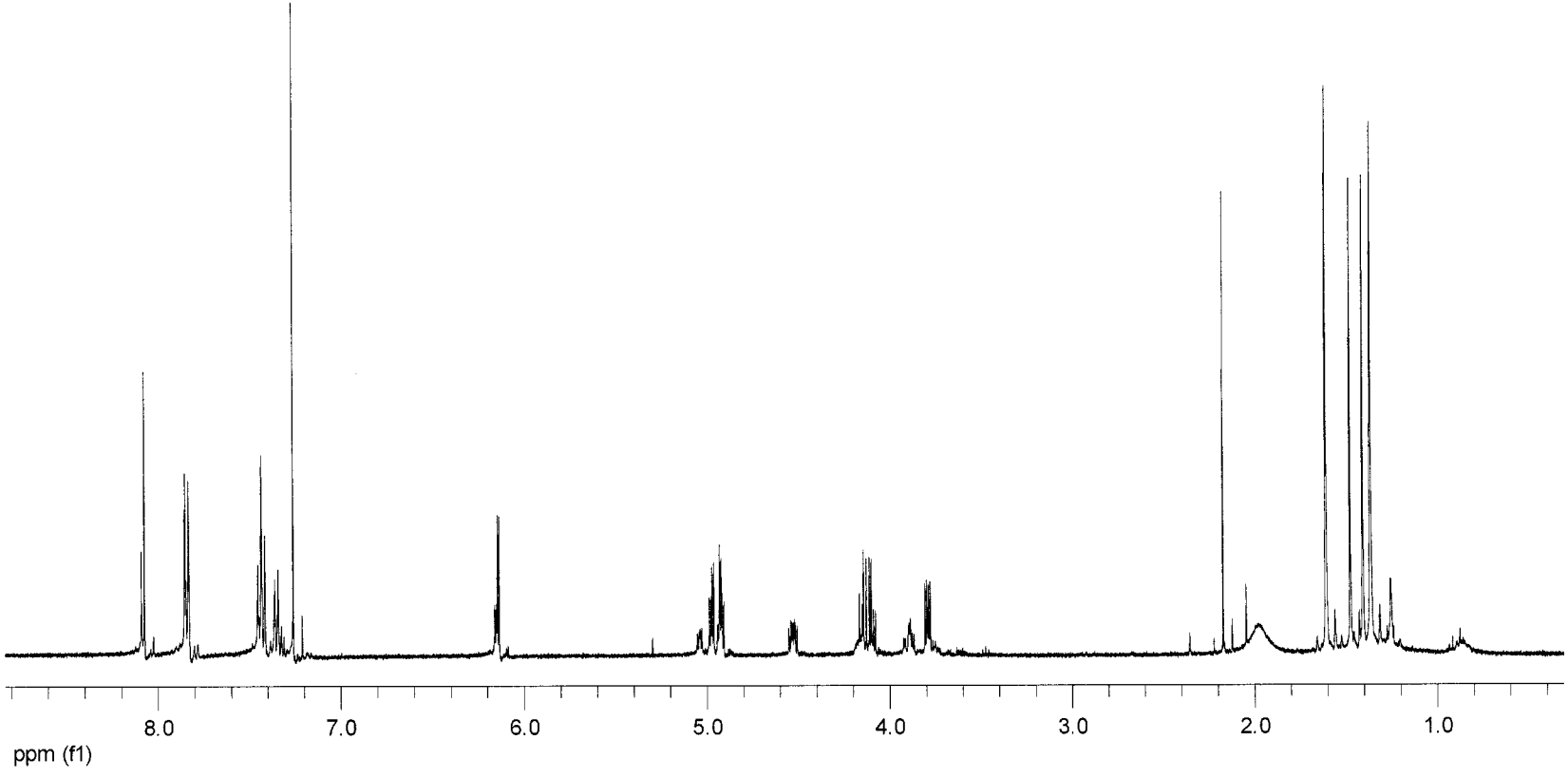

Figure 39: 400 MHz ^{1}H NMR spectrum of mannofuranosyl-4-phenyl-1*H*-[1,2,3]triazole (**13a**)

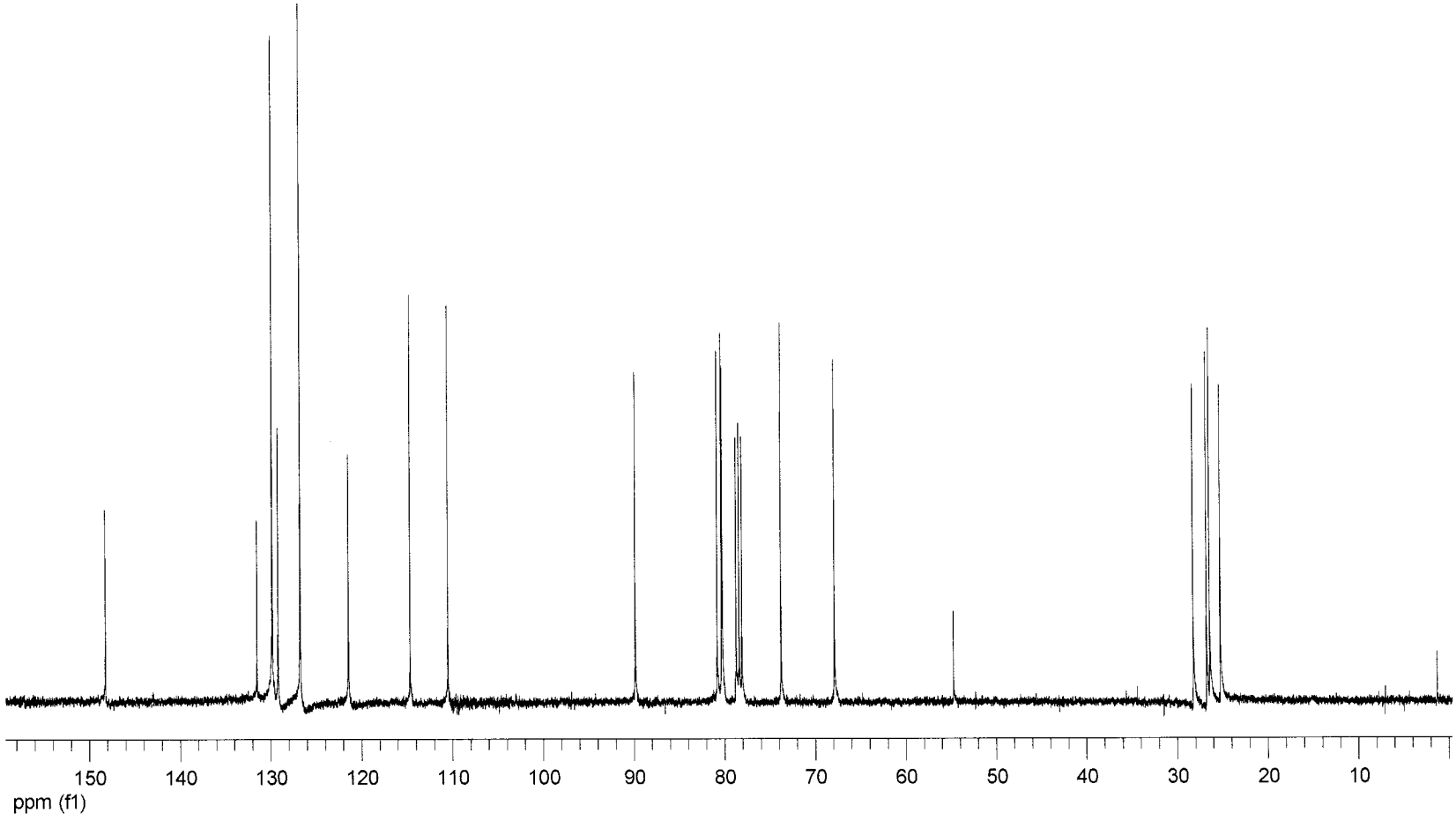

Figure 40: 100 MHz ^{13}C NMR spectrum of mannofuranosyl-4-phenyl-1*H*-[1,2,3]triazole (**13a**)

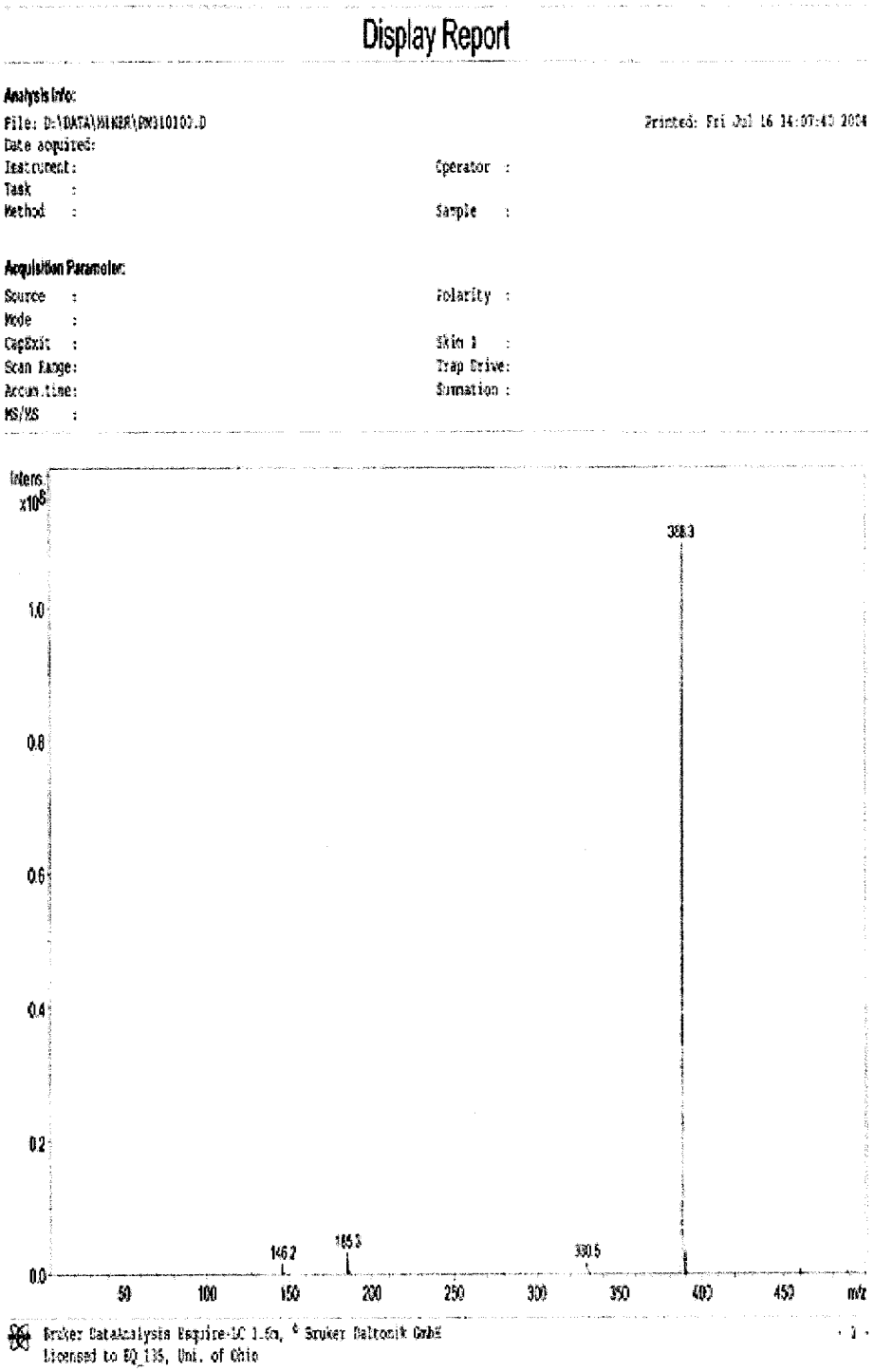

Figure 41: Mass spectrum of mannofuranosyl-4-phenyl-1*H*-[1,2,3]triazole (**13a**)

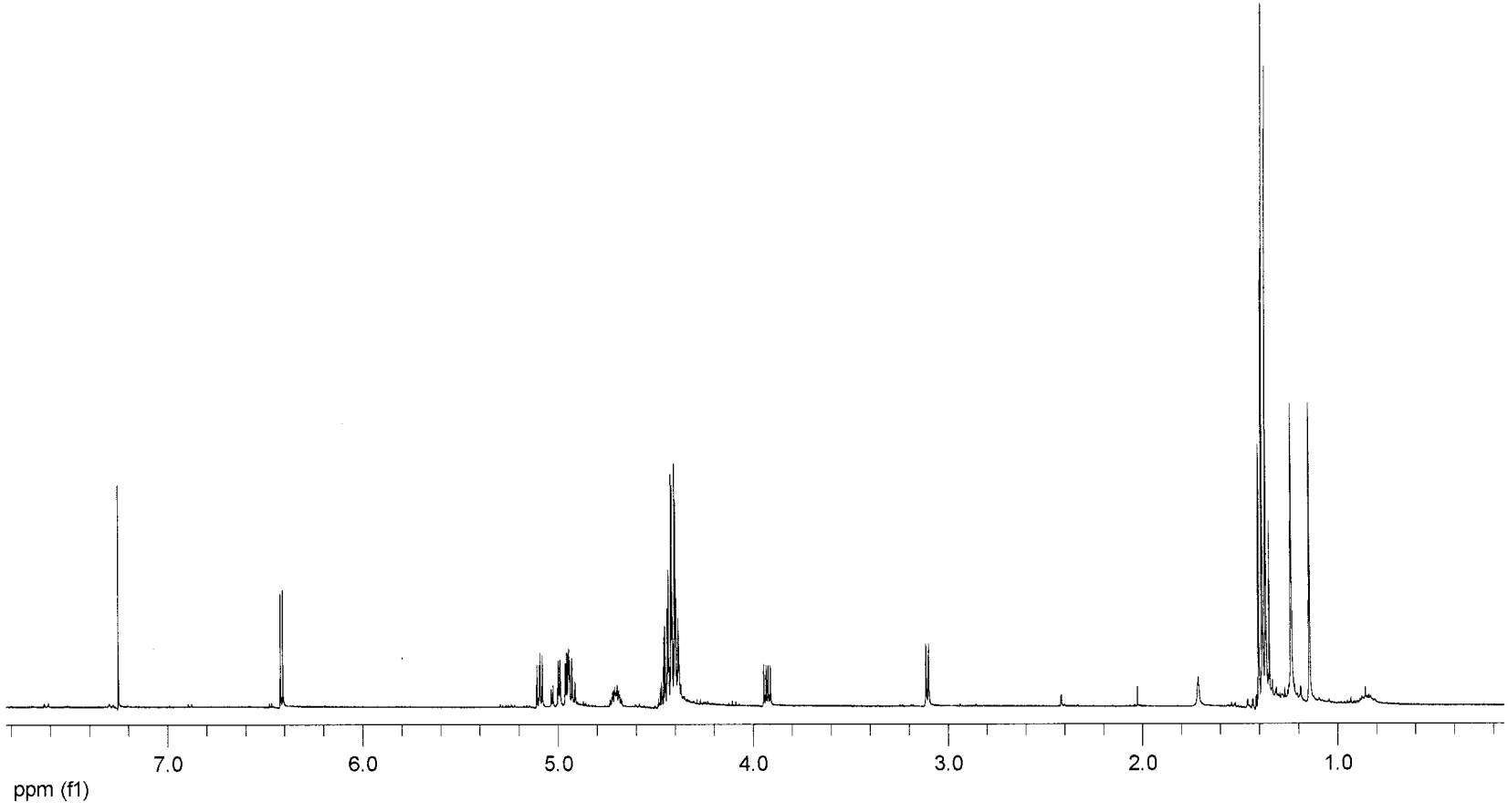

Figure 42: 400 MHz ^{1}H NMR spectrum of mannofuranosyl-1,6-*H*-[1,2,3]triazol-4,5-dicarboxylic acid diethyl esters (**14**)

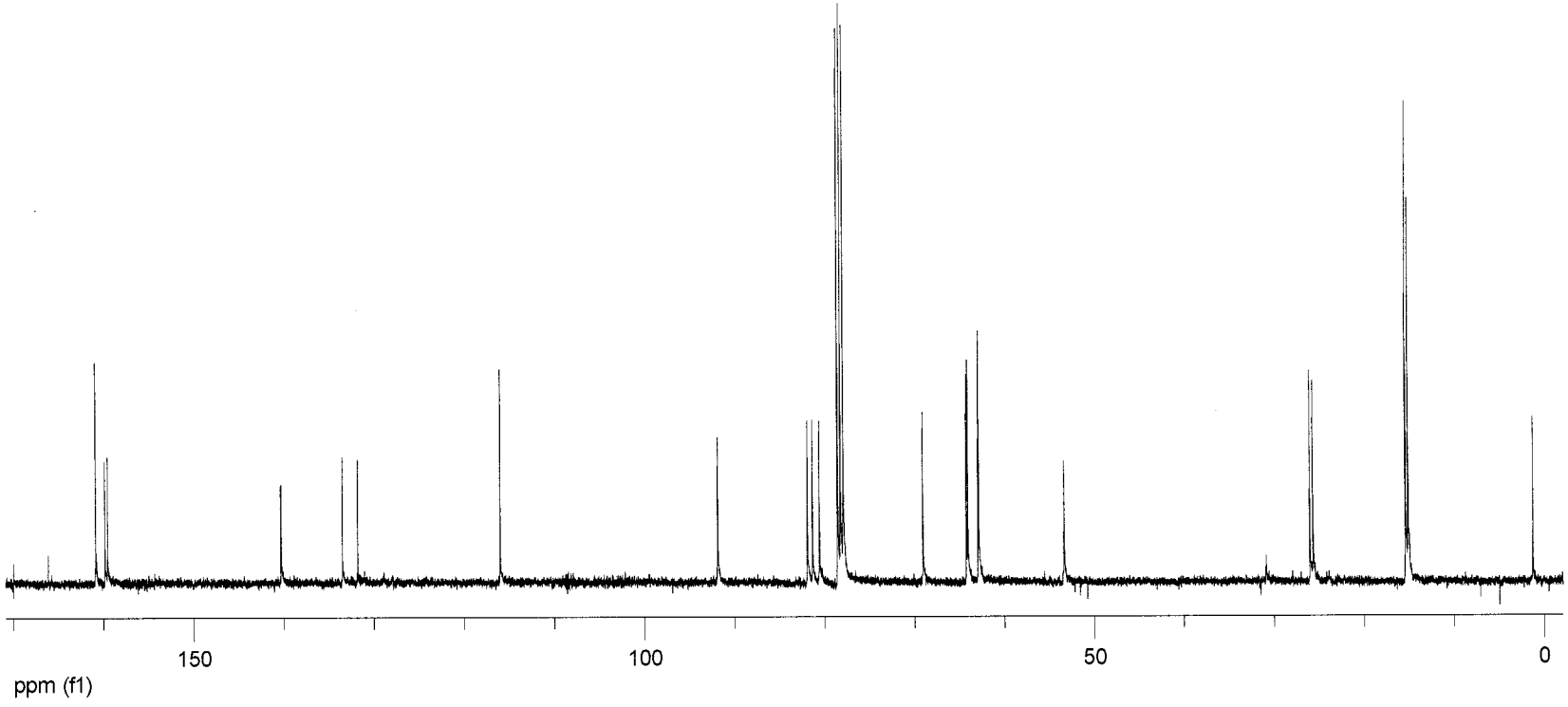

Figure 43: 400 MHz ^{13}C NMR spectrum of mannofuranosyl-1,6-*H*-[1,2,3]triazol-4,5-dicarboxylic acid diethyl esters (**14**)

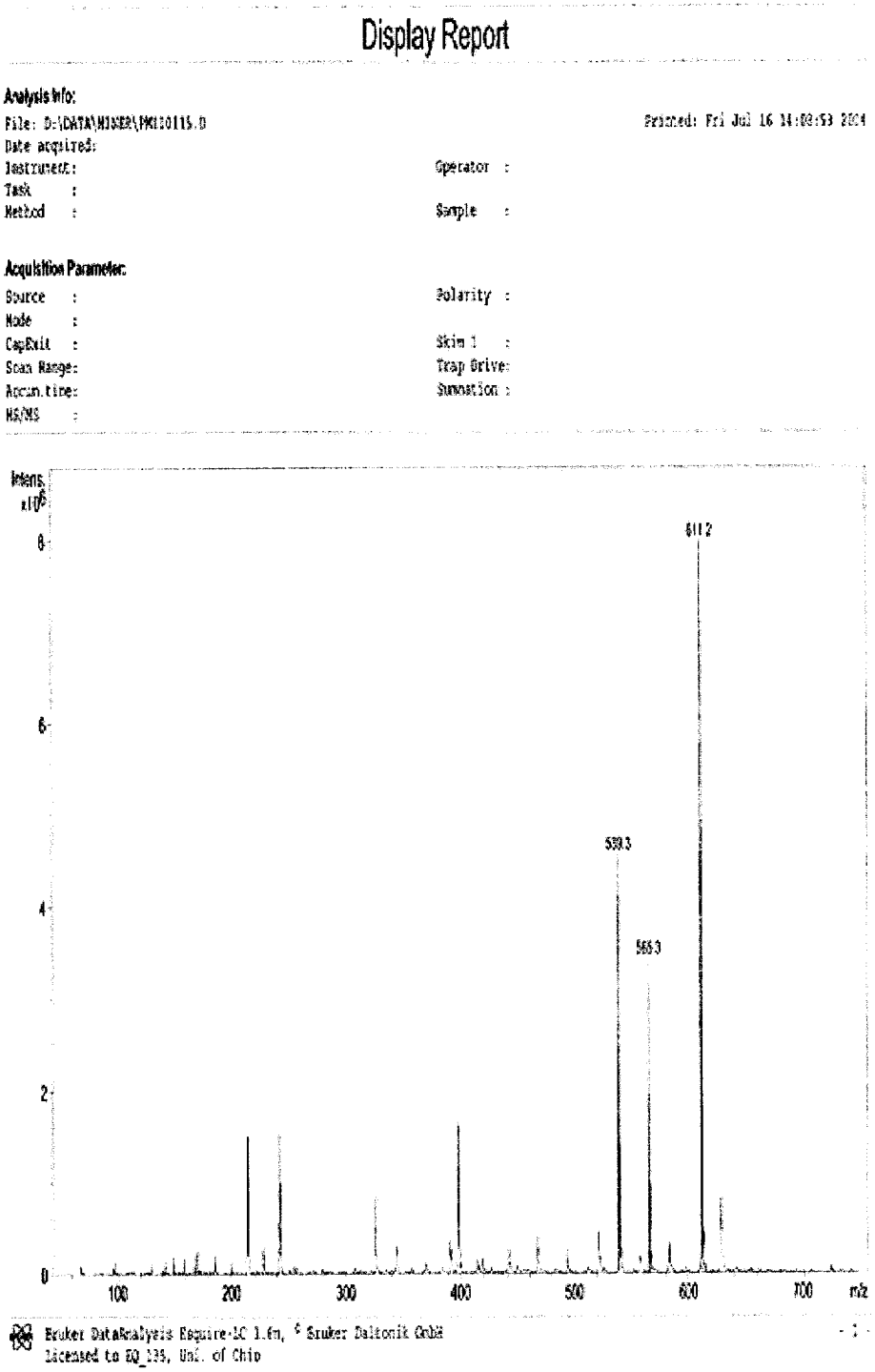

Figure 44: Mass spectrum of mannofuranosyl-1,6-1*H*-[1,2,3]triazol-4,5-dicarboxylic acid diethyl esters (**14**)

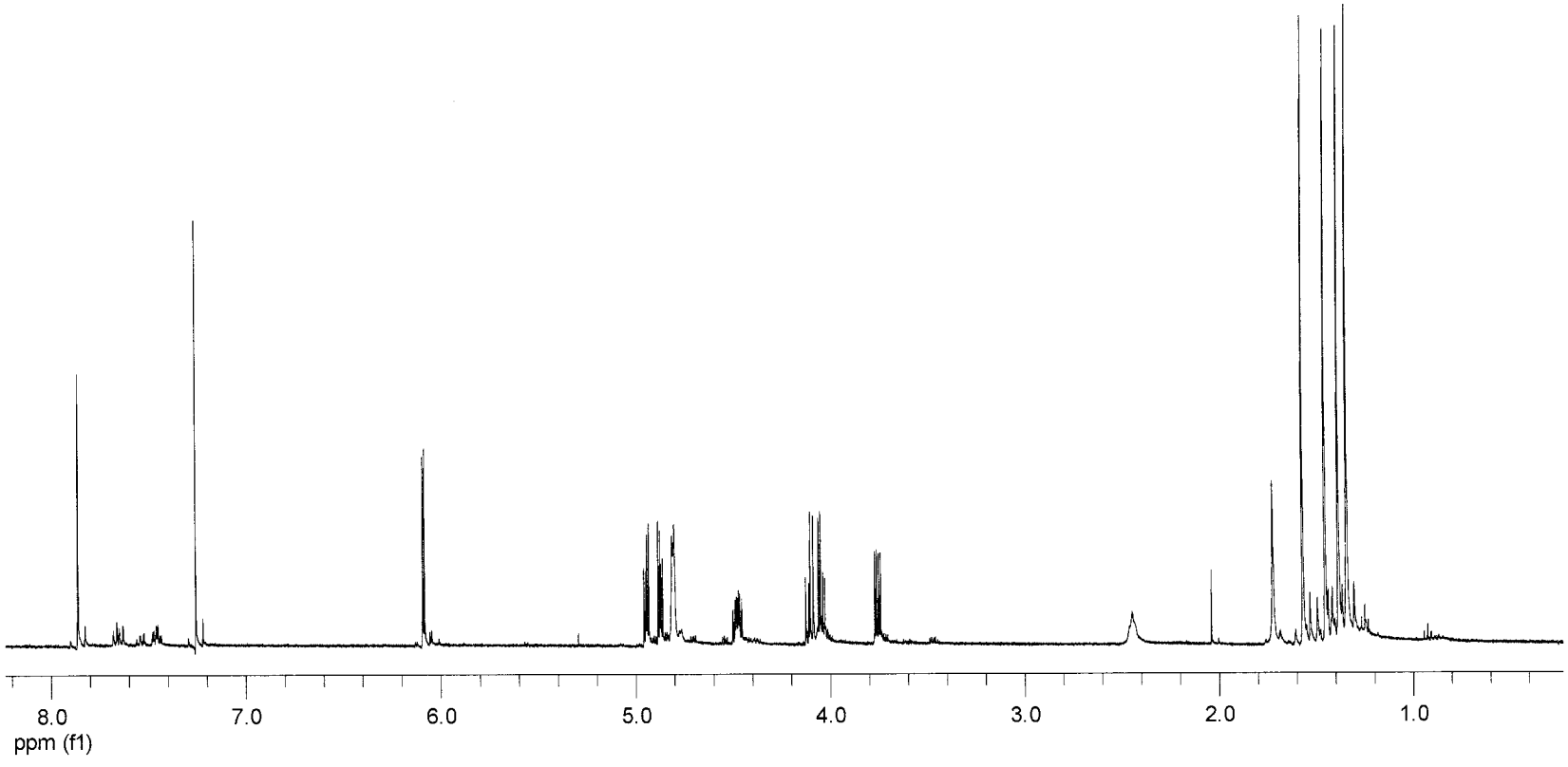

Figure 45: 400 MHz ^{1}H NMR spectrum of mannofuranosyl-1*H*-[1,2,3]triazol-4-yl methanol (**15**)

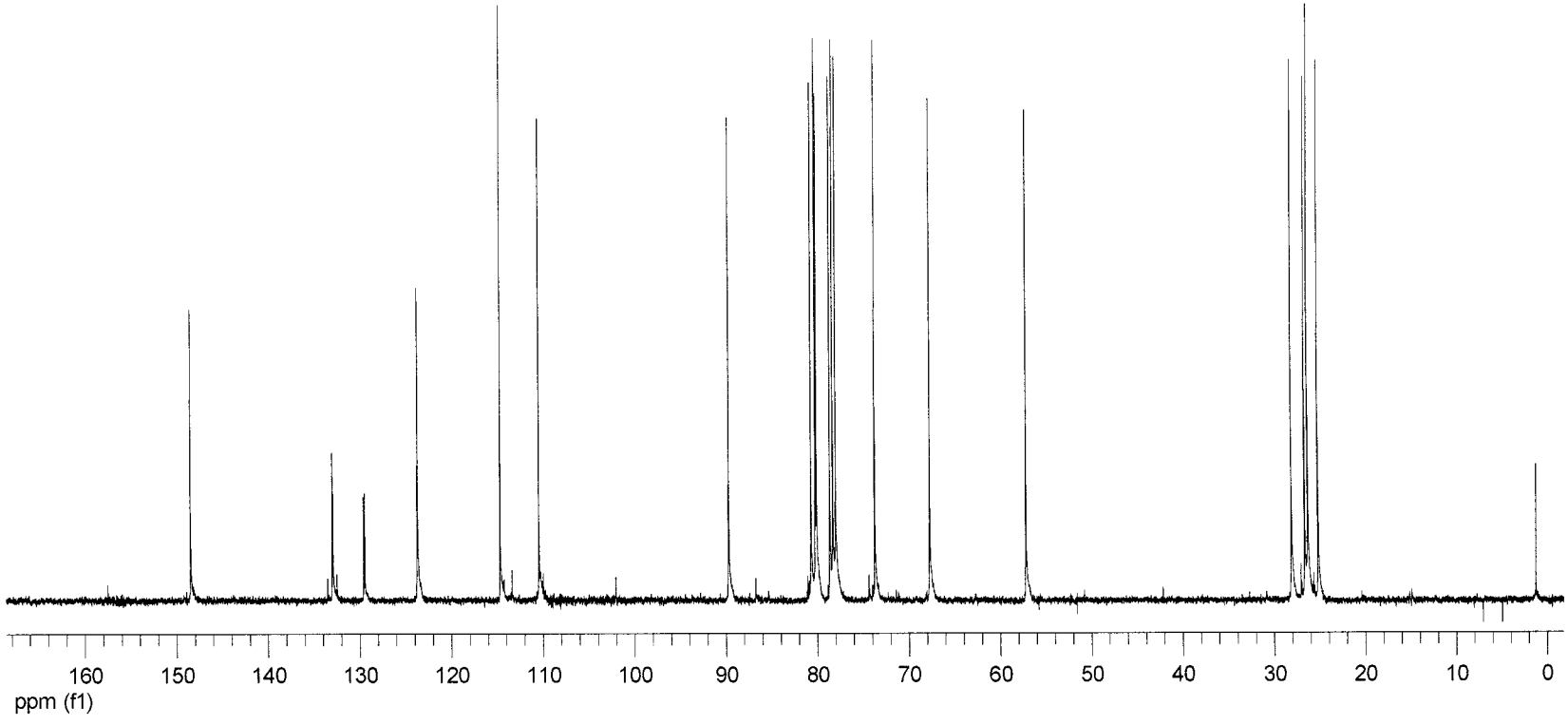

Figure 46: 100 MHz ^{13}C NMR spectrum of mannofuranosyl-1*H*-[1,2,3]triazol-4-yl methanol (**15**)

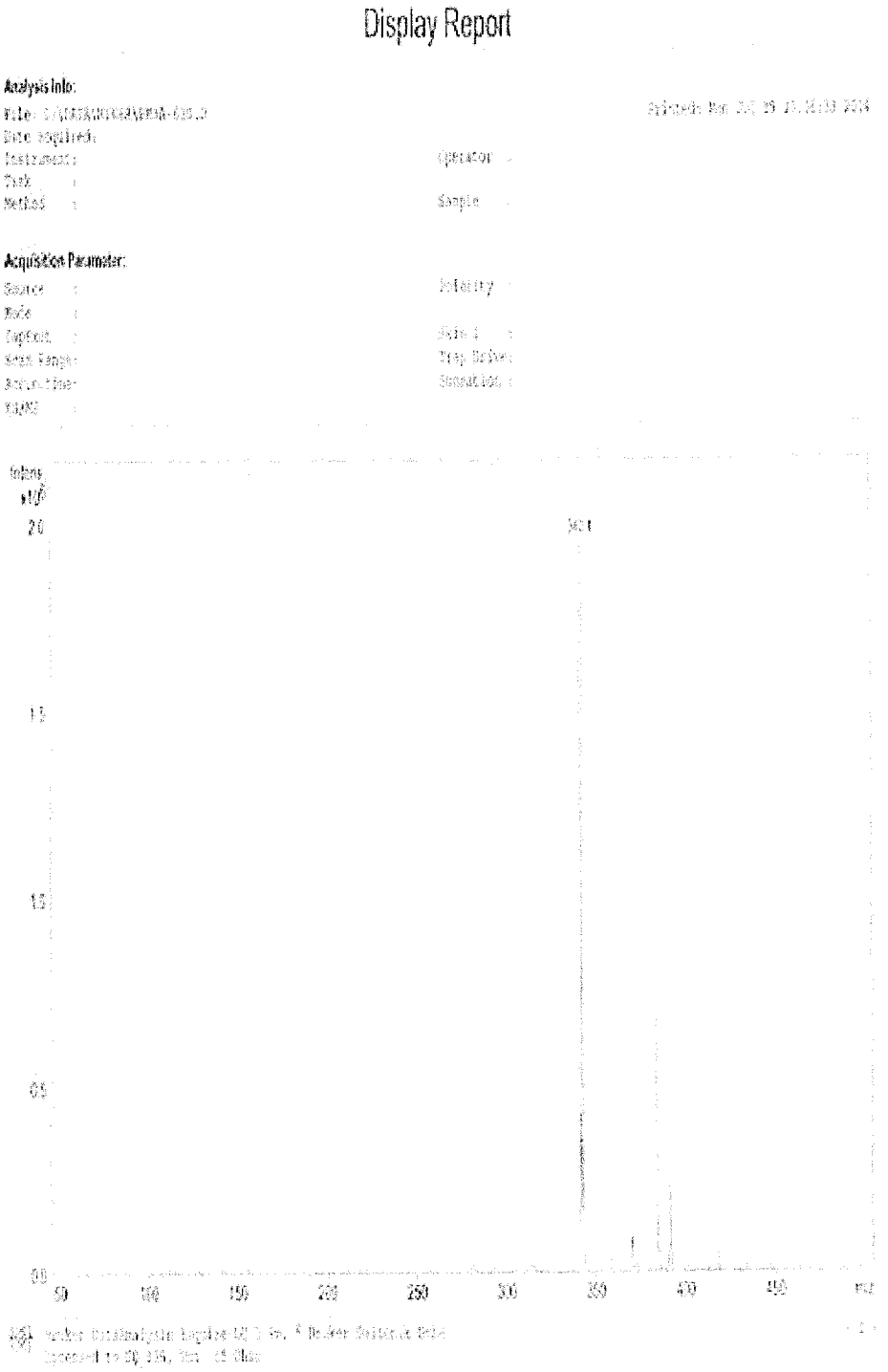

Figure 47: 100 MHz ^{13}C NMR spectrum of mannofuranosyl-1*H*-[1,2,3]triazol-4-yl methanol (**15**)

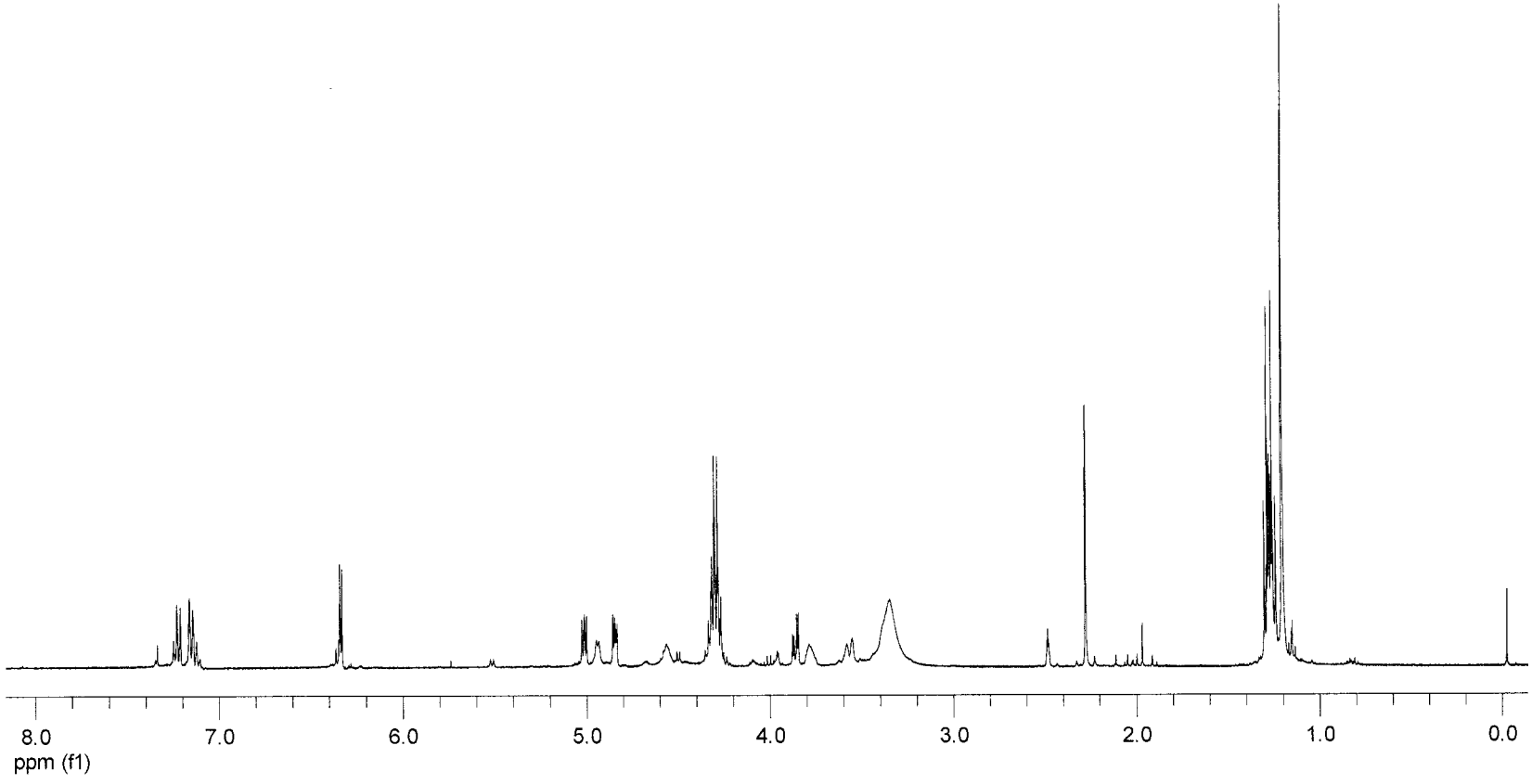

Figure 48: 400 MHz ^{1}H NMR spectrum of 1-(2,3-*O*-isopropylidene-β-D-mannofuranosyl)-1*H*-[1,2,3]triazol-4,5-dicarboxylic acid diethyl ester (**16**)

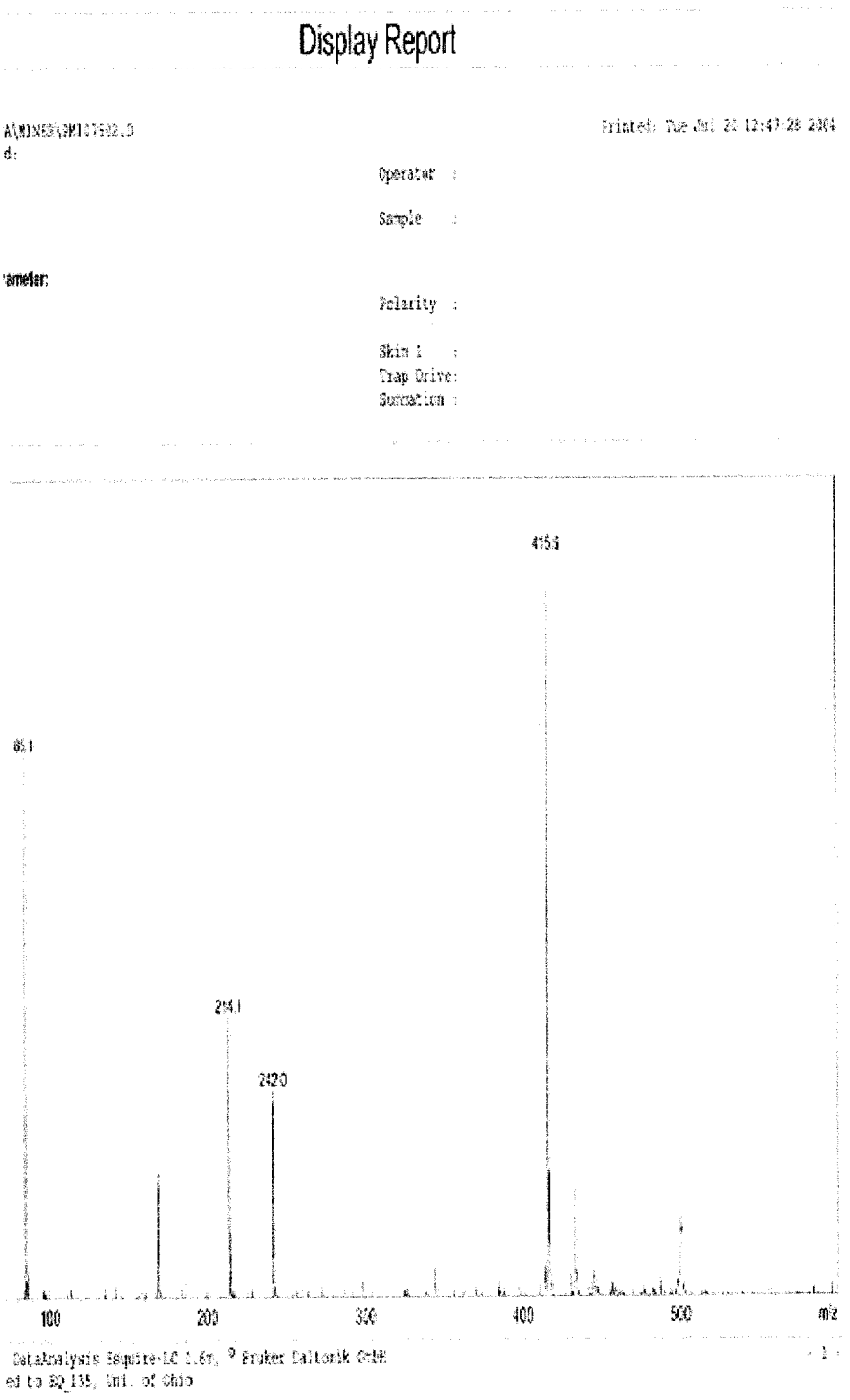

Figure 49: Mass spectrum of 1-(2,3-*O*-isopropylidene-β-D-mannofuranosyl)-1*H*-[1,2,3]triazol-4,5-dicarboxylic acid diethyl ester **(16)**

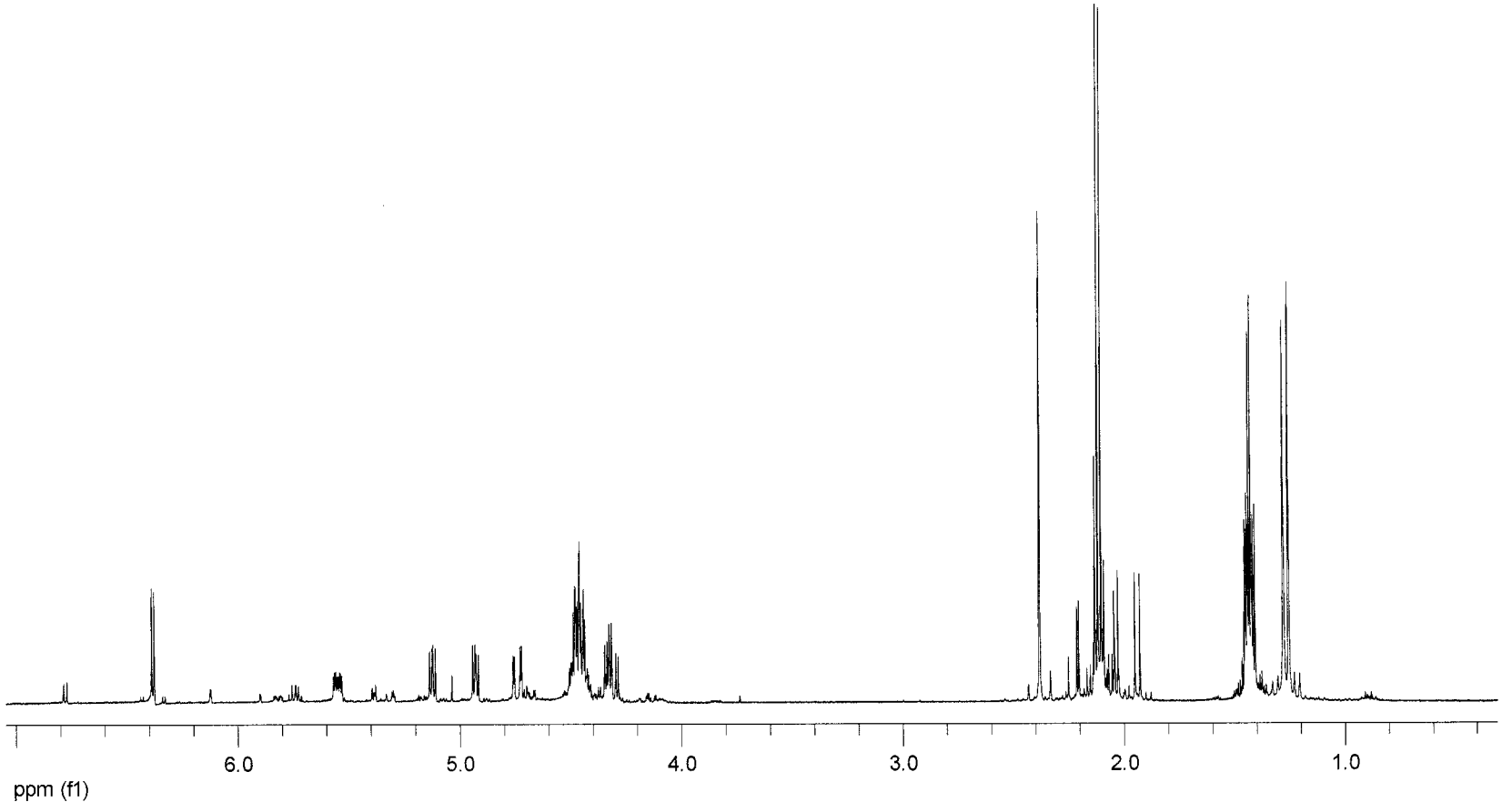

Figure 50: 400 MHz ^{1}H NMR spectrum of 1-(5,6-di-*O*-acetyl-2,3-*O*-isopropylidene-β-D-mannofuranosyl)-1*H*-[1,2,3]triazol-4,5-dicarboxylic acid diethyl ester (**17**)

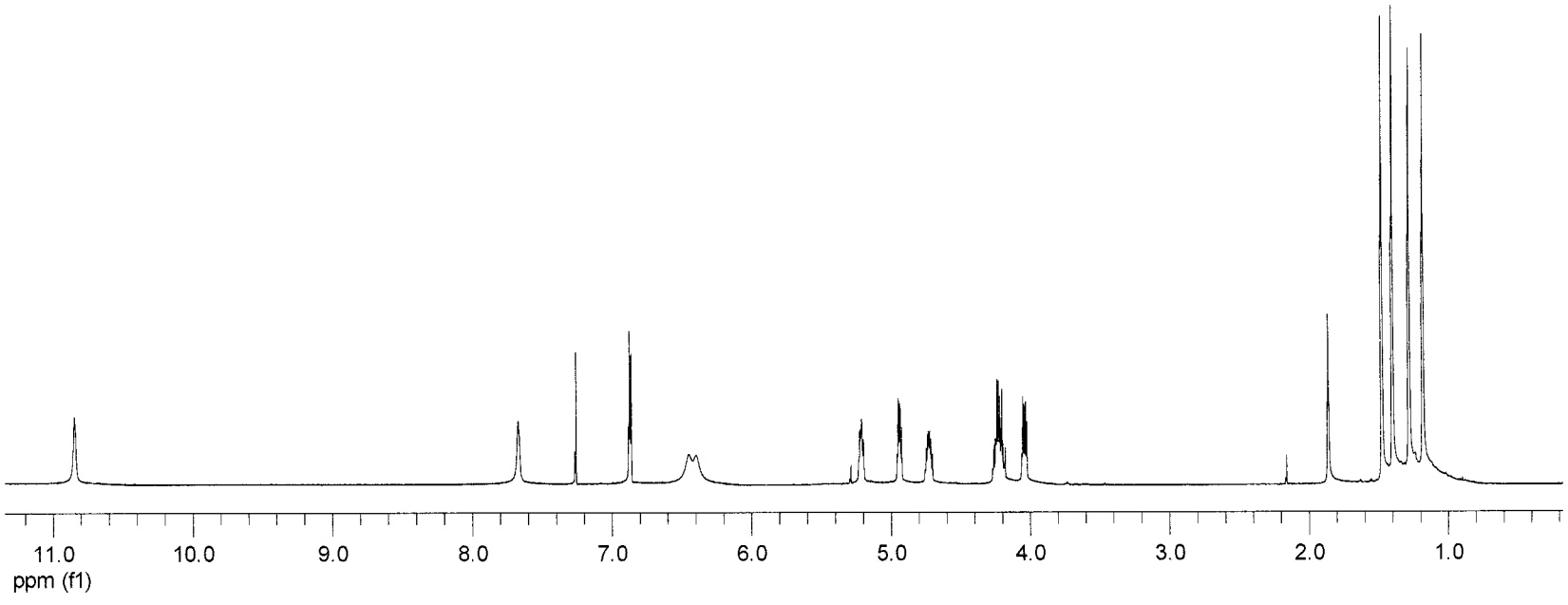

Figure 51: 400 MHz ^{1}H NMR spectrum of mannofuranosyl-1*H*-[1,2,3]-triazol-4,5-dicarboxylic acid diamide (**19**)

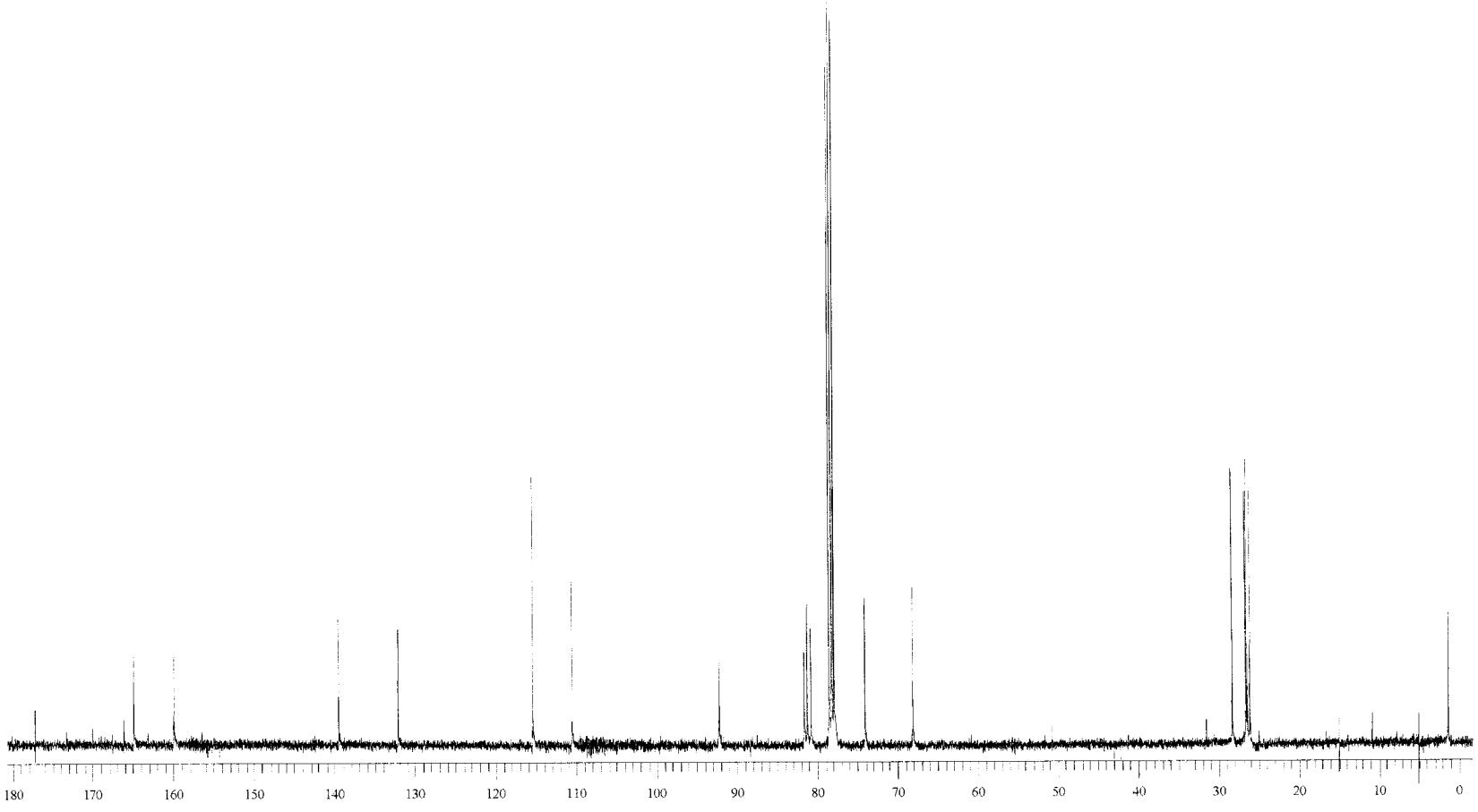

Figure 52: 100 MHz ^{13}C NMR spectrum of mannofuranosyl-1*H*-[1,2,3]-triazol-4,5-dicarboxylic acid diamide (**19**)

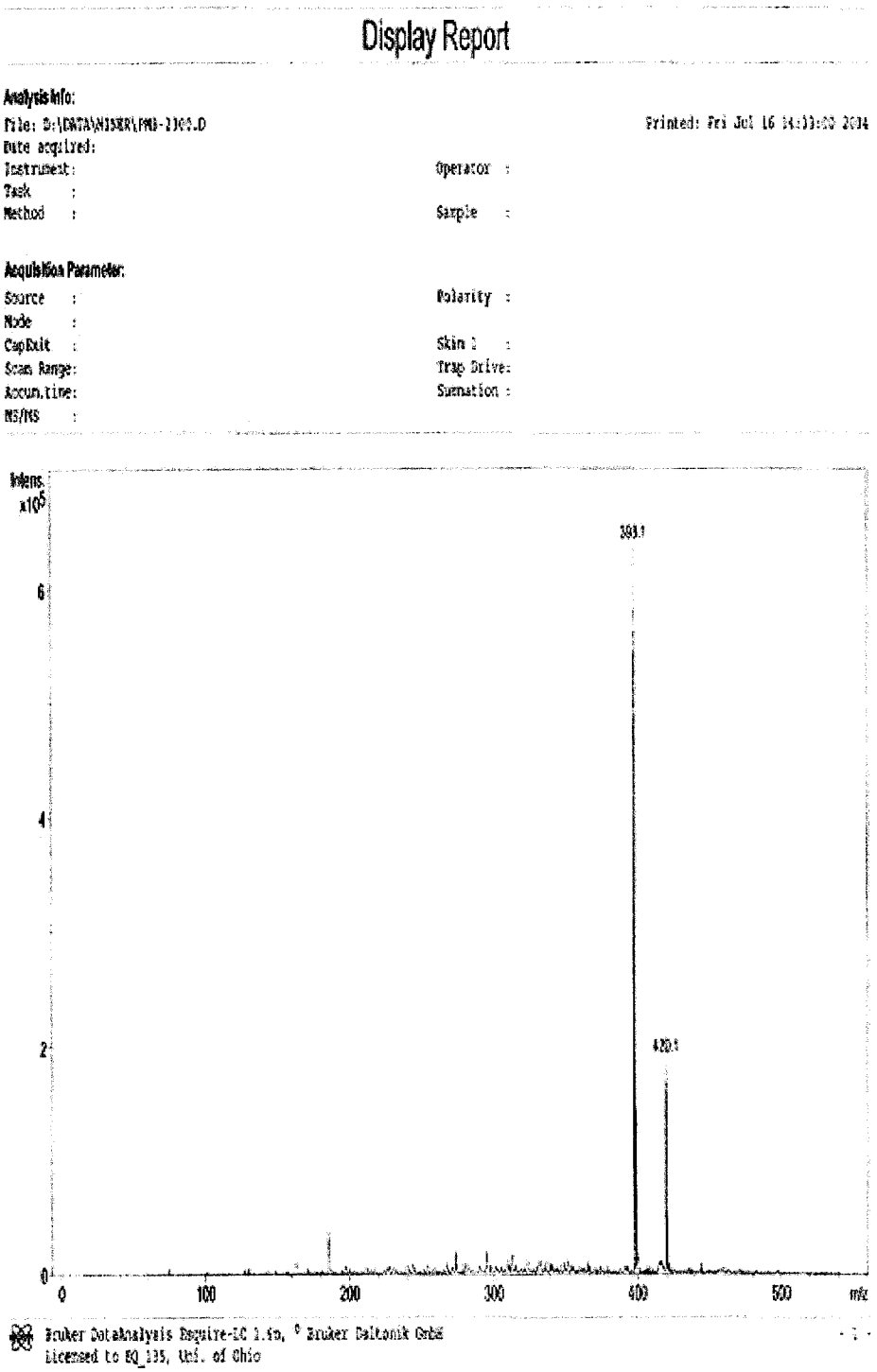

Figure 53: Mass spectrum of mannofuranosyl-1*H*-[1,2,3]-triazol-4,5-dicarboxylic acid diamide (**19**)

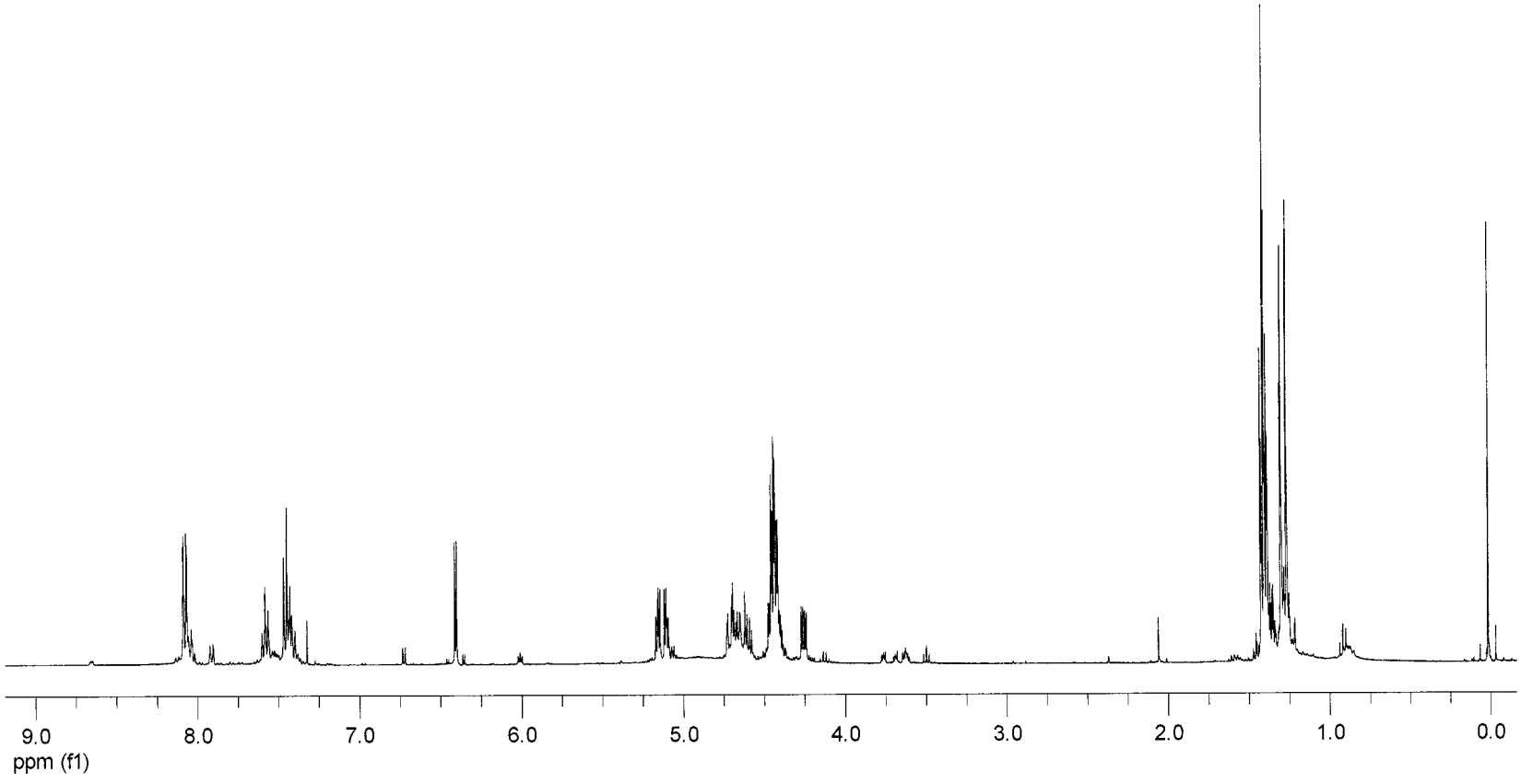

Figure 54: 400 MHz ^{1}H NMR spectrum of Bis(ester) **20**

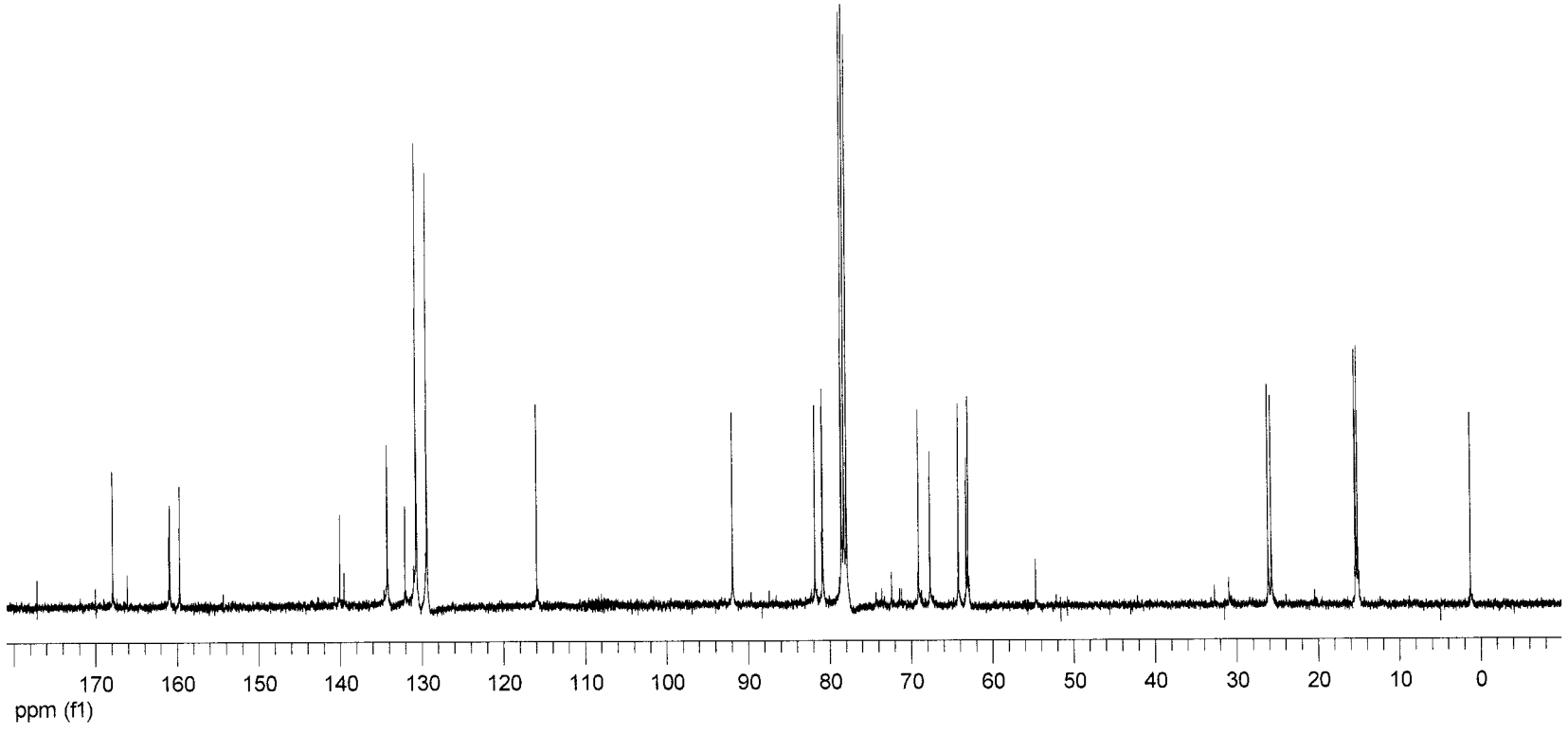

Figure 55: 100 MHz ^{13}C NMR spectrum of Bis(ester) **20**

Display Report

Analysis Info:

File: D:\DATA\MINNS\2-117003.D
Printed: Fri Jul 16 14:11:59 2004
Date acquired:
Instrument:
Operator :
Task :
Method :
Sample :

Acquisition Parameter:

Source :
Polarity :
Mode :
Cap.Exit :
Skim 1 :
Scan Range:
Trap Drive:
Accum.Time:
Summation :
MS/MS :

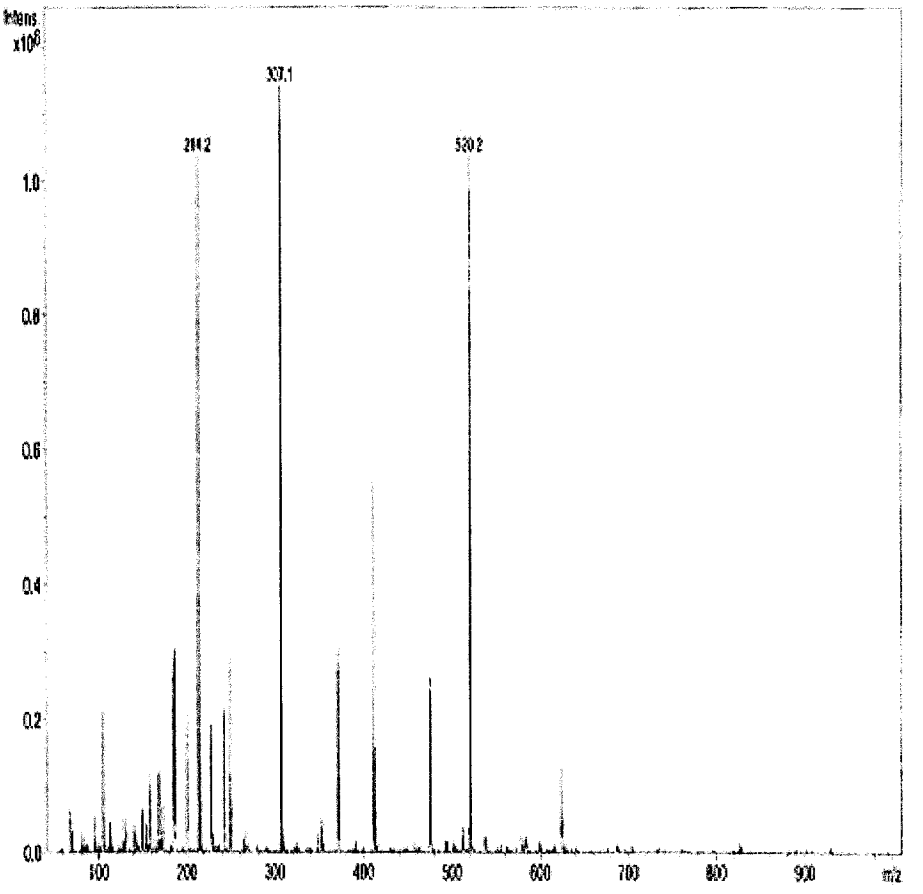

Bruker DataAnalysis Esquire-LC 1.6r, © Bruker Daltonik GmbH
Licensed to SQ_135, Uni. of Ohio

- 1 -

Figure 56: Mass spectrum of Bis(ester) **20**

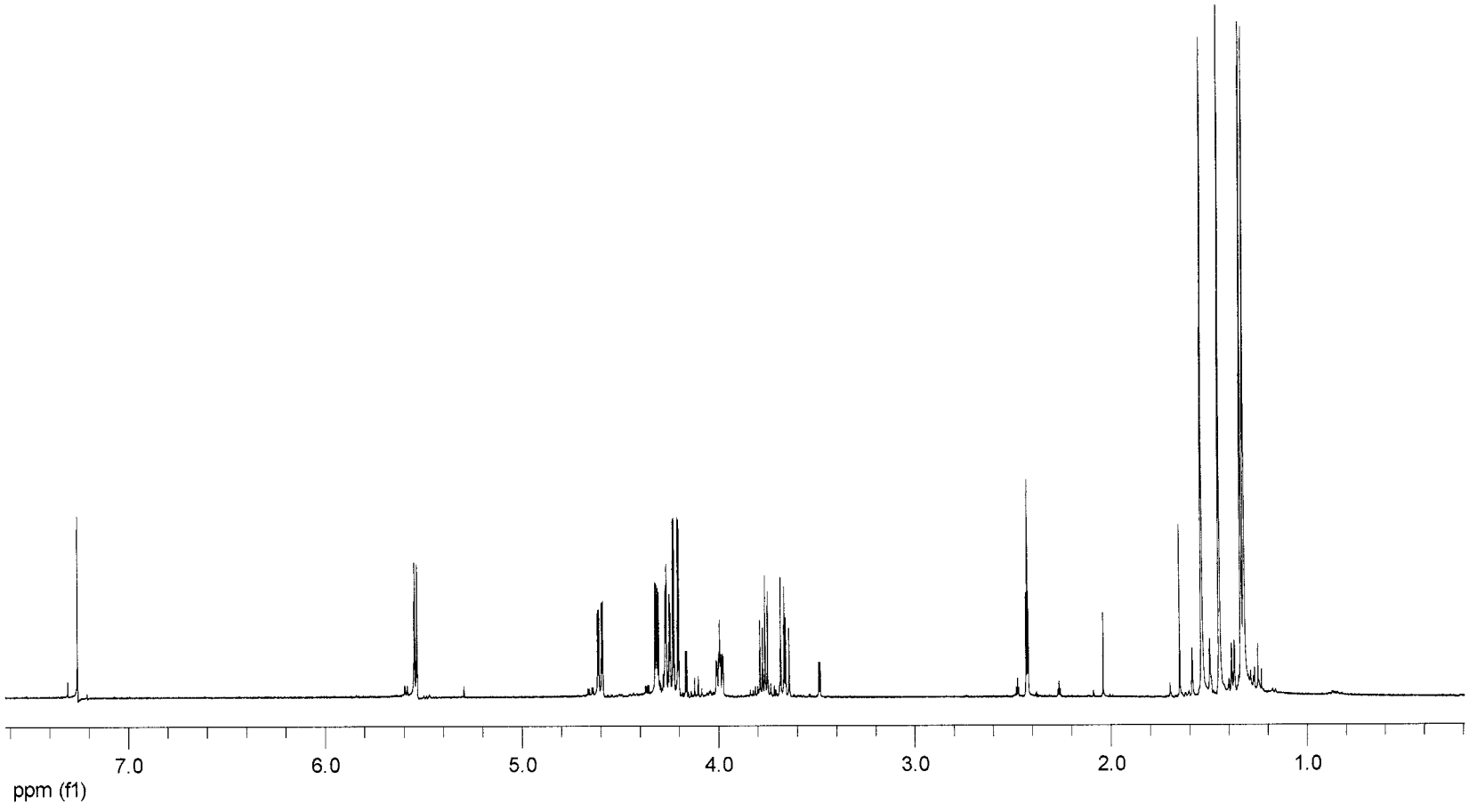

Figure 57: 400 MHz ^{1}H NMR spectrum of 1,2:3,4-di-*O*-isopropylidene-6-(prop-2-ynyloxy)-D-galactopyranose (**22**)

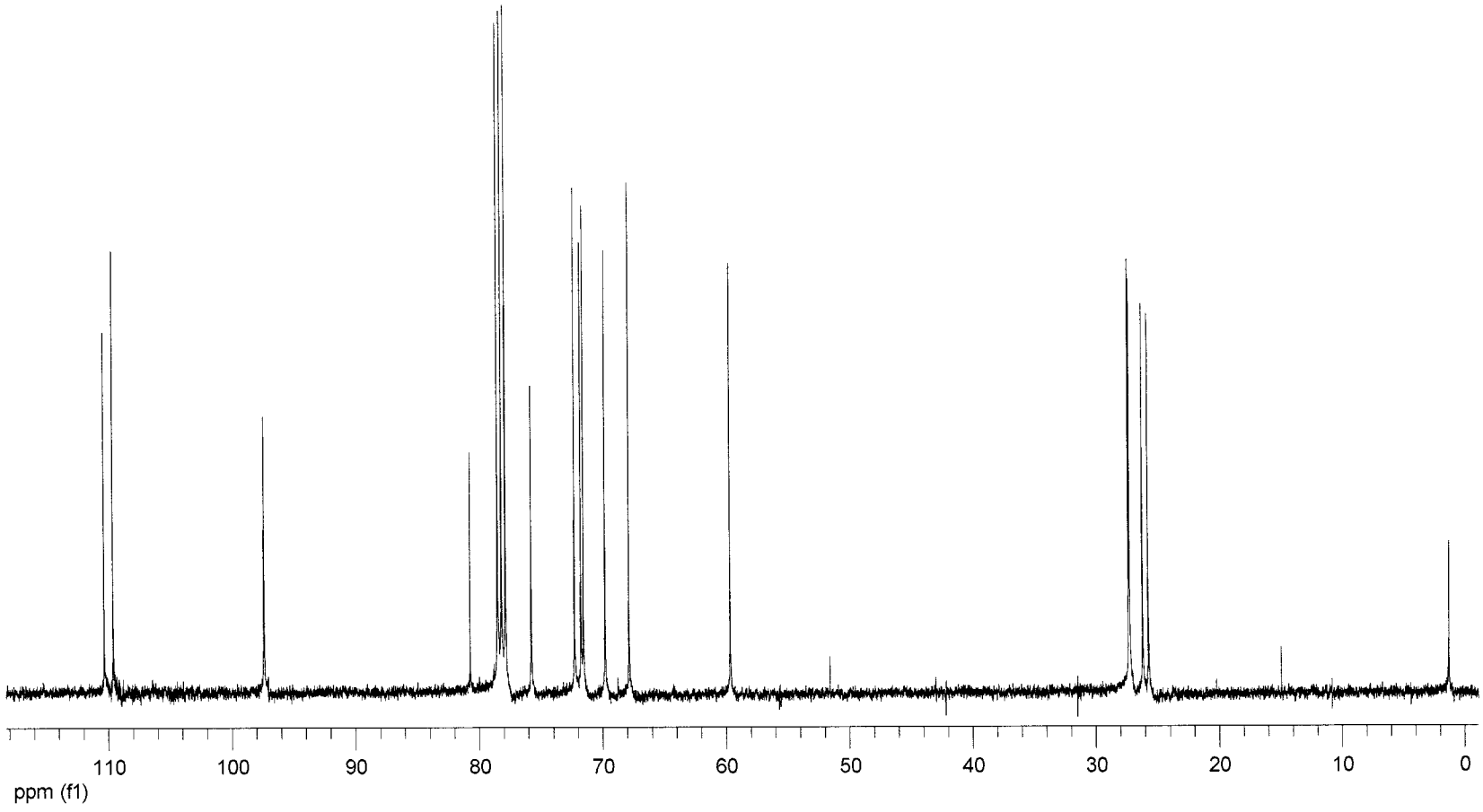

Figure 58: 100 MHz ^{13}C NMR spectrum of 1,2:3,4-di-*O*-isopropylidene-6-(prop-2-ynyloxy)-D-galactopyranose (**22**)

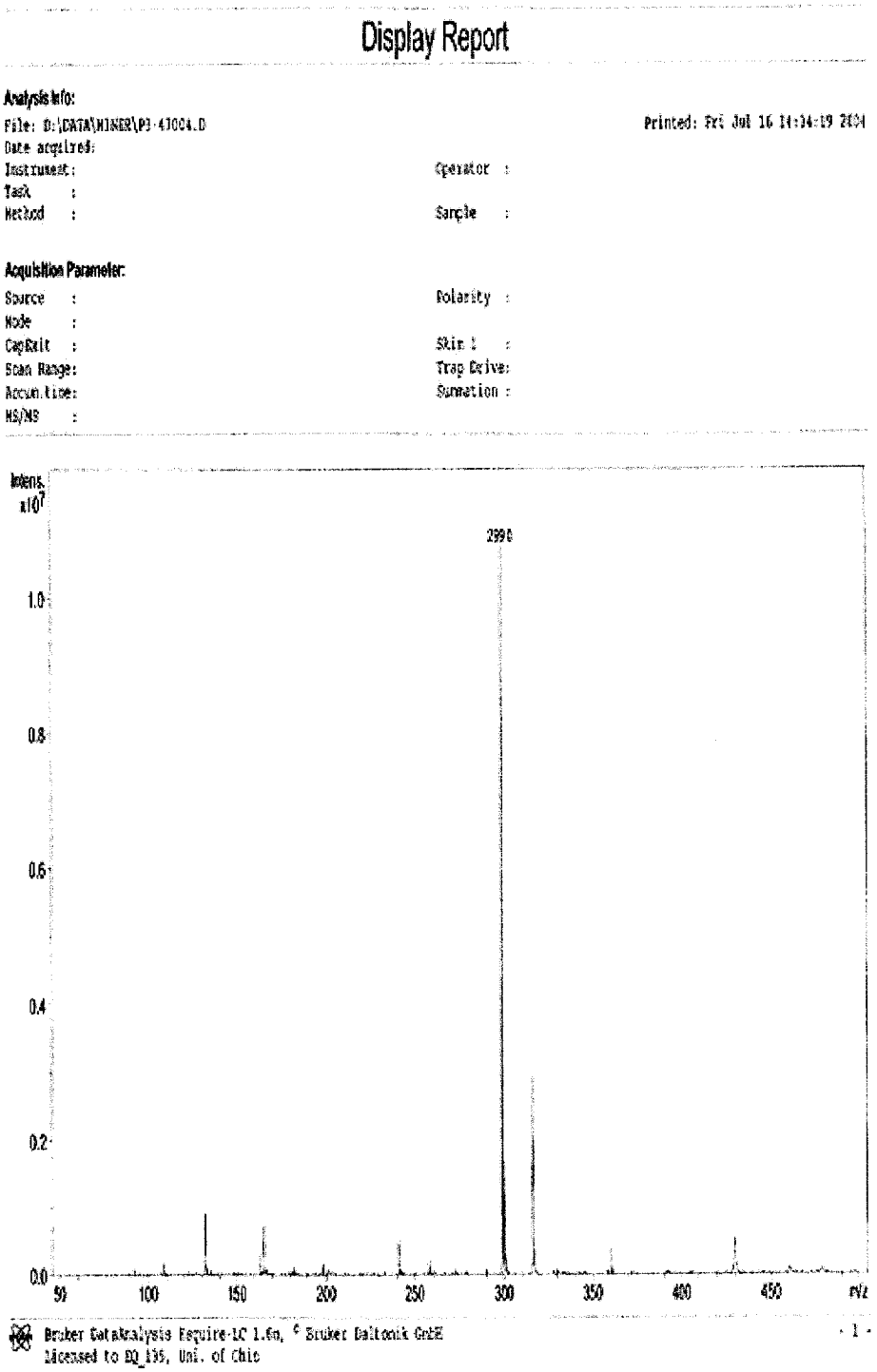

Figure 59: Mass spectrum of 1,2:3,4-di-*O*-isopropylidene-6-(prop-2-ynyloxy)-D-galactopyranose (**22**)

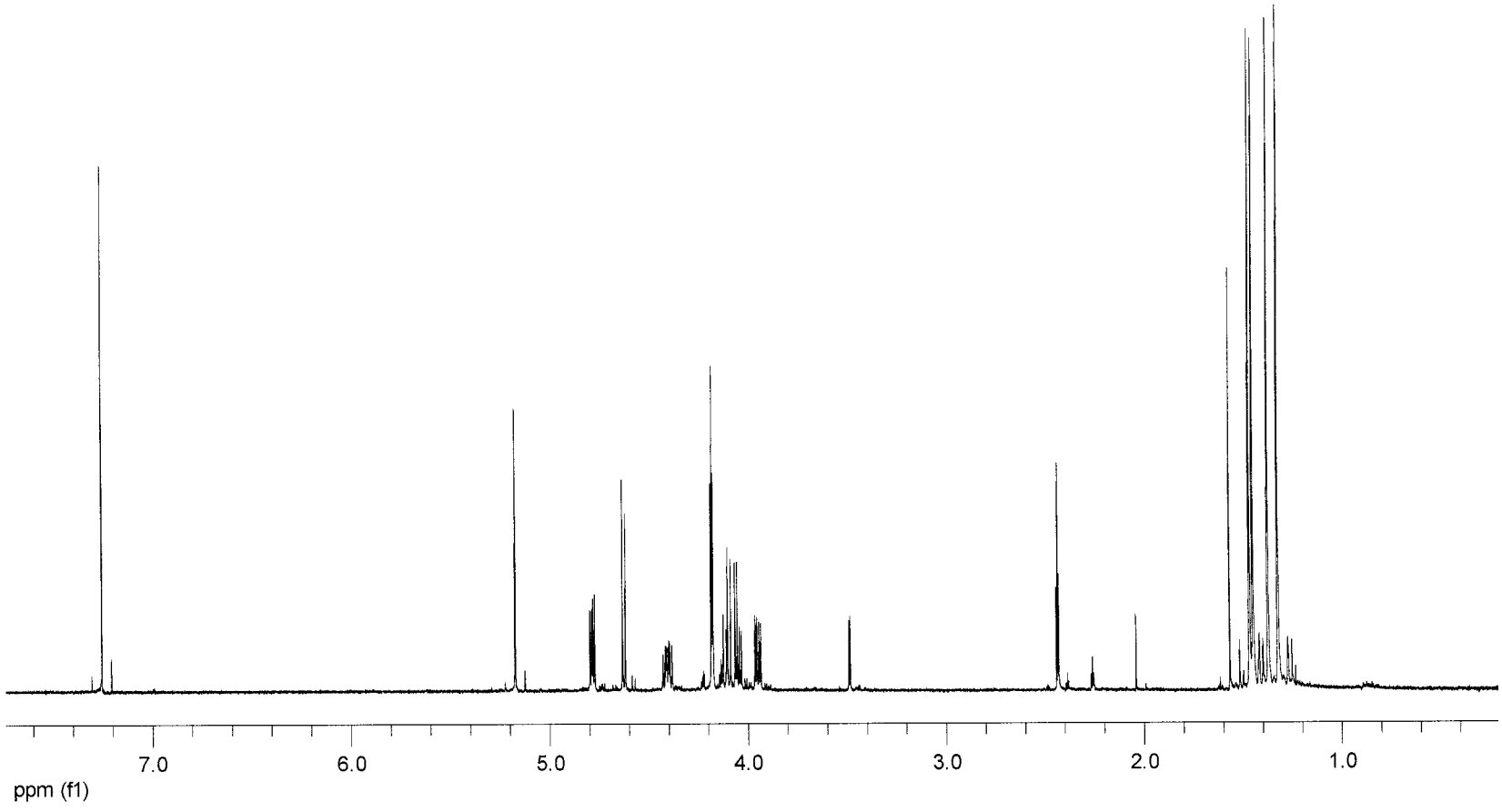

Figure 60: 400 MHz ^{1}H NMR spectrum of diacetone-D-mannose alkyne **23**

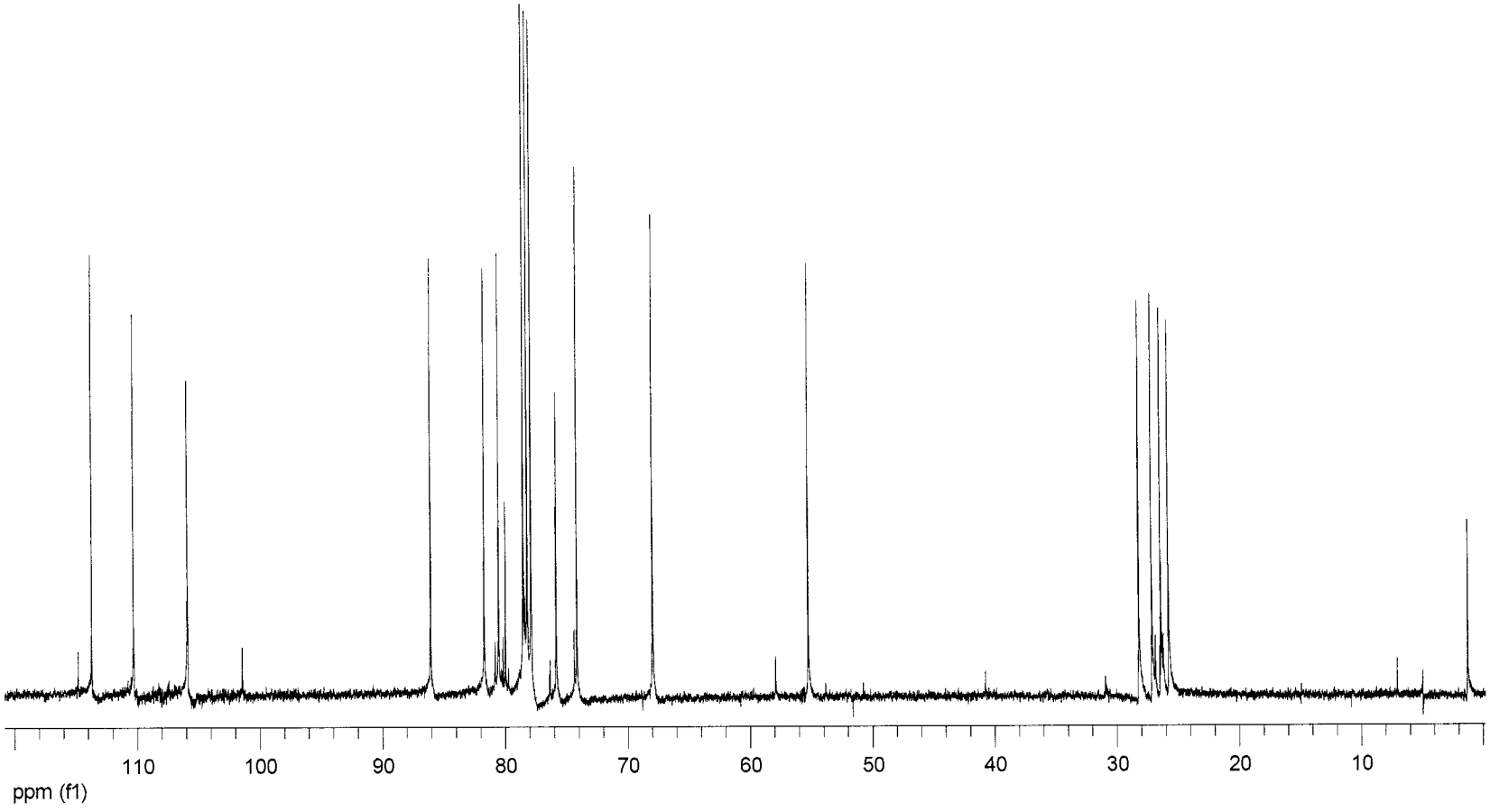

Figure 61: 100 MHz ^{13}C NMR spectrum of diacetone-D-mannose alkyne **23**

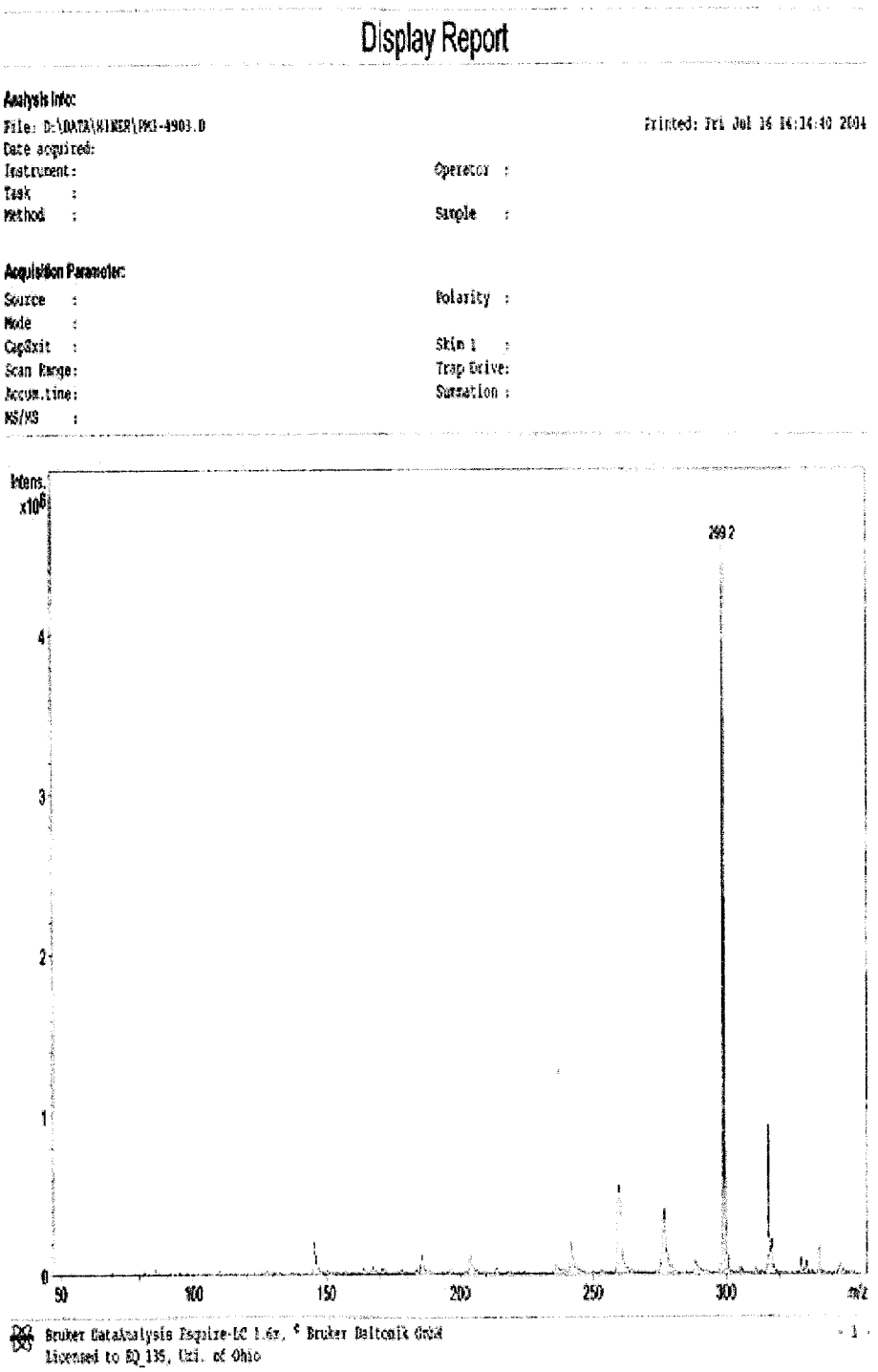

Figure 62: Mass spectrum of diacetone-D-mannose alkyne **23**

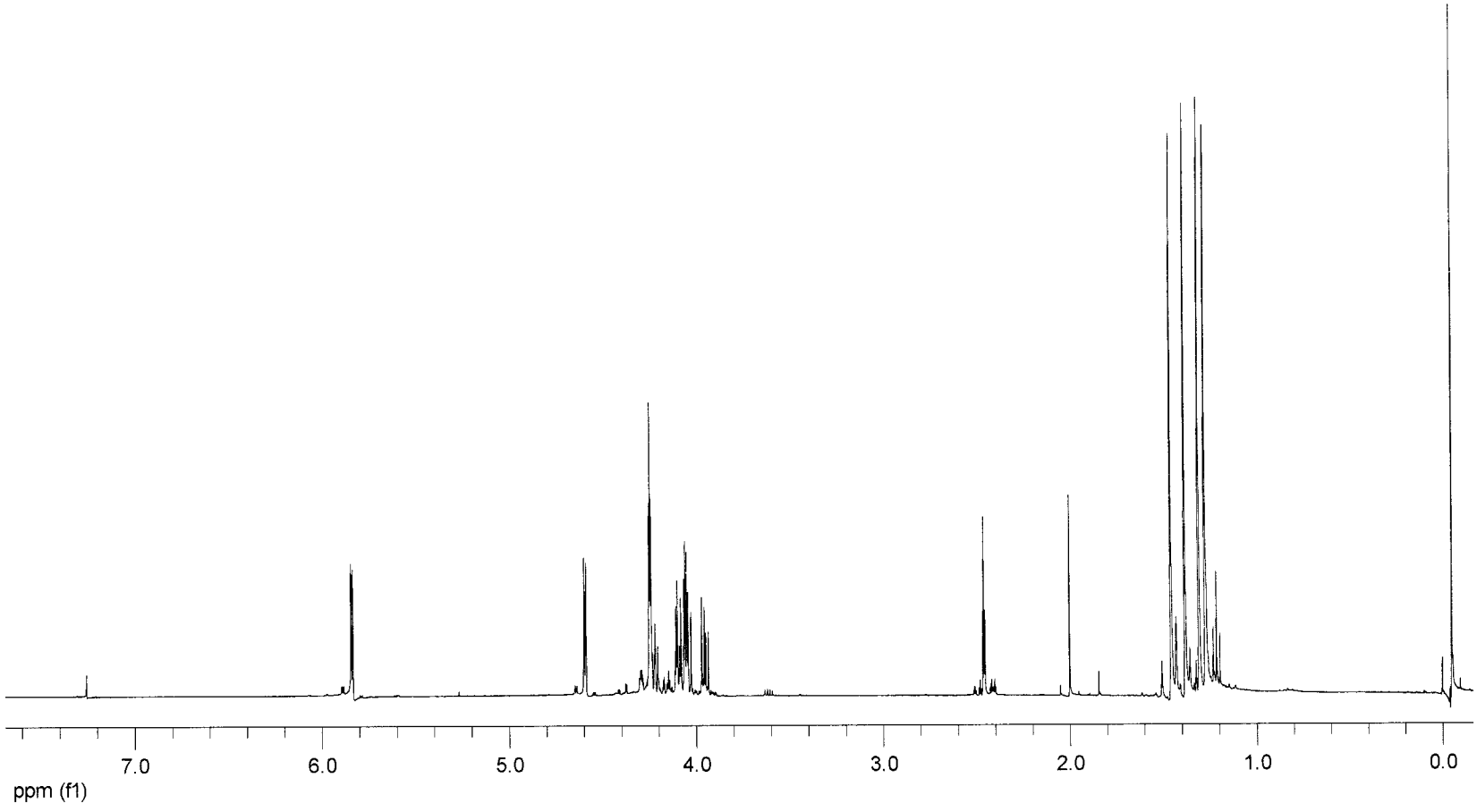

Figure 63: 400 MHz ^{1}H NMR spectrum of diacetone-D-glucofuranose alkyne **25**

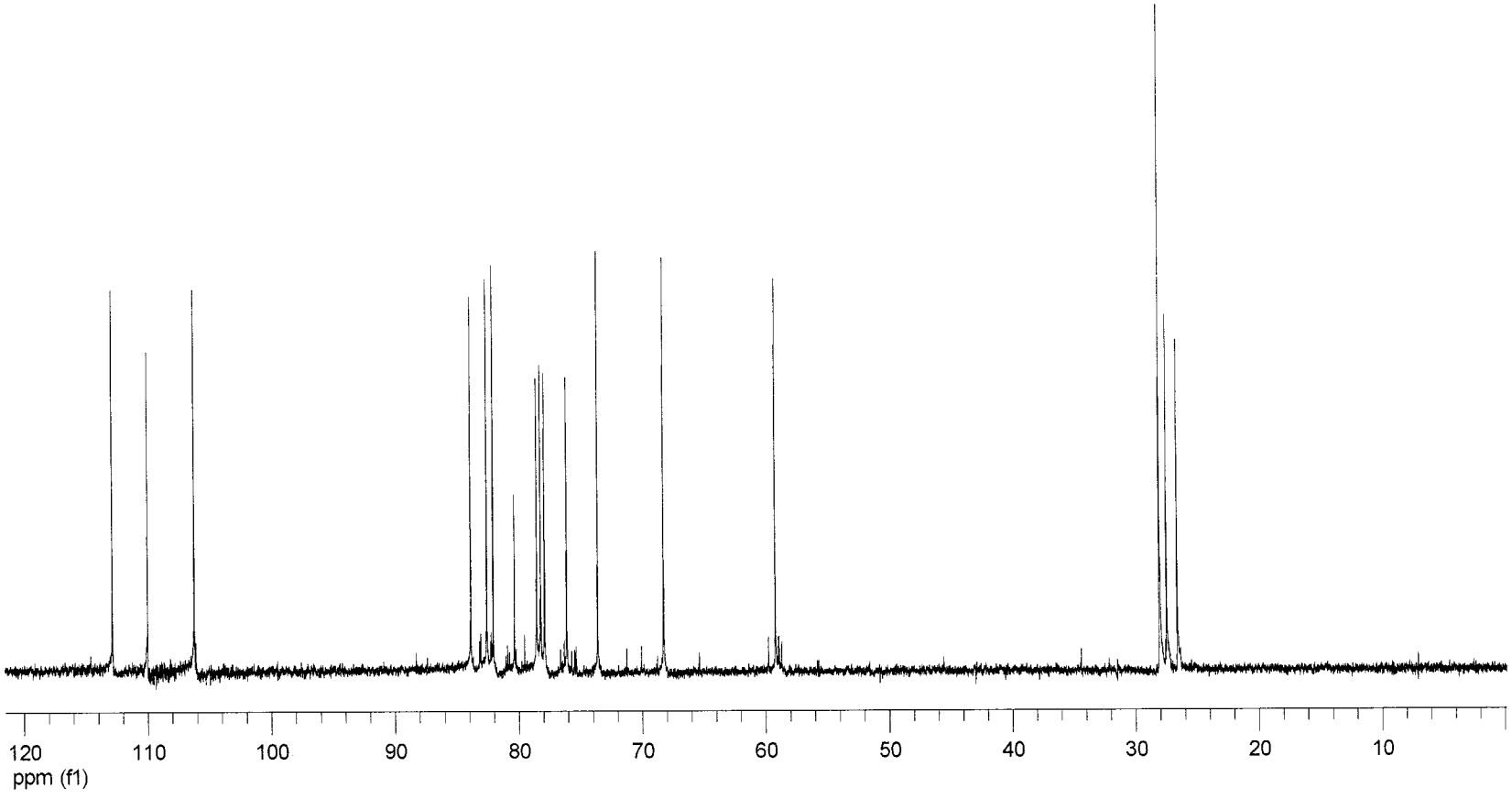

Figure 64: 100 MHz ^{13}C NMR spectrum of diacetone-D-glucofuranose alkyne **25**

Display Report

Analysis Info:

File: D:\DATA\MINER\PM5-51A4.D
Printed: Fri Jul 16 14:15:12 2004
Date acquired:
Instrument: Operator :
Task :
Method : Sample :

Acquisition Parameter:

Source : Polarity :
Mode :
CapExit : Skim 1 :
Scan Range: Trap Drive:
Accum.time: Correction :
MS/MS :

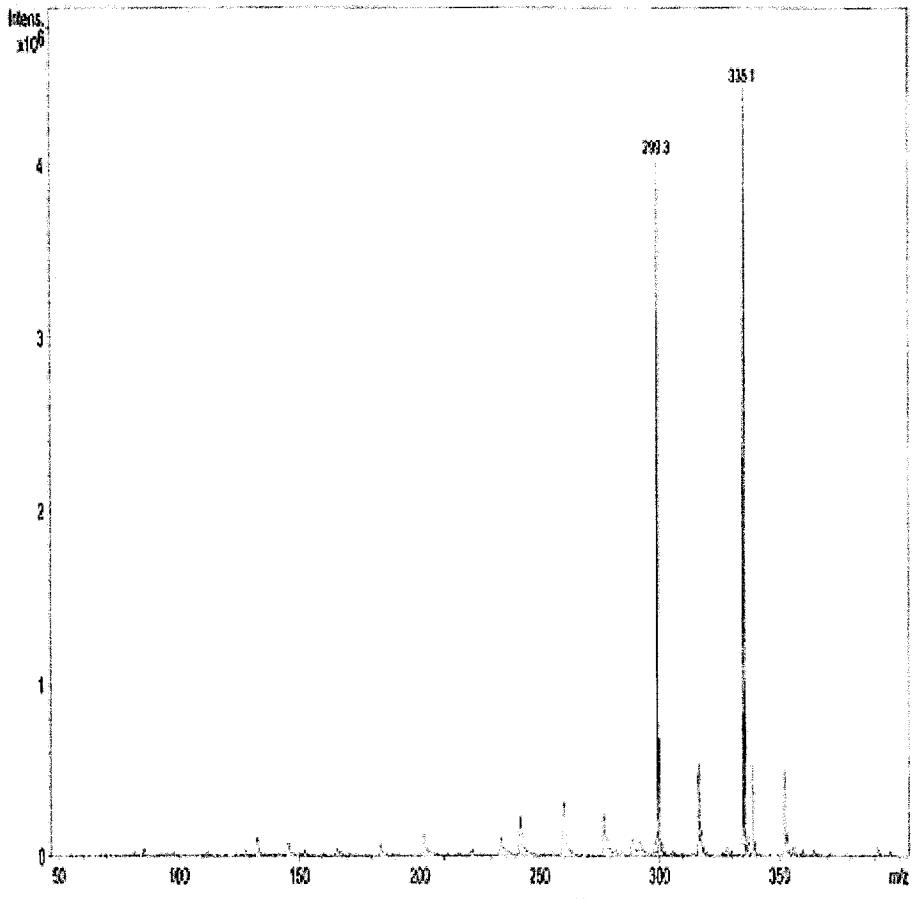

Bruker DataAnalysis Esquire-LC 3.4n, © Bruker Daltonik GmbH
Licensed to EQ_135, Uni. of Ohio
- 1 -

Figure 65: Mass spectrum of diacetone-D-glucofuranose alkyne **25**

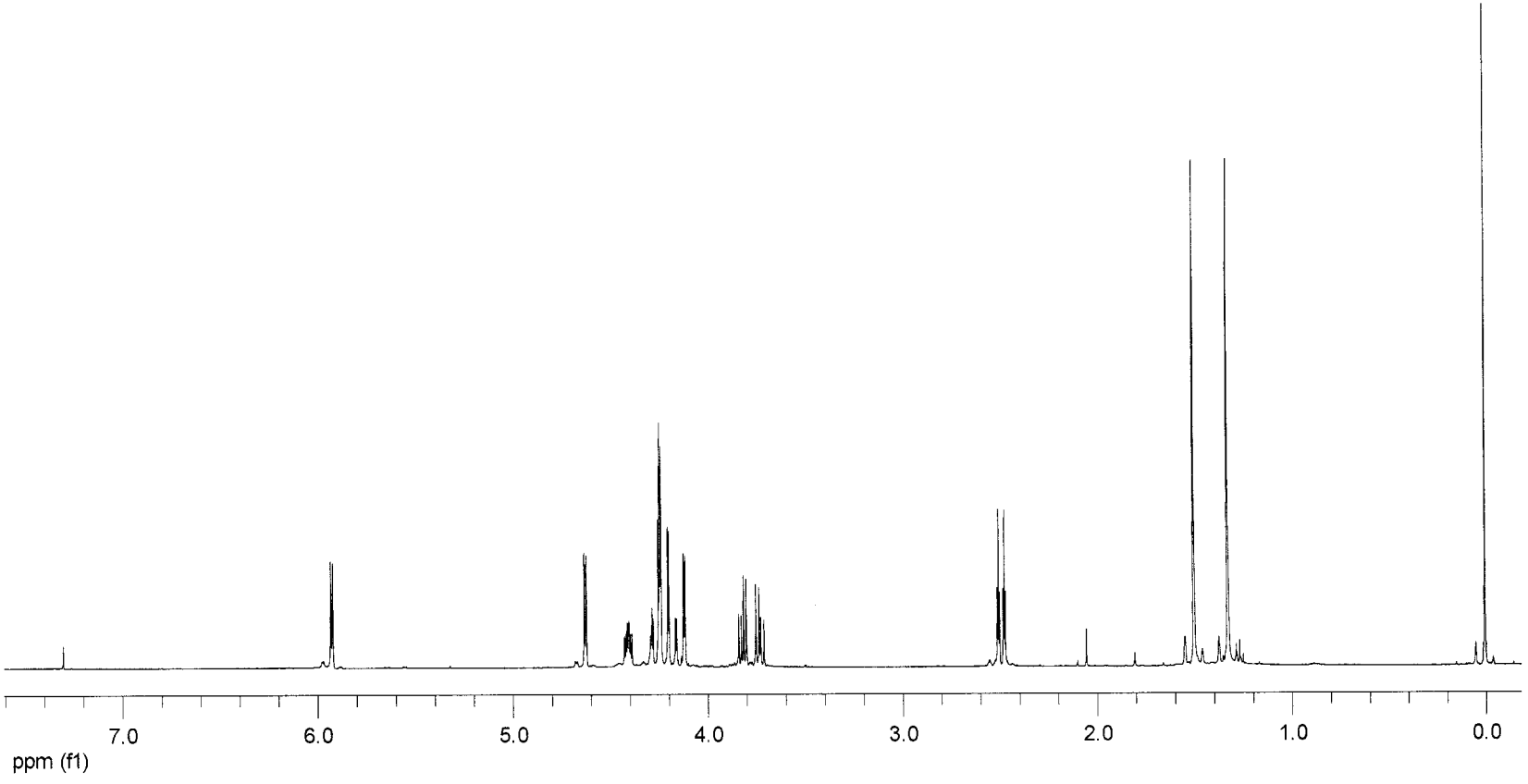

Figure 66: 400 MHz ^{1}H NMR spectrum of 1,2-*O*-isopropylidene-3,5-di-*O*-(prop-2-ynyloxy)-D-xylofuranose (**27**)

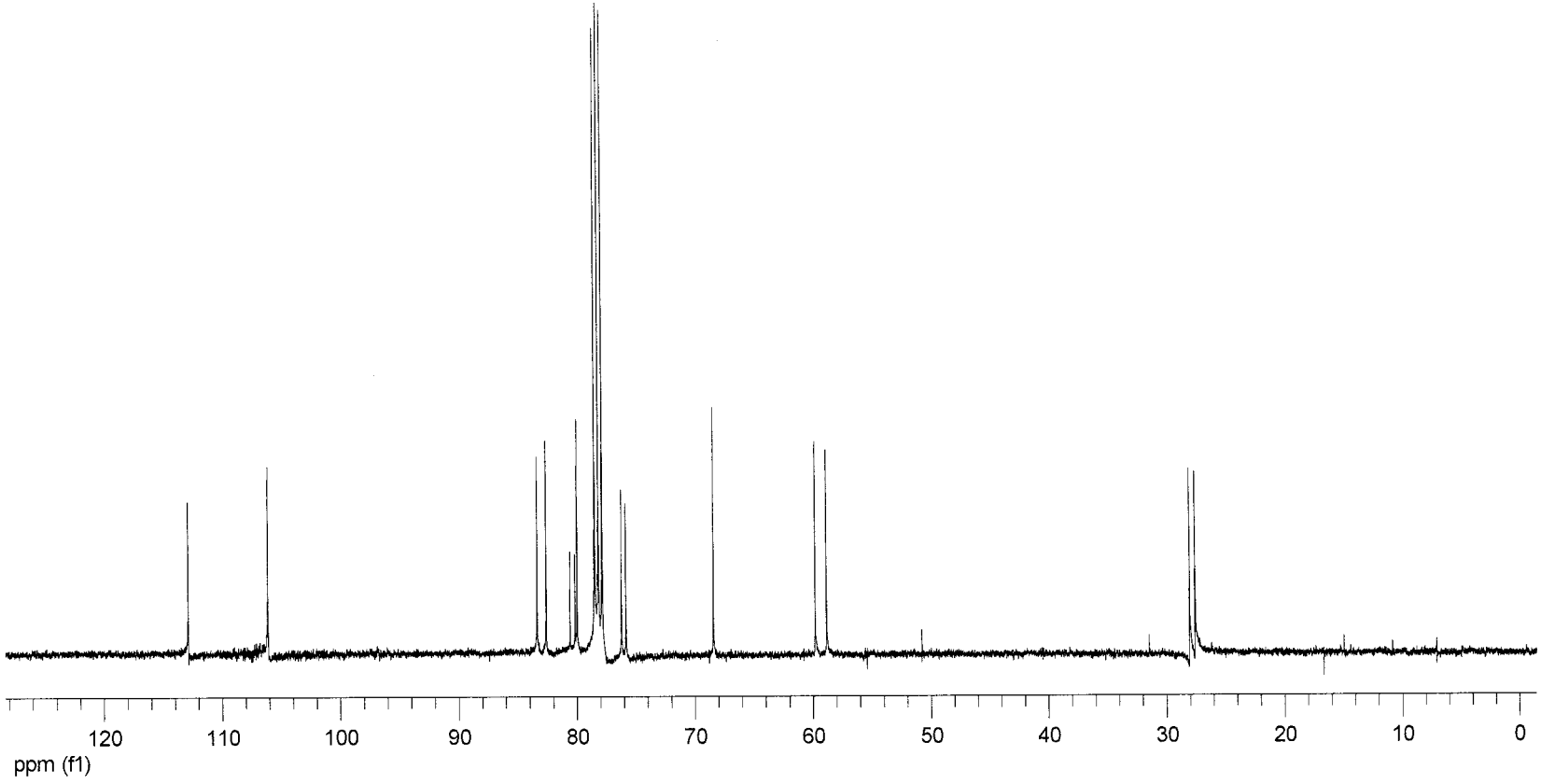

Figure 67: 100 MHz ^{13}C NMR spectrum of 1,2-*O*-isopropylidene-3,5-di-*O*-(prop-2-ynyloxy)-D-xylofuranose (**27**)

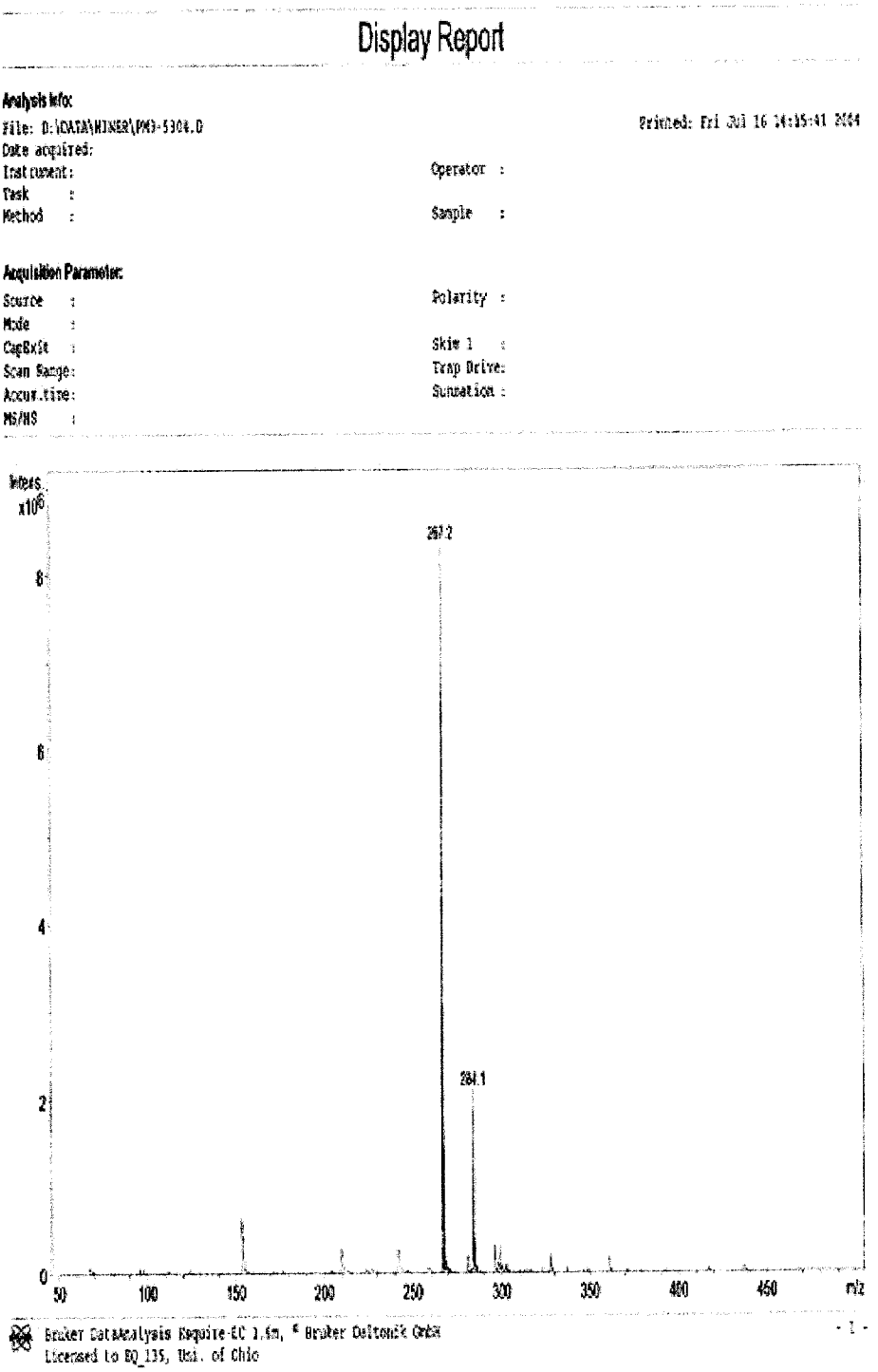

Figure 68: Mass spectrum of 1,2-*O*-isopropylidene-3,5-di-*O*-(prop-2-ynyloxy)-D-xylofuranose (**27**)

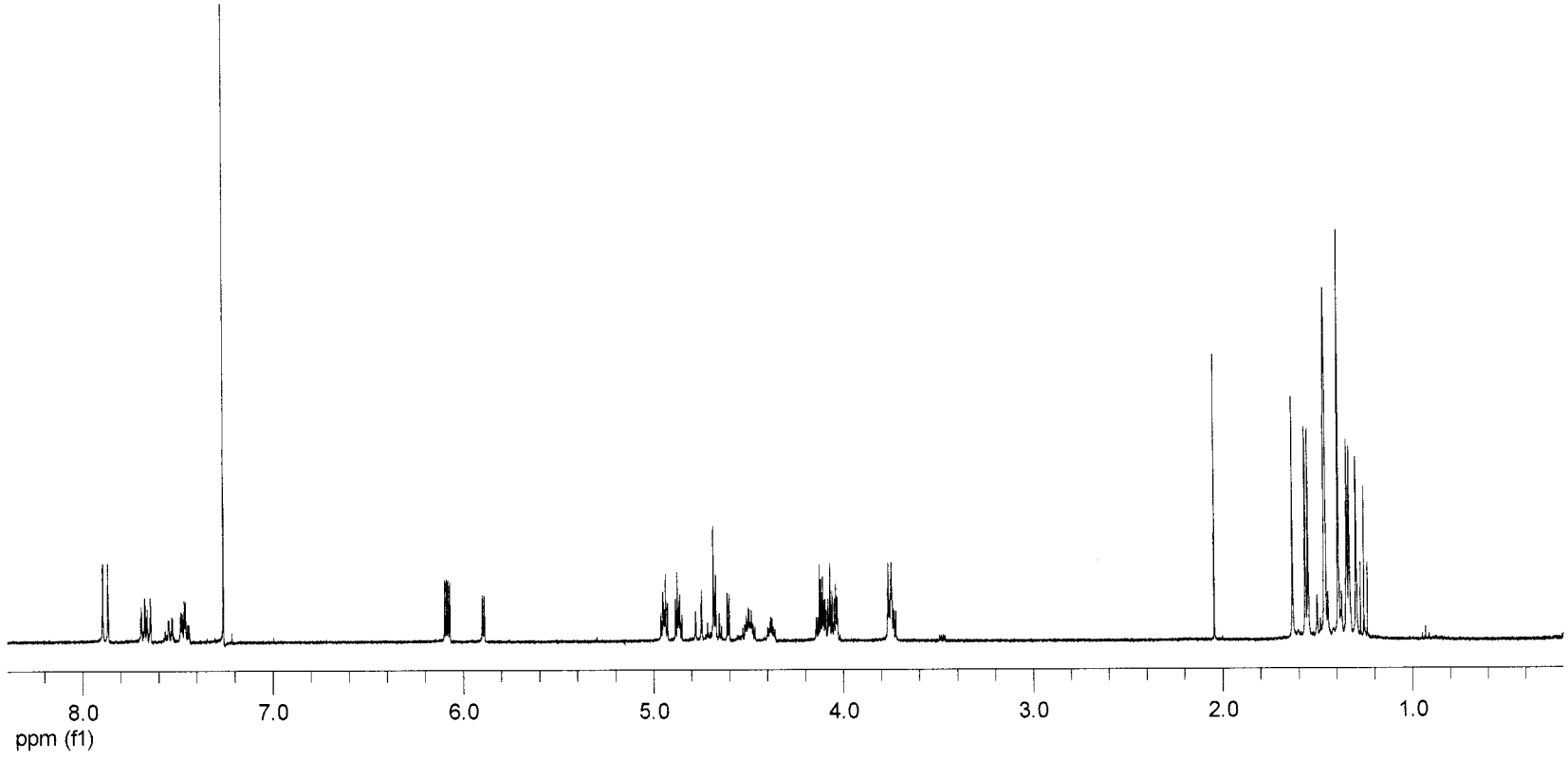

Figure 69: 400 MHz ^{1}H NMR spectrum of bistriazole **28**

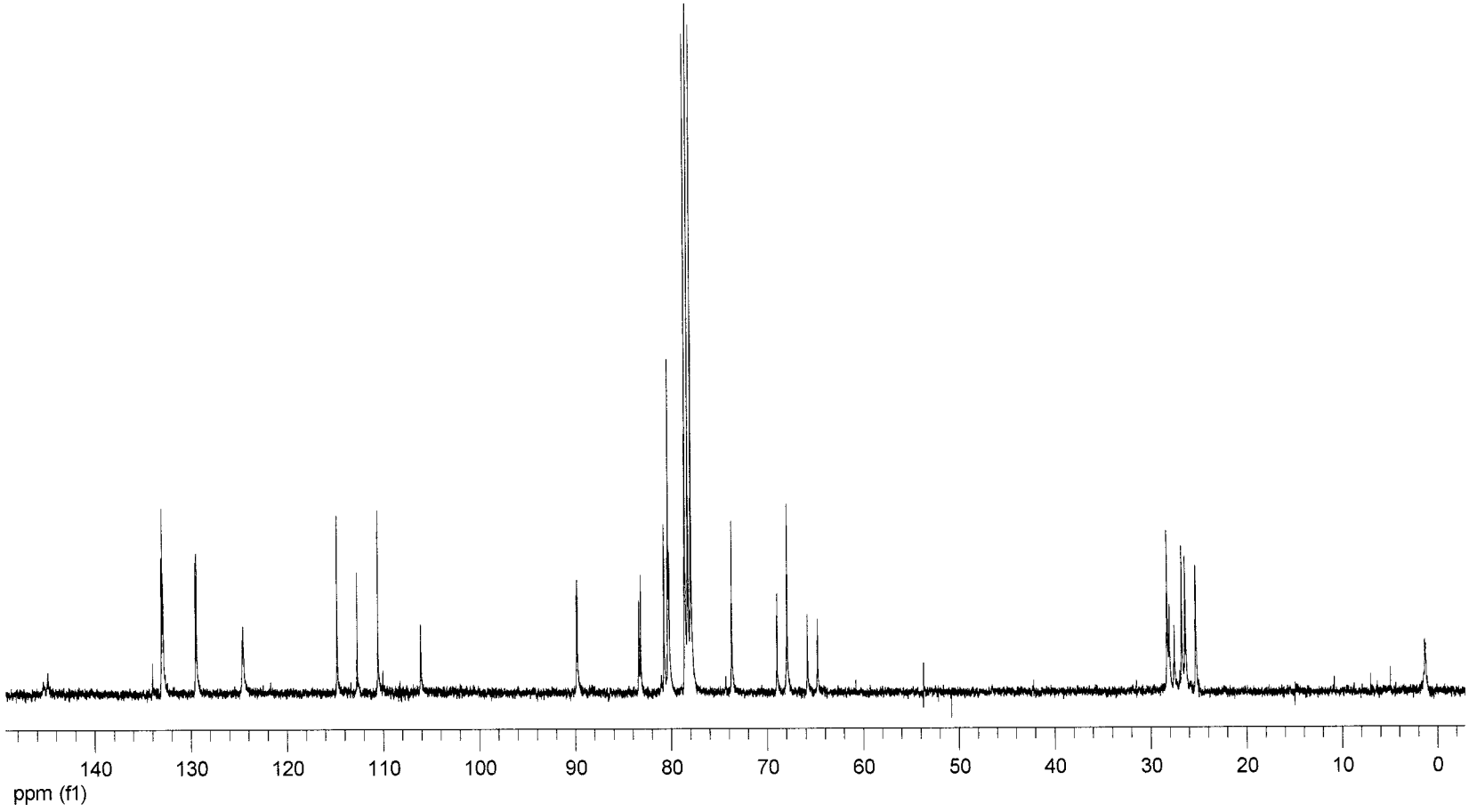

Figure 70: 100 MHz ^{13}C NMR spectrum of bistriazole **28**

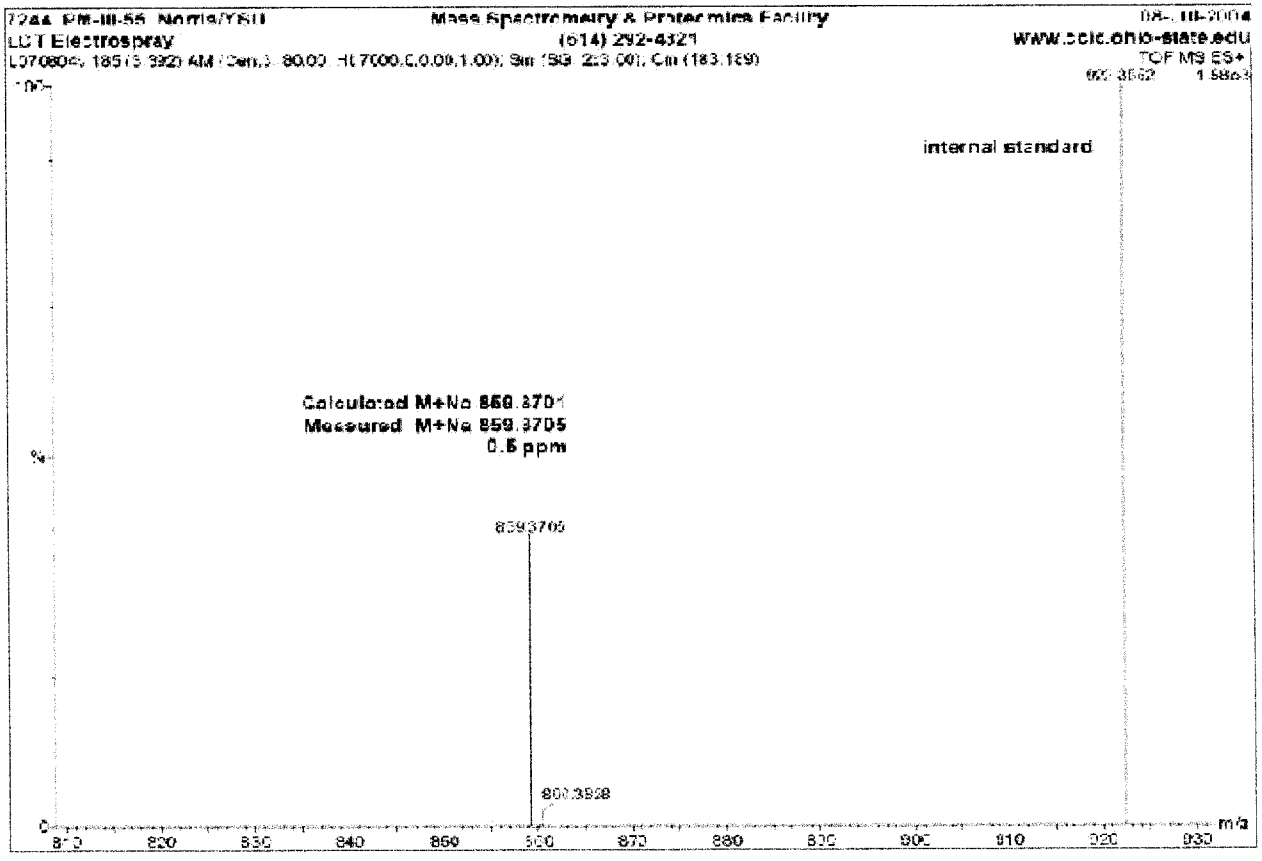

Figure 71: Mass spectrum of bistriazole **28**

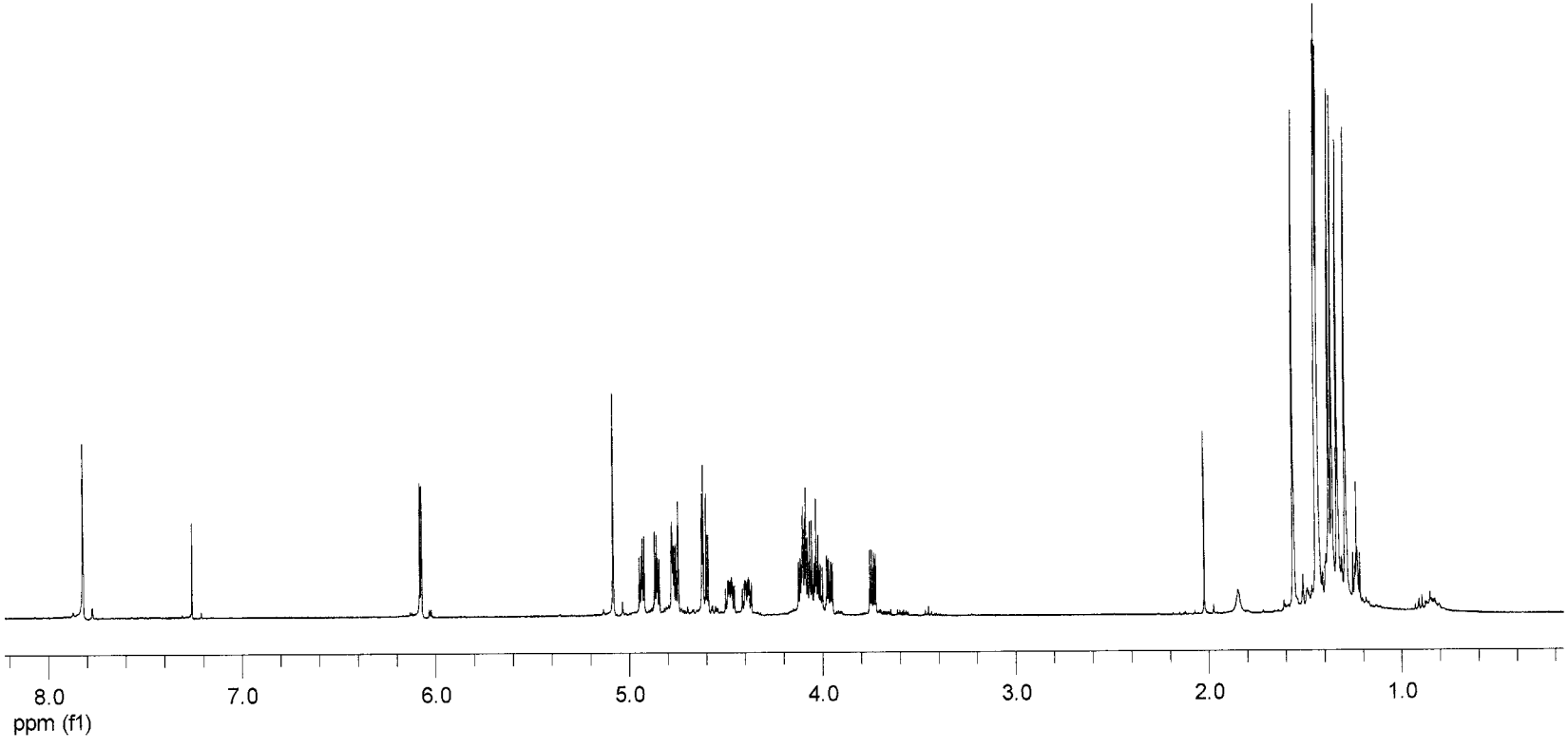

Figure 72: 400 MHz ^{1}H NMR spectrum of triazole **29**, a disaccharide analog

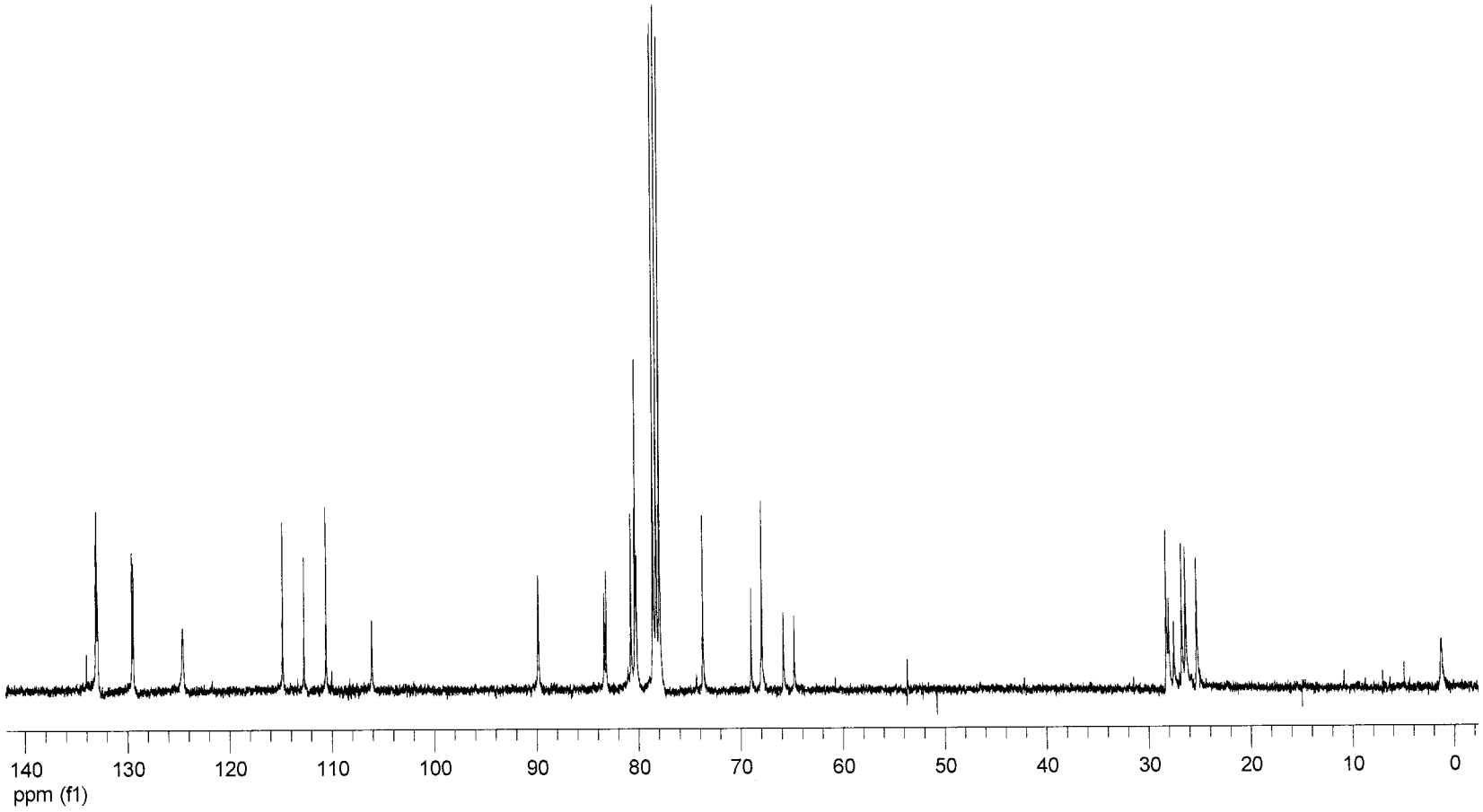

Figure 73: 100 MHz ^{13}C NMR spectrum of triazole **29**, a disaccharide analog

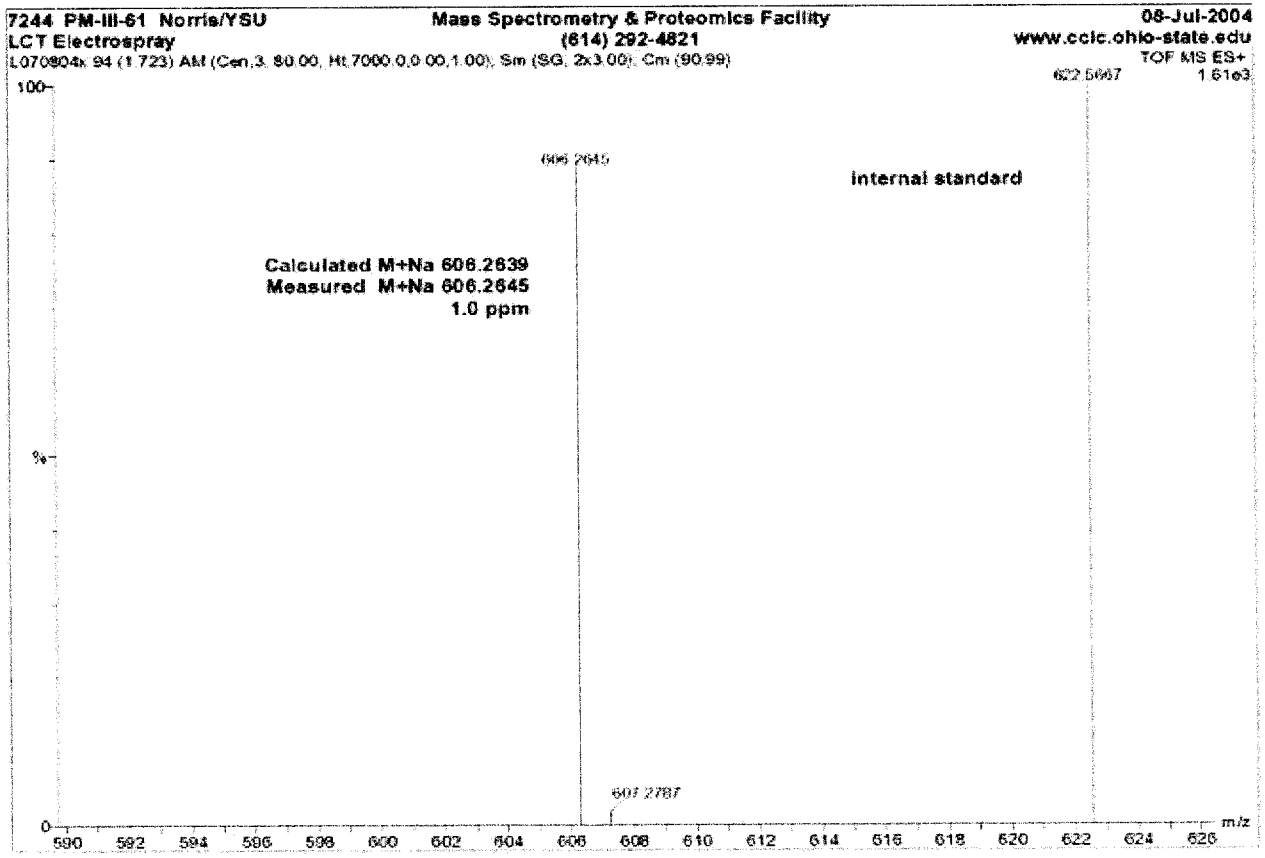

Figure 74: Mass spectrum of triazole **29**, a disaccharide analog

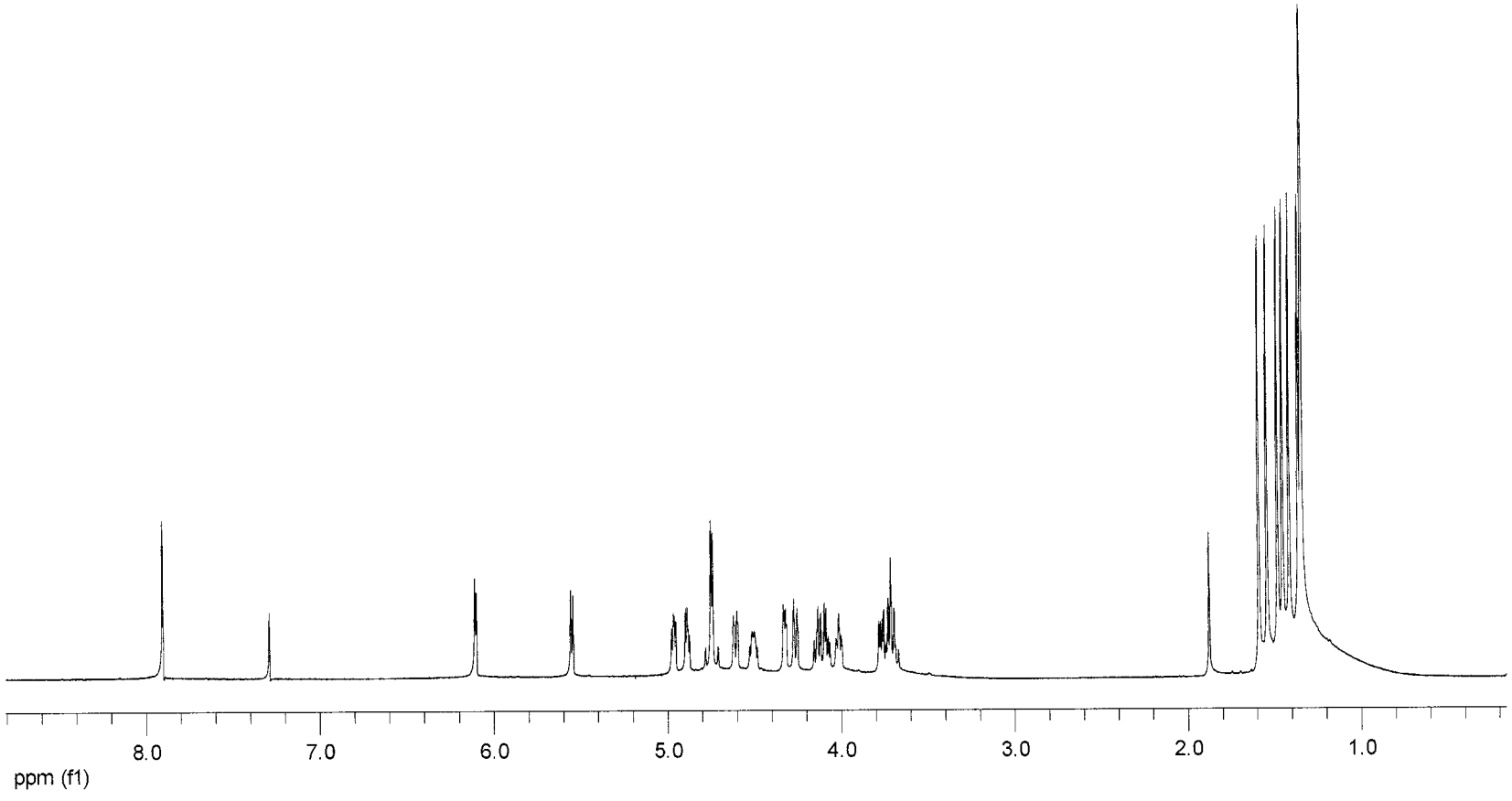

Figure 75: 400 MHz ^{1}H NMR spectrum of triazole **30**, a disaccharide analog

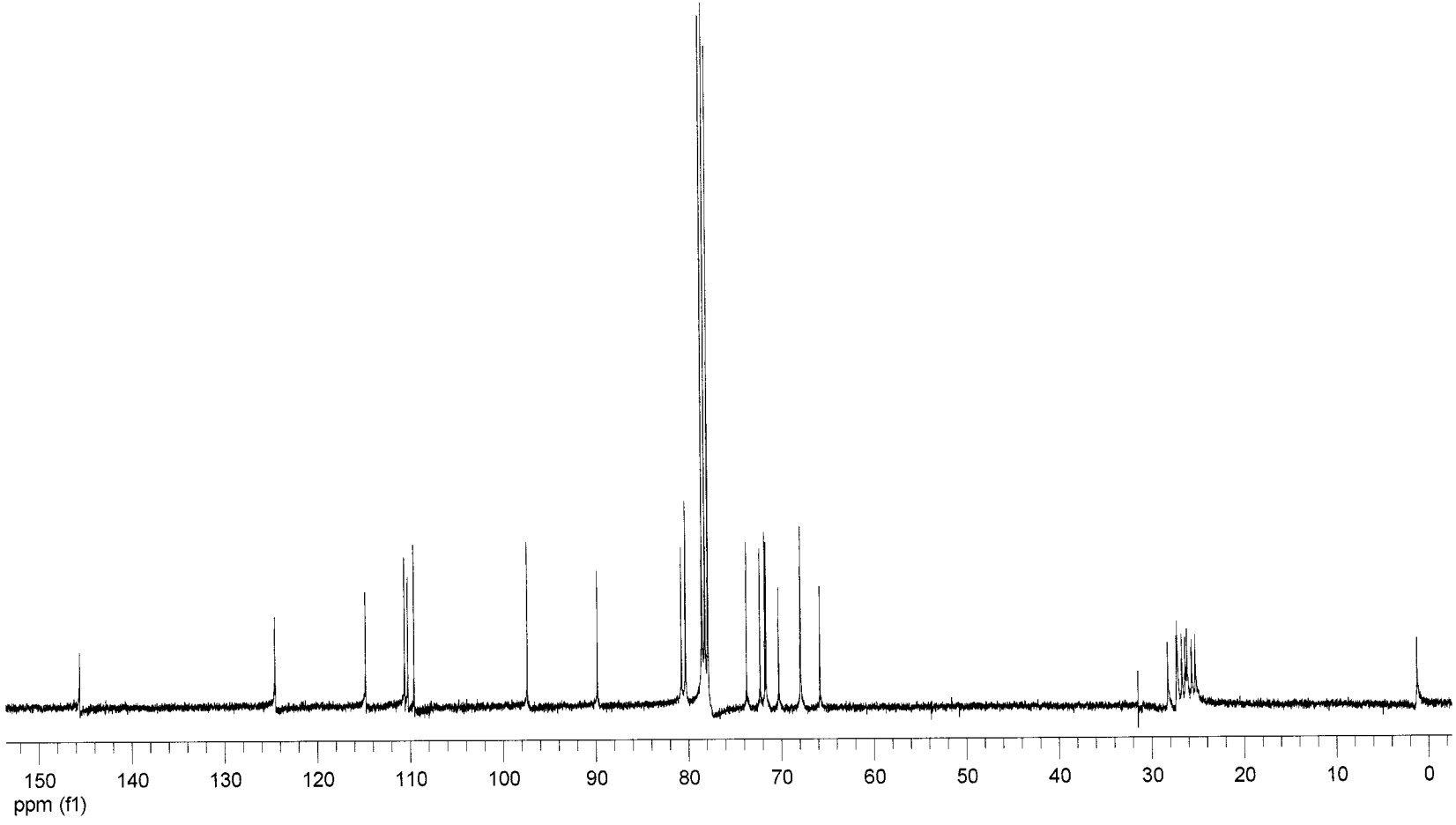

Figure 76: 100 MHz ^{13}C NMR spectrum of triazole **30**, a disaccharide analog

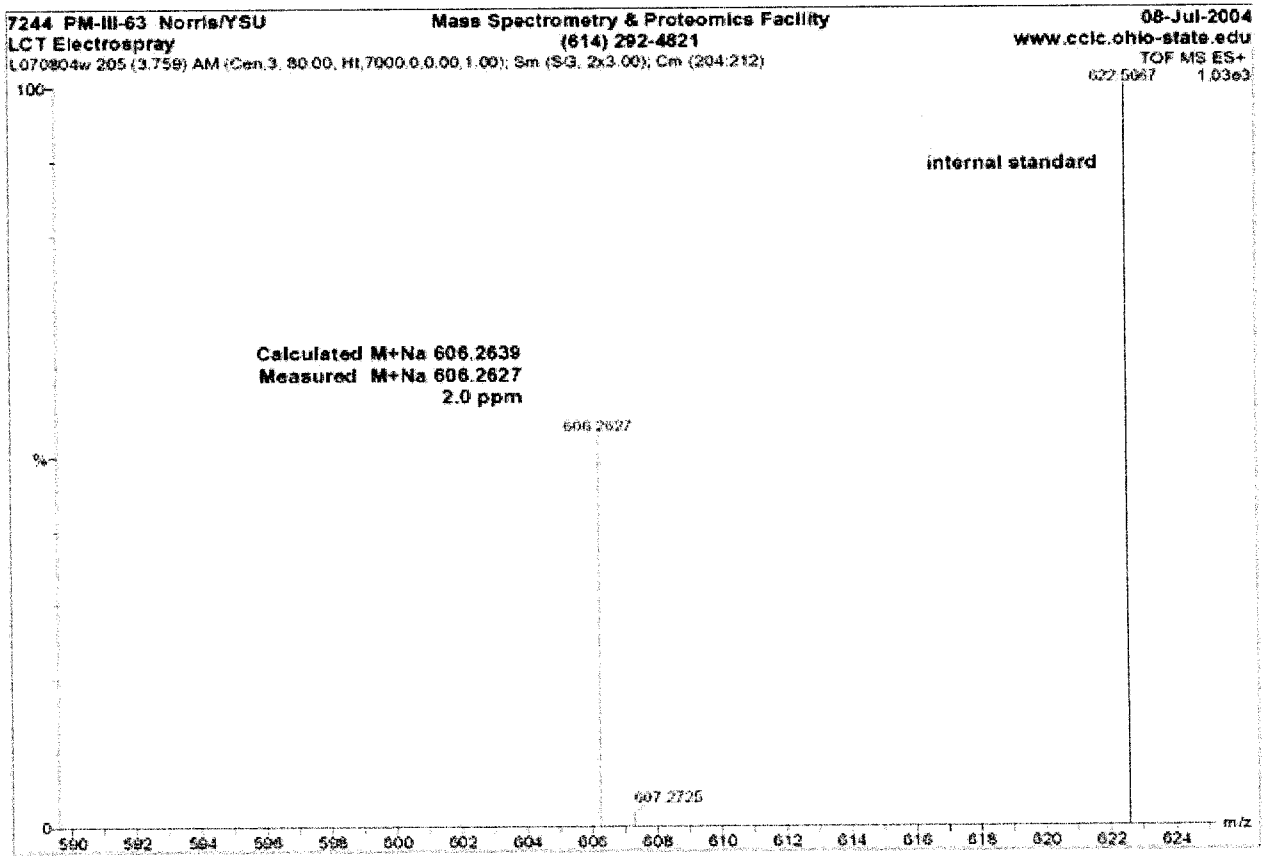

Figure 77: Mass spectrum of triazole **30**, a disaccharide analog

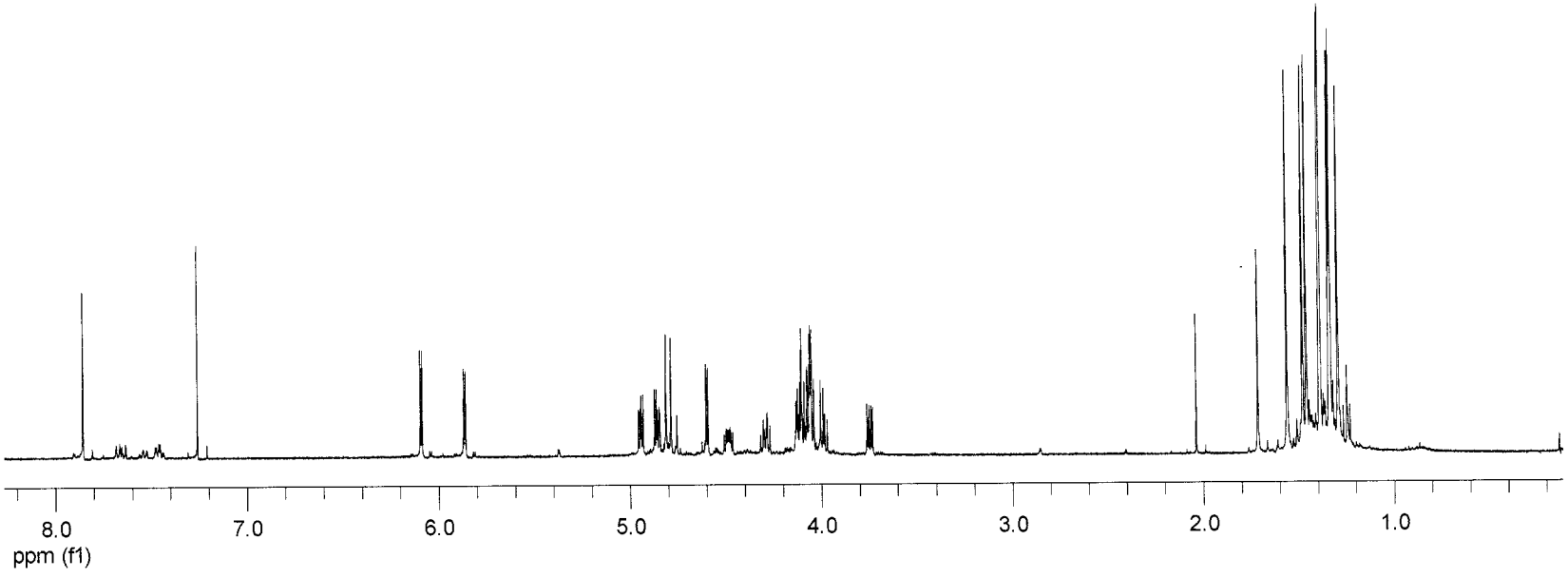

Figure 78: 400 MHz ^{1}H NMR spectrum of triazole **31**, a disaccharide analog

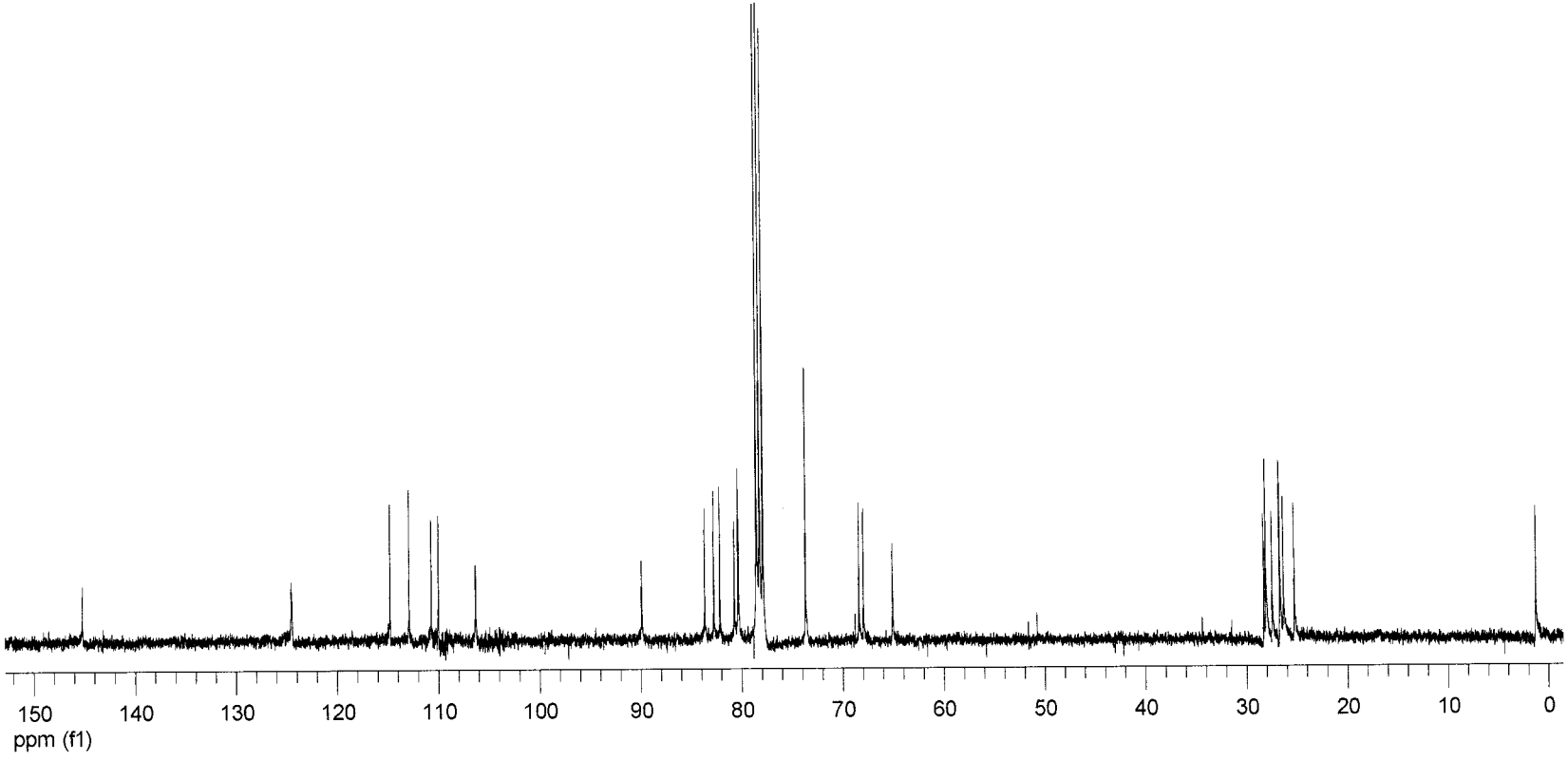

Figure 79: 100 MHz ^{13}C NMR spectrum of triazole **31**, a disaccharide analog

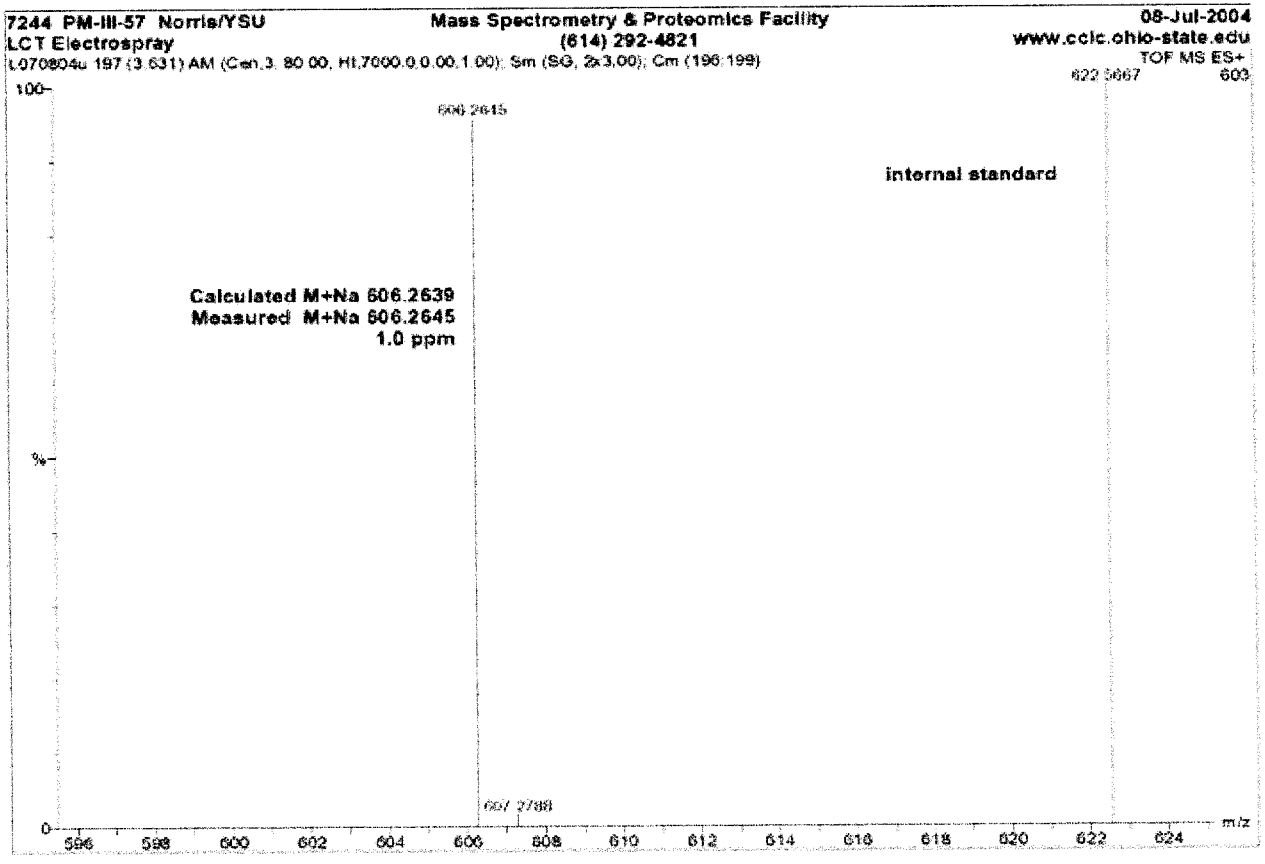

Figure 80: Mass spectrum of triazole **31**, a disaccharide analog

Appendix B

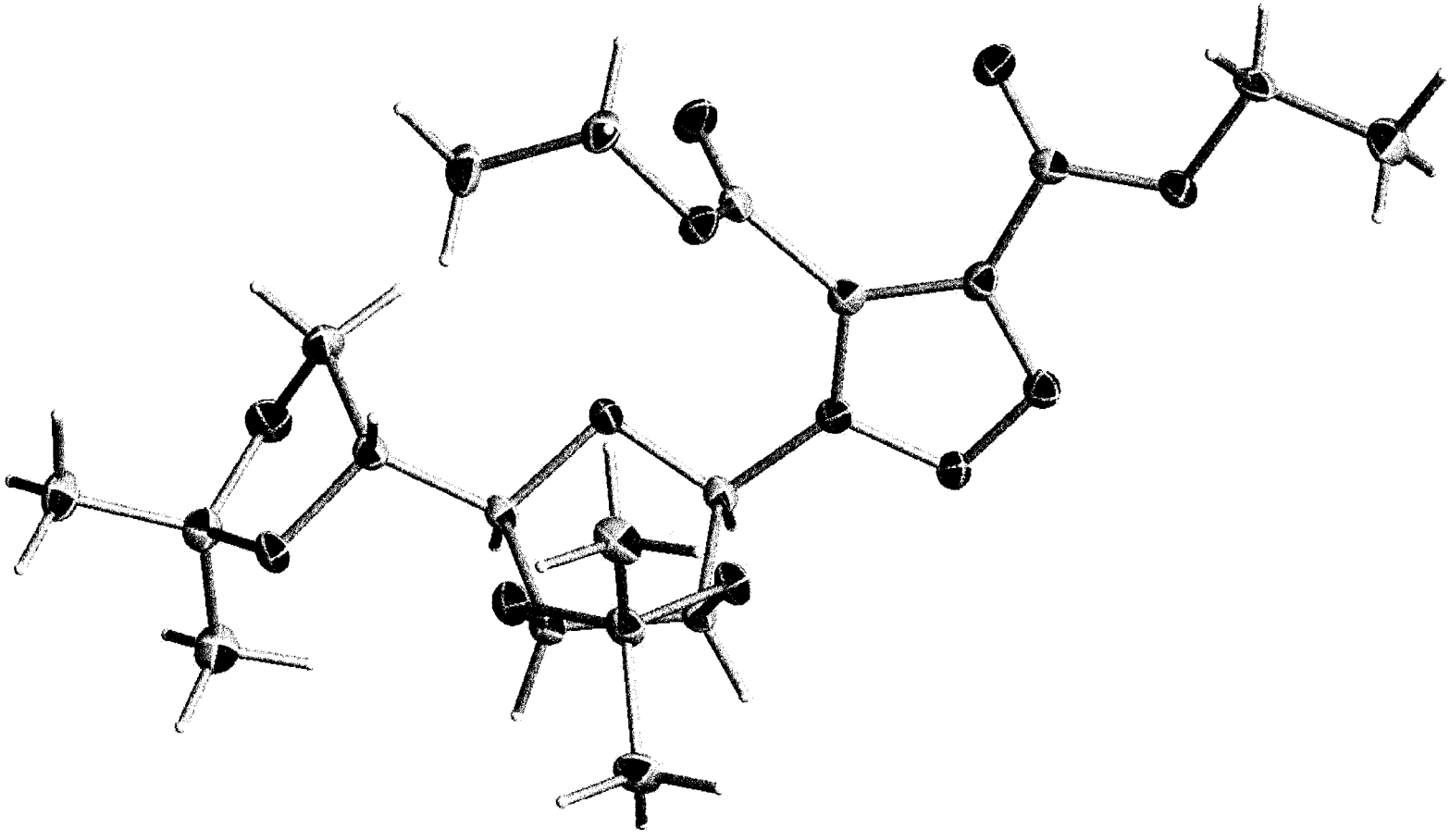

Figure 81: X-ray structure for 1-(2,3:5,6-di-*O*-isopropylidene-β-D-mannofuranosyl)-1*H*-[1,2,3]triazol-4,5-dicarboxylic acid diethyl ester (**9**)

Table 1. Crystal data and structure refinement for 03smhsm.

Identification code	03smhsm
Empirical formula	$C_{27}H_{41}N_6O_{22}$
Formula weight	455.46
Temperature	100(2) K
Wavelength	0.71073 A
Crystal system	Orthorhombic
Space group	P 2_1 2_1 2_1 (No. 19)
Unit cell dimensions	a = 8.6148(5) Å alpha = 90 deg. b = 10.4793(6) Å beta = 90 deg. c = 24.6873(15) Å gamma = 90 deg.
Volume, Z	2228.7(2) $Å^3$, 4
Density (calculated)	1.357 Mg/m^3
Absorption coefficient	0.108 mm^{-1}
F(000)	968
Crystal size	0.477 x 0.320 x 0.222 mm
Theta range for data collection	2.11 to 28.31 deg.
Limiting indices	-11<=h<=11, -13<=k<=13, -32<=l<=32
Reflections collected	23562
Independent reflections	5532 [R(int) = 0.0294]
Absorption correction	Empirical
Max. and min. transmission	1.0 and 0.812972
Refinement method	Full-matrix least-squares on F^2
Data / restraints / parameters	5532 / 0 / 295

Goodness-of-fit on F^2	1.357
Final R indices [I>2sigma(I)]	R1 = 0.0507, wR2 = 0.1191
R indices (all data)	R1 = 0.0510, wR2 = 0.1192
Absolute structure parameter	0.2(8)
Largest diff. peak and hole	0.397 and -0.231 e. $Å^{-3}$

Table 2. Atomic coordinates (x 10^4) and equivalent isotropic displacement parameters (A^2 x 10^3) for 03smhsm. U(eq) is defined as one third of the trace of the orthogonalized Uij tensor.

	x	y	z	U(eq)
O(7)	9339(2)	9991(1)	555(1)	16(1)
O(1)	9490(2)	7455(1)	1358(1)	15(1)
O(5)	6868(2)	4811(1)	1036(1)	15(1)
O(3)	7133(2)	9325(1)	1790(1)	16(1)
O(8)	12338(2)	12137(2)	797(1)	21(1)
O(2)	5976(2)	7652(1)	1374(1)	17(1)
N(1)	10291(2)	9320(2)	1796(1)	14(1)
N(3)	11240(2)	11046(2)	2124(1)	15(1)
O(9)	12404(2)	13140(1)	1607(1)	18(1)
O(4)	9291(2)	3948(2)	931(1)	21(1)
N(2)	10597(2)	9967(2)	2259(1)	15(1)
O(6)	11670(2)	8998(2)	556(1)	22(1)
C(3)	7029(2)	7082(2)	1748(1)	14(1)
C(15)	10651(2)	9575(2)	776(1)	15(1)
C(13)	10740(2)	9995(2)	1360(1)	13(1)
C(12)	5326(2)	9752(2)	1078(1)	21(1)
C(14)	11358(2)	11099(2)	1575(1)	15(1)
C(1)	9498(2)	8093(2)	1859(1)	14(1)
C(2)	7805(2)	8232(2)	2036(1)	13(1)
C(4)	8377(2)	6436(2)	1446(1)	13(1)
C(18)	12076(2)	12171(2)	1276(1)	15(1)
C(16)	9174(3)	9760(2)	-29(1)	19(1)
C(17)	8585(3)	8435(2)	-139(1)	25(1)
C(5)	7926(2)	5824(2)	912(1)	15(1)
C(19)	13027(3)	14283(2)	1348(1)	18(1)
C(7)	7062(3)	2812(2)	560(1)	23(1)
C(11)	4416(3)	8918(2)	1986(1)	22(1)
C(10)	5686(2)	8923(2)	1559(1)	17(1)
C(8)	7705(2)	3609(2)	1022(1)	18(1)
C(20)	12950(3)	15346(2)	1758(1)	27(1)
C(6)	9269(3)	5122(2)	640(1)	21(1)
C(9)	7580(3)	2958(2)	1566(1)	23(1)

Table 3. Bond lengths [A] and angles [deg] for 03smhsm.

O(7)-C(15)	1.328(2)
O(7)-C(16)	1.469(2)
O(1)-C(1)	1.407(2)
O(1)-C(4)	1.452(2)
O(5)-C(5)	1.433(2)
O(5)-C(8)	1.453(2)
O(3)-C(2)	1.419(2)
O(3)-C(10)	1.434(2)
O(8)-C(18)	1.205(2)
O(2)-C(3)	1.426(2)
O(2)-C(10)	1.431(2)
N(1)-C(13)	1.344(3)
N(1)-N(2)	1.354(2)
N(1)-C(1)	1.464(2)
N(3)-N(2)	1.302(2)
N(3)-C(14)	1.361(3)
O(9)-C(18)	1.334(2)
O(9)-C(19)	1.460(2)
O(4)-C(6)	1.424(3)
O(4)-C(8)	1.430(3)
O(6)-C(15)	1.196(3)
C(3)-C(4)	1.537(3)
C(3)-C(2)	1.550(3)
C(3)-H(3)	1.0000
C(15)-C(13)	1.510(3)
C(13)-C(14)	1.379(3)
C(12)-C(10)	1.503(3)
C(12)-H(19)	0.9800
C(12)-H(18)	0.9800
C(12)-H(17)	0.9800
C(14)-C(18)	1.479(3)
C(1)-C(2)	1.530(3)
C(1)-H(1)	1.0000
C(2)-H(2)	1.0000
C(4)-C(5)	1.516(3)
C(4)-H(4)	1.0000
C(16)-C(17)	1.504(3)
C(16)-H(21)	0.9900
C(16)-H(20)	0.9900
C(17)-H(24)	0.9800
C(17)-H(23)	0.9800
C(17)-H(22)	0.9800

C(5)-C(6)	1.526(3)
C(5)-H(5)	1.0000
C(19)-C(20)	1.505(3)
C(19)-H(26)	0.9900
C(19)-H(25)	0.9900
C(7)-C(8)	1.518(3)
C(7)-H(10)	0.9800
C(7)-H(9)	0.9800
C(7)-H(8)	0.9800
C(11)-C(10)	1.518(3)
C(11)-H(16)	0.9800
C(11)-H(15)	0.9800
C(11)-H(14)	0.9800
C(8)-C(9)	1.510(3)
C(20)-H(29)	0.9800
C(20)-H(28)	0.9800
C(20)-H(27)	0.9800
C(6)-H(7)	0.9900
C(6)-H(6)	0.9900
C(9)-H(13)	0.9800
C(9)-H(12)	0.9800
C(9)-H(11)	0.9800

C(15)-O(7)-C(16)	115.51(16)
C(1)-O(1)-C(4)	102.74(14)
C(5)-O(5)-C(8)	108.74(15)
C(2)-O(3)-C(10)	106.72(14)
C(3)-O(2)-C(10)	107.13(15)
C(13)-N(1)-N(2)	110.88(16)
C(13)-N(1)-C(1)	132.93(17)
N(2)-N(1)-C(1)	116.12(15)
N(2)-N(3)-C(14)	108.74(17)
C(18)-O(9)-C(19)	115.75(15)
C(6)-O(4)-C(8)	106.31(16)
N(3)-N(2)-N(1)	107.57(16)
O(2)-C(3)-C(4)	110.56(15)
O(2)-C(3)-C(2)	104.18(15)
C(4)-C(3)-C(2)	103.83(15)
O(2)-C(3)-H(3)	112.5
C(4)-C(3)-H(3)	112.5
C(2)-C(3)-H(3)	112.5
O(6)-C(15)-O(7)	127.23(19)
O(6)-C(15)-C(13)	122.89(18)
O(7)-C(15)-C(13)	109.81(16)
N(1)-C(13)-C(14)	104.15(17)
N(1)-C(13)-C(15)	126.65(17)

C(14)-C(13)-C(15)	129.12(18)
C(10)-C(12)-H(19)	109.5
C(10)-C(12)-H(18)	109.5
H(19)-C(12)-H(18)	109.5
C(10)-C(12)-H(17)	109.5
H(19)-C(12)-H(17)	109.5
H(18)-C(12)-H(17)	109.5
N(3)-C(14)-C(13)	108.66(18)
N(3)-C(14)-C(18)	123.92(18)
C(13)-C(14)-C(18)	127.40(18)
O(1)-C(1)-N(1)	109.03(15)
O(1)-C(1)-C(2)	106.94(15)
N(1)-C(1)-C(2)	113.05(16)
O(1)-C(1)-H(1)	109.2
N(1)-C(1)-H(1)	109.2
C(2)-C(1)-H(1)	109.2
O(3)-C(2)-C(1)	110.14(16)
O(3)-C(2)-C(3)	104.84(14)
C(1)-C(2)-C(3)	101.91(15)
O(3)-C(2)-H(2)	113.0
C(1)-C(2)-H(2)	113.0
C(3)-C(2)-H(2)	113.0
O(1)-C(4)-C(5)	110.45(15)
O(1)-C(4)-C(3)	104.38(14)
C(5)-C(4)-C(3)	114.49(16)
O(1)-C(4)-H(4)	109.1
C(5)-C(4)-H(4)	109.1
C(3)-C(4)-H(4)	109.1
O(8)-C(18)-O(9)	125.72(19)
O(8)-C(18)-C(14)	123.04(19)
O(9)-C(18)-C(14)	111.23(16)
O(7)-C(16)-C(17)	111.27(17)
O(7)-C(16)-H(21)	109.4
C(17)-C(16)-H(21)	109.4
O(7)-C(16)-H(20)	109.4
C(17)-C(16)-H(20)	109.4
H(21)-C(16)-H(20)	108.0
C(16)-C(17)-H(24)	109.5
C(16)-C(17)-H(23)	109.5
H(24)-C(17)-H(23)	109.5
C(16)-C(17)-H(22)	109.5
H(24)-C(17)-H(22)	109.5
H(23)-C(17)-H(22)	109.5
O(5)-C(5)-C(4)	106.87(15)
O(5)-C(5)-C(6)	102.67(15)
C(4)-C(5)-C(6)	113.06(17)

O(5)-C(5)-H(5)	111.3
C(4)-C(5)-H(5)	111.3
C(6)-C(5)-H(5)	111.3
O(9)-C(19)-C(20)	107.25(16)
O(9)-C(19)-H(26)	110.3
C(20)-C(19)-H(26)	110.3
O(9)-C(19)-H(25)	110.3
C(20)-C(19)-H(25)	110.3
H(26)-C(19)-H(25)	108.5
C(8)-C(7)-H(10)	109.5
C(8)-C(7)-H(9)	109.5
H(10)-C(7)-H(9)	109.5
C(8)-C(7)-H(8)	109.5
H(10)-C(7)-H(8)	109.5
H(9)-C(7)-H(8)	109.5
C(10)-C(11)-H(16)	109.5
C(10)-C(11)-H(15)	109.5
H(16)-C(11)-H(15)	109.5
C(10)-C(11)-H(14)	109.5
H(16)-C(11)-H(14)	109.5
H(15)-C(11)-H(14)	109.5
O(2)-C(10)-O(3)	104.39(15)
O(2)-C(10)-C(12)	108.77(17)
O(3)-C(10)-C(12)	108.89(16)
O(2)-C(10)-C(11)	110.12(17)
O(3)-C(10)-C(11)	110.59(17)
C(12)-C(10)-C(11)	113.65(18)
O(4)-C(8)-O(5)	105.21(16)
O(4)-C(8)-C(9)	108.65(17)
O(5)-C(8)-C(9)	109.51(17)
O(4)-C(8)-C(7)	111.59(18)
O(5)-C(8)-C(7)	108.36(17)
C(9)-C(8)-C(7)	113.20(18)
C(19)-C(20)-H(29)	109.5
C(19)-C(20)-H(28)	109.5
H(29)-C(20)-H(28)	109.5
C(19)-C(20)-H(27)	109.5
H(29)-C(20)-H(27)	109.5
H(28)-C(20)-H(27)	109.5
O(4)-C(6)-C(5)	101.87(16)
O(4)-C(6)-H(7)	111.4
C(5)-C(6)-H(7)	111.4
O(4)-C(6)-H(6)	111.4
C(5)-C(6)-H(6)	111.4
H(7)-C(6)-H(6)	109.3
C(8)-C(9)-H(13)	109.5

C(8)-C(9)-H(12)	109.5
H(13)-C(9)-H(12)	109.5
C(8)-C(9)-H(11)	109.5
H(13)-C(9)-H(11)	109.5
H(12)-C(9)-H(11)	109.5

Table 4. Anisotropic displacement parameters (A^2 x 10^3) for 03smhsm.
The anisotropic displacement factor exponent takes the form:
-2 pi^2 [h^2 a*^2 U11 + ... + 2 h k a* b* U12]

	U11	U22	U33	U23	U13	U12
O(7)	14(1)	20(1)	13(1)	-1(1)	-2(1)	2(1)
O(1)	13(1)	15(1)	17(1)	-3(1)	1(1)	-3(1)
O(5)	12(1)	11(1)	22(1)	-1(1)	-1(1)	0(1)
O(3)	12(1)	13(1)	23(1)	1(1)	-3(1)	0(1)
O(8)	25(1)	23(1)	15(1)	-2(1)	1(1)	-1(1)
O(2)	13(1)	16(1)	20(1)	-1(1)	-4(1)	1(1)
N(1)	10(1)	17(1)	14(1)	0(1)	-1(1)	1(1)
N(3)	13(1)	17(1)	16(1)	0(1)	-1(1)	0(1)
O(9)	21(1)	16(1)	17(1)	2(1)	1(1)	-5(1)
O(4)	15(1)	21(1)	28(1)	-2(1)	3(1)	4(1)
N(2)	14(1)	17(1)	14(1)	-2(1)	-2(1)	-2(1)
O(6)	14(1)	30(1)	21(1)	-8(1)	2(1)	3(1)
C(3)	13(1)	15(1)	14(1)	2(1)	-1(1)	0(1)
C(15)	14(1)	14(1)	17(1)	-1(1)	0(1)	-2(1)
C(13)	8(1)	17(1)	15(1)	0(1)	-1(1)	3(1)
C(12)	17(1)	22(1)	26(1)	7(1)	-4(1)	1(1)
C(14)	13(1)	18(1)	14(1)	-2(1)	-3(1)	1(1)
C(1)	13(1)	12(1)	15(1)	2(1)	-2(1)	-1(1)
C(2)	14(1)	13(1)	13(1)	1(1)	-1(1)	0(1)
C(4)	13(1)	11(1)	15(1)	2(1)	-1(1)	-1(1)
C(18)	10(1)	17(1)	17(1)	2(1)	-1(1)	2(1)
C(16)	27(1)	19(1)	12(1)	1(1)	-3(1)	0(1)
C(17)	35(1)	23(1)	17(1)	-2(1)	-8(1)	-7(1)
C(5)	13(1)	14(1)	16(1)	-1(1)	1(1)	-1(1)
C(19)	19(1)	19(1)	16(1)	6(1)	2(1)	-5(1)
C(7)	29(1)	15(1)	23(1)	-4(1)	-3(1)	2(1)
C(11)	14(1)	25(1)	28(1)	1(1)	4(1)	1(1)
C(10)	10(1)	19(1)	22(1)	-1(1)	0(1)	0(1)
C(8)	18(1)	16(1)	20(1)	-1(1)	-1(1)	3(1)
C(20)	40(1)	17(1)	25(1)	2(1)	3(1)	-8(1)
C(6)	18(1)	22(1)	22(1)	-4(1)	4(1)	0(1)
C(9)	28(1)	20(1)	21(1)	2(1)	-4(1)	2(1)

Table 5. Hydrogen coordinates (x 10^4) and isotropic displacement parameters (A^2 x 10^3) for 03smhsm.

	x	y	z	U(eq)
H(3)	6500	6492	2008	17
H(19)	6186	9709	819	32
H(18)	5185	10636	1198	32
H(17)	4372	9450	904	32
H(1)	10068	7564	2131	16
H(2)	7671	8216	2438	16
H(4)	8854	5775	1686	16
H(21)	10193	9876	-208	23
H(20)	8443	10391	-184	23
H(24)	8448	8319	-530	37
H(23)	7588	8312	45	37
H(22)	9336	7809	-3	37
H(5)	7446	6460	661	18
H(26)	12406	14503	1024	21
H(25)	14115	14138	1234	21
H(10)	7212	3266	217	34
H(9)	5952	2662	618	34
H(8)	7608	1992	546	34
H(16)	4717	8354	2284	33
H(15)	3446	8611	1824	33
H(14)	4265	9786	2124	33
H(29)	13351	16133	1596	41
H(28)	13578	15120	2075	41
H(27)	11869	15475	1869	41
H(7)	9065	4983	250	25
H(6)	10257	5593	683	25
H(13)	8051	3501	1844	34
H(12)	8124	2138	1553	34
H(11)	6484	2815	1653	34

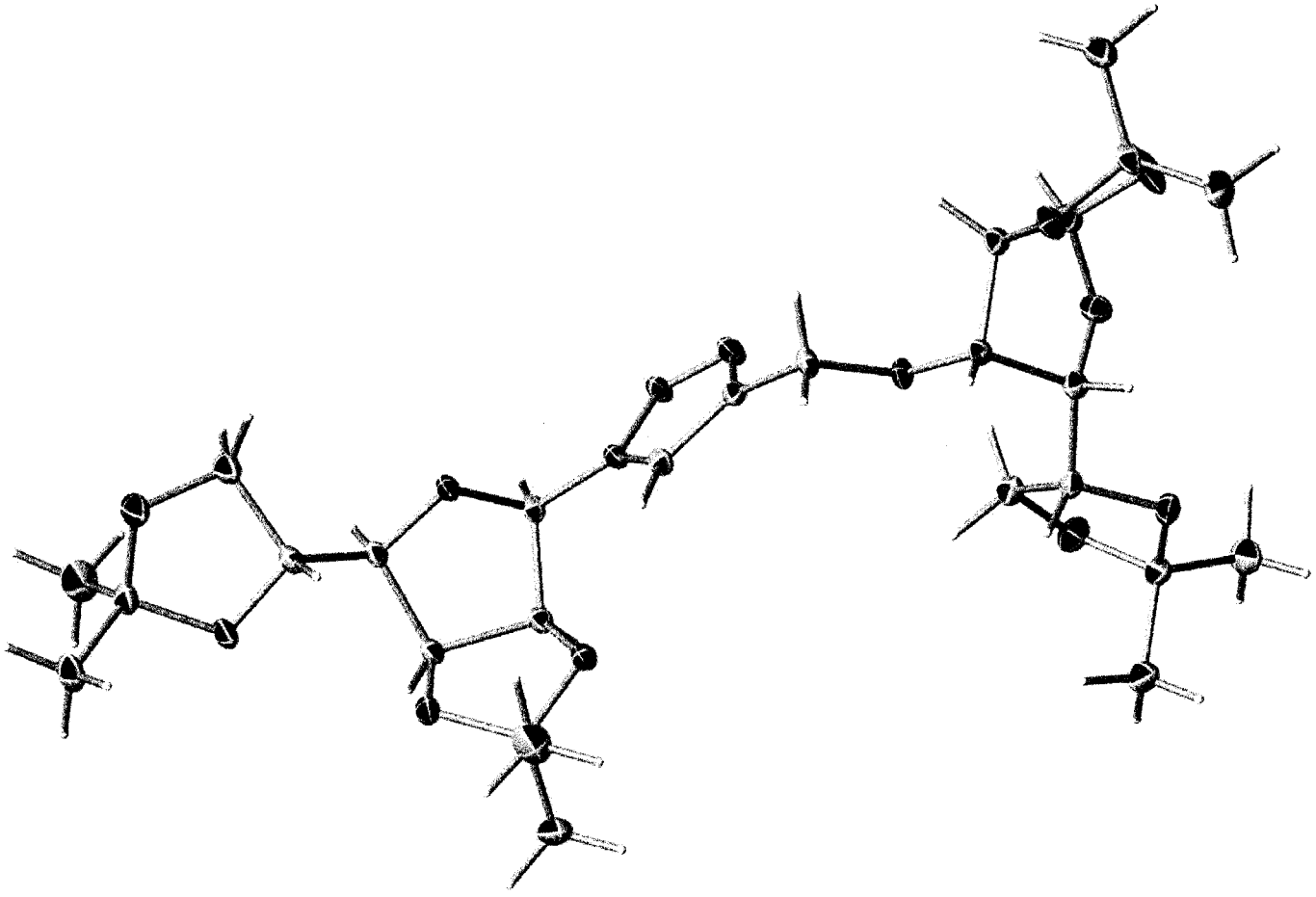

Figure 82: X-ray structure compound **31**, a disaccharide analog

Table 1. Crystal data and structure refinement for 04twpmdm.

Identification code	04twpmdm
Empirical formula	$C_{27}H_{41}N_3O_{11}$
Formula weight	583.63
Temperature	100(2) K
Wavelength	0.71073 Å
Crystal system	Monoclinic
Space group	P 2_1 (No. 4)
Unit cell dimensions	a = 10.0048(13) Å alpha = 90 deg. b = 10.3781(13) Å beta = 107.051(2) deg. c = 14.6612(19) Å gamma = 90 deg.
Volume, Z	1455.4(3) $Å^3$, 2
Density (calculated)	1.332 Mg/m^3
Absorption coefficient	0.103 mm^{-1}
F(000)	624
Crystal size	0.407 x 0.275 x 0.154 mm
Theta range for data collection	1.45 to 28.33 deg.
Limiting indices	-13<=h<=13, -13<=k<=13, -19<=l<=19
Reflections collected	15527
Independent reflections	7134 [R(int) = 0.0212]
Refinement method	Full-matrix least-squares on F^2
Data / restraints / parameters	7134 / 1 / 426
Goodness-of-fit on F^2	1.078
Final R indices [I>2sigma(I)]	R1 = 0.0425, wR2 = 0.1088

R indices (all data)	R1 = 0.0436, wR2 = 0.1098
Absolute structure parameter	0.6(5)
Largest diff. peak and hole	0.374 and -0.256 e. $Å^{-3}$

Table 2. Atomic coordinates (x 10^4) and equivalent isotropic displacement parameters (A^2 x 10^3) for 04twpmdm. U(eq) is defined as one third of the trace of the orthogonalized Uij tensor.

	x	y	z	U(eq)
O(1)	-1650(1)	6077(1)	-3492(1)	25(1)
O(2)	-654(1)	7260(1)	-2153(1)	21(1)
O(3)	344(1)	6636(1)	-80(1)	17(1)
O(4)	1915(1)	5334(1)	925(1)	17(1)
O(5)	1743(1)	4680(1)	-1080(1)	13(1)
O(6)	7240(1)	716(1)	4970(1)	19(1)
O(7)	7814(1)	2469(1)	4250(1)	21(1)
O(8)	4890(1)	417(1)	2118(1)	14(1)
O(9)	7320(1)	-856(1)	3353(1)	18(1)
O(10)	4963(1)	-3010(1)	2654(1)	18(1)
O(11)	7340(1)	-3077(1)	3115(1)	28(1)
N(1)	3443(1)	3607(1)	129(1)	13(1)
N(2)	4711(1)	3180(1)	106(1)	16(1)
N(3)	4910(1)	2061(1)	527(1)	18(1)
C(1)	-711(2)	8196(2)	-3672(1)	30(1)
C(2)	-2903(2)	7903(2)	-3178(1)	24(1)
C(3)	-1483(2)	7370(2)	-3141(1)	18(1)
C(4)	-409(2)	5408(2)	-2970(1)	24(1)
C(5)	-175(2)	5964(2)	-1978(1)	15(1)
C(6)	1324(2)	5987(2)	-1347(1)	13(1)
C(7)	1555(2)	6706(1)	-399(1)	14(1)
C(8)	2654(2)	5876(2)	327(1)	14(1)
C(9)	2996(2)	4838(1)	-311(1)	13(1)
C(10)	751(2)	6161(2)	875(1)	18(1)
C(11)	1188(2)	7271(2)	1571(1)	28(1)
C(12)	-418(2)	5351(2)	1025(2)	30(1)
C(13)	2831(2)	2749(2)	574(1)	14(1)
C(14)	3777(2)	1759(2)	819(1)	13(1)
C(15)	3684(2)	510(2)	1302(1)	15(1)
C(16)	4897(2)	-699(1)	2685(1)	13(1)
C(17)	5389(2)	-1890(2)	2254(1)	14(1)
C(18)	6994(2)	-1860(2)	2679(1)	16(1)
C(19)	6085(2)	-547(2)	3613(1)	14(1)
C(20)	6196(2)	773(2)	4061(1)	15(1)
C(21)	6702(2)	1874(2)	3540(1)	17(1)
C(22)	7818(2)	1979(2)	5158(1)	17(1)

C(23)	9329(2)	1871(2)	5768(1)	26(1)
C(24)	6916(2)	2811(2)	5597(1)	22(1)
C(25)	6133(2)	-3866(2)	2956(1)	18(1)
C(26)	6098(2)	-4839(2)	2173(1)	27(1)
C(27)	6119(2)	-4488(2)	3882(1)	29(1)

Table 3. Bond lengths [A] and angles [deg] for 04twpmdm.

O(1)-C(3)	1.429(2)
O(1)-C(4)	1.433(2)
O(2)-C(5)	1.4255(19)
O(2)-C(3)	1.4467(19)
O(3)-C(7)	1.4222(19)
O(3)-C(10)	1.4269(19)
O(4)-C(8)	1.4187(19)
O(4)-C(10)	1.4304(19)
O(5)-C(9)	1.4283(17)
O(5)-C(6)	1.4398(17)
O(6)-C(22)	1.427(2)
O(6)-C(20)	1.4333(18)
O(7)-C(21)	1.4225(19)
O(7)-C(22)	1.424(2)
O(8)-C(16)	1.4244(17)
O(8)-C(15)	1.4320(18)
O(9)-C(18)	1.406(2)
O(9)-C(19)	1.4329(19)
O(10)-C(17)	1.4220(18)
O(10)-C(25)	1.432(2)
O(11)-C(18)	1.412(2)
O(11)-C(25)	1.420(2)
N(1)-C(13)	1.3515(19)
N(1)-N(2)	1.3540(18)
N(1)-C(9)	1.4421(19)
N(2)-N(3)	1.3033(19)
N(3)-C(14)	1.361(2)
C(1)-C(3)	1.513(2)
C(1)-H(1A)	0.9800
C(1)-H(1B)	0.9800
C(1)-H(1C)	0.9800
C(2)-C(3)	1.511(2)
C(2)-H(2A)	0.9800
C(2)-H(2B)	0.9800
C(2)-H(2C)	0.9800
C(4)-C(5)	1.518(2)
C(4)-H(4A)	1.02(3)
C(4)-H(4B)	0.97(3)
C(5)-C(6)	1.514(2)
C(5)-H(5)	0.93(2)
C(6)-C(7)	1.535(2)
C(6)-H(6)	1.0000

C(7)-C(8)	1.548(2)
C(7)-H(7)	0.96(2)
C(8)-C(9)	1.529(2)
C(8)-H(8)	0.99(2)
C(9)-H(9)	1.0000
C(10)-C(12)	1.508(2)
C(10)-C(11)	1.516(2)
C(11)-H(11A)	0.9800
C(11)-H(11B)	0.9800
C(11)-H(11C)	0.9800
C(12)-H(12A)	0.9800
C(12)-H(12B)	0.9800
C(12)-H(12C)	0.9800
C(13)-C(14)	1.372(2)
C(13)-H(13)	0.95(2)
C(14)-C(15)	1.493(2)
C(15)-H(15A)	0.98(2)
C(15)-H(15B)	0.96(2)
C(16)-C(19)	1.530(2)
C(16)-C(17)	1.533(2)
C(16)-H(16)	0.961(19)
C(17)-C(18)	1.543(2)
C(17)-H(17)	0.955(18)
C(18)-H(18)	1.0000
C(19)-C(20)	1.509(2)
C(19)-H(19)	1.03(2)
C(20)-C(21)	1.540(2)
C(20)-H(20)	0.99(2)
C(21)-H(21A)	0.966(19)
C(21)-H(21B)	1.00(2)
C(22)-C(23)	1.518(2)
C(22)-C(24)	1.522(2)
C(23)-H(23A)	0.9800
C(23)-H(23B)	0.9800
C(23)-H(23C)	0.9800
C(24)-H(24A)	0.9800
C(24)-H(24B)	0.9800
C(24)-H(24C)	0.9800
C(25)-C(27)	1.507(2)
C(25)-C(26)	1.522(2)
C(26)-H(26A)	0.9800
C(26)-H(26B)	0.9800
C(26)-H(26C)	0.9800
C(27)-H(27A)	0.9800
C(27)-H(27B)	0.9800
C(27)-H(27C)	0.9800

C(3)-O(1)-C(4)	105.74(13)
C(5)-O(2)-C(3)	108.55(12)
C(7)-O(3)-C(10)	108.34(12)
C(8)-O(4)-C(10)	107.11(12)
C(9)-O(5)-C(6)	102.99(11)
C(22)-O(6)-C(20)	106.60(12)
C(21)-O(7)-C(22)	108.43(12)
C(16)-O(8)-C(15)	113.65(11)
C(18)-O(9)-C(19)	108.19(12)
C(17)-O(10)-C(25)	108.54(12)
C(18)-O(11)-C(25)	110.93(12)
C(13)-N(1)-N(2)	110.95(12)
C(13)-N(1)-C(9)	132.41(13)
N(2)-N(1)-C(9)	116.63(12)
N(3)-N(2)-N(1)	107.08(12)
N(2)-N(3)-C(14)	109.17(12)
C(3)-C(1)-H(1A)	109.5
C(3)-C(1)-H(1B)	109.5
H(1A)-C(1)-H(1B)	109.5
C(3)-C(1)-H(1C)	109.5
H(1A)-C(1)-H(1C)	109.5
H(1B)-C(1)-H(1C)	109.5
C(3)-C(2)-H(2A)	109.5
C(3)-C(2)-H(2B)	109.5
H(2A)-C(2)-H(2B)	109.5
C(3)-C(2)-H(2C)	109.5
H(2A)-C(2)-H(2C)	109.5
H(2B)-C(2)-H(2C)	109.5
O(1)-C(3)-O(2)	105.01(12)
O(1)-C(3)-C(2)	108.74(14)
O(2)-C(3)-C(2)	108.73(13)
O(1)-C(3)-C(1)	111.72(15)
O(2)-C(3)-C(1)	109.31(14)
C(2)-C(3)-C(1)	113.00(15)
O(1)-C(4)-C(5)	101.11(13)
O(1)-C(4)-H(4A)	109.8(14)
C(5)-C(4)-H(4A)	115.9(14)
O(1)-C(4)-H(4B)	112.1(14)
C(5)-C(4)-H(4B)	113.2(14)
H(4A)-C(4)-H(4B)	105(2)
O(2)-C(5)-C(6)	108.40(12)
O(2)-C(5)-C(4)	103.74(13)
C(6)-C(5)-C(4)	115.93(13)
O(2)-C(5)-H(5)	109.6(12)
C(6)-C(5)-H(5)	107.6(12)

C(4)-C(5)-H(5)	111.4(12)
O(5)-C(6)-C(5)	107.98(12)
O(5)-C(6)-C(7)	104.86(11)
C(5)-C(6)-C(7)	114.82(12)
O(5)-C(6)-H(6)	109.7
C(5)-C(6)-H(6)	109.7
C(7)-C(6)-H(6)	109.7
O(3)-C(7)-C(6)	110.89(12)
O(3)-C(7)-C(8)	104.32(12)
C(6)-C(7)-C(8)	103.88(12)
O(3)-C(7)-H(7)	109.5(12)
C(6)-C(7)-H(7)	114.0(11)
C(8)-C(7)-H(7)	113.8(12)
O(4)-C(8)-C(9)	110.45(12)
O(4)-C(8)-C(7)	104.58(12)
C(9)-C(8)-C(7)	102.30(12)
O(4)-C(8)-H(8)	113.0(12)
C(9)-C(8)-H(8)	112.1(12)
C(7)-C(8)-H(8)	113.7(13)
O(5)-C(9)-N(1)	109.66(11)
O(5)-C(9)-C(8)	105.14(12)
N(1)-C(9)-C(8)	116.49(12)
O(5)-C(9)-H(9)	108.4
N(1)-C(9)-H(9)	108.4
C(8)-C(9)-H(9)	108.4
O(3)-C(10)-O(4)	104.58(12)
O(3)-C(10)-C(12)	109.00(14)
O(4)-C(10)-C(12)	108.21(15)
O(3)-C(10)-C(11)	109.89(14)
O(4)-C(10)-C(11)	110.60(14)
C(12)-C(10)-C(11)	114.11(15)
C(10)-C(11)-H(11A)	109.5
C(10)-C(11)-H(11B)	109.5
H(11A)-C(11)-H(11B)	109.5
C(10)-C(11)-H(11C)	109.5
H(11A)-C(11)-H(11C)	109.5
H(11B)-C(11)-H(11C)	109.5
C(10)-C(12)-H(12A)	109.5
C(10)-C(12)-H(12B)	109.5
H(12A)-C(12)-H(12B)	109.5
C(10)-C(12)-H(12C)	109.5
H(12A)-C(12)-H(12C)	109.5
H(12B)-C(12)-H(12C)	109.5
N(1)-C(13)-C(14)	104.12(13)
N(1)-C(13)-H(13)	124.3(15)
C(14)-C(13)-H(13)	131.6(15)

N(3)-C(14)-C(13)	108.67(14)
N(3)-C(14)-C(15)	121.51(13)
C(13)-C(14)-C(15)	129.81(14)
O(8)-C(15)-C(14)	107.48(12)
O(8)-C(15)-H(15A)	109.2(11)
C(14)-C(15)-H(15A)	113.0(12)
O(8)-C(15)-H(15B)	111.4(13)
C(14)-C(15)-H(15B)	111.4(13)
H(15A)-C(15)-H(15B)	104.4(17)
O(8)-C(16)-C(19)	107.77(12)
O(8)-C(16)-C(17)	111.29(12)
C(19)-C(16)-C(17)	100.96(12)
O(8)-C(16)-H(16)	112.1(12)
C(19)-C(16)-H(16)	113.3(11)
C(17)-C(16)-H(16)	111.0(12)
O(10)-C(17)-C(16)	108.56(12)
O(10)-C(17)-C(18)	104.61(12)
C(16)-C(17)-C(18)	103.82(13)
O(10)-C(17)-H(17)	109.3(13)
C(16)-C(17)-H(17)	116.2(12)
C(18)-C(17)-H(17)	113.6(11)
O(9)-C(18)-O(11)	111.66(13)
O(9)-C(18)-C(17)	107.35(13)
O(11)-C(18)-C(17)	104.62(13)
O(9)-C(18)-H(18)	111.0
O(11)-C(18)-H(18)	111.0
C(17)-C(18)-H(18)	111.0
O(9)-C(19)-C(20)	111.08(13)
O(9)-C(19)-C(16)	104.20(12)
C(20)-C(19)-C(16)	114.80(13)
O(9)-C(19)-H(19)	110.4(12)
C(20)-C(19)-H(19)	108.3(12)
C(16)-C(19)-H(19)	108.0(12)
O(6)-C(20)-C(19)	107.93(13)
O(6)-C(20)-C(21)	103.63(12)
C(19)-C(20)-C(21)	116.80(13)
O(6)-C(20)-H(20)	110.0(13)
C(19)-C(20)-H(20)	108.3(13)
C(21)-C(20)-H(20)	109.9(13)
O(7)-C(21)-C(20)	105.08(12)
O(7)-C(21)-H(21A)	106.4(11)
C(20)-C(21)-H(21A)	116.3(12)
O(7)-C(21)-H(21B)	108.4(13)
C(20)-C(21)-H(21B)	109.5(13)
H(21A)-C(21)-H(21B)	110.7(17)
O(7)-C(22)-O(6)	104.92(12)

O(7)-C(22)-C(23)	107.84(14)
O(6)-C(22)-C(23)	108.87(14)
O(7)-C(22)-C(24)	110.67(14)
O(6)-C(22)-C(24)	110.21(13)
C(23)-C(22)-C(24)	113.91(14)
C(22)-C(23)-H(23A)	109.5
C(22)-C(23)-H(23B)	109.5
H(23A)-C(23)-H(23B)	109.5
C(22)-C(23)-H(23C)	109.5
H(23A)-C(23)-H(23C)	109.5
H(23B)-C(23)-H(23C)	109.5
C(22)-C(24)-H(24A)	109.5
C(22)-C(24)-H(24B)	109.5
H(24A)-C(24)-H(24B)	109.5
C(22)-C(24)-H(24C)	109.5
H(24A)-C(24)-H(24C)	109.5
H(24B)-C(24)-H(24C)	109.5
O(11)-C(25)-O(10)	105.78(13)
O(11)-C(25)-C(27)	109.37(15)
O(10)-C(25)-C(27)	108.75(14)
O(11)-C(25)-C(26)	109.64(15)
O(10)-C(25)-C(26)	110.05(14)
C(27)-C(25)-C(26)	112.98(15)
C(25)-C(26)-H(26A)	109.5
C(25)-C(26)-H(26B)	109.5
H(26A)-C(26)-H(26B)	109.5
C(25)-C(26)-H(26C)	109.5
H(26A)-C(26)-H(26C)	109.5
H(26B)-C(26)-H(26C)	109.5
C(25)-C(27)-H(27A)	109.5
C(25)-C(27)-H(27B)	109.5
H(27A)-C(27)-H(27B)	109.5
C(25)-C(27)-H(27C)	109.5
H(27A)-C(27)-H(27C)	109.5
H(27B)-C(27)-H(27C)	109.5

Table 4. Anisotropic displacement parameters (A^2 x 10^3) for 04twpmdm.
The anisotropic displacement factor exponent takes the form:
-2 pi^2 [h^2 a*^2 U11 + ... + 2 h k a* b* U12]

	U11	U22	U33	U23	U13	U12
O(1)	23(1)	24(1)	21(1)	-4(1)	-5(1)	6(1)
O(2)	21(1)	17(1)	19(1)	-1(1)	-3(1)	8(1)
O(3)	16(1)	22(1)	14(1)	4(1)	6(1)	6(1)
O(4)	20(1)	15(1)	16(1)	3(1)	7(1)	5(1)
O(5)	13(1)	10(1)	14(1)	1(1)	2(1)	2(1)
O(6)	24(1)	16(1)	13(1)	1(1)	-1(1)	0(1)
O(7)	21(1)	24(1)	16(1)	-1(1)	4(1)	-6(1)
O(8)	16(1)	12(1)	14(1)	4(1)	1(1)	0(1)
O(9)	14(1)	17(1)	22(1)	-3(1)	4(1)	0(1)
O(10)	16(1)	11(1)	25(1)	4(1)	4(1)	-1(1)
O(11)	16(1)	13(1)	48(1)	8(1)	-1(1)	1(1)
N(1)	12(1)	11(1)	14(1)	0(1)	3(1)	2(1)
N(2)	16(1)	16(1)	18(1)	3(1)	8(1)	7(1)
N(3)	19(1)	15(1)	21(1)	4(1)	9(1)	6(1)
C(1)	28(1)	35(1)	33(1)	10(1)	15(1)	3(1)
C(2)	15(1)	29(1)	25(1)	6(1)	3(1)	6(1)
C(3)	16(1)	20(1)	17(1)	3(1)	2(1)	4(1)
C(4)	24(1)	21(1)	21(1)	-4(1)	-3(1)	7(1)
C(5)	14(1)	13(1)	18(1)	2(1)	3(1)	3(1)
C(6)	14(1)	12(1)	13(1)	3(1)	4(1)	2(1)
C(7)	13(1)	10(1)	16(1)	1(1)	2(1)	2(1)
C(8)	15(1)	11(1)	16(1)	0(1)	1(1)	1(1)
C(9)	13(1)	9(1)	16(1)	3(1)	3(1)	-1(1)
C(10)	20(1)	18(1)	14(1)	2(1)	4(1)	6(1)
C(11)	33(1)	28(1)	22(1)	-8(1)	5(1)	9(1)
C(12)	27(1)	32(1)	35(1)	8(1)	17(1)	3(1)
C(13)	12(1)	13(1)	16(1)	1(1)	3(1)	1(1)
C(14)	15(1)	12(1)	12(1)	0(1)	3(1)	1(1)
C(15)	14(1)	12(1)	17(1)	4(1)	1(1)	1(1)
C(16)	15(1)	10(1)	13(1)	2(1)	4(1)	-1(1)
C(17)	18(1)	10(1)	15(1)	2(1)	4(1)	-1(1)
C(18)	18(1)	13(1)	18(1)	2(1)	6(1)	1(1)
C(19)	14(1)	14(1)	15(1)	1(1)	4(1)	0(1)
C(20)	16(1)	16(1)	13(1)	2(1)	2(1)	1(1)

C(21)	19(1)	14(1)	15(1)	1(1)	3(1)	-2(1)
C(22)	17(1)	18(1)	16(1)	-2(1)	3(1)	1(1)
C(23)	20(1)	30(1)	24(1)	-5(1)	-2(1)	3(1)
C(24)	22(1)	24(1)	19(1)	-4(1)	5(1)	1(1)
C(25)	19(1)	11(1)	22(1)	2(1)	1(1)	-1(1)
C(26)	33(1)	18(1)	28(1)	-3(1)	3(1)	7(1)
C(27)	41(1)	21(1)	24(1)	7(1)	7(1)	6(1)

Table 5. Hydrogen coordinates (x 10^4) and isotropic displacement parameters (A^2 x 10^3) for 04twpmdm.

	x	y	z	U(eq)
H(1A)	-617	9073	-3414	46
H(1B)	-1235	8217	-4351	46
H(1C)	220	7832	-3595	46
H(2A)	-2802	8793	-2944	36
H(2B)	-3316	7377	-2775	36
H(2C)	-3511	7884	-3837	36
H(6)	1939	6363	-1708	16
H(9)	3742	5177	-576	15
H(11A)	1464	6938	2225	42
H(11B)	403	7869	1485	42
H(11C)	1980	7724	1452	42
H(12A)	-146	5020	1679	45
H(12B)	-606	4627	575	45
H(12C)	-1262	5879	916	45
H(18)	7459	-1724	2169	20
H(23A)	9735	2735	5903	40
H(23B)	9860	1371	5425	40
H(23C)	9368	1437	6368	40
H(24A)	7326	3674	5726	33
H(24B)	6868	2420	6195	33
H(24C)	5972	2876	5152	33
H(26A)	5262	-5378	2063	41
H(26B)	6934	-5384	2369	41
H(26C)	6077	-4382	1584	41
H(27A)	5283	-5028	3775	44
H(27B)	6108	-3819	4351	44
H(27C)	6956	-5023	4122	44
H(4A)	-570(20)	4440(30)	-3032(17)	29(6)
H(4B)	370(30)	5560(20)	-3229(17)	28(6)
H(5)	-700(20)	5530(20)	-1649(14)	10(4)
H(7)	1830(20)	7590(20)	-419(13)	11(4)
H(8)	3490(20)	6360(20)	685(14)	18(5)
H(13)	1940(20)	2860(20)	666(15)	23(5)
H(15A)	2840(20)	440(20)	1509(14)	11(4)
H(15B)	3630(20)	-210(20)	876(15)	19(5)
H(16)	4000(20)	-849(19)	2785(13)	8(4)
H(17)	5081(19)	-1950(20)	1575(13)	10(4)
H(19)	5930(20)	-1210(20)	4098(15)	17(5)

H(20)	5280(20)	1000(20)	4145(15)	21(5)
H(21A)	7080(20)	1620(20)	3032(13)	11(5)
H(21B)	5930(20)	2520(20)	3307(16)	24(6)